Quantum correlations in systems of indistinguishable particles / Topological states of matter in a number conserving setting

Fernando Iemini de Rezende Aguiar

August 2015

Quantum correlations in systems of indistinguishable particles/Topological states of matter in a number conserving setting

Fernando Iemini de Rezende Aguiar

Orientador:

Prof. Dr. Reinaldo Oliveira Vianna

Tese apresentada à UNIVERSIDADE FEDERAL DE MINAS GERAIS - UFMG, como requisito parcial para a obtenção do grau de DOUTOR EM FÍSICA.

Belo Horizonte
Brasil
Agosto de 2015

Contents

A minha avó **Clotilde Iemini de Rezende Brasil**,
a qual sempre foi e sempre será meu grande exemplo.

Acknowledgments

Thanking all those who are part, directly or indirectly, of this work is by no means a simple task, since the large number of names to be remembered and the forgetfulness of some is natural. I thanks first and foremost to my family, my grandmother Clotilde Iemini de Rezende Brasil, my parents Rogers Tadeu Aguiar and Thaís Iemini de Rezende Aguiar, and my brothers Thiago and Marcelo Iemini de Rezende Aguar, their support and trust were indispensable.

To my colleagues of work and quantum discussions, Thiago Debarba, Thiago Maciel, André Tanus, and of course to my adviser Reinaldo O. Vianna, whose suggestions and advice were fundamental. His guidance helped me in all the time of research and writing of this thesis. To my longtime friends Lucas Costa Fonseca, José Guilherme, Helen Murta, Diogo Spinelli, Henrique Milani, Henrique Guimarães, Joao Antonio, Iury Marques Paiva, and all residents/ visitors of the Arantes Consulate. To my cousin André Iemini Godoy, to the Clockwork band members, to the basketball group, to all these by moments and unforgettable experiences, for memorable trips and pleasant conversations.

I would like also to express my sincere gratitude to my advisor Prof. Rosario Fazio during my internship period at Scuola Normale Superiore (SNS). I thanks for the continuous support of my PhD studies and related research, for his patience, motivation, and immense knowledge. I could not have imagined having a better advisor and mentor for such period. I would like to thank also the rest of the group and colleagues at SNS, with special attention to Davide Rossini and Leonardo Mazza, whose help and support in my studies were fundamental.

Finally, I thank everyone who has made my way as pleasant as possible.

-Este trabalho teve o apoio financeiro direto e indireto da **CAPES**, da **FAPEMIG** e do **CNPq**.

Abstract

This thesis is a contribution to the research field of three distinct subjects: quantum correlations in systems of indistinguishable particles, topological states of matter, and non-Markovian dynamics. The first two subjects are the main subjects of the thesis, in which was kept an exclusive dedication, while the last one fits as a satellite part in the thesis.

The first part of this thesis concerns to a proper understanding of quantum correlations in systems of indistinguishable particles. In this case, the space of quantum states is restricted to symmetric or antisymmetric subspaces, depending on the bosonic or fermionic nature of the system, and the particles are no longer accessible individually, thus eliminating the usual notions of separability and local measurements, and making the analysis of correlations much subtler. We completely review the distinct approaches for the entanglement in these systems, and based on its definitions we elaborate distinct methods in order to quantify the entanglement between the indistinguishable particles. Such methods have proven to be very useful and easy to handle, since they adapt common tools in the usual entanglement theory of distinguishable systems for the present indistinguishable case. We further propose a general notion of quantum correlation beyond entanglement (the quantumness of correlations) in these systems, by means of an "activation protocol". Such general notion is very helpful at the ongoing debate in the literature regarding the correct definition of particle entanglement, since it allows us to analyze the correlations between indistinguishable particles in a different, and more general, framework, settling some of its controversies. We then use our quantifiers to study the entanglement of indistinguishable particles on its particle partition in a specific model, namely extended Hubbard model, with focus on its behavior when crossing its quantum phase transitions.

The second part of this thesis concerns to the study of topological states of matter. Our analysis and results have as a basis the paradigmatic (non-number conserving) Kitaev model, which provides a minimal setting showcasing all the key aspects of topological states of matter in fermionic systems. Our analysis focus, however, in a number conserving setting. In such setting, we present two distinct ways to generate topological states completely similar to the Kitaev model: (i) in a Hamiltonian setting, we present an exactly solvable two-wire fermionic model which conserves the number of particles and features Majorana-like exotic quasiparticles at the edges; (ii) by means of a suitably engineered dissipative dynamics, we present how to generate such topological states as the dark states (steady-states) of the evolution.

In the third part of this thesis we analyze non-Markovian dynamics with the divisibility criterion, *i.e.*, the non-positivity of the dynamical matrix for some intermediate time. Particularly, we study a qubit interacting with an Ising model environment.

Resumo

Esta tese é uma contribuição para o campo de pesquisa de três assuntos distintos: correlações quânticas em sistemas de partículas indistinguíveis, estados topológicos da matéria, e dinâmica nao-Markoviana. Os primeiros dois assuntos são os temas pricipais desta tese, nos quais foi mantida uma dedicação exclusiva, enquanto o último assunto se encaixa mais como uma parte satélite na tese.

A primeira parte desta tese diz respeito a uma compreensão adequada das correlações quânticas em sistemas de partículas indistinguíveis. Neste caso, o espaço de estados quântico é restrito ao subspaço simétrico ou antisimétrico, dependendo da natureza bosônica ou fermiônica do sistema, e as partículas não são mais acessíveis individualmente, eliminando desta forma as noções habituais de separabilidade e medições locais, tornando a análise de suas correlações muito mais sutil. Nós revisamos as distintas abordagens para o emaranhamento nestes sistemas, e com base em tais definições elaboramos diferentes métodos a fim de quantificar o emaranhamento entre as partículas indistinguíveis. Tais métodos mostram-se muito úteis e fáceis de se manusear, uma vez que adaptam ferramentas comuns da teoria usual do emaranhamento em sistemas distinguíveis para o presente caso indistinguível. Propomos também uma noção geral de correlação quântica além do emaranhamento (o *quantumness of correlations*) nestes sistemas, por meio de um "protocolo de ativação". Tal noção é muito útil no debate em curso da literatura a respeito da definição correta para o emaranhamento entre as partículas indistinguíveis, uma vez que nos permite analisar suas correlações de uma ótica distinta, e mais geral, resolvendo algumas de suas constrovérsias. Em seguida, usamos nossos quantificadores para estudar o emaranhamento de partículas indistinguíveis em um modelo específico, o modelo Hubbard estendido, com foco em seu comportamento ao atravessar suas respectivas transições de fase quânticas.

A segunda parte desta tese diz respeito ao estudo de estados topológicas da matéria. Nossa análise e resultados têm como base o paradigmático modelo de Kitaev (não conserva o número de partículas), o qual fornece um ambiente mínimo apresentando todos os aspectos chave de estados topológicos em sistemas fermiônicos. Nossa análise foca-se, no entanto, em um cenário que conserve o número de partículas. Em tal cenário, apresentamos duas maneiras distintas para gerar estados topológicos completamente similares ao modelo de Kitaev: (i) em um cenário tipo Hamiltoniano, apresentamos um modelo fermiônico de dois fios, com solução exata, que conserva o número de partículas e apresenta quasipartículas exóticas tipo Majorana nas bordas;

(ii) por meio de uma dinâmica de dissipação adequadamente projetada, tais estados topológicos se apresentam como *dark states* (estados estacionários) da evolução.

Na terceira parte desta tese analisamos dinâmicas não-Markovianas com o critério de divisibilidade, ou seja, a não-positividade da matriz dinâmica em algum tempo intermediário. Particularmente, estudamos um qubit interagindo com um ambiente tipo Ising.

Publications Related to this Thesis

1. Fernando Iemini, Thiago. O. Maciel, Tiago. Debarba and Reinaldo O. Vianna
Quantifying Quantum Correlations in Fermionic Systems using Witness Operators
Quantum Inf. Process. **12**, 733 (2013).
see chapter 2

2. Fernando Iemini and Reinaldo O. Vianna
Computable Measures for the Entanglement of Indistinguishable Particles
Phys. Rev. A **87**, 022327 (2013).
see chapter 2

3. Fernando Iemini, Tiago Debarba and Reinaldo O. Vianna
Quantumness of correlations in indistinguishable particles
Phys. Rev. A **89**, 032324 (2014).
see chapter 3

4. Fernando Iemini, Thiago O. Maciel and Reinaldo O. Vianna
Entanglement of indistinguishable particles as a probe for quantum phase transitions in the extended Hubbard model
Phys. Rev. B **92**, 075423 (2015)
see chapter 4

5. Fernando Iemini, Leonardo Mazza, Davide Rossini, Rosario Fazio and Sebastian Diehl
Localized Majorana-like modes in a number conserving setting: An exactly solvable model
Phys. Rev. Lett. **115**, 156402 (2015)
see chapter 6

6. Fernando Iemini, Davide Rossini, Sebastian Diehl, Rosario Fazio and Leonardo Mazza
Dissipative topological superconductors in number-conserving systems
Phys. Rev. B **93**, 115113 (2016)
see chapter 7

7. Fernando Iemini, Andre T. Cesário and Reinaldo O. Vianna
   Witnessing non-Markovian dynamics with the divisibility criterion: a qubit interacting with an Ising model environment
   arXiv:1507.02267
   see chapter 8

• **Highlight and media coverage:** *"Férmions de Majorana em modelo solúvel"*, Destaque em Física no boletim da SBF (Sociedade Brasileira de Física), semana de 15 de Outubro de 2015, *url*: http://www.sbfisica.org.br/v1/index.php?option=com_content&view=article&id=706:2015-10-15-17-38-14&catid=151:destaque-em-fisica&Itemid=315

Introduction

This thesis is a contribution to the research field of three distinct subjects: (*I*) quantum correlations in systems of indistinguishable particles, (*II*) topological states of matter, and (*III*) non-Markovian dynamics. The first two topics are the main subjects of the thesis, in which it was kept an exclusive dedication, while the last one fits more like a satellite part in the thesis.

Part I.

The notion of entanglement is considered one of the main features of quantum mechanics, and became a subject of great interest in the last years, due to its primordial role in several distinct areas of physics, as Quantum Computation, Quantum Information [1, 2, 3, 4], Condensed Matter Physics [5], just to cite some. The subject was first addressed in the 1935's seminal paper by Einstein, Podolsky and Rosen [6], which originated the famous "EPR paradox", putting in evidence several basic concepts of nature, such as the notion of locality and physical reality. In the EPR paradox the quantum theory is confronted to the idea of a local realistic nature. Soon after the EPR publication, the subject has also attracted interest to another great name of science; Schrödinger [7, 8] discuss in his works the peculiarity of the phenomenon, historically being the author who introduced the term entanglement. While considering uncomfortable that the quantum theory would allow so unusual phenomena, as the idea of a non-local, non-realistic nature, he has considered them as the main feature of quantum mechanics: "I would not call that *one* but *the* characteristic trait of quantum mechanics; the one that enforces its entire departure from classical lines of thought" [7]. The subject has gained a major boost after John Bell, in the 1960's, proposed a test, called Bell inequalities [9], shifting EPR arguments to the domain of experimental physics. Experimental tests were then conducted some years later corroborating the quantum theory [10].

Despite widely studied in systems of distinguishable particles, less attention has been given to the study of entanglement, or even a more general notion of quantum correlations, in the case of indistinguishable particles. In this case, the space of quantum states is restricted to symmetric $\mathcal{S}$ or antisymmetric $\mathcal{A}$ subspaces, depending on the bosonic or fermionic nature of the system, and the particles are no longer accessible individually, thus eliminating the usual notions of separability and local measurements, and making the analysis of correlations much subtler. In fact, there are a multitude of distinct approaches and an ongoing debate around the entanglement

in these systems [11, 12, 13, 14, 15, 16, 17, 18, 19, 20, 21, 22, 23, 24, 25, 26]. Nevertheless, despite the variety, the approaches consist essentially in the analysis of correlations under two different aspects: the correlations genuinely arising from the entanglement between the particles ("entanglement of particles") [11, 12, 13, 14, 15, 16, 17, 18], and the correlations arising from the entanglement between the modes of the system ("entanglement of modes") [19, 20, 21, 22]. These two notions of entanglement are complementary, and the use of one or the other depends on the particular situation under scrutiny. For example, the correlations in eigenstates of a many-body Hamiltonian could be more naturally described by particle entanglement, whereas certain quantum information protocols could prompt a description in terms of entanglement of modes. Once one has opted for a certain notion of entanglement there are interesting methods in order to quantify it [14, 27, 28, 29, 30, 31, 32].

Entanglement is not, however, the only kind of correlation presenting non classical features, and a great effort has recently been directed towards characterizing a more general notion of quantum correlations, the *quantumness* of correlations. The quantumness of correlations is revealed in different ways, and there are a wide variety of approaches, sometimes equivalent, in order to characterize and quantify it, e.g., through the "activation protocol", where the non classical character of correlations in the system is revealed by a unavoidable creation of entanglement between system and measurement apparatus in a local measurement [34, 47]; or by the analysis of the minimum disturbance caused in the system by local measurements [48, 49, 52], which led to the seminal definition of *quantum discord* [48]; or even through geometrical approaches [53].

The first part of this thesis concerns in this way to a proper understanding of quantum correlations in systems of indistinguishable particles. We first review, in Chapter 1, the distinct approaches for the entanglement in these systems. In Chapter 2 and show how to quantify such entanglement by adapting the common tools used in the usual entanglement theory of distinguishable systems [27, 28]. In Chapter 3 we propose a general notion of quantum correlation beyond such entanglement (the quantumness of correlations) in these systems, by means of an "activation protocol" [14]. In Chapter 4 we then use our quantifiers to study the entanglement of indistinguishable particles on its particle partition in the extended Hubbard model, with focus on its behavior when crossing its quantum phase transitions [67].

Part II.

In a general perspective, matter has many distinct phases, such as ordinary gas, liquid and solid phases, as well as more interesting conductors, insulators, superfluids, and others phases. Despite formed by the same elementary particle constituents, each phase has striking different properties. The properties of a phase emerge from the pattern in which the particles are organized and correlated in the material. These different patterns are usually called the *order* of the phase.

In this thesis we study states which present a "*topological order*". The defining features of topological order, namely the existence of degenerate

ground states which (i) share the same thermodynamic properties and (ii) can only be distinguished by a global measurement, portend for a true many-body protection of quantum information. Thus, topological quantum computation has recently emerged as one of the most intriguing paradigms for the storage and manipulation of quantum information [85, 86].

Large part of the enormous attention devoted in the last years to topological superconductors owes to the exotic quasiparticles such as Majorana modes, which localize at their boundaries (edges, vortices, ...) [91, 92] and play a key role in several robust quantum information protocols [93]. Kitaev's p-wave superconducting quantum wire [89] provides a minimal setting showcasing all the key aspects of topological states of matter in fermionic systems. Various implementations in solid state [94, 95] and ultracold atoms [96] via proximity to superconducting or superfluid reservoirs have been proposed, and experimental signatures of edge modes were reported [97].

Kitaev's model is an effective mean-field model and its Hamiltonian does not commute with the particle number operator. Considerable activity has been devoted to understanding how this scenario evolves in a number-conserving setting [98, 99, 100, 101, 102]. This effort is motivated both by the fundamental interest in observing a topological parity-symmetry breaking while a U(1) symmetry is intact, and by an experimental perspective, as in several setups (e.g. ultracold atoms) number conservation is naturally present. It was realised that a simple way to promote particle number conservation to a symmetry of the model, while keeping the edge state physics intact, was to consider at least two coupled wires rather than a single one [98, 99, 100]. However, since attractive interactions are pivotal to generate superconducting order in the canonical ensemble, one usually faces a complex interacting many-body problem. Therefore, approximations such as bosonization [98, 99, 100], or numerical approaches [101] were invoked. An exactly solvable model of a topological superconductor in a number conserving setting, which would directly complement Kitaev's scenario, is missing.

The second part of this thesis concerns, in this way, to the study of topological states of matter in a number conserving setting. Our analysis and results have as a basis the paradigmatic (non-number conserving) Kitaev model. In Chapter 5 we briefly review the main characteristics of the Kitaev model and its topological phase. Later, in the next chapters, we present, in a number conserving setting, two distinct ways to generate topological states completely similar to the Kitaev model. In Chapter 6 we work in a Hamiltonian setting, presenting an exactly solvable two-wire fermionic model which conserves the number of particles and features Majorana-like exotic quasiparticles at the edges [115]. In Chapter 7, by means of a suitably engineered dissipative dynamics, we present how to generate such topological states as the dark states (steady-states) of the evolution [122].

***Part** III.*

The need to fight decoherence, to guarantee the proper working of the quantum enhanced technologies of information and computation [1], has renovated the motivation for the in-depth study of system-environment inter-

action dynamics. In particular, the Markovian or non-Markovian nature of the dynamics is of great interest [161]. Several witnesses and measures have been proposed in order to characterize the non-Markovianity of quantum processes [162]. For instance, the information flow between system and environment, quantified by the distinguishability of any two quantum states [163, 164], or by the Fisher information [165], or mutual information [166]; the Loschmidt echo [167, 168]; the entanglement between system and environment [169].

In Chapter 8 of this thesis we study, by means of the divisibility criterion, *i.e.*, the non-positivity of the dynamical matrix for some intermediate time, characterizing the dynamics of a qubit interacting with an arbitrary quadratic fermionic environment. We obtain an analytical expression for the Kraus decomposition of the quantum map, and check its non-positivity with a simple function. With an efficient sufficient criterion to map the non-Markovian regions of the dynamics, we analyze the particular case of an environment described by the Ising Hamiltonian with a transverse field [160].

Part I

Quantum correlations in systems of indistinguishable particles

CHAPTER 1

Entanglement in system of indistinguishable particles

In this chapter we review some selected topics in entanglement theory, chosen because of their relevance in this thesis. In Sec.1.1 we review concepts of entanglement theory in systems of distinguishable particles, which will make the subsequent discussions for the indistinguishable case clearer. In Sec.1.2 we discuss in detail the main approaches of entanglement in systems of indistinguishable particles.

1.1 Distinguishable subsystems - general view

Let us see a simple scenario which can highlight some of the peculiar features of quantum entanglement. Consider the case of two distinguishable particles, which primarily can interact, and after some time, are spatially separated. Let us first suppose that its quantum state is given by the product form $|\psi\rangle = |\phi_A\rangle \otimes |\phi_B\rangle \in \mathcal{H}_A^{d_a} \otimes \mathcal{H}_B^{d_b}$, where $|\phi_A\rangle \in H_A^{d_a}$ and $|\phi_B\rangle \in H_B^{d_b}$. In such a state, local operations in one of the particles, $\{\mathcal{I} \otimes \hat{\Phi}, \hat{\Phi} \otimes \mathcal{I}\}$, do not change the state of the other particle. States described in such a product form are called separable states, and can be generated by only performing local operations on its parts, and classical communication between them (LOCC operations). We could consider, however, a different state which cannot be described in a product form, such as the *singlet* state,

$$|\psi\rangle = \frac{|\uparrow\downarrow\rangle - |\downarrow\uparrow\rangle}{\sqrt{2}} \tag{1.1}$$

where $\{|\uparrow\rangle, |\downarrow\rangle\}$ are the eigenstates of the σ_z operator. Such a state is an entangled state, commonly called as EPR state, and it can not be generated from a separable state by any LOCC operations. Moreover, if we have access only to one of its particles, the state is described by the partial trace over the

other particle,

$$\rho_A = Tr_B(|\psi\rangle\langle\psi|) = \frac{\mathcal{I}}{2}, \tag{1.2}$$

it corresponds to a maximally mixed state (similarly for $\rho_B = \frac{\mathcal{I}}{2}$). This means that if we measure spin A along any axis, the result is completely random — we find spin up with probability $1/2$ and spin down with probability $1/2$. Therefore, if we perform any local measurement of A or B, we acquire no information about the preparation of the state. Quoting Schrödinger: "the best possible knowledge of a *whole* does not necessarily include the best possible knowledge of all its *parts*"[7].

Entangled states are interesting because they exhibit correlations that have no classical analog. The definition of an entangled state is related to the impossibility to describe it in the usual product form (as a separable state). Formally, separable states, are defined as,

Definition 1.1. *Given a partition of the Hilbert space in N distinguishable parts, $\mathcal{H} = \mathcal{H}_1 \otimes \mathcal{H}_2 \otimes ... \otimes \mathcal{H}_N$, the separable states in this partition are the quantum states $\{\sigma_{sep}\}$ which can be described as a convex decomposition of pure states in the product form, i.e.,*

$$\sigma_{sep} = \sum_i p_i \, \sigma_1^i \otimes \sigma_2^i \otimes ... \otimes \sigma_N^i \quad ; \quad \sum_i p_i = 1 \tag{1.3}$$

where $\sigma_k \in \mathcal{H}_k$. A quantum state is entangled in such a partition if it cannot be described as a separable state.

The determination of separability in a arbitrary quantum state is not a trivial task. Several criteria were formulated, as the famous Peres-Horodecki [33] criteria, which relates the set of separable states with its invariance to partial transpositions in one of its parts. In this work we will not only investigate the separability problem in general systems, but also study the quantification of its entanglement. This is a very important concept due to the several applications of entanglement as a resource, e.g., in Quantum Information and Computation [1, 2, 3, 4].

1.2 Indistinguishable particles

As aforementioned, in systems of indistinguishable particles the analysis of entanglement and quantum correlations between the particles becomes much subtler. The quantum states are now restricted to the symmetric ($\mathcal{S}$) or antisymmetric ($\mathcal{A}$) subspaces, depending on the bosonic or fermionic nature of the system, and the particles are no longer accessible individually, thus eliminating the usual notions of separability and local measurements. Notice first that one cannot analyze the system under the usual paradigm of *separability and locality*, where the reduced states obtained by partial trace are mixed ($\rho_r = Tr_{2...N}(|\psi\rangle\langle\psi|)$), whenever the global state is pure and entangled. Therefore, in the case of indistinguishable particles, the use of partial trace over the particles to characterize entanglement should be carefully reviewed, since it would suggest that all pure fermionic states are entangled, given that

their reduced states are always mixed. In order to generalize the notion of entanglement for systems of indistinguishable particles, the approach based on the algebra of observables sheds light on the problem and allows us to go beyond the paradigm of separability and locality.

In Sec.1.2.1 we present the concept of entanglement of modes. The discussion for the particles entanglement is given in Sec.1.2.2, where we show a detailed presentation of the main approaches based on algebra of observables and their restrictions; we also discuss about exchange-correlations in these systems, an intrinsic quantum correlation due to particle statistics.

1.2.1 Modes entanglement

Usually, the analysis of entanglement in indistinguishable particles is realized under two distinct aspects: the correlation between the modes of the system ("entanglement of modes") [19, 20, 21, 22], and the correlations arising genuinely from the entanglement between the particles ("entanglement of particles") [11, 12, 13, 14, 15, 16, 17, 18]. We will analyse in this section the former one.

The notion of entanglement of modes is a relatively simple concept. It constitutes the entanglement between the occupation number of the possible "degrees of freedom" (modes) of the system. The notion reconnects us to the usual entanglement theory, where the subsystems (modes) are distinguishable, and in this way one can employ all the tools commonly used in distinguishable quantum systems in order to analyse their correlations.

In the fermionic case, for example, the modes notion can be realized by mapping the quantum state in its number representation as follows,

$$\begin{aligned} f^\dagger_{j_1}...f^\dagger_{j_N}|vac\rangle \quad &\longrightarrow \quad |0...1_{j_1}...1_{j_N}...0\rangle \\ \hat{\mathcal{A}}(\mathcal{H}_1^M \otimes ... \otimes \mathcal{H}_N^M) \quad &\longrightarrow \quad (\mathcal{H}_1^2 \otimes ... \otimes \mathcal{H}_M^2) \end{aligned} \tag{1.4}$$

where $\{f_j^\dagger\}_{j=1}^M$ is an arbitrary set of M fermionic operators for the system. We will denote hereafter as "configuration representation" ("number representation") the left (right) side of the above equations. Such equation corresponds to a mapping to distinguishable qubits, represented by the occupied ($|1\rangle_j$) or unoccupied ($|0\rangle_j$) modes, which then allows one to employ all the tools commonly used in distinguishable quantum systems in order to analyse their correlations. One could, for example, use the von Neumann entropy of the reduced state representing a block with ℓ modes, in order to quantify the entanglement between the block with the rest of the system. The reduced state is obtained by the partial trace in the number representation, $\rho_\ell = Tr_{j\notin\ell}(|\psi\rangle\langle\psi|)$. Notice that, in the modes notion, local observables in the modes may involve correlations between the particles, e.g., "$f_j^\dagger f_{j+1}^\dagger f_{j+1} f_j$" despite acting locally in the $(j, j+1)$ block, describes pairing correlations between the particles. The algebra of local observables in the modes, defined in the number representation space, is generated by,

$$\begin{aligned} \Omega_{loc} = \{ &\hat{O}_1 \otimes \mathcal{I}_{2,M} \,;\, \mathcal{I} \otimes \hat{O}_2 \otimes \mathcal{I}_{3,M} \,;\, \cdots \\ &\cdots \,;\, \mathcal{I}_{1,(M-1)} \otimes \hat{O}_M \;||\; \hat{O}_j^\dagger = \hat{O}_j \} \end{aligned} \tag{1.5}$$

where $\mathcal{I}_{i,j} = \mathcal{I}_i \otimes \mathcal{I}_{i+1} \otimes \cdots \otimes \mathcal{I}_j$, and $\mathcal{I}$ is the identity operator. The unentangled states are those which can be completely described by such local observables. It is known that such states are simply the separable states in the usual tensor product form, i.e., $|\psi\rangle_{un} = |\phi_1\rangle \otimes |\phi_2\rangle \otimes \cdots \otimes |\phi_M\rangle$.

The above analysis extends in a similar way to the bosonic case, just noticing that the maximal occupation number of bosons in a mode is not restricted to a single boson, but all of the bosons could occupy the same mode. An interesting feature that should be recalled, concerns the fact that the number representation mapping, as presented in Eq.(1.4), is not bijective, i.e., there are states in the number representation space which have no counterpart in the configuration representation space. Such a problem is simply due the particle number conservation, and can thus be solved by mapping the entire Fock space with its number representation space. More precisely, given a system with M modes, and its respective fermionic Fock space,

$$\mathcal{F}(M)_f = |vac\rangle\langle vac| \oplus \mathcal{H}_1^M \oplus \mathcal{A}(\mathcal{H}_1^M \otimes \mathcal{H}_2^M) \oplus \cdots \oplus \mathcal{A}(\mathcal{H}_1^M \otimes \cdots \mathcal{H}_M^M), \quad (1.6)$$

or bosonic one,

$$\mathcal{F}(M)_b = |vac\rangle\langle vac| \oplus \mathcal{H}_1^M \oplus \mathcal{S}(\mathcal{H}_1^M \otimes \mathcal{H}_2^M) \oplus \cdots \oplus \mathcal{S}(\mathcal{H}_1^M \otimes \cdots \mathcal{H}_{M^M}^M), \quad (1.7)$$

where $\oplus$ is the matrix direct sum, defined as,

$$\oplus_{i=1}^k X_i = \begin{pmatrix} X_1 & & & \\ & X_2 & & \\ & & \ddots & \\ & & & X_k \end{pmatrix}; \quad (1.8)$$

the complete mapping to the number representation space is given, in the fermionic case, as

$$\mathcal{F}(M)_f \longleftrightarrow (\mathcal{H}_1^2 \otimes ... \otimes \mathcal{H}_M^2) \quad (1.9)$$

and in the bosonic case as,

$$\mathcal{F}(M)_b \longleftrightarrow (\mathcal{H}_1^M \otimes ... \otimes \mathcal{H}_M^M) \quad (1.10)$$

Example: An example makes the previous discussions clearer. Consider a fermionic (bosonic) state described by a single Slater determinant (permanent), within a four dimensional single particle space dimension $\{a_j^\dagger\}_{j=1}^4$. Given the state $|\psi\rangle = (\frac{a_1^\dagger + a_2^\dagger}{\sqrt{2}})(\frac{a_3^\dagger + a_4^\dagger}{\sqrt{2}})|vac\rangle$, the mapping onto its number representation leads to,

$$\begin{aligned} |\psi\rangle &\mapsto (\frac{|10\rangle + |01\rangle}{\sqrt{2}}) \otimes (\frac{|10\rangle + |01\rangle}{\sqrt{2}}) \\ &= \frac{1}{2}(|1010\rangle + |1001\rangle + |0110\rangle + |0101\rangle). \end{aligned} \quad (1.11)$$

Such a state is entangled or not depending on its modes partition. For example, if we analyse the correlations between the first mode with the rest, taking its reduced state,

$$\rho_1 = Tr_{2,3,4}(\rho) = \frac{1}{2}(|1\rangle\langle 1| + |0\rangle\langle 0|), \quad (1.12)$$

it corresponds to a maximally mixed state, and consequently this mode is maximally entangled with the rest. If, however, we analyse the correlations of pairs of modes, and take the reduced state of the first two modes,

$$\rho_{1,2} = Tr_{3,4}(\rho) = (|10\rangle + |01\rangle)(\langle 10| + \langle 01|), \tag{1.13}$$

we see that there is no entanglement between them.

1.2.2 Particle entanglement

In this section, we will work with the correlations genuinely arising from the entanglement between the particles. An interesting approach follows considering the proper algebra of "local observables", *i.e.*, the one composed by observables which do not involve correlations between the indistinguishable particles. In this way, analogous to the distinguishable case, the unentangled states can be defined as those states which can be completely described by such algebra. It is not hard to conclude that such algebra, defined in the configuration representation space, is generated simply by the single-particle observables,

$$\begin{aligned}\Omega_{loc} = \big\{&\hat{O} \otimes \mathcal{I}_{2,N} + \mathcal{I} \otimes \hat{O} \otimes \mathcal{I}_{3,N} + \cdots \\ &\cdots + \mathcal{I}_{1,(N-1)} \otimes \hat{O} \;||\; \hat{O}^\dagger = \hat{O}\big\},\end{aligned} \tag{1.14}$$

where N is the number of particles. Equivalently, using the second quantization formalism, the above set is given by number conserving quadratic operators $\Omega_{loc} = \{(a_i^\dagger a_j + H.c.) \,|\, i,j = 1,...,L\}$. The states that can be completely described by such algebra compose the set of unentangled states, where every particle is not entangled with any other. Intuitively, we would expect that this set corresponds to the set of single-Slater determinant/permanent states, with a fixed number of particles; more precisely, for a system with N fermions (bosons), it is given by,

$$|\psi\rangle_{un} = a_{j_1}^\dagger a_{j_2}^\dagger ... a_{j_N}^\dagger |vac\rangle, \tag{1.15}$$

where $\{a_j^\dagger\}$ is an arbitrary set of fermionic (bosonic) operators, recalling that these operators are not "quasiparticles" with particle-hole superpositions, as usual in a Bogoliubov transformation, and the above states have a fixed number of fermions (bosons). In fact, distinct approaches confirmed such intuitive set of unentangled states [11, 12, 13, 14, 15, 16, 17, 18, 25, 26, 32] (the only correlations in such states are the exchange correlations, due to the antissimetrization, which does not constitute in entanglement). For example, in [11] the authors analysis follows by using a very elegant mathematical formalism, called GNS (Gelfand–Naimark–Segal) construction, for the case of two fermions, each one with dimension $d = 3$ or 4, and two bosons with dimension $d = 3$; in [18, 25, 26], the authors propose a "Generalized Entanglement (GE)" measure, obtaining a simple formula for the "partial trace" in such algebra restriction, and the set o fermionic unentangled states for an arbitrary number of particles; or also in [14], not restricted only to the entanglement

notion, but to a general idea of quantum correlations (the *quantumness* of correlations), we generalize the idea of "activation protocol" [34] (as used for distinguishable particles in order to characterize their correlations) for indistinguishable particles, obtaining the same set of states with no *quantumness* as the above unentangled one.

We extend now the above discussions in order to make the notion of particle entanglement clearer. Firstly we will discuss the role of the exchange correlations in a system of indistinguishable particles, providing the idea of why, intuitively, it should not be considered as entanglement. We also show some cases where would be possible to treat the particles as effectively distinguishable, recovering the usual entanglement theory. We also present, in more detail, the previous mentioned approaches for the particle entanglement based on algebra of observables; more precisely, we present the GE measure and the GNS construction. We leave the discussion of quantumness of correlations to another chapter (see Chapter 3).

Exchange-correlations

Consider a general system, with N indistinguishable fermionic/bosonic particles, characterized by the single particle wave functions $\{|\phi_j\rangle_{j=1}^{M}\}$, which have a non negligible overlap between the moduli of their spatial wave function $\phi_j(x) = \langle x|\phi_j\rangle$, *i.e.*, $|\phi_j(x)|^2|\phi_\ell(x)|^2 \neq 0$, where $\{|x\rangle\}$ is the spatial position wave function basis. A general state for this system can be given by,

$$|\psi\rangle = \sum_{i_1,\ldots,i_N=1}^{M} c_{i_1,\ldots,i_N}\, \mathcal{A}/\mathcal{S}|\phi_{i_1}\ldots\phi_{i_N}\rangle, \tag{1.16}$$

or in second quantization formalism, as

$$|\psi\rangle = \sum_{i_1,\ldots,i_N=1}^{M} c_{i_1,\ldots,i_N}\, a^\dagger_{\phi_{i_1}}\ldots a^\dagger_{\phi_{i_N}}|vac\rangle. \tag{1.17}$$

where $\{a^\dagger_{\phi_j}\}$ are fermionic/bosonic creation operators. Generally, such Slater determinants/permanents contain correlations due to the exchange statistics of the indistinguishable particles, called *exchange correlations* in the language of Hartree-Fock theory. However, if the moduli of the spatial wave functions $\phi_j(x)$ have only a vanishing overlap, these exchange correlations will also tend to zero for any physically meaningful operator. For example, given a system with two fermions described by a single Slater-determinant, $|\psi\rangle = \frac{1}{\sqrt{2}}(|\phi\,\chi\rangle - |\chi\,\phi\rangle)$, and an arbitrary physical operator $\hat{O}$, its expectation value is given by,

$$\langle\hat{O}\rangle = \int O(x_1,x_2)\psi^*(x_1,x_2)\psi(x_1,x_2)dx_1dx_2, \tag{1.18}$$

where $O(x_1,x_2) = \langle x_1,x_2|\hat{O}|x_1,x_2\rangle$, and

$$\psi(x_1,x_2) = \langle x_1,x_2|\psi\rangle = \frac{1}{\sqrt{2}}[\phi(x_1)\chi(x_2) - \chi(x_1)\phi(x_2)] \tag{1.19}$$

We also have that,

$$\psi(x_1,x_2)^*\psi(x_1,x_2) = \frac{1}{2}\Big\{|\phi(x_1)|^2|\chi(x_2)|^2 + |\chi(x_1)|^2|\phi(x_2)|^2 + \\ -(\phi(x_1)^*\chi(x_1)\phi(x_2)\chi(x_2)^* + H.c.)\} \tag{1.20}$$

where the last term is the commonly called *exchange term* in Hartree-Fock theory. Noticing that $O(x_1,x_2) = O(x_2,x_1)$ must be symmetric under particle exchange, we can expand the expectation value in two parts,

$$\langle\hat{O}\rangle = \int O(x_1,x_2)\Big(|\phi(x_1)|^2|\chi(x_2)|^2 - Re[\phi(x_1)\chi(x_1)^*\phi(x_2)\chi(x_2)^*]\Big)dx_1dx_2. \tag{1.21}$$

We see in this way that, if the moduli of the spatial wave functions have a vanishing overlap, $|\phi(x_i)|^2|\chi(x_i)|^2 \sim 0$, the second term in the above equation, related to the exchange terms in the wave function, will also vanish, and the expectation value of the operator is reduced to

$$\langle\hat{O}\rangle \sim \int O(x_1,x_2)|\phi(x_1)|^2|\chi(x_2)|^2dx_1dx_2, \tag{1.22}$$

which is equivalent to two uncorrelated and distinguishable particles in a state $|\psi\rangle \sim |\phi\,\chi\rangle$. This situation is generically realized when the supports of the single particle wave functions are essentially centered around locations being sufficiently apart from each other. In this case, the (anti)symmetrization has no physical effects, and we would be able to "distinguish" the particles; see Fig.1.1 for a schematic representation. Thus, we easily conclude that such exchange correlations should not constitute as entanglement, since it vanishes with the particles spatial separation, and it is not a non-local correlation as in the usual entanglement theory.

CHSH inequality: Bell test experiments, or Bell inequalities [9], are formulated to test some theoretical consequences of entanglement, as the notion of locality and realism. A local theory is based on the assumption that spatially distant events are independent, having no instantaneous ("faster than light") interactions between each other. Under realism it is assumed that all objects must objectively have a pre-determined value for any measurement before the measurement is made. Thus, the Bell inequality consists of a though-experimental test which sets limits on the expectation values for its observables, based on the assumption of a *local hidden variable (LHV) theory*, i.e., a theory with underlying inaccessible variables (hidden variables) consistent with the principle of locality and realism.

Let us focus now on a specific generalization of Bell's original inequality, the CHSH inequality, introduced by John Clauser, Michael Horne, Abner Shimony and R. A. Holt [35]. Such inequality involves the correlation of two space-like separated spin measurements, $\hat{\sigma}_L(\vec{a})$ and $\hat{\sigma}_R(\vec{b})$, along the $\vec{a}$ and $\vec{b}$ directions, respectively. The CHSH inequality is given by,

$$CHSH : |E(\vec{a},\vec{b}) + E(\vec{a},\vec{b'}) - E(\vec{a'},\vec{b}) + E(\vec{a'},\vec{b'})| \leq 2, \tag{1.23}$$

where $E(\vec{a},\vec{b})$ is the expectation value for the pair of spin measurements $(\hat{\sigma}_L(\vec{a}),\hat{\sigma}_R(\vec{b}))$. For simplicity we normalized $E(\vec{a},\vec{b})$, such that $|E(\vec{a},\vec{b})| \leq 1$.

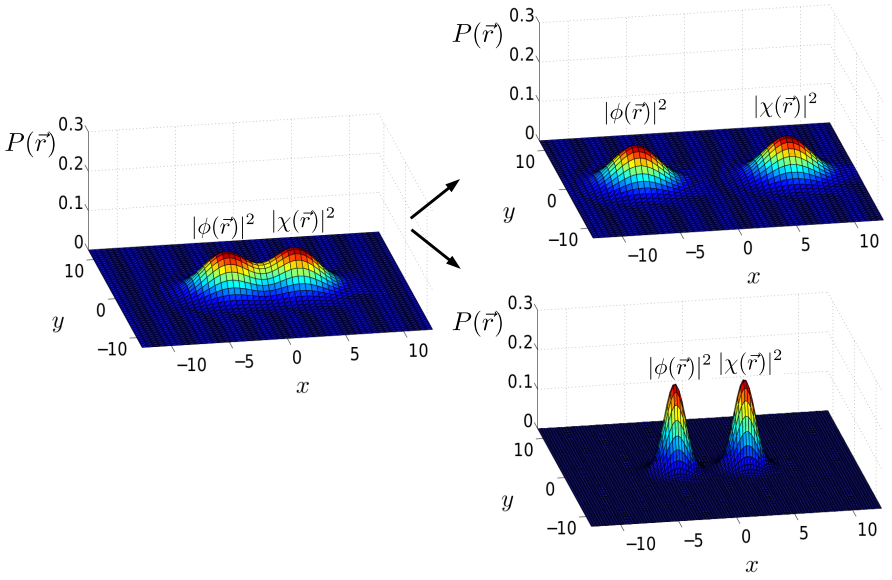

Figure 1.1: Spatial probability distribution $P(\vec{r}) = |\phi(x)|^2$, or $|\chi(x)|^2$, for two single particle modes, $|\phi\rangle$ and $|\chi\rangle$, with gaussian spatial probability distributions, $f(\vec{r}) \approx e^{-\frac{|\vec{r}-\vec{r}_0|^2}{2\sigma_0^2}}$, $\vec{r} = (y, x)$, centered around $(0, +x_o)$ and $(0, -x_o)$, respectively. Consider a state composed of indistinguishable particles, with support in these modes, as $|\psi\rangle = a_\phi^\dagger a_\chi^\dagger |vac\rangle$ (Eq.(1.19)). In Fig-left, the spatial distributions are centered around $x_o \sim 3$, and have a non-negligible overlap; in this case, exchange-correlations have physical effects and must be taken into account. In Fig-right, the single particle modes are: *(upper)* spatially separated from each other, with supports centered around $x \approx 2x_o$, describing for example the indistinguishable particles being spatially separated from each other; or *(bottom)* have a smaller gaussian variance, $\sigma \approx \sigma_o/2$, as for example, if we consider the modes as representing the particles probability distribution at two separated potential wells, then raising the potential barrier would decrease the tunneling of the particles between the wells, and in this way the gaussian distributions would be more localized. In these cases the modes spatial distributions have a negligible overlap, and exchange-correlations have no physical effects anymore. We could associate local Hilbert spaces ($\mathcal{H}_A$, $\mathcal{H}_B$) centered at the modes distributions, and the quantum state would be effectively represented by $\psi \sim |\phi\rangle_A |\psi\rangle_B$, with distinguishable particles A and B.

Any LHV theory must satisfies the above bound for all pairs of measurements. It is, however, not hard to show that violation of the CHSH inequality is predicted by quantum theory, *i.e.*, using the EPR state (Eq.1.1) it is possible to obtain, for certain spin measurements directions, the value of $2\sqrt{2}$ in the inequality.

Following the previous discussions on exchange correlations, the space-like separated spin measurements can here be represented by operators centered on the spatially separated wave functions $|\phi\rangle$ and $|\chi\rangle$ (considering $|\phi(x_i)|^2|\chi(x_i)|^2 \sim 0$). Taking into account also the spin degrees of freedom for the indistinguishable particles, these operators have their support as follows: $\hat{\sigma}_L(\vec{a}) \subset \{|\phi\uparrow\rangle, |\phi\downarrow\rangle\}$, and $\hat{\sigma}_R(\vec{b}) \subset \{|\chi\uparrow\rangle, |\chi\downarrow\rangle\}$. Thus, the expectation value for an arbitrary spin measurement correlation is given by,

$$E(\vec{a},\vec{b}) = \langle\psi|\Big(\hat{\sigma}_L(\vec{a})\otimes\hat{\sigma}_R(\vec{b}) + \hat{\sigma}_R(\vec{b})\otimes\hat{\sigma}_L(\vec{a})\Big)|\psi\rangle, \tag{1.24}$$

which is symmetric under particle exchange. If the quantum state is a simple single Slater determinant, *e.g.*, $|\psi\rangle = \frac{(|\phi\uparrow,\chi\uparrow\rangle - |\chi\uparrow,\phi\uparrow\rangle)}{\sqrt{2}}$, its expectation value is reduced to,

$$E(\vec{a},\vec{b}) = \langle\phi\uparrow|\hat{\sigma}_L(\vec{a})|\phi\uparrow\rangle\,\langle\chi\uparrow|\hat{\sigma}_R(\vec{b})|\chi\uparrow\rangle, \tag{1.25}$$

since $\hat{\sigma}_L(\vec{a})\otimes\hat{\sigma}_R(\vec{b})|\chi\uparrow,\phi\uparrow\rangle = \hat{\sigma}_R(\vec{b})\otimes\hat{\sigma}_L(\vec{a})|\phi\uparrow,\chi\uparrow\rangle = 0$. The expectation value is equivalent to a spin measurement $\hat{\sigma}_L(\vec{a})\otimes\hat{\sigma}_R(\vec{b})$ on distinguishable particles A and B, described by the separable state $|\psi\rangle \sim |\phi\uparrow\rangle_A \otimes |\chi\uparrow\rangle_B$. Thus, such a single Slater determinant state cannot violate the CHSH inequality for any $\vec{a}$ and $\vec{b}$ direction. On the other hand, if the state is not just a single Slater determinant, *e.g.*,

$$|\psi\rangle = \frac{1}{\sqrt{2}}\Big(f^\dagger_{\phi\uparrow}f^\dagger_{\chi\uparrow} + f^\dagger_{\phi\downarrow}f^\dagger_{\chi\downarrow}\Big)|vac\rangle, \tag{1.26}$$

the expectation value is reduced to,

$$E(\vec{a},\vec{b}) = \langle\psi^-_{dist}|\hat{\sigma}_L(\vec{a})\otimes\hat{\sigma}_R(\vec{b})|\psi^-_{dist}\rangle, \tag{1.27}$$

where $|\psi^-_{dist}\rangle = \frac{1}{\sqrt{2}}(|\phi\uparrow\rangle_A|\chi\uparrow\rangle_B + |\phi\downarrow\rangle_A|\chi\downarrow\rangle_B)$ represents an entangled state with distinguishable particles A and B, which violates the CHSH inequality for specific measurement directions $\vec{a}$ and $\vec{b}$.

Generalized entanglement (GE)

In [18, 25, 26] the authors generalize the notion of partial trace when we restrict the total algebra of observables to a subset Ω, obtaining the reduced state corresponding to such restriction. As in the standard entanglement theory, if the quantum state is a pure state, a sufficient condition for it to be an unentangled state relates to the fact that its reduced state is pure (or an extremal state, as we will discuss later). Thus, a candidate of quantifier for the entanglement of a pure quantum state can be given by a function sensitive to the mixedeness (loss of purity) of the reduced state. In their work it is used the purity function, *i.e.*, $Purity(\rho) = Tr(\rho^2)$. In the case of a mixed quantum

state we can define an unentangled state as usual, *i.e.*, the states which can be described as a convex decomposition of pure unentangled states.

In the context of indistinguishable particles, the subset Ω of observables relative to "local observables" are simply the single particles observables (Eq.(1.14)), as discussed previously . Let $\{X_\alpha\}$ be an orthonormal basis of Ω, $Tr(X_\alpha X_\beta) = \delta_{\alpha\beta}$. Thus, for every density operator $\rho \in \mathcal{F}(M)_f$ or $\mathcal{F}(M)_b$, the reduced state $\hat{\mathcal{P}}_\Omega[\rho]$ corresponding to the Ω restriction of the total algebra of observables, is defined by,

$$\rho \longrightarrow \hat{\mathcal{P}}_\Omega[\rho] = \sum_\alpha Tr(\rho X_\alpha) X_\alpha \tag{1.28}$$

The partial trace mapping $\hat{\mathcal{P}}_\Omega[\rho]$ can be roughly seen as a projection over the subspace spanned by the algebra of observables Ω. A pure state $|\psi\rangle$ is defined as *generalized entangled (generalized unentangled)* relative to the restricted Ω algebra of observables, if it induces a reduced mixed (pure) state by the mapping $|\psi\rangle \mapsto \hat{\mathcal{P}}_\Omega[|\psi\rangle]$. Notice that a reduced state is pure, in a general sense, if it cannot be described as a convex decomposition of any other states, being also called an *extremal* state. We could have for example that $\hat{\mathcal{P}}_\Omega[|\psi\rangle] = K|\psi\rangle$, where K is a constant, but notice that $\hat{\mathcal{P}}_\Omega[|\psi\rangle]$ is as extremal as $|\psi\rangle$.

A possible measure for the entanglement of a pure quantum state can be given by the purity of its reduced state. Assuming X_α to be Hermitian, $X_\alpha = X_\alpha^\dagger$, it can be easily computed as,

$$\begin{aligned} Purity\big(\hat{\mathcal{P}}_\Omega[|\psi\rangle]\big) &= Tr\left[\sum_{\alpha,\beta} Tr(\rho X_\alpha) Tr(\rho X_\beta) X_\alpha X_\beta\right] \\ &= \sum_\alpha \langle X_\alpha\rangle^2 \end{aligned} \tag{1.29}$$

where $\langle X_\alpha\rangle = Tr(\rho X_\alpha)$ denotes the expectation value of the observable X_α in the pure state $|\psi\rangle$. An import property to be noticed in the above defined purity, is its invariance under group transformations; if a new basis $\widetilde{X}_\alpha$ is chosen, the purity remains unchanged, $\sum_\alpha \left\langle \widetilde{X}_\alpha \right\rangle^2 = \sum_\alpha \langle X_\alpha\rangle^2$. It is common to proper renormalize the purity measure for an Ω algebra by setting K such that $Purity\big(\hat{\mathcal{P}}_\Omega[|\psi\rangle]\big) = 1$ f or the generalized unentangled states.

As shown in [26], for the cases where Ω is a Lie algebra, the generalized unentangled states relative to Ω satisfy the following equivalent statements:
(i) $|\psi\rangle$ is generalized unentangled relative to Ω;
(ii) $\hat{\mathcal{P}}_\Omega[|\psi\rangle]$ has maximum purity;
(iii) $\hat{\mathcal{P}}_\Omega[|\psi\rangle]$ is an extremal state;
(iv) $|\psi\rangle$ is the unique ground state of some Hamiltonian H in Ω;

In the case of fermions, a basis for the Ω algebra can be given by $\{f_j^\dagger f_\ell;\ 1 \leq j, \ell \leq M\}$, where M is the number of modes of the system. The interesting feature of this basis is that it satisfies the following commutation relation,

$$\left[f_i^\dagger f_j, f_k^\dagger f_\ell\right] = \delta_{kj} f_i^\dagger f_\ell - \delta_{i\ell} f_k^\dagger f_j, \tag{1.30}$$

providing a realization of the unitary Lie algebra $u(M)$ in the Fock space $\mathcal{F}(M)_f$. Thus, the fermionic unentangled states relative to Ω are single-Slater determinant states with fixed particle number, since they constitute the ground states of number conserving quadratic Hamiltonians. As shown in [18], their purity can be analytically computed and is given by $Purity(\hat{\mathcal{P}}_\Omega[|\psi\rangle]) = M/2$. Any state which cannot be described by a single Slater determinant with a fixed particle number has a lower purity, *e.g.*, any state with coherence superposition between different particle number sectors.

GNS construction

In [11], the authors deal with the partial trace mapping, or subsystems representation, for general systems (*e.g.*, systems of indistinguishable particles), by a different approach, more precisely, using the *GNS construction*, which allows us to obtain the reduced states respective to a restricted algebra of observables. The GNS construction, formulated in 1940s by Gel'fand, Naimark and Segal, allows one to reconstruct the Hilbert space from an "abstract algebra of observables" $\mathcal{A}$, and a linear functional w representing the quantum state. More precisely, a linear functional w acting on abstract observables $a \in \mathcal{A}$ can be generically represented, by the GNS construction, in terms of a density matrix ρ_w and operators $\hat{\pi}_w(a)$ in a induced Hilbert space $\mathcal{H}_w$:

$$\begin{array}{ccc} \left\{ \begin{array}{l} a \in \mathcal{A} \\ w \end{array} \right. & \xleftrightarrow{\text{GNS}} & \left\{ \begin{array}{l} \hat{\pi}_w(a) \\ \rho_w \end{array} \right. \in \mathcal{H}_w \\ \text{abstract algebra of observables and states} & & \text{Hermitian observables and density matrix in a Hilbert space} \end{array} \tag{1.31}$$

This formulation is very useful when dealing with subsystems representation and entanglement. In this approach all that is needed in order to describe a subsystem is the specification of its subalgebra of observables $\mathcal{A}_o \subset \mathcal{A}$. Given such a specification one readily obtain the reduced functional w_o for such a subalgebra, and then performing the GNS construction, $(w_o, \mathcal{A}_o) \longleftrightarrow (\rho_{w_o}, \hat{\pi}_{w_o}) \in \mathcal{H}_{w_o}$, one gets the *reduced* state ρ_{w_o} describing the subsystem. In this way, the restriction of the original state to the subalgebra provides a physically motivated generalization for the concept of partial trace. The characterization of entanglement follows analogously as in the GE approach where, *e.g.*, given an initially pure quantum state, its entanglement can be computed by analysing the mixedeness (loss of purity) of its reduced state.

In [11] the authors show how to use such approach for several distinct systems, as for example, in systems of indistinguishable particles. In the case of two fermions, each one with dimension $d = 3, 4$, it is obtained that single Slater determinant states, with a fixed particle number, have no entanglement when the restricted subalgebra corresponf to single-particle observables (Eq.(1.14)). The same is obtained for two bosons, with dimension $d = 3$. The results thus agree with our intuitive expectation, as discussed previously.

CHAPTER 2

Computable measures for the entanglement of indistinguishable particles

In this chapter we discuss particle entanglement in systems of indistinguishable bosons and fermions, in finite Hilbert spaces, with focus on operational measures for its quantification. We essentially show how to adapt the common tools used in the usual entanglement theory of distinguishable systems. It is very interesting to use such adapted measures, since we recover all of its well known properties. For example, by using an adapted entropy of entanglement, we know it is not increasing under single-particle operations. More precisely, we show how to use Negativity, entanglement witnesses, and any measure sensitive to mixedeness (loss of purity) of the single-particle reduced state, in order to quantify the entanglement of particles in system of indistinguishable particles. We prove interesting relations between all the presented measures. We also obtain analytic expressions to quantify the entanglement of particles for the eigenstates of homogeneous D-dimensional Hamiltonians with certain symmetries.

This chapter is organized as follows. In Sec.2.1 we show how the purity of the single-particle reduced state can be used as a measure for pure states, analysisng the fermionic and bosonic case separately, seem they have non trivial differences. In Sec.2.2 we analyse the Negativity as a measure. In Sec.2.4 we discuss entanglement witnesses measures, and its duality with Robustness of entanglement measures; we show how to compute such measures based on semi-definite programs (SDPs), which can be solved efficiently with arbitrary accuracy. In Sec.2.5 we make some remarks about the different measures for the entanglement of particles, and discuss how they compare for pure states with single-particle Hilbert space with the smallest non trivial dimension, proving some interesting relations. In Sec.2.6 we show how to use the tools

presented in the previous sections in the context of entanglement in many-body systems, computing analytically the entanglement for the eigenstates of certain symmetric Hamiltonians. We conclude in Sec.2.7.

2.1 Single-particle reduced density matrix

In this section we show how the single-particle reduced state can provide information about the entanglement of pure states. We show how any measure based on the mixedeness of the reduced state, *e.g.* the von Neumann entropy, can be used in order to quantify the entanglement.

2.1.1 Fermions

As previously discussed, fermionic pure states with no entanglement are described by single Slater determinants with fixed particle number. The single-particle reduced states ($\sigma_{r_{(Sl_1)}}$) of a single Slater determinant have a particularly interesting form, and stand for the pure states in the "N-representable" reduced space (single-particle reduced space respective to the antisymmetric space of N fermions) [36]. Recall that pure states are those states which can not be described as a convex decomposition of any other state; in this way they are the *extremal* states of such space.

Single-particle reduced fermionic state without particle entanglement: Given a pure fermionic state with no particle entanglement, i.e., a single Slater determinant with a fixed particle number, $|\psi\rangle = f^\dagger_{\phi_1} f^\dagger_{\phi_2} ... f^\dagger_{\phi_N} |vac\rangle$, where $\{f^\dagger_{\phi_i}\}_{i=1}^d$ are orthonormal modes, we have the equivalence:

$$\sigma_{r_{(Sl_1)}} \equiv \frac{1}{N} \sum_{i=1}^{N} f^\dagger_{\phi_i} |0\rangle\langle 0| f_{\phi_i} \iff |\psi\rangle = f^\dagger_{\phi_1} f^\dagger_{\phi_2} ... f^\dagger_{\phi_N} |vac\rangle, \tag{2.1}$$

where $\sigma_{r_{(Sl_1)}} = Tr_1 ... Tr_{N-1}(|\psi\rangle\langle\psi|)$ is the single-particle reduced state (Tr_i is the partial trace over particle i). The interesting feature that should be noticed follows from the fact that $\sigma_{r_{(Sl_1)}}$ stands as a pure state (extremal state) in the reduced space $\mathcal{H}^d$, see Fig.2.1 for a schematic view. Aware of it, it is straightforward to conclude that shifted positive semidefinite functions of the purity for the single-particle reduced state can be used to measure the entanglement of particles of a pure fermionic state; a result similar to that obtained by Paskauskas and You [29] or Plastino *et al.* [30]. Using, for example, the von Neumann entropy ($S(\rho) = Tr(-\rho \ln \rho)$), we see that,

$$S[\rho_r = Tr_1 ... Tr_{N-1}(|\psi\rangle\langle\psi|)] \geq S(\sigma_{r_{(Sl_1)}}) = \ln N, \tag{2.2}$$

and thus a measure E for the entanglement of particles of a pure fermionic state can be defined as a shifted von Neumann entropy of the single-particle reduced state.

Shifted von Neumann entropy of entanglement for pure states:

$$E(|\psi\rangle\langle\psi|) = S(\rho_r) - \ln N. \tag{2.3}$$

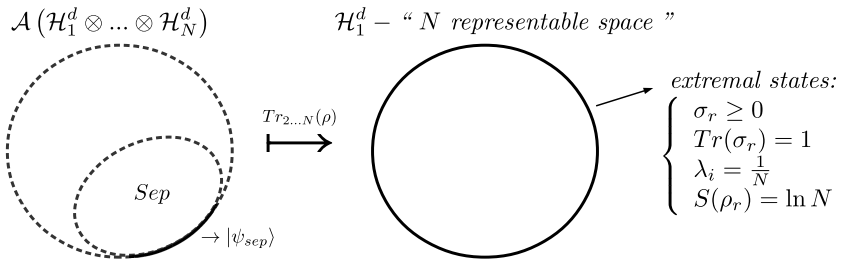

Figure 2.1: Schematic view for the partial trace mapping of fermionic states. The antisymmetric space of states, a convex set of states, is represented by the left dashed and larger curve. Its convex subset of unentangled states "*Sep*" is represented by its inner dashed curve. The pure (extremal) states are localized at the border of the space. The partial trace over the pure unentangled states leads to pure (extremal) states in the single particle reduced space, called N representable space.

The case of pure states is easy due to the unique form of their respective single-particle reduced states, which is no longer the case for mixed states. If σ is a mixed unentangled state, *i.e.*, can be described by a convex decomposition of unentangled pure states, its single-particle reduced state in the N-representable reduced space is:

$$\sigma_r \equiv Tr_1...Tr_{N-1}(\sigma) = \sum_i p_i \sigma^i_{r_{(Sl_1)}}, \tag{2.4}$$

which is not necessarily an extremal state anymore.

It is easy to check that, as expected, the particle entanglement measure as here defined is non-increasing under single-particle symmetric operations ("local symmetric operations") [27], which follows from the entropy of entanglement properties.

2.1.2 Bosons

For systems of indistinguishable bosonic particles, despite the physically motivated notion of entanglement, characterizing the set of unentangled states, presented in the last chapter, there are in the literature some different definitions and some debates about the proper definition and correponding set of unentangled states for bosonic particles. For example, in [37] Eckert *et al.* base their analysis in the characterization of what they call *useful correlations* in systems of indistinguishable particles, defining a concurrence measure in order to quantify the entanglement. It is obtained that the set of unentangled bosonic states is actually smaller than the one we presented in this work; it is generated by single Slater permanent states, but only those states where all of their bosons occupy the same mode.

We will analyse in this section, for completeness, both cases, corresponding specifically to the two distinct sets of unentangled states:

Bosonic pure state with no particle entanglement: A bosonic pure state $|\psi\rangle \in \mathcal{S}(\mathcal{H}_1^d \otimes \cdots \otimes \mathcal{H}_N^d)$ without particle entanglement can be written as:

$$\text{Definition 1.} \qquad |\psi\rangle = \prod_{i=1}^{N_o} \frac{(b_{\phi_i}^\dagger)^{n_{\phi_i}}|vac\rangle}{\sqrt{(n_{\phi_i}!)}}, \tag{2.5}$$

$$\text{Definition 2.} \qquad |\psi\rangle = \frac{1}{\sqrt{N!}}(b_\phi^\dagger)^N|vac\rangle, \tag{2.6}$$

where $b_{\phi_i}^\dagger = \sum_{k=1}^d u_{ik}\, b_k^\dagger$ ($\{b_{\phi_i}^\dagger\}$ is a set of orthonormal operators in the index i, U is a unitary matrix of dimension dN_o, N_o is the number of distinct occupied states, and n_{ϕ_i} is the number of bosons in the state ϕ_i. Unentangled mixed states are those that can be written as convex combinations of unentangled pure states. We clearly see that the set of states without particle entanglement according to Definition 1 includes the set derived from Definition 2, since the later is a particular case of the former, with $N_o = 1$.

In one hand, definition 2 mirrors the case of distinguishable particles. Therefore one can use the entropy of the one-particle reduced state $S(\rho_r)$ to quantify the entanglement. On the other hand, the problem is delicate for definition 1, since the equivalence between pure states without particle entanglement and the single-particle reduced states is no longer uniquely defined by the analogous of Eq.(2.1). The entropy of the one-particle reduced state gives information about the particle entanglement, but as a quantifier it must be better understood. We know that a unentangled bosonic pure state, according to Eq.(2.5), has the following one-particle reduced state:

$$\begin{aligned} \sigma_r(\phi_i,\phi_j) &= \frac{1}{N} Tr(b_{\phi_j}^\dagger b_{\phi_i}|\psi\rangle\langle\psi|) = \begin{cases} \frac{1}{N} n_{\phi_i}, & \text{if } \phi_i = \phi_j \\ 0, & \text{otherwise,} \end{cases} \\ \sigma_r &= \frac{1}{N}\sum_{i=1}^{N_o} n_{\phi_i} b_{\phi_i}^\dagger |vac\rangle\langle vac| b_{\phi_i}. \end{aligned} \tag{2.7}$$

where $\sigma_r(\phi_i,\phi_j)$ is a matrix element of σ_r. The entropy of the one-particle reduced state assumes the special values (see Fig.2.2 for a schematic view):

$$S(\sigma_r) = -\sum_{i=1}^{N_o} (\frac{n_{\phi_i}}{N}) \ln(\frac{n_{\phi_i}}{N}). \tag{2.8}$$

Note that $0 \leq S(\sigma_r) \leq \ln N$, and therefore when $S(\rho_r) > \ln N$, the pure state ρ is *entangled*. The pure state is also *entangled* if $S(\rho_r)$ is not one of the values given by Eq.(2.8). Take for example the case of two bosons: we have either $N_o = 1, n_{\phi_i} = 2$ and thus $S(\sigma_r) = 0$, or $N_o = 2, n_{\phi_i} = 1$ and $S(\sigma_r) = \ln 2$. Given an arbitrary pure state ρ of two bosons, if $S(\rho_r) = 0$ we can say with certainty that the state has no particle entanglement, but if $S(\rho_r) = \ln 2$ we cannot conclude anything, for either a state with no particle entanglement, e.g. $|\psi\rangle = b_{\phi_i}^\dagger b_{\phi_j}^\dagger |vac\rangle$, or an entangled one, e.g. $|\psi\rangle = \frac{1}{\sqrt{3}}(c_i b_{\phi_i}^\dagger b_{\phi_i}^\dagger + c_j b_{\phi_j}^\dagger b_{\phi_j}^\dagger + c_k b_{\phi_k}^\dagger b_{\phi_k}^\dagger)|vac\rangle$, with $c_{i,j,k} \in \mathcal{R}$, and $S(\rho_r) \subset (0, \ln 3]$, could have the same von Neumann entropy for the one-particle reduced state.

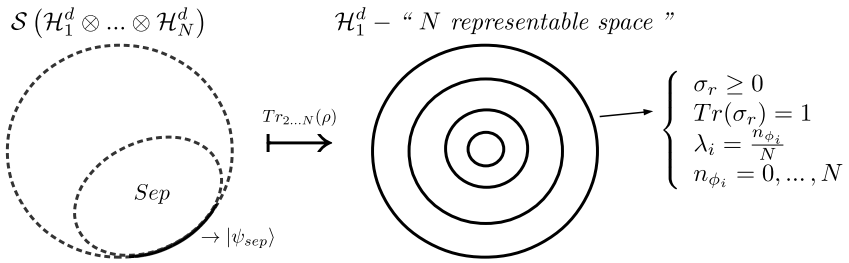

Figure 2.2: Schematic view for the partial trace mapping of bosonic states. The bosonic space of states, a convex set of states, is represented by the left dashed and larger curve. Its convex subset of unentangled states "*Sep*", as defined in Eq.(2.5), is represented by its inner dashed curve. The pure (extremal) states are localized at the border of the space. The partial trace over the pure unentangled states does not leads only to pure (extremal) states in the single particle reduced space, but also to mixed states with specific von Neumann entropies.

2.2 Negativity

In this section we show how the usual Negativity measure can be used also in system of indistinguishable particles, in order to quantify its entanglement.

2.2.1 Fermions

As aforementioned in the previous section, the case of pure states is easy due to the unique form of the unentangled single-particle reduced states, which is no longer the case for mixed states. Though not obvious, but straightforward to prove as we show at the end of this section, we can measure the entanglement of particles of mixed fermionic states by the following shifted Negativity.

Shifted Negativity:

$$Neg(\rho) = \begin{cases} \left\|\rho^{T_i}\right\|_1 - N & \text{if } \left\|\rho^{T_i}\right\|_1 > N, \\ 0 & \text{otherwise,} \end{cases} \tag{2.9}$$

where T_i is the partial transpose over the i-th particle, and $\|.\|_1$ is the trace-norm. If ρ is a single Slater determinant, its trace-norm is N, and it is smaller in the case of a unentangled mixed state. Note, however, that we do not know if there are entangled fermionic states whose Negativity is null, similarly to the case of distinguishable subsystems, where we may have the known PPT entangled states.

2.2.2 Bosons

In one hand, definition 2 of unentangled bosonic states mirrors the case of distinguishable particles. Therefore one can use the usual Negativity $\left\|\rho^{T_i}\right\|_1 - 1$ to quantify the entanglement. On the other hand, the problem is

delicate for definition 1, since the equivalence between pure states without particle entanglement and the single-particle reduced states is no longer uniquely defined by the analogous of Eq.(2.1). The shifted Negativity given by Eq.(2.9) is still valid, but now we do know that there are entangled states with $\left\|\rho^{T_i}\right\|_1 < N$.

2.2.3 Proof

In this section we calculate the trace-norm of the partial transpose of a unentangled fermionic/bosonic state, *i.e.*, $\left\|\sigma^{T_i}\right\|_1 = Tr[(\sigma^{T_i}, \sigma^{T_i^\dagger})^{\frac{1}{2}}]$, thus proving the *shifted negativity* (Eq.(2.9)). We do so by the explicit diagonalization of the operator $(\sigma^{T_i}\sigma^{T_i^\dagger})$. Consider first the case of a fermionic/bosonic pure state $\sigma = |\psi\rangle\langle\psi|$, as given by Eq.(1.15)/(2.5) which can be rewritten as:

$$\sigma = C \sum_{\pi\pi'} \epsilon_\pi \epsilon_{\pi'} P_\pi |\phi_1\phi_2...\phi_N\rangle\langle\phi_N...\phi_2\phi_1| P_{\pi'}, \tag{2.10}$$

with $|\psi\rangle = \sqrt{C}\sum_\pi \epsilon_\pi P_\pi |\phi_1\phi_2...\phi_N\rangle$, where ϕ_i, ϕ_j are either equal or orthonormal, P_π are the permutation operators, ϵ_π is the permutation parity ($\epsilon = \pm 1$ for fermions, $\epsilon = 1$ for bosons), and $C = (N!)^{-1}$ for fermions or $C = [N!\prod_{i=1}^{N_o}(n_{\phi_i}!)]^{-1}$ for bosons. From now on we omit the normalization C and introduce the following notation:

$$P_\pi|\phi_1...\phi_N\rangle = |\pi(\phi_1...\phi_N)\rangle = |\pi(\phi_1)\pi(\phi_2)...\pi(\phi_N)\rangle. \tag{2.11}$$

Now we perform the partial transpose on the first particle explicitly:

$$\sigma^{T_1} = \sum_{\pi\pi'} \epsilon_\pi \epsilon_{\pi'} \left|\pi'(\phi_1)\pi(\phi_2...\phi_N)\right\rangle\left\langle\pi'(\phi_N...\phi_2)\pi(\phi_1)\right|; \tag{2.12}$$

$$(\sigma^{T_1})^\dagger = \sigma^{T_1}; \tag{2.13}$$

$$\begin{aligned}\sigma^{T_1}\sigma^{T_1} \quad = \quad & \sum_{\pi,\pi',\tilde\pi,\tilde\pi'} \epsilon_\pi\epsilon_{\pi'}\epsilon_{\tilde\pi}\epsilon_{\tilde\pi'} \left|\pi'(\phi_1)\pi(\phi_2...\phi_N)\right\rangle \\ & \left\langle\pi'(\phi_N...\phi_2)\pi(\phi_1)\right|\left\langle\tilde\pi'(\phi_1)\tilde\pi(\phi_2...\phi_N)\right\rangle\left\langle\tilde\pi'(\phi_N...\phi_2)\tilde\pi(\phi_1)\right|\end{aligned} \tag{2.14}$$

$$\begin{aligned}\sigma^{T_1}\sigma^{T_1} \quad = \quad & \sum_{\pi',\tilde\pi} \epsilon_{\pi'}\epsilon_{\tilde\pi}\left\langle\pi'(\phi_N...\phi_2)\right|\left.\tilde\pi(\phi_2...\phi_N)\right\rangle\left|\pi'(\phi_1)\right\rangle\langle\tilde\pi(\phi_1)| \otimes \\ & \sum_{\pi,\tilde\pi'} \epsilon_\pi\epsilon_{\tilde\pi'}\left\langle\pi(\phi_1)\right|\left.\tilde\pi'(\phi_1)\right\rangle|\pi(\phi_2...\phi_N)\rangle\left\langle\tilde\pi'(\phi_N...\phi_2)\right|.\end{aligned} \tag{2.15}$$

We analyze only the bosonic case, and the fermions follow by setting $N_o = N$ and $n_{\phi_i} = 1$. Consider the first line of Eq.2.15. As states ϕ_i are not necessarily orthogonal, and may be the same, we have contributions when the permutations $\pi', \tilde\pi$ are equal and in some cases even when they are different. It can be seen that there are $n_k[(N-1)!]$ permutations such that $\pi'(\phi_1) = \phi_k$, and for each of these there are $\prod_{i=1}^{N_o}(n_{\phi_i}!)$ permutations $\tilde\pi$ such that $\tilde\pi(\phi_1) = \phi_k$, resulting in non null contributions $\langle\pi'(\phi_N...\phi_2)|\tilde\pi(\phi_2...\phi_N)\rangle \neq 0$. If $\tilde\pi(\phi_1) \neq \phi_k$ then the contribution is null $\langle\pi'(\phi_N...\phi_2)|\tilde\pi(\phi_2...\phi_N)\rangle = 0$

(simply note that the set $\{\tilde{\pi}(\phi_2...\phi_N)\}$ always has n_k states "ϕ_k", whereas $\{\pi'(\phi_N...\phi_2)\}$ has only $n_k - 1$). The first line of Eq.2.15 thus reduces to:

$$\sum_{k=1}^{N_o} n_k[(N-1)!]\,[\prod_{i=1}^{N_o}(n_{\phi_i}!)]\,|\phi_k\rangle\langle\phi_k|. \tag{2.16}$$

Now we analyze the second line of Eq.2.15. This term has non null contributions only if $\pi(\phi_1) = \tilde{\pi}'(\phi_1)$. For permutations of the type $\pi(\phi_1) = \tilde{\pi}'(\phi_1) = \phi_k$, the matrix $|\pi(\phi_2...\phi_N)\rangle\langle\tilde{\pi}'(\phi_N...\phi_2)|$ can assume $\frac{(N-1)!}{(n_k-1)!\prod_{i=1,(i\neq k)}^{N_o}(n_{\phi_i}!)} = \frac{n_{\phi_k}(N-1)!}{\prod_{i=1}^{N_o}(n_{\phi_i}!)}$ distinct combinations from the elements of the set $\{\pi(\phi_2...\phi_N)\}$. Note that there are $\prod_{i=1}^{N_o}(n_{\phi_i}!)$ permutations of type $\pi(\phi_1) = \phi_k$ generating the same "ket" $|\pi(\phi_2...\phi_N)\rangle$ (or "bra" $\langle\tilde{\pi}'(\phi_N...\phi_2)|$). Thus we have,

$$\sum_{\pi,\tilde{\pi}'}\epsilon_\pi\epsilon_{\tilde{\pi}'}\langle\pi(\phi_1)|\tilde{\pi}'(\phi_1)\rangle\,|\pi(\phi_2...\phi_N)\rangle\langle\tilde{\pi}'(\phi_N...\phi_2)| = [\prod_{i=1}^{N_o}(n_{\phi_i}!)]^2\,|\psi_k\rangle\langle\psi_k|, \tag{2.17}$$

where $|\psi_k\rangle = \sum_i|\pi_k^i(\phi_2...\phi_N)\rangle$, being $\pi_k^i(\phi_2...\phi_N)$ all the possible permutations such that $\pi_k^i(\phi_1) = \phi_k$, and $\left\langle\pi_k^i(\phi_2...\phi_N)\middle|\pi_k^j(\phi_2...\phi_N)\right\rangle = \delta_{ij}$. We have then $\langle\psi_k|\psi_{k'}\rangle = \frac{n_{\phi_k}(N-1)!}{\prod_{i=1}^{N_o}(n_{\phi_i}!)}\delta_{kk'}$, and finally the second line of Eq.2.15 is reduced to:

$$\sum_{k=1}^{N_o}[\prod_{i=1}^{N_o}(n_{\phi_i}!)]^2\,|\psi_k\rangle\langle\psi_k| \quad = \quad [\prod_{i=1}^{N_o}(n_{\phi_i}!)]\,(N-1)!\sum_{k=1}^{N_o} n_{\phi_k}\frac{|\psi_k\rangle\langle\psi_k|}{\langle\psi_k|\psi_k\rangle}. \tag{2.18}$$

From Eq.(2.16) and Eq.(2.18) and remembering to reintroduce the normalization constant C, we obtain:

$$\left\||\psi\rangle\langle\psi|^{T_A}\right\|_1 = \frac{(\sum_{k=1}^{N_o}\sqrt{n_{\phi_k}})^2}{N} \leq N. \tag{2.19}$$

The last step follows by noting that $\sum_{k=1}^{N_o} n_k = N$, and thus $\sum_{k=1}^{N_o}\sqrt{n_k} \leq N$. As the trace-norm is a convex function, we can write for uncorrelated mixed states: $\left\|\sum_j p_j\sigma_j^{T_i}\right\|_1 \leq \sum_j p_j\left\|\sigma_j^{T_i}\right\|_1$, and we are done.

2.3 Concurrence

A measure of fermionic and bosonic entanglement was proposed in [37] as the analogous of Wootters concurrence [38]. Such measure, called Slater concurrence (C_S), is valid only for two-fermion states with a four-dimensional single-particle Hilbert space $\mathcal{A}(\mathcal{H}^4 \otimes \mathcal{H}^4)$, or two-boson states with a two-dimensional single-particle Hilbert space $\mathcal{S}(\mathcal{H}^2 \otimes \mathcal{H}^2)$, i.e. the antisymmetric and symmetric spaces of lowest dimension which can have entangled states.

The Wooters concurrence for two distinguishable qubits ($\mathcal{H}_1^2 \otimes \mathcal{H}_2^2$), is given as follows. First we define the temporal inversion operator $\mathcal{D}$, also

called spin flip transformation when we consider the qubits as spin degrees of freedom,

$$\mathcal{D} = (\sigma_y \otimes \sigma_y)\mathcal{K}, \tag{2.20}$$

where σ_y is the Pauli matrix, and $\mathcal{K}$ is the anti-linear operator of complex conjugation, which acts in an arbitrary state as $\mathcal{K}\sum_{i,j} c_{i,j}|ij\rangle = \sum_{i,j} c^*_{i,j}|ij\rangle$. In this way, given the dual state $\widetilde{\rho} = \mathcal{D}\rho\mathcal{D}^{-1}$, the Wooters concurrence for states $\rho \in (\mathcal{H}^2 \otimes \mathcal{H}^2)$ is given by,

$$C_W(\rho) = max(0, \lambda_4 - \lambda_3 - \lambda_2 - \lambda_1), \tag{2.21}$$

where $\lambda_i's$ are, in descending order of magnitude, the square roots of the singular values of the matrix $R = \rho\widetilde{\rho}$.

The concurrence for fermions and bosons follows a similar reasoning. In order to define the Slater concurrence for fermions, it is introduced some operators. Let $\mathcal{U}_{ph}$ be the operator of particle-hole transformation:

$$\mathcal{U}_{ph} f_i^\dagger \mathcal{U}_{ph}^\dagger = f_i, \qquad \mathcal{U}_{ph}|0\rangle = \prod_{i=1}^{d} f_i^\dagger |0\rangle, \tag{2.22}$$

where d is the single-particle Hilbert space dimension. Similarly, define $\mathcal{K}$ as the anti-linear operator of complex-conjugation, satisfying the following relations:

$$\mathcal{K} f_i^\dagger \mathcal{K} = f_i^\dagger, \qquad \mathcal{K} f_i \mathcal{K} = f_i, \qquad \mathcal{K}|0\rangle = |0\rangle. \tag{2.23}$$

Thus, given the operator $\mathcal{D} = \mathcal{K}\mathcal{U}_{ph}$, and the dual states $\widetilde{\rho} = \mathcal{D}\rho\mathcal{D}^{-1}$, we have that the Slater concurrence for states $\rho \in \mathcal{A}(\mathcal{H}^4 \otimes \mathcal{H}^4)$ is given by

$$C_S(\rho) = max(0, \lambda_6 - \lambda_5 - \lambda_4 - \lambda_3 - \lambda_2 - \lambda_1), \tag{2.24}$$

where $\lambda_i's$ are, in descending order of magnitude, the square roots of the singular values of the matrix $R = \rho\widetilde{\rho}$.

Analogously, we can define the concurrence for the bosonic case, where the dualization operator is now defined as $\mathcal{D} = \mathcal{R}\mathcal{K}$, and the operator $\mathcal{R}$ acts as

$$\mathcal{R} b_i^\dagger \mathcal{R}^\dagger = \sum_{j=1}^{2} \sigma_{ji}^y b_j^\dagger. \tag{2.25}$$

Thus, given the dual state $\widetilde{\rho} = \mathcal{D}\rho\mathcal{D}^{-1}$, the Slater concurrence for bosonic states $\rho \in \mathcal{S}(\mathcal{H}^2 \otimes \mathcal{H}^2)$ is given by

$$C_{\mathcal{B}}(\rho) = max(0, \lambda_4 - \lambda_3 - \lambda_2 - \lambda_1), \tag{2.26}$$

where $\lambda_i's$ are, in descending order of magnitude, the square roots of the singular values of the matrix $R = \rho\widetilde{\rho}$. It is important to recall that the bosonic Slater concurrence follows Eq.(2.6) as the set of unentangled states.

2.4 Entanglement witnesses and robustness

In this section we show how to use entanglement witnesses as a necessary and sufficient criterion for the entanglement of a quantum state. We also present the equivalence between the optimal entanglement witnesses with physically motivated entanglement quantifiers, as the known Robustness of entanglement. By duality Lagrangean from theory of convex optimization we show their equivalence. We then show how to compute such measures with good accuracy based on semi-definite programs (SDPs).

2.4.1 Entanglement witnesses

Entanglement witnesses are hermitian operators (observables) whose expectation values contain information about the entanglement of a quantum state, being in this way a great tool for the study of entanglement in quantum systems. Central to a formal definition of such operators is the important Hahn-Banach theorem, or its simplified version also called as *Hahn-Banach theorem of separation*:

Definição 2.1. ***Hahn-Banach theorem of separation.*** *Let $\mathcal{S}$ be a compact and convex set, in a Banach* [1] *space of finite dimension, and ρ a point which does not belong to this set. Thus we can always find an hyperplane W which separates ρ from $\mathcal{S}$.*

A schematic illustration of the theorem is given in Fig.2.3. If we identify the set $\mathcal{S}$ as the set of unentangled (separable) states, we see that is always possible to determine if a state is or not entangled by looking for such an hyperplane of separation. That is why such hyperplanes are also called as entanglement witnesses. We can also see the theorem by the perpective of "distances", or better, expectation values $Tr(W\rho)$, leading to the following definition of witnesses operators:

Definição 2.2. *An operator W is a entanglement witness for a given state entangled (separable) state ρ if $Tr(W\sigma) \geq 0$ for all separable states σ, and $Tr(W\rho) < 0$ ($Tr(W\rho) > 0$).*

When we work with entanglement witnesses, several times we are more interested in just a specific subset of such operators, the called optimal entanglement witnesses, OEW. There are, however, two different definitions of OEW. The first one, introduced by Lewenstein [39], is based on the quantity of of states detected by the witness, *i.e.*, the witness W is optimal if the set $\{\rho\}$ of entangled states detected is maximized. The second definition, which is the one we will use in this work, refers to a particular quantum state: *W_{opt} is the optimal witness to the quantum state ρ if,*

$$Tr(W_{opt}\rho) = \min_{W \in \mathcal{M}} Tr(W\rho), \tag{2.27}$$

where $\mathcal{M}$ represents a compact subset of the entire set of entanglement witnesses $\mathcal{W}$.

[1] Hilbert space of limited operators.

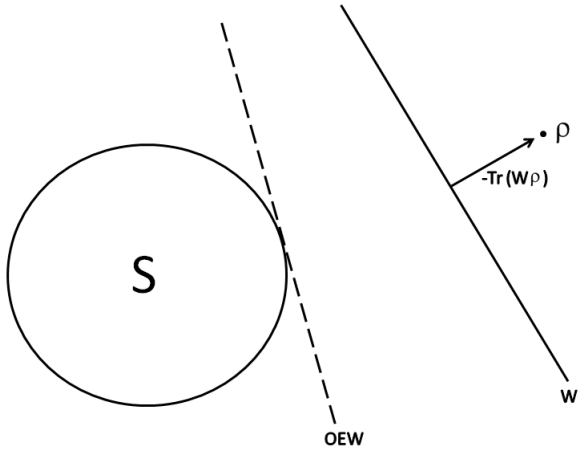

Figure 2.3: Schematic illustration of the Hahn-Banach theorem of separation, showing the convex set S, a point ρ outside of this set, and two possible hyperplanes W and OEW which separates the set from the point. OEW is the optimal entanglement witness, according to the definition in Eq.(2.27).

Actually, the choice of the set $\mathcal{M}$ can determine different measures of entanglement [40], showing that the OEW can be used as a tool not only as a sufficient criterion of separability, but also as a quantifier for the entanglement. A proper definition for these quantifiers can be given as:

$$E(\rho) = max(0, -\min_{W \in \mathcal{M}} Tr(W\rho)) \tag{2.28}$$

We will analyse in this work some specific cases for such a OEW quantifier, linking with the Robustness of entanglement measures.

2.4.2 Robustness of entanglement

The Robustness of entanglement measure is based on the idea of resistence of the state entanglement against pre-determined, or arbitrary, mixtures. More precisely, given an entangled state ρ, its robustness is the minimum necessary of a mixture with another state, such that the entanglement is suppressed. Formally, a definition may be given as follows:

Definition 2.3. *Given a quantum state $\rho \in \mathcal{H}_{\mathcal{T}}$, and $\phi_M \in \mathcal{X} \subset \mathcal{H}_{\mathcal{T}}$, the robustness $\mathcal{R}(\rho)$ is defined as the minimum amount "s" necessary to the mixture $\rho_M = \frac{1}{1+s}(\rho + s\phi_M)$ be a separable state, i.e.,*

$$\mathcal{R}(\rho) = \min_{\phi_M \in \mathcal{X}} \left(\min_{s \geq 0} s \ : \ \rho_M = \frac{1}{1+s}(\rho + s\phi_M) \in Sep \right) \tag{2.29}$$

Notice that the minimization must be realized over both variables "s" and ϕ_M, and it is computationally a quite hard task to be computed.

There were proposed different types of robustness in the litarature, each one based on a different motivation and leading to different specific space of mixtures $\mathcal{X}$. We will present three main types: the random robustness, generalized robustness, and the robustness of entanglement [41, 42].

·**Robustness of entanglement:** $\mathcal{R}(\rho) : \mathcal{X} \in \mathcal{S}$**.**

In this definition the interference mixed state are arbitrary separable states, which can in this way be prepared locally. Such a measure can be interpreted as the quantification of a "smart" interference at the quantum state by the local observers [41]. The term "smart" comes from the fact that, given that the local parts know the quantum state, they can shape at their best an interference in their local subsystems in order to suppress the entanglement of the state.

·**Random robustness,** $\mathcal{R}_a(\rho) : \mathcal{X} \equiv I$**.**

This definition follows as a particular case of the previous mentioned Robustness of entanglement, where the interference now corresponds to the white noise.

·**Generalized robustness,** $\mathcal{R}_g(\rho) : \mathcal{X} \in \mathcal{H}_\mathcal{T}$**.**

In the previous definitions the mixture was restricted to separable states. We could however consider the possibility of the quantum state interfering with an entangled state, as usual in many body dynamics. It is known that even mixtures of entangled states, can result in separable states. The Generalized robustness in this way encloses all the possible mixtures (interference).

There are some interesting properties between the robustness that might be presented, such as:

· clearly, the there is the following hierarchy between the measures:

$$\mathcal{R}_g(\rho) \leq \mathcal{R}(\rho) \leq \mathcal{R}_a(\rho) \tag{2.30}$$

· as shown by Steiner [42], the Generalized robustness and the Robustness of entanglement have the same value for pure states:

$$\mathcal{R}_g(\rho) = \mathcal{R}(\rho), \quad \text{if } \rho = |\psi\rangle\langle\psi|. \tag{2.31}$$

This is a very surprising result, since the volume of the space of states for high dimensions becomes dominated by entangled states, and the probability to find a separable state decays exponentially with the Hilbert space dimension; thus it would be expected that the Generalized robustness possessed smaller values than the Robustness of entanglement.

· The optimal mixed state ϕ_M for the Generalized robustness of pure states is not unique; in fact there are infinitely many possible optimal mixtures.

2.4.3 Duality: OEW $\sim$ Robustness

In this section we show how to relate OEW measures (Eq.(2.28)) with the Robustness measures (Eq.(2.29)) previously presented, using concepts of

Lagrangean duality from theory of convex optimization [2]. We will present the detailed calculations for the case of Generalized robustness, since the other cases follow in a similar way.

The Generalized robustness can be computed by OEW if we restrict the subset of witnesses to $\mathcal{M} = \{W \in \mathcal{W} \,|\, W \leq I\}$ in Eq.(2.28). Let us see how it works. In Lagrangean duality a minimization task can be seen under two distinct aspects, called primal and dual problem. In our case, we use as the primal problem the approach under entanglement witnesses, given by the following minimization task,

$$\begin{aligned} \text{minimize} \quad & Tr(W\rho) \\ \text{under the constraints} \quad & W \leq I \\ & Tr(W\sigma) \geq 0\,, \forall \sigma \in Sep \end{aligned} \tag{2.32}$$

The Lagrangean of this problem is given by,

$$\mathcal{L}(W, X, h(\sigma)) = Tr(W\rho) + Tr[X(W - I)] - \int\limits_{\sigma \in Sep} h(\sigma) Tr(W\sigma) d\sigma \tag{2.33}$$

From the Lagrangean, we can obtain the dual function $g(X, h(\sigma))$, given by infimum over the domain $W \in \mathcal{M}$. We see that,

$$\begin{aligned} g(X, h(\sigma)) &= \inf_{W \in \mathcal{M}} \mathcal{L}(W, X, h(\sigma)) \\ &= \begin{cases} -Tr(X), & \text{if} \quad Tr\, W(\rho + X - \int\limits_{\sigma \in Sep} h(\sigma)\sigma d\sigma) = 0 \\ -\infty, & \text{otherwise} \end{cases} \end{aligned}$$

The dual function is finite if the trace condition given above is satisfied. Thus, the dual problem, which consists of a maximization of the dual function under its constraints, is given by,

$$\begin{aligned} \text{minimize} \quad & Tr(X) \\ \text{under the constraints} \quad & h(\sigma) \geq 0 \\ & X \geq 0 \\ & \rho + X = \int\limits_{\sigma \in Sep} h(\sigma)\sigma d\sigma \end{aligned} \tag{2.34}$$

Denoting $X = s\phi_M$, where ϕ_M is an arbitrary state and $s > 0$, we finally have the equivalence between of the dual problem with the Generalized robustness.

The same analysis can also be performed for the other robustness. We obtain:

$$\mathcal{R}_g(\rho) = max(0, -\min_{W \leq \mathcal{I}} Tr(W\rho)), \tag{2.35}$$

$$\mathcal{R}(\rho) = max(0, -\min_{Tr(W\sigma) \leq 1, \forall \sigma \in \mathcal{S}} Tr(W\rho)), \tag{2.36}$$

$$\mathcal{R}_a(\rho) = max(0, -\min_{Tr(W)=1} Tr(W\rho)), \tag{2.37}$$

[2] See Appendix 2.8 for the main ideas about Lagrangean duality and theory of convex optimization used in this chapter. An interested reader is encouraged to consult [43].

2.4.4 Semi-definite programs (SDPs)

Despite the entanglement witnesses constitute an excellent tool in the entanglement theory, there is nevertheless a large difficulty in computing them, seem the hard minimization task related to its determination. We will show in this section how to settle this problem, based on optimization methods for semi-definite programs (SDPs).

An SDP is a class of problems which are characterized by the optimization of a linear functional under convex constraints. Formally, given the complex vectors $c, x, F_i \in \mathcal{C}^m$, an SDP is given by the following minimization problem:

$$\text{minimize } c^\dagger x \text{ constrained to}$$

$$F_i^\dagger x \geq 0, \quad i = 1, ..., k; \tag{2.38}$$

where the vector c determines the function to be minimized, x is the vector of the variables, and F_i's represent the "k" convex constraints associated to the variables. It is worth mentioning that in a SDP there are no local minimum solutions, since it is a convex optimization problem. Once you map your problem to an SDP format, as above, you are in very good hands since there are several efficient methods for its optimization, and the problem can thus be solved with arbitrary accuracy.

We can easily identify the determination of witnesses and optimal witnesses with an SDP, where the linear functional to be minimized is simply the trace function, $Tr(W\rho)$, while the convex constraints are given by Eqs.(2.35), (2.36) and (2.37). The main problem remains in the computational implementation of the constraints over *all infinitely many* separable states, $Tr(W\sigma) \geq 0, \forall \sigma \in Sep$. We will show in this way a method, proposed by Brandao and Vianna [44, 45], on how to efficiently solve this implementation problem, where by using just a finite set of constraints, it is possible to mimic the infinitely many constraints over the separable states. The central idea follows from the following SDP:

Theorem 2.1. *A quantum state $\rho \in (\mathcal{H}_1 \otimes \cdots \otimes \mathcal{H}_n)$ is entangled iff the optimal value of the following SDP is negative:*

$$\textit{minimize } Tr(W\rho) \textit{ constrained to}$$

$$\sum_{i_{n-1}=1}^{d_{n-1}} \cdots \sum_{i_1=1}^{d_1} \sum_{j_1=1}^{d_1} \cdots \sum_{j_{n-1}=1}^{d_{n-1}} (c_{j_{n-1}}^{i^*} \cdots c_{j_1}^{i^*} c_{\ell_1}^{i} \cdots c_{\ell_{n-1}}^{i}) \, W^i_{j_{n-1}\cdots j_1 \, \ell_1 \cdots \ell_{n-1}} \geq 0,$$

$$\forall c_{j_k}^i, c_{\ell_k}^i \in \mathcal{C}, \quad 1 \leq k \leq (n-1), \tag{2.39}$$

where d_k is the dimension of $\mathcal{H}_k$, $W^i_{j_{n-1}\cdots j_1 \, \ell_1 \cdots \ell_{n-1}} = \langle j_{n-1}|_{n-1} \otimes \cdots \otimes \langle j_1|_1 W |\ell_1\rangle_1 \otimes \cdots \otimes |\ell_{n-1}\rangle_{n-1} \in \mathcal{B}(\mathcal{H}_n)$ and $|j\rangle_k$ is an orthonormal basis on $\mathcal{H}_k$. If ρ is entangled, the matrix W which minimizes the problem corresponds to the OEW of ρ.

Proof. We know that a quantum state is entangled iff there is a witness operator W such that $Tr(W\rho) < 0$ and $Tr(W\sigma) > 0$ for all separable states. Consider a general separable state, $\sigma_{1,\cdots,n} \in (\mathcal{H}_1 \otimes \cdots \otimes \mathcal{H}_n)$ given by,

$$\sigma_{1,\cdots,n} = \sum_i p_i |\phi_i\rangle_1\langle\phi_i| \otimes \cdots \otimes |\chi_i\rangle_{n-1}\langle\chi_i| \otimes |\tau_i\rangle_n\langle\tau_i|; \tag{2.40}$$

the positivity condition of the witness over all separable states can be written as,

$$\langle\tau_i|_n \otimes \underbrace{\langle\chi_i|_{n-1} \otimes \cdots \otimes \langle\phi_i|_1 W |\phi_i\rangle_1 \otimes \cdots \otimes |\chi_i\rangle_{n-1}}_{\text{Functional} \in \mathcal{B}(\mathcal{H}_n)} \otimes |\tau_i\rangle_n \geq 0, \quad \forall i. \tag{2.41}$$

Notice, however, that the positivity of above functional is sufficient to satisfy the inequality. Expanding the local states as $|\phi_i\rangle_k = \sum_j c_j^i |j\rangle_k$, where $|j\rangle_k$ is an orthonormal basis for the local space $\mathcal{H}_k$, follows directly that the matrix W solving the problem minimization problem corresponds to the OEW of ρ. □

We see now that, even if we reduce the number of constraints in the above theorem, *i.e.*, if we set $i = 1, ..., M$, where M is a finite number, we are still generating infinitely many constraints from the functional of Eq.(2.41): each constraint given by a fixed i in the functional, satisfy the positivity over infinitely many possible local states "$|\tau\rangle_n$". Such a relaxation of an infinite number of contraints to a finite number can be made in a probabilistic way, where the constraints are chosen according to a probability distribution $\mathcal{P}$. In this way, the OEW obtained from the relaxation is the closest possible from the exact solution (with no relaxation), less an ϵ probability of violation, *i.e.*, that $Tr(W\sigma) < 0$. This probability is lowered as the number of constraints "i" is increased. Numerical simulations with this method showed a great accuracy even for very small values of i.

2.4.5 Indistinguishable particles

We will show in this section how to generalise all the previous concepts of entanglement witnesses, Robustness, and the duality between them, for the case where the system is composed of indistinguishable particles. When we deal with systems of indistinguishable (fermionic) bosonic particles, we know that the space of states is restricted to the (anti)symmetric subspaces. In our analysis we will properly assimilate this restriction on the witnesses operators, and in the robustness mixtures.

OEW ∼ Robustness

Let us first see the fermionic case, since the bosonic case follows similarly. In the fermionic case, if we restrict the witness operators to the antisymmetric space $\{W = \mathcal{A}W\mathcal{A}^\dagger\}$, with the the constraint $\{W \leq \mathcal{A}\}$, by duality theory we define the Fermionic Generalized Robustness ($R_g^{\mathcal{F}}$); while the constraint $\{Tr(W) = D_a\}$, where D_a is the antisymmetric N-particle Hilbert space dimension, defines the Fermionic Random Robustness ($R_r^{\mathcal{F}}$); and the constraint

$\{Tr(W) \leq 1\}$ defines the Fermionic Robustness of Entanglement ($R^{\mathcal{F}}$). These quantifiers correspond to the minimum value of s ($s \geq 0$), such that

$$\sigma = \frac{\rho + s\varphi}{1+s} \tag{2.42}$$

is a unentangled fermionic state, where φ is an arbitrary fermionic state (entangled or not) in the case of $R_g^{\mathcal{F}}$, an arbitrary unentangled fermionic state in the case of $R^{\mathcal{F}}$, and the maximally mixed fermionic state ($\mathcal{A}/D_a$) in the case of $R_r^{\mathcal{F}}$. We see the completely similarity with the usual distinguishable systems, where the only difference now is that all the states and operators are restricted to the *physical* subspace, the antissymetric under particles exchange. Analogous relations follows for the bosonic case, recallling now that the restricitons are defined in the symmetric space.

Example: In order to exemplify the above assertions, let us see the case of the Fermionic Generalized Robustness. In an analogous way as in Sec. 2.4.3, we will apply the concepts of Lagrange duality from theory of convex optimization in order to analyse the OEW problem and its dual Robustness. The primal problem (OEW) is given by,

$$\begin{aligned} \text{minimize} \quad & Tr(W\rho) \\ \text{under the constraints} \quad & W \leq \mathcal{A} \\ & W = \mathcal{A}W\mathcal{A}^{\dagger} \\ & Tr(W\sigma) \geq 0\,,\ \forall \sigma \in Sep \end{aligned} \tag{2.43}$$

where the set Sep corresponds here to the set of unentangled fermionic states. The Lagrangean of the problem is given by,

$$\mathcal{L}(W, X, h(\sigma)) = Tr(W\rho) + Tr[X(W - \mathcal{A})] - \int\limits_{\sigma \in Sep} h(\sigma) Tr(W\sigma) d\sigma \tag{2.44}$$

From the Lagrangean we obtain the dual function $g(X, h(\sigma))$, given by the infimum over the domain $W \in \mathcal{M}$, such that $W = \mathcal{A}W\mathcal{A}^{\dagger}$. We have that,

$$\begin{aligned} g(X, h(\sigma)) &= \inf_{W \in \mathcal{M}} \mathcal{L}(W, X, h(\sigma)) \\ &= \begin{cases} -Tr(X), & \text{if} \quad Tr\, W(\rho + X - \int\limits_{\sigma \in Sep} h(\sigma)\sigma d\sigma) = 0 \\ -\infty, & \text{otherwise} \end{cases} \end{aligned}$$

Thus the dual function is finite iff the above trace condition is satisfied. In this way, the dual problem is given by,

$$\begin{aligned} \text{minimize} \quad & Tr(X) \\ \text{under the constraints} \quad & h(\sigma) \geq 0 \\ & X \geq 0 \\ & \rho + X = \int\limits_{\sigma \in Sep} h(\sigma)\sigma_{\mathrm{A}} d\sigma \end{aligned} \tag{2.45}$$

which is simply the Generalized Robustness of Entanglement.

SDPs

We now adapt Brandão and Vianna's [44] technique in order to obtain a new algorithm to determine OEWs for indistinguishable fermions or bosons. The method for obtaining the OEW is based on semidefinite programs (SDPs), which can be solved efficiently with arbitrary accuracy.

The method has the same formulation for both fermionic and bosonic particles. We will present the SDP formulation specifically for the OEW and its Generalized Robustness of Entanglement measure, but any other case follows trivially from this one by just exchanging the witnesses subspace, as discussed previously. Recall that the central obstacle in order to obtain the OEW is the generation of the positivity constraint over all unentangled states, in our case, over all single-Slater determinant/permanent states.

Theorem 2.2. *A quantum state ρ with N indistinguishable fermionic/bosonic particles is entangled if and only if the optimal value of the following SDP is negative:*

$$\text{minimize } Tr(W\rho) \text{ subject to}$$

$$\begin{cases} \sum_{i_{N-1}=1}^{d} \cdots \sum_{i_1=1}^{d} \sum_{j_1=1}^{d} \cdots \sum_{j_{N-1}=1}^{d} (c_{i_{N-1}}^{N-1^*} \cdots c_{i_1}^{1^*} c_{j_1}^{1} \cdots c_{j_{N-1}}^{N-1} \times \\ W_{i_{N-1}\cdots i_1 j_1 \cdots j_{N-1}}) \geq 0, \\ \forall c_i^k \in \mathcal{C},\ 1 \leq k \leq (N-1),\ 1 \leq i \leq d, \\ \Gamma W \Gamma^\dagger = W, \\ W \leq \Gamma, \end{cases} \tag{2.46}$$

where d is the dimension of the single particle Hilbert space, $\{a_\ell^\dagger\}$ is an orthonormal basis of fermionic/bosonic creation operators, Γ is the antisymmetrization/symmetrization operator, and $W_{i_{N-1}\cdots i_1 j_1 \cdots j_{N-1}} = a_{i_{N-1}} \cdots a_{i_1} W a_{j_1}^\dagger \cdots a_{j_{N-1}}^\dagger \in \mathcal{B}(\mathcal{H}_1^d)$ is an operator acting on the space of one fermion/boson. If ρ is a fermionic entangled state, the operator W that minimizes the problem corresponds to the OEW of ρ; othewise, if ρ is a bosonic state, the operator is a "quasi-optimal" entanglement witness.

Proof. It is known that a state is entangled if and only if there exists a witness operator W such that $Tr(W\rho) < 0$ and $Tr(W\sigma) \geq 0$ for every unentangled state σ. Consider a general unentangled state as given by,

$$\sigma = \sum_{j_1,\ldots,j_N} p_{j_1,\ldots,j_N} \widetilde{a}_{j_1}^\dagger \cdots \widetilde{a}_{j_N}^\dagger |vac\rangle\langle vac| \widetilde{a}_{j_N} \cdots \widetilde{a}_{j_1}, \tag{2.47}$$

where $\sum p_{j_1,\ldots,j_N} = 1$, and $\widetilde{a}_{j_k}^\dagger = \sum_i c_i^k a_i^\dagger$. The semi-positivity condition $Tr(W\sigma) \geq 0$ is equivalent to:

$$\langle 0| \widetilde{a}_{j_N} \widetilde{a}_{j_{N-1}} \cdots \widetilde{a}_{j_1} W \widetilde{a}_{j_1}^\dagger \cdots \widetilde{a}_{j_{N-1}}^\dagger \widetilde{a}_{j_N}^\dagger |0\rangle \geq 0, \tag{2.48}$$

Note however that, in order to satisfy such a condition, it is sufficient that the operator $\widetilde{a}_{j_{N-1}} \cdots \widetilde{a}_{j_1} W \widetilde{a}_{j_1}^\dagger \cdots \widetilde{a}_{j_{N-1}}^\dagger$ be positive semidefinite. Expanding such a term in the canonical basis $\{a_j^\dagger\}$ we obtain exactly the first constraint in Eq.2.46. The others contraints follow from the definition of Fermionic/Bosonic Generalized Robustness of Entanglement.

In one hand such a witness operator is the OEW in the case of fermionic particles, but on the other hand it is not optimal in the case of bosonic particles, due to its complicated structure of unentangled states. The entanglement witness W does not detect bosonic entangled states of the form $a_1^\dagger \cdots a_{N-1}^\dagger \widetilde{a}_N^\dagger |0\rangle$, where $\widetilde{a}_N^\dagger$ is not orthogonal to $a_i^\dagger|_{i=1}^{N-1}$, a problem which does not arise in the fermionic case due to the Pauli exclusion principle. In numerical tests, we noticed that the quality of W improves with the increasing of the single-particle Hilbert space dimension. □

The minimization problem given above is again solved by means of probabilistic relaxations, as done in [44], where the set of infinite constraints is exchanged by a finite sample. Thus the witness operator obtained is such that satisfies most of the constraints in Eq.2.46. The small probability (ϵ) for a constraint to be violated (i.e. $Tr(W\sigma) < 0$) diminishes as the size of the sample of constraints increases.

2.5 Measures interrelations

In this section we highlight the relationships among the measures of particle entanglement for fermionic and bosonic pure states in the smallest dimension, $\mathcal{A}(\mathcal{H}^4 \otimes \mathcal{H}^4)$ and $\mathcal{S}(\mathcal{H}^2 \otimes \mathcal{H}^2)$, respectively. While the fermionic case resembles that of distinguishable qubits, the bosonic case is more intricate, due to the structure of the unentangled states.

For pure states of distinguishable qubits, $\rho = |\psi\rangle\langle\psi| \in \mathcal{B}(\mathcal{H}^2 \otimes \mathcal{H}^2)$, it is well known the following equivalence for Generalized Robustness $\mathcal{R}_g(\rho)$, Robustness of Entanglement $\mathcal{R}_e(\rho)$, Random Robustness $\mathcal{R}_r(\rho)$, Wooters Concurrence $C_W(\rho)$, Negativity $Neg(\rho)$, and Entropy of Entanglement $E(\rho)$ [38, 41, 42, 46]:

$$\mathcal{R}_g(\rho) = \mathcal{R}_e(\rho) = \frac{1}{2}\mathcal{R}_r(\rho) = C_W(\rho) = Neg(\rho) \propto E(\rho). \tag{2.49}$$

Recall that $E(\rho)$ is the Shannon entropy of the eigenvalues $(\lambda, 1-\lambda)$ of the reduced one-qubit state, and $C_W = 2\sqrt{\lambda(1-\lambda)}$.

For pure two-fermion states, $\rho = |\psi\rangle\langle\psi| \in \mathcal{B}(\mathcal{A}(\mathcal{H}^4 \otimes \mathcal{H}^4))$, we have found similar relations:

$$\mathcal{R}_g^{\mathcal{F}}(\rho) = \mathcal{R}_e^{\mathcal{F}}(\rho) = \frac{2}{3}\mathcal{R}_r^{\mathcal{F}}(\rho) = C_S^{\mathcal{F}}(\rho) = \frac{1}{2}Neg(\rho) \propto E(\rho). \tag{2.50}$$

Note that $Neg(\rho)$, and $E(\rho)$ are the shifted measures. The relations between Robustness and Slater concurrence were observed numerically by means of optimal entanglement witnesses [27], and now we prove them. Based on the Slater decomposition $|\psi\rangle = \sum_i z_i a_{2i-1}^\dagger a_{2i}^\dagger |0\rangle$, where $a_i^\dagger = \sum_k U_{ik} f_k^\dagger$, we can write the following optimal decomposition (*viz* Eq.(2.42)):

$$\sigma_{opt} = \frac{1}{1+t}(\rho + t\phi_{opt}), \tag{2.51}$$

$$\phi_{opt} = \frac{1}{2}(a_1^\dagger a_3^\dagger |0\rangle\langle 0| a_3 a_1 + a_2^\dagger a_4^\dagger |0\rangle\langle 0| a_4 a_2). \tag{2.52}$$

Now we show that when $t = C_S^{\mathcal{F}}(\rho)$, σ_{opt} is unentangled and in the border of the uncorrelated states. We know that the Slater concurrence of the state is invariant under unitary local symmetric maps Φ. We can always choose Φ such that the single particle modes $\{a_i^\dagger\}$ are mapped into the canonical modes $\{f_i^\dagger\}$ [3]. Therefore $\Phi\sigma_{opt} \to \sigma'_{opt} = \frac{1}{1+t}(|\psi'\rangle\langle\psi'| + t\phi'_{opt})$, where $|\psi'\rangle = \sum_i z_i f_{2i-1}^\dagger f_{2i}^\dagger$, and $\phi'_{opt} = \frac{1}{2}(f_1^\dagger f_3^\dagger|0\rangle\langle 0|f_3 f_1 + f_2^\dagger f_4^\dagger|0\rangle\langle 0|f_4 f_2)$.

The Slater concurrence of σ'_{opt} is given by $C_S^{\mathcal{F}}(\sigma'_{opt}) = \max(0, \lambda_4 - \lambda_3 - \lambda_2 - \lambda_1)$, where $\{\lambda_i\}_{i=1}^4$ are the eigenvalues, in non-decreasing order, of the matrix $\sqrt{\sigma'_{opt}\widetilde{\sigma}'_{opt}}$, with $\widetilde{\sigma}'_{opt} = (\mathcal{K}\mathcal{U}_{ph})\sigma'_{opt}(\mathcal{K}\mathcal{U}_{ph})^\dagger$, being $\mathcal{K}$ the complex conjugation operator, and $\mathcal{U}_{ph}$ the particle-hole transformation. Consider the following matrix:

$$\sqrt{\sigma'_{opt}\widetilde{\sigma}'_{opt}} = \sqrt{\frac{1}{(1+t)^2}(\rho'\widetilde{\rho}' + t(\rho'\widetilde{\phi}'_{opt} + \phi'_{opt}\widetilde{\rho}') + t^2\phi'_{opt}\widetilde{\phi}'_{opt})}. \tag{2.53}$$

Note that "$\sigma'_{opt}, \rho', \phi'_{opt}$" and their dual are all real matrices. With the aid of Eqs.(2.51) and (2.52), it is easy to see that $\rho'\widetilde{\phi}'_{opt} = \phi'_{opt}\widetilde{\rho}' = 0$, $\phi'_{opt}\widetilde{\phi}'_{opt} = \frac{1}{2}\phi'_{opt}$, and that $\rho'\widetilde{\rho}'$ is orthogonal to $\phi'_{opt}\widetilde{\phi}'_{opt}$. Thus Eq.(2.53) reduces to:

$$\sqrt{\sigma'_{opt}\widetilde{\sigma}'_{opt}} = \frac{1}{(1+t)}(\sqrt{\rho'\widetilde{\rho}'} + \frac{t}{\sqrt{2}}\sqrt{\phi'_{opt}}). \tag{2.54}$$

The eigenvalues of $\sqrt{\rho'\widetilde{\rho}'}$ are easily obtained by means of its Slater decomposition, and the only non null eigenvalue is given by $C_S^{\mathcal{F}}(\rho')$. $\sqrt{\phi'_{opt}}$ has just two non null eigenvalues, which are equal, given by $\frac{1}{\sqrt{2}}$ (viz. Eq.(2.52)). Therefore the eigenvalues of the Eq.2.53 are "$\frac{1}{(1+t)}(C_S^{\mathcal{F}}(\rho'), \frac{t}{2}, \frac{t}{2}, 0)$", and according to the definition of the Slater concurrence follows directly that $C_S^{\mathcal{F}}(\sigma'_{opt}) = 0$ if and only if $t \geq C_S^{\mathcal{F}}(\rho')$.

We end this section by considering pure two-boson states, $\rho = |\psi\rangle\langle\psi| \in \mathcal{B}(\mathcal{S}(\mathcal{H}^2 \otimes \mathcal{H}^2))$. We have the following relations, which can be easily verified:

$$C_S^{\mathcal{B}}(\rho) = Neg(\rho)_{def.2} \propto E(\rho)_{def.2} \tag{2.55}$$

In considering the measures corresponding to definition 1 of unentangled states (Eq.2.5), we see that they are related differently, since the Negativity will always be zero for such states ($\left\|\rho^{T_i}\right\|_1 \leq 2$). This is due to the use of the upper limit in Eq.(2.19). We could however, instead of using this upper limit, obtain analytically the values of $\left\|\rho^{T_i}\right\|_1$ corresponding to the unentangled pure states, which would be equal to $\left\|\rho^{T_i}\right\|_1 = 1$ or 2, and perform a similar analysis to that made for the $S(\rho_r)_{def.1}$ in Eq.2.8. Thus it would be possible to relate the

[3] Given the canonical single particle basis $\{f_i^\dagger\}$, and any other orthonormal single particle basis $\{a_i^\dagger\}$, where $a_k^\dagger = \sum_j u_{kj} f_j^\dagger$, a unitary local symmetric map Φ transforms the canonical basis as follows: $f_k^\dagger \mapsto \sum_j v_{kj} f_j^\dagger$, where v_{kj} is a unitary matrix. The basis $\{a_i^\dagger\}$ is given, after such transformation, by $a_k^\dagger \mapsto \sum_{j,l} u_{kj}(v_{jl} f_l^\dagger)$. We can always choose Φ such that $v = u^\dagger$, and thereby we have $\{a_i^\dagger\} \mapsto \{f_i^\dagger\}$.

Negativity and the Entropy of Entanglement according to definition 1. We see therefore that the relations between the distinct measures are similar to the distinguishable case when we consider the definition 2 (Eq.2.6) of particle entanglement, possessing some discrepancies when we consider the definition 1.

2.6 Homogeneous D-Dimensional Hamiltonians

Given the easy computability of the entanglement measures presented above, in particular the Negativity and functions of the purity of the single-particle reduced state, in this section we employ them to quantify entanglement of particles in many-body systems, described by homogeneous Hamiltonians with certain symmetries.

Consider the Hamiltonian of a D-dimensional lattice, with N indistinguishable particles of spin Σ, L^D sites (with the closure boundary condition, $L+1=1$), and the orthonormal basis $\{a^\dagger_{\vec{i}\sigma}, a_{\vec{i}\sigma}\}$ of creation and annihilation operators for the particles in that lattice, where $\vec{i}=(i_1,..,i_D)$ is the spatial position vector, and $\sigma=-\Sigma,(-\Sigma+1),...,(\Sigma-1),\Sigma$ is the spin in the direction $\hat{S_z}$. If the eigenstates are degenerate, we can use the Negativity to quantify their entanglement, and if the eigenstates are non-degenerate, we can also use any function of the purity of their reduced state as a quantifier. For example, the purity function, *i.e.*, $Tr(\rho_r^2)$, is lower than $1/N$ if (if and only if, in the case of fermions) the state is entangled. Thus we can define the measure "E" based on the purity function as $E(|\psi\rangle\langle\psi|)=\max\{0,\frac{1}{N}-Tr(\rho_r^2)\}$. If, however, the Hamiltonian has some symmetries, it is possible to obtain an analytic expression for the particle entanglement of their eigenstates according to the von Neumann entropy of its single-particle reduced state. Let the Hamiltonian be *homogeneous*, and with the following properties: (1) their eigenstates are non-degenerate, and (2) the Hamiltonian commutes with the spin operator S_z (thus S_z and the Hamiltonian share the same eigenstates), if ρ is one its eigenstates, we have then:

$$Tr(a^\dagger_{\vec{i}\sigma}a_{\vec{j}\sigma}\,\rho)=Tr(a^\dagger_{(\vec{i}+\vec{\delta})\sigma}a_{(\vec{j}+\vec{\delta})\sigma}\,\rho), \tag{2.56}$$

$$Tr(\underbrace{a^\dagger_{\vec{i}\sigma}a_{\vec{j}\bar{\sigma}}}_{\sigma\neq\bar{\sigma}}\,\rho)=0,\quad \forall\vec{i},\vec{j}, \tag{2.57}$$

where Eq.(2.56) follows from the translational invariance property of the quantum state due to the homogeneity of the Hamiltonian, while Eq.(2.57) follows directly from S_z conservation (condition (2)). By condition (1) of non-degeneracy and the results of the previous sections, we known that the von Neumann entropy of the single-particle reduced state can be used as a quantifier of the particle entanglement. Let us calculate it.

We know that matrix elements of the reduced state are given by $\rho_r(\vec{i}\sigma,\vec{j}\bar{\sigma})=\frac{1}{N}\,Tr(a^\dagger_{\vec{j}\bar{\sigma}}a_{\vec{i}\sigma}|\psi\rangle\langle\psi|)$ and, according to Eq.(2.57), subspaces of the reduced state with different spin "σ" are disjoint. We can therefore diagonalize the reduced

state in these subspaces separately. Eq.(2.56) together with the boundary condition fix the reduced state to a circulant matrix. More precisely, for the unidimensional case ($D = 1$), given the subspace with spin "σ" and $\{a^\dagger_{i\sigma}\}_{i=1}^{L}$, the reduced state is given by the following $L \times L$ matrix:

$$\rho_r^\sigma = \frac{1}{N}\begin{pmatrix} x_0 & x_1 & \cdots & x_{L-2} & x_{L-1} \\ x_{L-1} & x_0 & x_1 & & x_{L-2} \\ \vdots & x_{L-1} & x_0 & \ddots & \vdots \\ x_2 & & \ddots & \ddots & x_1 \\ x_1 & x_2 & \cdots & x_{L-1} & x_0 \end{pmatrix}, \tag{2.58}$$

$$x_\delta = \left\langle a^\dagger_{(j+\delta)\sigma} a_{j\sigma} \right\rangle, \tag{2.59}$$

$$x_0 = \left\langle a^\dagger_{j\sigma} a_{j\sigma} \right\rangle = n_{j\sigma} \underbrace{=}_{eq.2.56} n_{i\sigma} = \frac{N_\sigma}{L}, \tag{2.60}$$

where $N_\sigma = \sum_{j=1}^{L} n_{j\sigma}$. The terms x_δ are simply the quadratures of the model, and can be obtained in several ways, *e.g.* directly from one-particle Green's function, by computational methods like quantum Monte Carlo, or by the Density Matrix Renormalization Group method (DMRG). The eigenvalues $\{\lambda_k^\sigma\}$ are given by a Fourier transformation of the quadratures,

$$\lambda_k^\sigma = \frac{1}{L}\sum_{\delta=0}^{L-1} e^{ik\delta} x_\delta, \quad k = \left[0, \frac{2\pi}{L}, ..., (L-1)\frac{2\pi}{L}\right]. \tag{2.61}$$

Thus the particle entanglement of that eigenstate can be calculated from $S(\rho_r) = -\sum_{j,\sigma} \lambda_j^\sigma \log \lambda_j^\sigma$.

For higher dimensions, given the subspace of a single-particle with spin "σ" and $\{a^\dagger_{\vec{i}\sigma}\}_{i=1}^{L^D}$, the characteristic vector of its circulant matrix (*e.g.* the matrix first line) is given by,

[D=2] :

$$\vec{v}_c = \Big([x_{00} \cdots x_{(L-1)0}] \quad [x_{01} \cdots x_{(L-1)1}] \quad \cdots \quad \cdots \quad [x_{0(L-1)} \cdots x_{(L-1)(L-1)}] \Big), \tag{2.62}$$

[D=3]:

$$\vec{v}_c = \begin{pmatrix} v^{2D}_{z=0} & v^{2D}_{z=1} & ... & v^{2D}_{z=(L-1)} \end{pmatrix}, \tag{2.63}$$

where $v^{2D}_{z=\ell} = \begin{pmatrix} [x_{00\ell} \cdots x_{(L-1)0\ell}] & [x_{01\ell} \cdots x_{(L-1)1\ell}] & \cdots & [x_{0(L-1)\ell} \cdots x_{(L-1)(L-1)\ell}] \end{pmatrix}$ is the characteristic vector of the plane $z = \ell$, and $x_{\delta_x\delta_y\delta_z} = \left\langle a^\dagger_{(\ell+\delta_x)(m+\delta_y)(n+\delta_z)\sigma} a_{(\ell mn)\sigma} \right\rangle$.

Thus, the eigenvalues $\{\lambda_j^\sigma\}_{j=1}^{L^D}$ of the reduced state are given by:

$$[\text{D=2}]: \quad \lambda_j^\sigma = \sum_{\ell,m=0}^{L-1} x_{\ell m} w_j^{\ell+mL}, \tag{2.64}$$

$$[\text{D=3}]: \quad \lambda_j^\sigma = \sum_{\ell,m,n=0}^{L-1} x_{\ell mn} w_j^{\ell+mL+nL^2}, \tag{2.65}$$

where $w_j = \exp \frac{2\pi i j}{L^D}$. If we wished to obtain the particle entanglement according to the purity function, as presented in the beginning of this section, we would easily obtain the following expression:

$$E(|\psi\rangle\langle\psi|) = \max\{0, \frac{1}{N} - \frac{L^D}{N^2} \sum_{\vec{\delta},\sigma} \left| \left\langle a^\dagger_{(\vec{i}+\vec{\delta})\sigma} a_{\vec{i}\sigma} \right\rangle \right|^2 \} \tag{2.66}$$

for any fixed spatial position vector "$\vec{i}$". Note however that, although the calculation of the purity function is simple even for the case of a general Hamiltonian, since it is just the sum over the one-particle Green's function $\left\langle a^\dagger_{\vec{i}\tilde{\sigma}} a_{\vec{k}\sigma} \right\rangle$ (note that $Tr(\rho_r^2) = \frac{1}{N^2} \sum_{\vec{i},\vec{k},\sigma,\tilde{\sigma}} \left| \left\langle a^\dagger_{\vec{i}\tilde{\sigma}} a_{\vec{k}\sigma} \right\rangle \right|^2$) and thus does not require the diagonalization of the single-particle reduced state, the measure according to the von Neumann entropy can be more interesting, given its wide application in quantum information theory.

2.7 Conclusion

Entanglement of distinguishable particles is related to the notion of separability, *i.e.* the possibility of describing the system by a simple tensor product of individual states. In systems of indistinguishable particles, the symmetrization or antisymmetrization of the many-particle state eliminates the notion of separability, and the concept of entanglement becomes subtler. If one is interested in the different modes (or configurations) the system of indistinguishable particles can assume, it is possible to use the same tools employed in systems of distinguishable particles to calculate the *entanglement of modes*. On the other hand, if one is interested in the genuine entanglement between the particles, as discussed in the present work, one needs new tools. In this case, we have seen that entanglement of particles in fermionic systems is simple, in the sense that the necessary tools are obtained by simply antisymmetrizing the distinguishable case, and one is led to the conclusion that unentangled fermionic systems are represented by convex combinations of Slater determinants. The bosonic case, however, does not follow straightforwardly by symmetrization of the distinguishable case. The possibility of multiple occupation implies that a many-particle state of Slater rank one in one basis can be of higher rank in another basis. This ambiguity reflects on the possibility of multiple values of the von Neumann entropy for the one-particle reduced state of a pure many-particle state. Aware of the subtleties of the bosonic case, we have proven that a *shifted* von Neumann entropy and a *shifted* Negativity can

be used to quantify entanglement of particles. We presented fermionic and bosonic entanglement witnesses, and showed an algorithm able to efficiently determine OEW's for such systems. We have shown, however, that the bosonic entanglement witness are not completely optimal, due to the possibility of multiple occupation. Nonetheless, numerical calculations have shown that the bosonic witness improves with the increase of the single-particle Hilbert space dimension. Finally, we have illustrated how the tools presented in this article could be useful in analysing the properties of entanglement in many-body systems, obtaining in particular analytic expressions for the entanglement of particles according to the von Neumann entropy of the single-particle reduced state in homogeneous D-dimensional Hamiltonians.

Though we have not yet studied quantum correlations beyond entanglement, we mention that the *quantumness or nonclassicality* of states of indistinguishable particles can be reduced to the calculation of bipartite entanglement between the main system and an ancilla, following the *activation protocol* introduced by Piani *et al.* [34]. In this case, besides the usual symmetrization of operations to preserve indistinguishability, one must be more careful with the phraseology, for a *system of indistinguishable particles* cannot be classical. We will defer this discussion to Chapter 3.

2.8 Appendix: Duality and theory of convex optimization

In optimization theory, we can usually exchange the original problem, called primal problem, by an alternative formulation, called dual problem [43]. This link is realized by the Lagrangean of the problem. Consider the following primal optimization problem:

$$\begin{aligned} \text{minimize} \quad & f_o(x) \\ \text{under the constraints} \quad & f_i(x) \leq 0\,, \quad i = 1, ..., m \\ & h_i(x) = 0\,, \quad i = 1, ..., n \end{aligned} \tag{2.67}$$

where $x \in \mathcal{D}$ is the variable of the problem, f_o the function to be minimized, and f_i, h_i, the constraints. Denote the optimum value of the problem as given by p^*, *i.e.*, $f(x_{opt}) = p^*$.

The Lagrangean L of the problem encloses all of its information, given by the objective function to be minimized with its weighted constraints as follows,

$$L(x, \lambda, \mu) = f_0(x) + \sum_{i=1}^{m} \lambda_i f_i(x) + \sum_{i=1}^{n} \mu_i h_i(x), \tag{2.68}$$

where λ_i, μ_i are called Lagrangean multipliers. The minimization of the Lagrangean over the domain of the primal variables x provides the dual Lagrangean function $g(\lambda, \mu)$,

$$g(\lambda, \mu) = \inf_{x \in \mathcal{D}} (f_0(x) + \sum_{i=1}^{m} \lambda_i f_i(x) + \sum_{i=1}^{n} \mu_i h_i(x)) \tag{2.69}$$

A central property of such a dual Lagrangean relies on the fact that, for any $\lambda \succeq 0$ and μ, it provides a lower bound over the optimal primal minimization problem,

$$g(\lambda, \mu) \leq p^* \tag{2.70}$$

Proof. Consider $\widetilde{x}$ as a possible point of the problem, *i.e.* , $f_i(\widetilde{x}) \leq 0$ and $h_i(\widetilde{x}) = 0$, and let $\lambda \succeq 0$. Thus, the Lagrangean $L(\widetilde{x}, \lambda, \mu)$ will be limited by the objective function f_0 on such a point,

$$L(\widetilde{x}, \lambda, \mu) = f_0(\widetilde{x}) + \sum_{i=1}^{m} \lambda_i f_i(\widetilde{x}) + \sum_{i=1}^{n} \mu_i h_i(\widetilde{x}) \leq f_0(\widetilde{x}) \tag{2.71}$$

We see in this way that,

$$g(\lambda, \mu) = \inf_{x \in \mathcal{D}} L(x, \lambda, \mu) \leq L(\widetilde{x}, \lambda, \mu) \leq f_0(\widetilde{x}), \tag{2.72}$$

and since such a inequality is valid for all possible points of the problem, the proof for Eq.(2.70) follows directly. □

It raises now the question on what cases such an inequality would be saturated, obtaining $g(\lambda^*, \mu^*) = p^*$? If so, we would have two equivalent formulations for the same problem: the primal problem as given in Eq.(2.67), and its dual problem,

$$\begin{aligned} \text{maximize} \quad & g(\lambda, \mu) \\ \text{under the constraint} \quad & \lambda \succeq 0 \end{aligned} \tag{2.73}$$

In general such a inequality saturation is not valid. For some specific cases , however, it is possible to show the complete saturation, as for example, in cases where the optimization problem is convex,

$$\begin{aligned} \text{minimize} \quad & f_0(x) \\ \text{under the constraint} \quad & f_i(x) \leq 0\,, \quad i = 1, ..., m \\ & Ax = B\,, \end{aligned} \tag{2.74}$$

where $f_0, ..., f_m$ are convex functions. In such convex optimization problems we have that $d^* = p^*$.

CHAPTER 3

Quantumness of correlations in indistinguishable particles

The notion of entanglement, first noted by Einstein, Podolsky, and Rosen [6], is considered one of the main features of quantum mechanics, and became a subject of great interest in the last few years due to its primordial role in quantum computation and quantum information [1, 2, 3, 4]. However, entanglement is not the only kind of correlation presenting non classical features, and a great effort has recently been directed towards characterizing a more general notion of quantum correlations, the *quantumness* of correlations. The quantumness of correlations is revealed in different ways, and there are a wide variety of approaches, sometimes equivalent, in order to characterize and quantify it, e.g., through the "activation protocol", where the non classical character of correlations in the system is revealed by a unavoidable creation of entanglement between system and measurement apparatus in a local measurement [34, 47]; or by the analysis of the minimum disturbance caused in the system by local measurements [48, 49, 52], which led to the seminal definition of *quantum discord* [48]; or even through geometrical approaches [53].

As discussed in the previous chapters, the notion of entanglement in systems of indistinguishable particles has two distinct approaches: the correlations genuinely arising from the entanglement between the particles ("entanglement of particles") and the correlations arising from the entanglement between the modes of the system ("entanglement of modes"). These two notions of entanglement are complementary, and the use of one or the other depends on the particular situation under scrutiny. For example, the correlations in eigenstates of a many-body Hamiltonian could be more naturally described by particle entanglement, whereas certain quantum information protocols could prompt a description in terms of entanglement of modes.

The correlations between modes in a system of indistinguishable particles

is subsumed in the usual analysis of correlations in systems of distinguishable ones. Thus we will, in this work, characterize and quantify a general notion of quantum correlations (not necessarily entanglement) genuinely arising between indistinguishable particles. We will call these correlations by quantumness of correlations, to distinguish from entanglement, and it has an interpretation analogous to the quantumness of correlations in systems of distinguishable particles, as we will see. One must however be careful with such phraseology, since systems of indistinguishable particles always have *exchange correlations* coming from the symmetric or antisymmetric nature of the wavefunction. The intrinsic exchange correlations are not included in the concept of the quantumness of correlations. We will discuss these issues in more detail throughout the chapter.

The chapter is organized as follow. In Sec.3.1 we briefly review the notion of quantumness of correlations in distinguishable subsystems, and their interplay with the measurement process via the activation protocol. In Sec. 3.2 we introduce the activation protocol for systems of indistinguishable particles; and in Sec.3.3 we characterize and quantify the quantumness of correlations in these systems. We conclude in Sec.3.4.

3.1 Quantumness of correlations

The concept of quantumness of correlations is related to the amount of inaccessible information of a composed system if we restrict to the application of local measurements on the subsystems [48, 49, 50, 51]. Since quantumness of correlations can be created with local operations on the subsystems, it is also called as the quantum properties of classical correlations [48, 51]. A model for the description of a measurement process is given via decoherence [54], where in order to measure a quantum system we must interact it with a measurement apparatus, which is initially uncorrelated with the quantum system. This interaction, given by a unitary evolution, creates correlations between them, and thereby the measurement outcomes will be registered on the apparatus eigenbasis. A protocol that allows us to understand the interplay between a measurement process and the quantumness of correlations in a system is known as the *nonclassical correlations activation protocol*. This protocol shows that if and only if the system is strictly classically correlated, i.e., has no quantumness of correlations, there exists a local measurement on the subsystems that does not create entanglement between system and measurement apparatus [34, 47, 55]; or rather, if the system has quantumness of correlations, then it will inevitably create entanglement with the apparatus measurement in a local measurement process, hence the reference to "activation". A direct corollary of this protocol allows us to quantify the amount of quantumness of correlations by measuring the minimal amount of entanglement created between the system and the measurement apparatus during a local measurement process [56].

Given, for instance, a bipartite system S described by the state ρ_S, in order to apply a von Neumann measurement in this system we must interact it with a measurement apparatus $\mathcal{M}$, initially in an arbitrary state $|0\rangle\langle 0|_{\mathcal{M}}$.

Suppose that we are able to apply global von Neumann measurements in such a system, e.g., a von Neumann measurement in the system eigenbasis $\{|i\rangle\}_S$, $\rho_S = \sum_i \lambda_i |i\rangle\langle i|$. The system and the measurement apparatus must interact under the action of the following unitary transformation: $U_{S:\mathcal{M}}|i\rangle_S|0\rangle_{\mathcal{M}} = |i\rangle_S|i\rangle_{\mathcal{M}}$. We see that the interaction simply creates classical correlations between them: $\tilde{\rho}_{S:A} = U_{S:A}(\rho_S \otimes |0\rangle\langle 0|_A)U_{S:A}^\dagger = \sum_i \lambda_i |i\rangle\langle i| \otimes |i\rangle\langle i|$. If however we are restricted to apply local measurements, the measurement process will create entanglement between system and apparatus by their corresponding coupling unitary $U'_{S:A}$, unless the state is strictly classically correlated, as stated by the activation protocol. The minimal amount of entanglement $E(\tilde{\rho}_{S:A})$ which is created in a local measurement process is quantified by the quantumness of correlations $Q(\rho_S)$ of the system, i.e.,

$$Q(\rho_S) = \min_{U_{S:A}} E(\tilde{\rho}_{S:A}). \tag{3.1}$$

Different entanglement measures will lead, in principle, to different quantifiers for the quantumness of correlations. The only requirement is that the entanglement measure be monotone under LOCC maps [34, 47, 56]. Other measures of quantumness can be recovered with the activation protocol: the quantum discord [47], one-way work deficit [47], relative entropy of quantumness [34] and the geometrical measure of discord via trace norm [57], are some examples.

3.2 Activation protocol for indistinguishable particles

As aforesaid, quantum correlations between distinguishable particles can be interpreted via a unavoidable entanglement created with the measurement apparatus in a partial von Neumann measurement on the particles [47, 34], i.e., in a measurement corresponding to a non-degenerate local observable. Note that although the approach is based on projective measurements, it is valid and well defined also for POVMs: once the dimension and the partitioning of the ancilla can be arbitrarily chosen, general measurements can be realized through a direct application of the Naimark's dilation theorem. In systems of indistinguishable particles the notion of "local measurement" will be implemented through the algebra of single-particle observables (see for example Ref.[11] for a detailed discussion), and based on this identification we will set up an "activation protocol" for indistinguishable particles. The importance to study the correlations, particularly the entanglement, in terms of subalgebras of observables has been emphasized in [11, 21, 25, 58, 59, 60], and in the previous chapters, proving to be a useful approach for such analysis. The algebra of single-particle observables is generated by,

$$\begin{aligned}\mathcal{O}_{sp} = \quad & M \otimes \mathcal{I} \otimes \cdots \otimes \mathcal{I} + \mathcal{I} \otimes M \otimes \cdots \otimes \mathcal{I} + \cdots + \\ & \mathcal{I} \otimes \cdots \otimes \mathcal{I} \otimes M,\end{aligned} \tag{3.2}$$

where M is an observable in the Hilbert space of a single particle. We can express this algebra in terms of fermionic or bosonic creation $\{a_i^\dagger\}$ and annihilation $\{a_i\}$ operators, depending on the nature of the particles in the

system. The algebra is generated by number conserving quadratic observables $\mathcal{O}_{sp} = \sum_{ij} M_{ij} a_i^\dagger a_j$ that can be diagonalized as $\mathcal{O}_{sp} = \sum_k \lambda_k \tilde{a}_k^\dagger \tilde{a}_k$, where $\tilde{a}_k^\dagger = \sum_j U_{kj} a_j^\dagger$ and U is the unitary matrix which diagonalizes M. Thus, since it is a non-degenerate algebra, the eigenvectors of their single-particle observables will be given by single Slater determinants, or permanents, for fermionic and bosonic particles respectively; more precisely, given by the set $\{\tilde{a}_{\vec{k}}^\dagger |vac\rangle\}$ where $\vec{k} = (k_1, \cdots, k_n)$, $k_i \in \{1, 2, ..., dim_{single-particle}\}$, represents the states of occupation of n particles, $\tilde{a}_{\vec{k}}^\dagger = \tilde{a}_{k_1}^\dagger \tilde{a}_{k_2}^\dagger \cdots \tilde{a}_{k_n}^\dagger |vac\rangle$, $dim_{single-particle}$ is the single-particle dimension and $|vac\rangle$ is the vacuum state. The measurement of single-particle observables is therefore given by a von Neumann measurement, which we shall call hereafter as single-particle von Neumann measurement, according to the complete set of rank one projectors $\{\tilde{\Pi}_{\vec{k}} = \tilde{a}_{\vec{k}}^\dagger |vac\rangle\langle vac| \tilde{a}_{\vec{k}}\}$, $\sum_{\vec{k}} \tilde{\Pi}_{\vec{k}} = \mathcal{I}_{\mathcal{A}(\mathcal{S})}$, being $\mathcal{I}_{\mathcal{A}}$ and $\mathcal{I}_{\mathcal{S}}$ the identity of the antisymmetric and symmetric subspaces, respectively.

Recall that a measurement can be described by coupling the system to a measurement apparatus, being the measurement outcomes obtained by measuring the apparatus in its eigenbasis. Given a quantum state $\rho_{\mathcal{Q}}$, and a measurement apparatus $\mathcal{M}$ in a pure initial state $|0\rangle_{\mathcal{M}}$, such that $\rho_{\mathcal{Q},\mathcal{M}} = \rho_{\mathcal{Q}} \otimes |0\rangle\langle 0|_{\mathcal{M}}$, their coupling is given by applying a unitary U on the total state that will correlate system and apparatus, $\tilde{\rho}_{\mathcal{Q},\mathcal{M}} = U(\rho_{\mathcal{Q}} \otimes |0\rangle\langle 0|_{\mathcal{M}})U^\dagger$. Such unitary U realizes a single-particle von Neumann measurement $\{\Pi_{\vec{k}}\}$ if for any quantum state $\rho_{\mathcal{Q}}$ holds: $Tr_{\mathcal{M}}(U(\rho_{\mathcal{Q}} \otimes |0\rangle\langle 0|_{\mathcal{M}})U^\dagger) = \sum_{\vec{k}} \Pi_{\vec{k}} \rho_{\mathcal{Q}} \Pi_{\vec{k}}^\dagger$.

It is not hard to see how the unitary U must act in order to realize the $\{\Pi_{\vec{k}} = a_{\vec{k}}^\dagger |vac\rangle\langle vac| a_{\vec{k}}\}$, $\sum_{\vec{k}} \Pi_{\vec{k}} = \mathcal{I}_{\mathcal{A}(\mathcal{S})}$ measurement. Let us first consider the following notation, $\{a_{\vec{k}}^\dagger |vac\rangle\} = \left\{ \left| f(\vec{k}) \right\rangle \right\}$, $f(\vec{k}) \in \{1, 2, .., dim_{\mathcal{A}(\mathcal{S})}\}$, being f a bijective function of the sets $\{\vec{k}\}$ and $\{1, 2, .., dim_{\mathcal{A}(\mathcal{S})}\}$, and $dim_{\mathcal{A}(\mathcal{S})}$ is the dimension of the antisymmetric or symmetric subspaces. Given that the apparatus has at least the same dimension as the system, the unitary is given by,

$$U \left| f(\vec{k}) \right\rangle_{\mathcal{Q}} \otimes |j\rangle_{\mathcal{M}} = \left| f(\vec{k}) \right\rangle_{\mathcal{Q}} \otimes \left| j \oplus f(\vec{k}) \right\rangle_{\mathcal{M}}. \tag{3.3}$$

It is easy to show that such operator is indeed unitary; note that

$$U = \sum_{\vec{k},j} \left| f(\vec{k}) \right\rangle \left| j \oplus f(\vec{k}) \right\rangle \left\langle f(\vec{k}) \right| \langle j|, \tag{3.4}$$

thus,

$$UU^\dagger = \sum_{\vec{k},j,\vec{k}',j'} \delta_{\vec{k},\vec{k}'} \delta_{j,j'} \left| f(\vec{k}) \right\rangle \left| j \oplus f(\vec{k}) \right\rangle \left\langle f(\vec{k}') \right| \left\langle j' \oplus f(\vec{k}') \right|, \tag{3.5}$$

and since $\{\left| f(\vec{k}) \right\rangle_{\mathcal{Q}}\}_{\vec{k}}$ and $\{\left| j \oplus f(\vec{k}) \right\rangle_{\mathcal{M}}\}_j$ form a complete set, we have that $UU^\dagger = \mathcal{I}_{\mathcal{A}(\mathcal{S})} \otimes \mathcal{I}_{\mathcal{M}}$.

Defined the coupling unitary, we are now able to analyze the entanglement created between system and apparatus in a single-particle von Neumann measurement, $E_{\mathcal{Q},\mathcal{M}}$. Given a quantum state $\rho_{\mathcal{Q}}$, we intend to quantify the

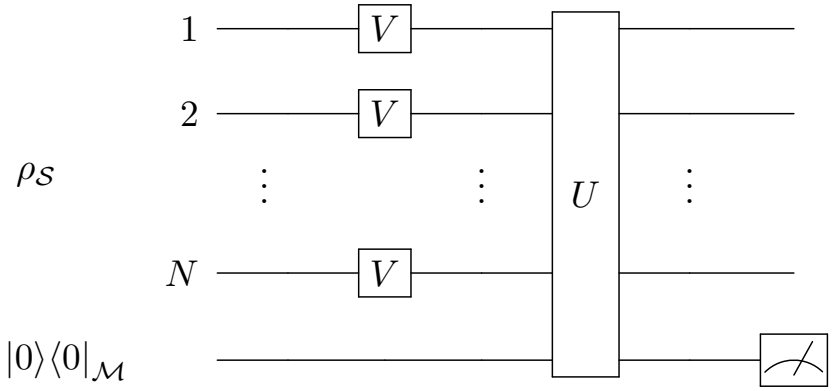

Figure 3.1: Activation protocol for a system of indistinguishable particles, where $\rho_{\mathcal{S}}$ is the state of the system, $|0\rangle\langle 0|_{\mathcal{M}}$ represents the measurement apparatus, V is the single-particle unitary transformations and U the unitary (as given by Eq.(3.3)) respective to a single-particle von Neumann measurement.

minimum of such entanglement over all single-particle von Neumann measurements, $\min_U E_{\mathcal{Q},\mathcal{M}}\left[U(\rho_{\mathcal{Q}} \otimes |0\rangle\langle 0|_{\mathcal{M}})U^\dagger\right]$. This quantity then corresponds to the quantumness of correlation in systems of indistinguishable particles. Note that such minimization is analogous to the activation protocol given in [34], but now for systems of indistinguishable particles, where the minimization is carried out on the single-particle unitary transformations $V^{\otimes n}$, see Fig.3.1.

3.3 Results

Regardless of which entanglement measure is used, let us first see which set of states does not generate entanglement after the activation protocol, i.e., has no quantumness of correlations. We find that this set $\{\xi\}$ is given by states that possess a convex decomposition in orthonormal pure states described by single Slater determinants, or permanents,

$$\xi = \sum_{\vec{k}} p_{\vec{k}}\, \tilde{a}^\dagger_{\vec{k}} |vac\rangle\langle vac| \tilde{a}_{\vec{k}} \quad , \quad \sum_{\vec{k}} p_{\vec{k}} = 1, \tag{3.6}$$

where $\tilde{a}^\dagger_{\vec{k}}|vac\rangle = V^{\otimes n} a^\dagger_{\vec{k}}|vac\rangle$, V is a unitary matrix, and $\{a^\dagger_{\vec{k}}\}$ an orthonormal set of creation operators.

Proof. We shall first show that states given by Eq.(3.6) do not generate entanglement, and then that they are the only ones. Let U be the coupling unitary corresponding to the $\{\Pi_{\vec{k}} = a^\dagger_{\vec{k}}|vac\rangle\langle vac|a_{\vec{k}} = \left|f(\vec{k})\right\rangle\left\langle f(\vec{k})\right|\}$, $\sum_{\vec{k}} \Pi_{\vec{k}} = \mathcal{I}_{\mathcal{A}(\mathcal{S})}$ measurement. Applying the activation protocol on states given by Eq.(3.6),

using $\bar{V} = V^\dagger$ as the single-particle unitary transformation, it follows that:

$$\begin{aligned}\rho_{\mathcal{Q}:\mathcal{M}} &= U\Big[(\bar{V}^{\otimes n}\xi\bar{V}^{\dagger\otimes n})_{\mathcal{Q}} \otimes |0\rangle\langle 0|_{\mathcal{M}}\Big]U^\dagger \\ &= \sum_{\vec{k}} p_{\vec{k}} \left|f(\vec{k})\right\rangle\left\langle f(\vec{k})\right|_{\mathcal{Q}} \otimes \left|f(\vec{k})\right\rangle\left\langle f(\vec{k})\right|_{\mathcal{M}},\end{aligned} \tag{3.7}$$

where $\rho_{\mathcal{Q}:\mathcal{M}} \in Sep(\mathcal{Q}\otimes\mathcal{M})$. The demonstration that such states correspond to the unique states that do not generate entanglement is given below. A separable state between system and measurement apparatus can be given by,

$$\sigma = \sum_i p_i |\psi_i\rangle\langle\psi_i|_{\mathcal{Q}} \otimes |\phi_i\rangle\langle\phi_i|_{\mathcal{M}}, \tag{3.8}$$

noting that the sets $\{|\psi_i\rangle\}$ and $\{|\phi_i\rangle\}$ are not necessarily orthogonal. Since the activation protocol corresponds to a unitary operation, thus invertible, there must exist a set $\{|\eta_i\rangle\}$ of states for the system such that,

$$U(V^{\otimes n})\,|\eta_i\rangle_{\mathcal{Q}} \otimes |0\rangle_{\mathcal{M}} = |\psi_i\rangle_{\mathcal{Q}} \otimes |\phi_i\rangle_{\mathcal{M}}, \tag{3.9}$$

and $\rho_{\mathcal{Q}} = \sum_i p_i\,|\eta_i\rangle\langle\eta_i|$. Expanding $\{|\eta_i\rangle\}$ on the basis $\{a^\dagger_{\vec{k}}|vac\rangle\}$ "transformed" by $V^{\dagger\otimes n}$,

$$|\eta_i\rangle = \sum_{\vec{k}} c^{(i)}_{\vec{k}}\; V^{\dagger\otimes n}\; a^\dagger_{\vec{k}}|vac\rangle, \tag{3.10}$$

we see from Eqs.(3.9) and (3.10) that,

$$U(V^{\otimes n})\,|\eta_i\rangle \otimes |0\rangle = \sum_{\vec{k}} c^{(i)}_{\vec{k}}\; a^\dagger_{\vec{k}}|vac\rangle \otimes \left|f(\vec{k})\right\rangle = |\psi_i\rangle \otimes |\phi_i\rangle. \tag{3.11}$$

The above factorization condition imposes the following restriction: $c^{(i)}_{\vec{k}} = \gamma_i\,\delta_{\{\vec{k},g(i)\}}$, $\|\gamma_i\| = 1$, $g : \{i\} \mapsto \{\vec{k}\}$. Therefore,

$$\begin{aligned}\rho_{\mathcal{Q}} &= \sum_i p_i\,|\eta_i\rangle\langle\eta_i|, \\ &= \sum_i p_i\,(\sum_{\vec{k}} \gamma_i\,\delta_{\{\vec{k},g(i)\}}\; a^\dagger_{\vec{k}}|vac\rangle) \\ &\quad (\sum_{\vec{k}'}\langle vac|a_{\vec{k}'}\;\gamma_i^*\;\delta_{\{\vec{k}',g(i)\}}), \\ &= \sum_i p_i\;\underbrace{\|\gamma_i\|}_{1}\; a^\dagger_{g(i)}|vac\rangle\langle vac|a_{g(i)},\end{aligned} \tag{3.12}$$

i.e, the states with no quantumness of correlations as given by Eq.(3.6). □

Example. Let us show an example of the approach in order to clarify the formalism and the above analysis. An interesting case concerns to the controversial bosonic quantum state $|\psi_b\rangle = \frac{1}{2}(b_0^\dagger b_0^\dagger + b_1^\dagger b_1^\dagger)|vac\rangle \in \mathcal{S}(\mathcal{H}^2 \otimes \mathcal{H}^2)$, where $\{b_i^\dagger\}$ are the bosonic creation operators. Note that such a state can actually be described by a single Slater permanent $|\psi_b\rangle = b_+^\dagger b_-^\dagger|vac\rangle$, being $b_\pm^\dagger = \frac{1}{\sqrt{2}}(b_0^\dagger \pm b_1^\dagger)$. Defining the coupling unitary U corresponding to the

$\{\Pi_{\vec{k}} = b_{\vec{k}}^\dagger|vac\rangle\langle vac|b_{\vec{k}}\}$, $\sum_{\vec{k}}\Pi_{\vec{k}} = \mathcal{I}_{\mathcal{S}}$, $\{\vec{k}\} = \{(0,0),(0,1),(1,1)\}$ measurement, and using the notation,

$$b_0^\dagger b_0^\dagger|vac\rangle = |0\rangle,\ b_0^\dagger b_1^\dagger|vac\rangle = |1\rangle,\ b_1^\dagger b_1^\dagger|vac\rangle = |2\rangle, \tag{3.13}$$

we have that the unitary acts as follows,

$$U|k\rangle_{\mathcal{Q}} \otimes |0\rangle_{\mathcal{M}} = |k\rangle_{\mathcal{Q}} \otimes |k\rangle_{\mathcal{M}}. \tag{3.14}$$

Applying this unitary on the bosonic state, we generate an entangled state between system and apparatus, $U(|\psi_b\rangle_{\mathcal{Q}} \otimes |0\rangle_{\mathcal{M}}) = \frac{1}{2}(b_0^\dagger b_0^\dagger|vac\rangle \otimes |0\rangle + b_1^\dagger b_1^\dagger|vac\rangle \otimes |2\rangle)$, but this is not a unavoidable entanglement in order to realize that measurement, since we could apply, before the unitary coupling, the following single-particle unitary transformation, $V : |+\rangle = |0\rangle + i|1\rangle \mapsto |0\rangle, |-\rangle = |0\rangle - i|1\rangle \mapsto |1\rangle$, i.e,

$$V \otimes V : \begin{cases} b_+^\dagger \mapsto b_0^\dagger, \\ b_-^\dagger \mapsto b_1^\dagger. \end{cases} \tag{3.15}$$

We see now that the coupling between system and apparatus does not generate entanglement between them, $U\left[(V \otimes V)|\psi_b\rangle_{\mathcal{Q}} \otimes |0\rangle_{\mathcal{M}}\right] = U(b_0^\dagger b_1^\dagger|vac\rangle_{\mathcal{Q}} \otimes |0\rangle_{\mathcal{M}}) = b_0^\dagger b_1^\dagger|vac\rangle_{\mathcal{Q}} \otimes |1\rangle_{\mathcal{M}} \in Sep(\mathcal{Q} \otimes \mathcal{M})$, and thus such a state has no quantumness of correlations.

An important result to be emphasized in this analysis via the activation protocol relates to the establishment of an equivalence between the quantumness of correlations with the *distinguishable* bipartite entanglement between system and apparatus, showing the usefulness of the correlations between indistinguishable particles. Note that the set $\{\xi\}$ is simply the antisymmetrization or symmetrization of the distinguishable classically correlated states (states with distinguishable particles with no quantumness of correlations), and all their correlations are due to the exchange correlations; the activation protocol then shows that any kind of correlations between indistinguishable particles beyond the mere exchange correlations can always be activated or mapped into distinguishable bipartite entanglement between $\mathcal{Q} : \mathcal{M}$.

The correlations between indistinguishable particles can thereby be characterized by different types: the entanglement, the quantumness of correlations as discussed in this chapter, the correlations generated merely by particle statistics (exchange correlation), and the classical correlations. In fact, there are quantum states whose particles are classically correlated, not even possessing exchange correlations, such as pure bosonic states with all their particles occupying the same degree of freedom, $|\psi_b\rangle = \frac{1}{\sqrt{n!}}(b_i^\dagger)^n|vac\rangle$, or mixed states described by an orthonormal convex decomposition of such pure states, $\chi_b = \sum_i \frac{1}{n}(b_i^\dagger)^n|vac\rangle\langle vac|(b_i)^n$. See Fig.3.2 for a schematic picture of these different kinds of correlations. Interesting questions to raise concern how the notion of entanglement of particles is related to the quantumness of correlations, and if they are equivalent for pure states. We can note from Eq.(3.6) that, for pure states, the set with no quantumness of correlations is described by states with a single Slater determinant, or permanent, which is equivalent to the set of unentangled pure states. Concerning mixed states,

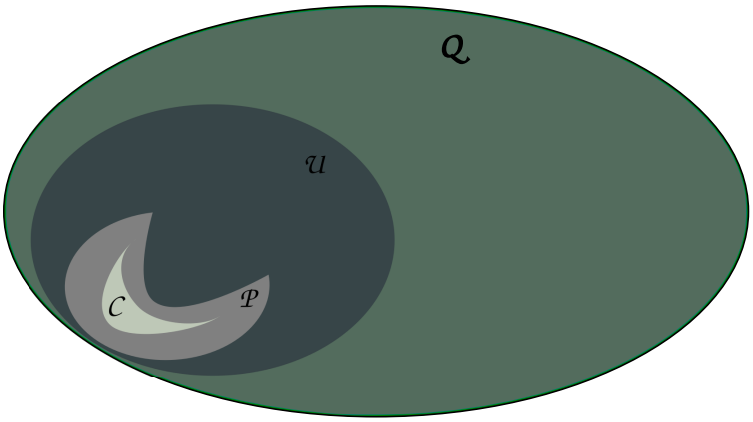

Figure 3.2: Schematic picture of the distinct types of correlations in systems of indistinguishable particles. The larger set ($\mathcal{Q}$) denotes the set of all fermionic, or bosonic, quantum states; the blue area ($\mathcal{U}$) represents the convex set of states with no entanglement; the gray area ($\mathcal{P}$) represents the non convex set of states with no quantumness of correlations, as defined in this chapter (Eq.(3.6)); and the light gray area ($\mathcal{C}$) represents the non convex set of states with no exchange correlations due to the particle statistics, possessing only classical correlations. Note that for fermionic particles, the set $\mathcal{C}$ is a null set. The following hierarchy is identified: $\mathcal{C} \subset \mathcal{P} \subset \mathcal{U} \subset \mathcal{Q}$.

it becomes clear that the set given by Eq.(3.6) is a subset of the unentangled one, thereby being quantumness of correlations a more general notion of correlations than entanglement.

According to the activation protocol, different entanglement measures will lead, in principle, to different quantifiers for the quantumness of correlations. We can thus define the measure Q_E for quantumness of correlations, associated with the entanglement measure E, as follows,

$$Q_E(\rho_{\mathcal{Q}}) = \min_V E(\tilde{\rho}_{\mathcal{Q},\mathcal{M}}), \tag{3.16}$$

where $\tilde{\rho}_{\mathcal{Q},\mathcal{M}} = U\Big[(V^{\otimes n}\rho_{\mathcal{Q}}V^{\dagger\otimes n}) \otimes |0\rangle\langle 0|_{\mathcal{M}}\Big]U^{\dagger}$.

We shall consider two different entanglement measures for the bipartite entanglement, the physically motivated distillable entanglement E_D [61] and the relative entropy of entanglement E_r [62, 63]. Note that the output states of the activation protocol have the so called maximally correlated form [64] between system and measurement apparatus, $\tilde{\rho}_{\mathcal{Q},\mathcal{M}} = \sum_{\vec{l},\vec{l}'} \chi^V_{\vec{l},\vec{l}'} \left|f(\vec{l})\right\rangle\!\left\langle f(\vec{l}')\right|_{\mathcal{Q}} \otimes \left|f(\vec{l})\right\rangle\!\left\langle f(\vec{l}')\right|_{\mathcal{M}}$, being $\chi^V_{\vec{l},\vec{l}'} = (\Pi^V_{\vec{l}})^{\dagger}\rho_{\mathcal{Q}}(\Pi^V_{\vec{l}'})$, where $\Pi^V_{\vec{l}} = V^{\otimes n}\Pi_{\vec{l}}$ (see appendix). It is known that the entanglement for such states according to the distillable entanglement [65], as well as for the relative entropy of entanglement [64], is given by $E_{D(r)}(\tilde{\rho}_{\mathcal{Q},\mathcal{M}}) = S(\tilde{\rho}_{\mathcal{Q}}) - S(\tilde{\rho}_{\mathcal{Q},\mathcal{M}})$, where $S(\rho) = -Tr(\rho\ln\rho)$ is the von Neumann entropy. The first term is given by $S(\tilde{\rho}_{\mathcal{Q}}) = S\Big(\sum_{\vec{l}}(\Pi^V_{\vec{l}})^{\dagger}\rho_{\mathcal{Q}}(\Pi^V_{\vec{l}})\left|f(\vec{l})\right\rangle\!\left\langle f(\vec{l})\right|\Big)$, i.e., the entropy of the projected state $\rho_{\mathcal{Q}}$ according to a single-particle von

Neumann measurement, and the second term is simply given by $S(\tilde{\rho}_{\mathcal{Q},\mathcal{M}}) = S(\rho_{\mathcal{Q}})$, since it is invariant under unitary transformations. Thus we have that the quantumness of correlations measure is given by,

$$Q_{E_{D(r)}}(\rho_{\mathcal{Q}}) = \min_{V}\Big[S\Big(\sum_{\vec{l}}(\Pi_{\vec{l}}^{V})^{\dagger}\rho_{\mathcal{Q}}(\Pi_{\vec{l}}^{V})\Big|f(\vec{l})\Big\rangle\Big\langle f(\vec{l})\Big|\Big) - S(\rho_{\mathcal{Q}})\Big], \tag{3.17}$$

which corresponds to the notion of minimum disturbance caused in the system by single-particle measurements. This result is in agreement with the analysis made in [66] for the particular case of two-fermion systems, and to the best of our knowledge is the only study attempting to characterize and quantify a more general notion of correlations between indistinguishable particles. Using analogous arguments as those in [53], it is possible to prove the Eq.(3.17) is an equivalent expression to,

$$Q_{E_{D(r)}}(\rho_{\mathcal{Q}}) = \min_{\xi} S(\rho_{\mathcal{Q}} \parallel \chi), \tag{3.18}$$

where $S(\rho \parallel \chi) = Tr(\rho \ln \rho - \rho \ln \chi)$ is the relative entropy. The above equation introduces a geometrical approach to the particle correlation measure. Notably we see that, as well as for the quantumness of correlations in distinguishable subsystems, the correlations between indistinguishable particles defined in this chapter has a variety of equivalent approaches in order to characterize and quantify it, as shown by the activation protocol (Eq.3.16), minimum disturbance (Eq.3.17) and geometrical approach(Eq.3.18).

3.4 Conclusion

In this work we discussed how to define a more general notion of correlation, called quantumness of correlations, in fermionic and bosonic indistinguishable particles, and presented equivalent ways to quantify it, addressing the notion of an activation protocol, the minimum disturbance in a single-particle von Neumann measurement, and a geometrical view for its quantification. An important result of our approach concerns to the equivalence of these correlations to the entanglement in distinguishable subsystems via the activation protocol, thus settling its usefulness for quantum information processing. It is interesting to note that the approach used in this work is essentially based on the definition of the algebra of single-particle observables, dealing here with the algebra of indistinguishable fermionic, or bosonic, single-particle observables, but we could apply the same idea for identical particles of general statistics, e.g. braid-group statistics, simply by defining the correct single-particle algebra of observables.

3.5 Appendix: maximally correlated states

Let us show that the output states of the activation protocol for indistinguishable particles have the so called maximally correlated form between system and measurement apparatus. If $\{a_{\vec{k}}^{\dagger}|vac\rangle\} = \left\{\left|f(\vec{k})\right\rangle\right\}$ is the system basis, U

is the coupling unitary given by Eq.(3.3), and V is the unitary respective to the single particle transformation, we have that,

$$\begin{aligned} V^{\otimes n}\, a^{\dagger}_{\vec{k}}|vac\rangle &= (\sum_{l_1} v_{k_1 l_1} a^{\dagger}_{l_1}) \cdots (\sum_{l_n} v_{k_n l_n} a^{\dagger}_{l_n})|vac\rangle, \\ &= \sum_{\vec{l}} v_{k_1 l_1} \cdots v_{k_n l_n} \Big| f(\vec{l}) \Big\rangle, \end{aligned} \tag{3.19}$$

where $v_{k_i l_j}$ are the matrix elements of V. A general state for the system can be given as,

$$\rho_{\mathcal{Q}} = \sum_{\vec{k},\vec{k'}} p_{\vec{k},\vec{k'}} \Big| f(\vec{k}) \Big\rangle \Big\langle f(\vec{k'}) \Big|; \tag{3.20}$$

thereby,

$$\begin{aligned} V^{\otimes n} \rho_{\mathcal{Q}} V^{\dagger \otimes n} &= \sum_{\vec{k},\vec{k'},\vec{l},\vec{l'}} p_{\vec{k},\vec{k'}} (v_{k_1 l_1} \cdots v_{k_n l_n}) \, (v_{k'_1 l'_1} \cdots v_{k'_n l'_n})^{\dagger} \Big| f(\vec{l}) \Big\rangle \Big\langle f(\vec{l'}) \Big|, \\ &= \sum_{\vec{l},\vec{l'}} \chi^{V}_{\vec{l},\vec{l'}} \Big| f(\vec{l}) \Big\rangle \Big\langle f(\vec{l'}) \Big|, \end{aligned} \tag{3.21}$$

where $\chi^{V}_{\vec{l},\vec{l'}} = \sum_{\vec{k},\vec{k'}} p_{\vec{k},\vec{k'}} (v_{k_1 l_1} \cdots v_{k_n l_n}) \, (v_{\vec{k'}_1 l'_1} \cdots v_{\vec{k'}_n l'_n})^{\dagger}$. The output states of the activation protocol thus have the form,

$$\begin{aligned} \rho_{\mathcal{Q}:\mathcal{M}} &= U \Big[(V^{\otimes n} \rho_{\mathcal{Q}} V^{\dagger^{\otimes n}}) \otimes |0\rangle\langle 0|_{\mathcal{M}} \Big] U^{\dagger} \\ &= \sum_{\vec{l},\vec{l'}} \chi^{V}_{\vec{l},\vec{l'}} \Big| f(\vec{l}) \Big\rangle \Big\langle f(\vec{l'}) \Big|_{\mathcal{Q}} \otimes \Big| f(\vec{l}) \Big\rangle \Big\langle f(\vec{l'}) \Big|_{\mathcal{M}}, \end{aligned} \tag{3.22}$$

i.e., the maximally correlated form.

CHAPTER 4

Entanglement of indistinguishable particles as a probe for quantum phase transitions in the extended Hubbard model

We investigate the quantum phase transitions of the extended Hubbard model at half-filling with periodic boundary conditions employing the entanglement of particles, as opposed to the more traditional entanglement of modes. Our results show that the entanglement has either discontinuities or local minima at the critical points. We associate the discontinuities to first order transitions, and the minima to second order ones. Thus we show that the entanglement of particles can be used to derive the phase diagram, except for the subtle transitions between the phases SDW-BOW, and the superconductor phases TS-SS.

4.1 Introduction

The connection between two important disciplines of Physics, namely quantum information theory and condensed matter physics, has been the subject of great interest recently, generating much activity at the border of these fields, with numerous interesting questions addressed so far [5]. In particular, the properties of entanglement in many-body systems, and the analysis of its behavior in critical systems deserve special attention.

In this work [67] we deal with the entanglement of indistinguishable fermionic particles in the one dimensional extended Hubbard model (EHM).

We focus in the half-filling case. The model is a generalisation of the Hubbard model [68, 69], which encompasses more general interactions between the fermionic particles, such as an inter-site interaction, thus describing more general phenomena and a richer phase diagram. Precisely, it is given by,

$$\begin{aligned} H_{EHM} &= -t\sum_{j=1}^{L}\sum_{\sigma=\uparrow,\downarrow}(a^{\dagger}_{j,\sigma}a_{j+1,\sigma}+a^{\dagger}_{j+1,\sigma}a_{j,\sigma})+ \\ &\quad + U\sum_{j=1}^{L}\hat{n}_{j\uparrow}\hat{n}_{j\downarrow}+V\sum_{j=1}^{L}\hat{n}_{j}\hat{n}_{j+1}, \end{aligned} \tag{4.1}$$

where L is the lattice size, $a^{\dagger}_{j,\sigma}$ and $a_{j,\sigma}$ are creation and annihilation operators, respectively, of a fermion with spin σ at site j, $\hat{n}_{j,\sigma}=a^{\dagger}_{j,\sigma}a_{j,\sigma}$, $\hat{n}_{j}=\hat{n}_{j,\uparrow}+\hat{n}_{j,\downarrow}$, and we consider periodic boundary conditions (PBC), $L+1=1$. The hopping (tunnelling) between neighbor sites is parametrized by t, while the on-site and inter-site interactions are given by U and V, respectively. Despite the apparent simplicity of the model, it exhibits a very rich phase diagram, which includes several distinct phases, namely: charge-density wave (CDW), spin-density wave (SDW), phase separation (PS), singlet (SS) and triplet (TS) superconductors, and a controversial bond-order wave (BOW). A more detailed description of the model and its phases will be given in the next section.

Our numerical analysis is performed employing entanglement measures for indistinguishable particles introduced recently [27, 28, 14], in conjunction with the density-matrix renormalisation group approach (DRMG)[70, 71], which has established itself as a leading method for the simulation of one dimensional strongly correlated quantum lattice systems. DMRG is a numerical algorithm for the efficient truncation of the Hilbert space of strongly correlated quantum systems based on a rather general decimation prescription. The algorithm has achieved unprecedented precision in the description of static, dynamic and thermodynamic properties of one dimensional quantum systems, quickly becoming the method of choice for numerical studies.

The chapter is organized as follows. In Sec. 4.2 we review the model and its phase diagram. In Sec. 4.3 we present our results. We conclude in Sec. 4.4.

4.2 Extended Hubbard Model

In this section we give a detailed description of the extended Hubbard model [68, 69], and its distinct phases in the half-filling case. The reader familiar with the subject may skip this section.

Many efforts have been devoted to the investigation of the EHM's phase diagram at half-filling, using both analytical and numerical methods [72, 73, 74, 75, 76, 77, 78, 79]. Despite the apparent simplicity of the model, it exhibits a very rich phase diagram which includes several distinct phases: charge-density wave (CDW), spin-density wave (SDW), phase separation (PS), singlet (SS) and triplet (TS) superconductors, and a controversial bond-order wave (BOW). See Fig.4.1 for a schematic drawing of the phase diagram at half-filling.

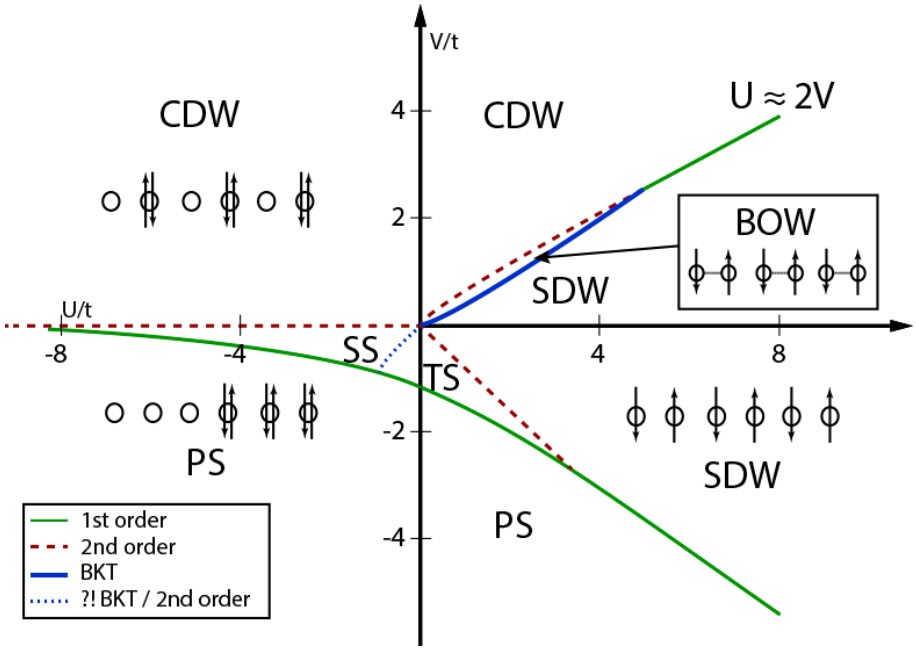

Figure 4.1: Phase diagram of the half-filled extended Hubbard model in one dimension. The distinct phases correspond to the charge-density wave (CDW), the spin-density wave (SDW), phase separation (PS), singlet (SS) and triplet (TS) superconducting phases, and bond-order wave (BOW). The order of the quantum phase transitions is identified by the different line shapes. The order of the two superconducting phases transition (blue dotted line) is controversial, being identified as a BKT transition [73], or a second order transition [72].

In the strong coupling limit ($|U|, |V| \gg t$), one can qualitatively characterize its phases as given by a charge-density wave, spin density wave and a phase separation. For a strong repulsive on-site interaction ($U > 0$, $U \gg V$), the ground state avoids double occupancy and the spin density is periodic along the lattice, leading to an antiferromagnetic ordering, namely spin-density wave. Its order parameter is given by,

$$\mathcal{O}_{sdw}(k) = \frac{1}{L}\sum_{m,n} e^{ik(m-n)}[\langle\sigma_m^z\sigma_n^z\rangle - \langle\sigma_m^z\rangle\langle\sigma_n^z\rangle], \tag{4.2}$$

where $\sigma_j^z = \frac{1}{2}(\hat{n}_{j\uparrow} - \hat{n}_{j\downarrow})$. In the limit $U \to \infty$, the ground state is dominated by the following configurations:

$$|\psi\rangle_{sdw} \approx \frac{1}{\sqrt{2}}(\,|\uparrow,\downarrow,\uparrow,\downarrow,\ldots,\uparrow_{L-1},\downarrow_L\rangle + \\ +|\downarrow,\uparrow,\downarrow,\uparrow,\ldots,\downarrow_{L-1},\uparrow_L\rangle\,), \tag{4.3}$$

where the state is described in the real space mode representation, in which each site can be in the following set of configurations: $\{|0\rangle, |\uparrow\rangle, |\downarrow\rangle, |\uparrow\downarrow\rangle\}$.

Considering a strong repulsive inter-site interaction ($V > 0$, $V \gg U$), a periodic fermionic density is generated, leading to a charge-density wave. Its order parameter is given by,

$$\mathcal{O}_{cdw}(k) = \frac{1}{L}\sum_{m,n} e^{ik(m-n)}[\langle \hat{n}_m \hat{n}_n \rangle - \langle \hat{n}_m \rangle \langle \hat{n}_n \rangle]. \tag{4.4}$$

In the limit $V \to \infty$, the ground state is dominated by the following configurations,

$$|\psi\rangle_{cdw} \approx \frac{1}{\sqrt{2}}\,(\,|\uparrow\downarrow, 0, \uparrow\downarrow, 0, \ldots, \uparrow\downarrow_{L-1}, 0\rangle + \\ + |0, \uparrow\downarrow, 0, \uparrow\downarrow, \ldots, 0, \uparrow\downarrow_{L}\rangle\,). \tag{4.5}$$

In the range of strong attractive interactions ($U, V < 0$ or $U > 0$, $V < 0$ with $|V| \gg |U|$), the fermions cluster together, and the ground state becomes inhomogeneous, with different average charge densities in its distinct spatial regions. Such a phase is called phase separated state. In the limit $V \to -\infty$, the ground state is dominated by the following configurations,

$$|\psi\rangle_{ps} \approx \frac{1}{\sqrt{L}} \sum_{\{\hat{\Pi}\}} \hat{\Pi}\Big|\uparrow\downarrow, \uparrow\downarrow, \ldots, \uparrow\downarrow_{(\frac{L}{2})}, 0, \ldots, 0\Big\rangle, \tag{4.6}$$

where $\{\hat{\Pi}\}$ is the set of translation operators.

In the weak coupling limit, different phases appear. For small attractive inter-site interactions ($V < 0$), superconducting phases are raised, characterized by the pairing correlations,

$$\Delta_x = \frac{1}{\sqrt{L}}\sum_j a_{j,\uparrow} a_{j+x,\downarrow}, \tag{4.7}$$

with the respective order parameter $\mathcal{O}_s = \sum_{x,x'} \langle \Delta_x^\dagger \Delta_{x'} \rangle$. If the on-site interactions are lower than the inter-site interactions ($U \leq 2V$), the fermions will pair as a singlet superconductor, characterized by nearest-neighbor ($\Delta_{ss_{nn}}$) or on-site (Δ_{ss_o}) singlet pairing correlations given by,

$$\begin{aligned} \Delta_{ss_{nn}} &= \Delta_x - \Delta_{-x} \\ &= \frac{1}{\sqrt{L}}\sum_j (a_{j,\uparrow} a_{j+x,\downarrow} - a_{j,\downarrow} a_{j+x,\uparrow}), \end{aligned} \tag{4.8}$$

$$\Delta_{ss_o} = \Delta_0 = \frac{1}{\sqrt{L}}\sum_j a_{j,\uparrow} a_{j,\downarrow}, \tag{4.9}$$

where $x = 1$. On the other hand, if the on-site interactions are higher than the inter-site interactions ($U \geq 2V$), we have a triplet superconductor, characterized by nearest-neighbor triplet pairing correlations ($\Delta_{ts_{nn}}$) given by,

$$\begin{aligned} \Delta_{ts_{nn}} &= \Delta_x + \Delta_{-x} \\ &= \frac{1}{\sqrt{L}}\sum_j (a_{j,\uparrow} a_{j+x,\downarrow} + a_{j,\downarrow} a_{j+x,\uparrow}), \end{aligned} \tag{4.10}$$

where $x = 1$.

Note that the difference between the singlet and triplet pairing correlations is simply a plus or minus sign. It can be clarified if we consider, for example, the case of two fermions in a singlet or triplet spin state, given by $(|ij\rangle \pm |ji\rangle)\,(|\uparrow\downarrow\rangle \mp |\downarrow\uparrow\rangle)$. Expanding this state, we have,

$$\begin{aligned} & |ij\rangle(|\uparrow\downarrow\rangle \mp |\downarrow\uparrow\rangle) \pm |ji\rangle(|\uparrow\downarrow\rangle \mp |\downarrow\uparrow\rangle) \\ = \;& |i\uparrow, j\downarrow\rangle \mp |i\downarrow, j\uparrow\rangle \pm |j\uparrow, i\downarrow\rangle - |j\downarrow, i\uparrow\rangle \\ = \;& (|i\uparrow, j\downarrow\rangle - |j\downarrow, i\uparrow\rangle) \mp (|i\downarrow, j\uparrow\rangle - |j\uparrow, i\downarrow\rangle) \\ = \;& \left(a^\dagger_{i\uparrow}a^\dagger_{j\downarrow} \mp a^\dagger_{i\downarrow}a^\dagger_{j\uparrow}\right)|vac\rangle, \end{aligned} \tag{4.11}$$

where the lower/upper sign corresponds to the singlet/triplet pairing correlation.

The last phase in the diagram is the controversial bond-order-wave (BOW). By studying the EHM ground state broken symmetries, using level crossings in excitation spectra, obtained by exact diagonalization, Nakamura [73] argued for the existence of a novel bond-order-wave phase for small to intermediate values of positive U and V, in a narrow strip between CDW and SDW phases. This phase exhibits alternating strengths of the expectation value of the kinetic energy operator on the bonds, and is characterized by the following order parameter,

$$\begin{aligned} \mathcal{O}_{bow}(k) = \frac{1}{L}\sum_{m,n} e^{ik(m-n)}[&\langle B_{m,m+1}B_{n,n+1}\rangle \\ &-\langle B_{m,m+1}\rangle\langle B_{n,n+1}\rangle], \end{aligned} \tag{4.12}$$

where $B_{m,m+1} = \sum_\sigma (a^\dagger_{m,\sigma}a_{m+1,\sigma} + H.c.)$ is the kinetic energy operator associated with the mth bond. Nakamura argued that the CDW-SDW transition is replaced by two separate transitions, namely: (i) a continuous CDW-BOW transition; and (ii) a Berezinskii-Kosterlitz-Thouless (BKT) spin-gap transition from BOW to SDW. Such remarkable proposal was later confirmed by several works [74, 75, 76, 77, 78, 79], employing different numerical methods, like DMRG, Monte Carlo or exact diagonalization. Nevertheless, while the BOW-CDW phase boundary can be well resolved, since it involves a standard second order (continuous) phase transition, the SDW-BOW boundary is more difficult to locate, for it involves a BKT transition in which the spin gap opens exponentially slowly as one enters the BOW phase. The precise location of the BOW phase is then still a subject of debate. To the best of our knowledge, the best estimates for the transitions, taking $U/t = 4$, correspond to a CDW-BOW transition at $V/t \approx 2.16$ [74, 75, 78, 79], and to a BOW-SDW transition in the range $V/t \approx 1.88 - 2.00$ [74, 75, 78, 79], or $V/t = 2.08 \pm 0.02$ [76].

4.3 Entanglement and Quantum Phase Transitions

The computation of the single particle correlations, and consequently the entanglement of particles, was numerically performed using DMRG. Although DMRG is less accurate for problems with periodic boundary conditions (PBC)

than with open boundary conditions (OBC), from the Physical viewpoint PBC are strongly preferable over OBC, as boundary effects are eliminated and finite size extrapolations can be performed for much smaller system sizes. In this work we analyze the extended Hubbard model considering PBC. Our simulations were performed for systems up to $L = 352$ sites, always keeping a large enough dimension (m) for the renormalized matrices (ranging from $m = 100$ to 1000) and number of sweeps (~ 20 sweeps), in order to obtain an accurate precision. In Fig.4.2 (all figures and tables with our results are at the end of the chapter), we see that m ranging from 200 to 300 is enough for an entanglement accuracy of the order of $\mathcal{O}(10^{-4})$. The accuracy for the ground state energy, as well as the truncation error, using such parameters, are of the order of $\mathcal{O}(10^{-7})$.

Our results for the entanglement of particles in the extended Hubbard model at half-filling are shown in Fig.4.3, to be dissected below. It is remarkable that such picture highlights the known phase diagram of the model. We first note that, as expected, we have a maximum of entanglement at the strong coupling limits ($E_p \to 1$), and as we decrease the interactions between the particles, the entanglement tends also to decrease, until the unentangled case for the non interacting Hamiltonian ($U = V = 0$). The figure thus presents the shape of a valley around this point. Following then the discontinuities and the local minimum points in the entanglement, we can easily identify the quantum phase transitions, except for both the subtle SDW-BOW transition, and the transition between the superconductor phases TS-SS. In the former case, one needs to recall that the observation of the BOW phase is by itself a hard task, since its gap opens exponentially slowly, and also that there are evidences that such transition is of infinite order [80, 81]. Therefore we believe that a possible detection of such transition by the entanglement of particles would require higher precision numerical analysis as well as the study of larger lattice sizes. Concerning the TS-SS transition, on the one hand the order of the two superconducting phases transition is controversial, being identified as a BKT transition [73] as well as a second order one [72] in the literature. On the one hand, we would be led to strengthen the result of a BKT transition, since our entanglement does not detect it. On the other hand, it is reasonable the apathy of the entanglement of particles on distinguishing the two phases, since the correlations between the particles in the two superconducting phases have essentially the same characteristics. Thus it is hard to precisely conclude the reason for the failure to detect such transition with our measure of entanglement.

The discontinuities in the entanglement are directly identified with the first order quantum phase transitions, whereas the minimum points are identified with the second order quantum phase transitions. When crossing a first order transition, the ground state energy presents a discontinuity and consequently also its observables. In this way, the eigenvalues "λ_k" of the single particle reduced density matrix (Eq.(2.61)), and the entanglement obtained from them, should present a discontinuity. The occurrence of the minimum points are due to the divergence of the correlation length when approaching the second order transitions. As described in the previous section,

the eigenvalues "λ_k" are given in momentum space by the Fourier transform of the real space quadratures "$\left\langle a^{\dagger}_{j\sigma} a_{l\sigma} \right\rangle$" (Eq.(2.61)). In this way, if we are close to the transitions, such real space quadratures tend to become delocalised or spread out along the lattice, thus leading to more localised eigenvalue distributions in momentum space, and consequently to smaller von Neumann entropies. It is worth remarking that such behavior is the opposite of the entanglement of modes, where the sites are maximally entangled at the second order transitions. As an example, see in Fig.4.4 the eigenvalue distribution for a system with $L = 128$ sites when crossing the BOW-CDW quantum phase transition.

We present now the entanglement behavior in some specific slices of the phase diagram with $L = 128$, in order to clarify the above discussion and results. More specifically, we show the entanglement behavior in the PS-SS-CDW, PS-SS-SDW, and PS-SDW-CDW transitions. Notice that our finite-size scaling analysis showed that in thermodynamic limit the entanglement behavior is qualitatively similar (see Appendix), with a scaling inversely proportional to the lattice size, $E_p = aL^{-1} + b$, where a and b are constants.

4.3.1 PS-SS-CDW

In Fig.4.5 we see the entanglement behavior across the PS-SS-CDW phases. We clearly see, for any fixed attractive on-site interaction ($U/t < 0$), a discontinuity in the entanglement followed by a local minimum point, as we increase the value of the inter-site interactions V/t. The discontinuity is related to the first order transition PS-SS, while the local minimum is related to the second order transition SS-CDW. We see, however, that the SS-CDW transition is not located exactly at $V/t = 0$, as expected from the phase diagram described in the literature, but at a value close to this one. We believe that this discrepancy is related to finite-size effects.

4.3.2 PS-TS-SDW

In Fig.4.6 we see the entanglement behavior across the PS-TS-SDW phases. We see again the two kinds of behavior for any fixed attractive inter-site interaction ($V/t < 0$): a first discontinuity, related to the first order transition PS-TS, followed by a local minimum point related to the second order transition TS-SDW. Note that, for large values of the attractive inter-site interaction, $V/t \simeq -1.5$, the discontinuity and minimum converge to the same point, and there is no TS phase anymore.

4.3.3 PS-SDW-(BOW)-CDW

In Fig.4.7 we see the entanglement behavior across the PS-SDW-BOW-CDW phases. We see that, as we increase the value of the inter-site interactions, for any fixed repulsive on-site interactions ($U/t > 0$), the entanglement identifies two transitions. Firstly we see a discontinuity, related to the first order transition PS-SDW, followed then by: (i) a discontinuity, when considering large

U/t, or (ii) a local minimum point, when considering small U/t. Such discontinuity is related to the first order SDW-CDW transition, while the minimum points are related to the second order BOW-CDW transition (the SDW-BOW transition is not seen, as aforementioned). We see that the transitions to the CDW phase occur at $U \approx 2V$. Performing a finite-size scaling analysis (see Appendix) we obtain that, for $U/t = 4$, the BOW-CDW transition is located at $V/t = 2.11 \pm 0.01$, which is slightly lower than the literature results, namely $V/t \approx 2.16$ [74, 75, 78, 79].

4.4 Conclusion

We studied the entanglement of indistinguishable particles in the extended Hubbard model at half-filling, with focus on its behavior when crossing the quantum phase transitions. Our results showed that the entanglement either has discontinuities, or presents local minima, at the critical points. We identified the discontinuities as first order transitions, and the minima as second order transitions. In this way, we concluded that the entanglement of particles can "detect" all transitions of the known diagram, except for the subtle transitions between the superconductor phases TS-SS, and the transition SDW-BOW.

It is also interesting to compare our results with other entanglement measures, such as the entanglement of modes, which was widely studied in several models, as well as in the extended Hubbard model [82, 83, 81]. Gu *et al.* [82] firstly showed that the entanglement of modes, i.e., the entanglement of a single site with the rest of the lattice, could detect three main symmetry broken phases, more specifically, the CDW, SDW and PS. Other phases were not identified due to the fact that they are associated to off-diagonal long-range order. Further investigation were performed analysing the block-block entanglement [83, 81], i.e., the entanglement of a block with l sites with the rest of the lattice ($L - l$ sites), showing that this more general measure could then detect the transition to the superconducting phase, as well as the bond-order phase. The measure, however, could not detect the SS-TS transition, besides presenting some undesirable finite-size effects in the PS phase. On the other hand, the entanglement of particles studied in this work showed no undesirable finite-size effects in the PS phase, but could not detect the superconductor SS-TS transition either. Regarding the BOW phase, from the above discussion we see that it would be worth to analyze more general measures for the entanglement of particles, which goes beyond single particle information. Some steps in this direction were made in [12], where a notion of entanglement of "subgroups" of indistinguishable particles was defined.

4.5 Appendix: Finite-size scaling analysis

In this appendix we perform a finite-size scaling analysis in the system entanglement, in order to extract information about the ground state of the model. We obtained that the entanglement behavior is qualitatively the same for lattices larger than $L \approx 100$, with just small differences of the order of

$\mathcal{O}(10^{-2})$ in its magnitude. In a general way, the entanglement scales with the inverse of the lattice size, $E_p = aL^{-1} + b$, where a and b are constants. See in Fig.4.8 , for example, the entanglement scaling for the SDW-BOW-CDW phase transitions. In Tab. I we show the computed values for the scaling constants at different points in the phase diagram, as highlighted in Fig.4.3.

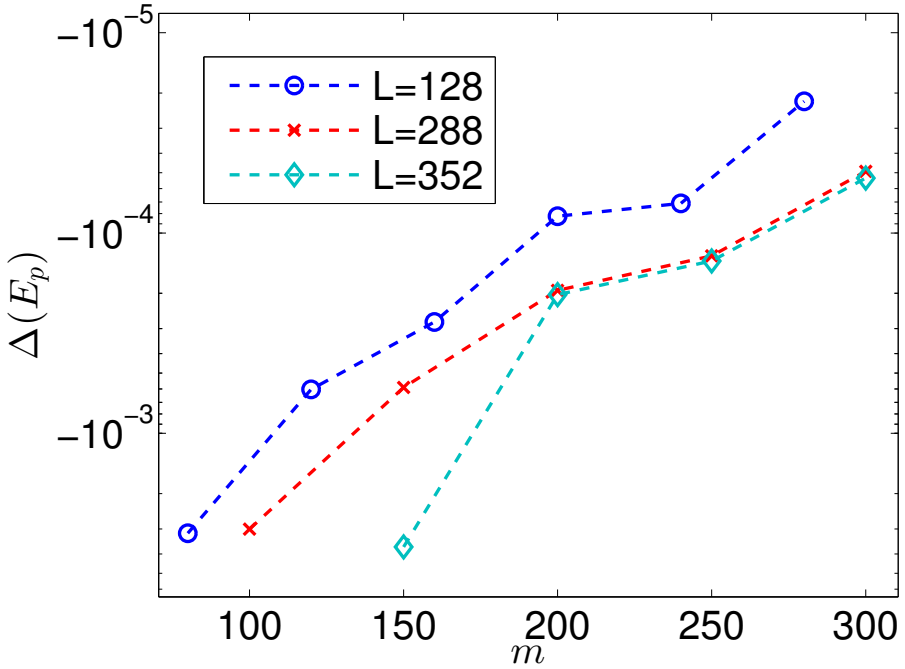

Figure 4.2: Accuracy analysis for the computation of entanglement of particles using DMRG. It is shown the accuracy of the entanglement, $\Delta(E_p) = E_p(m) - E_p(m-50)$, as a function of m (dimension of the renormalized matrices), at the point $U = 4, V = 2.11$, and using 20 sweeps in the computation, which is enough for the ground state convergence.

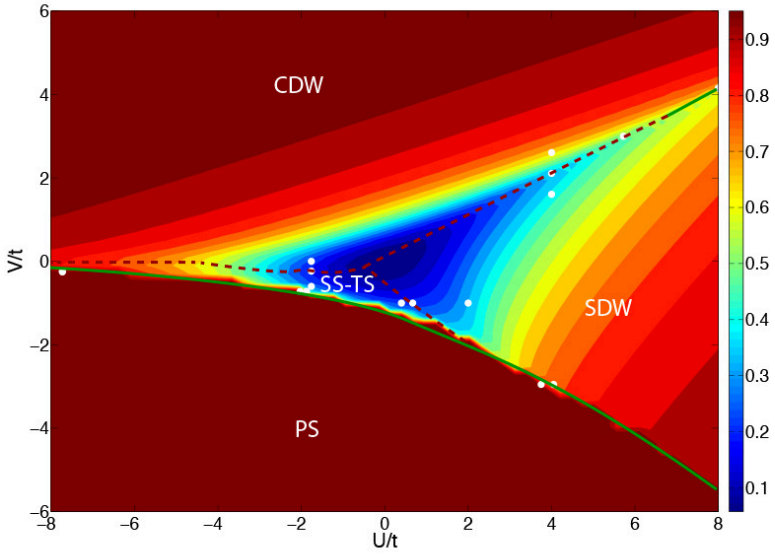

Figure 4.3: Contour map for the entanglement of particles "E_p" as a function of the interaction terms V/t and U/t, in a system with $L = 128$ sites at half-filling. The entanglement behavior in the thermodynamic limit, $L \to \infty$, keeping fixed the filling $n = N/L = 1$, is qualitatively the same, with slight differences of the order of $\mathcal{O}(10^{-2})$ in its magnitude; see Appendix 4.5 for a detailed discussion. The (green) continuous line denotes the discontinuity at the entanglement function, while the (red) dashed line denotes the local minima. The white dots correspond to the points where we performed a detailed finite-size scaling analysis (see Table I in Appendix 4.5).

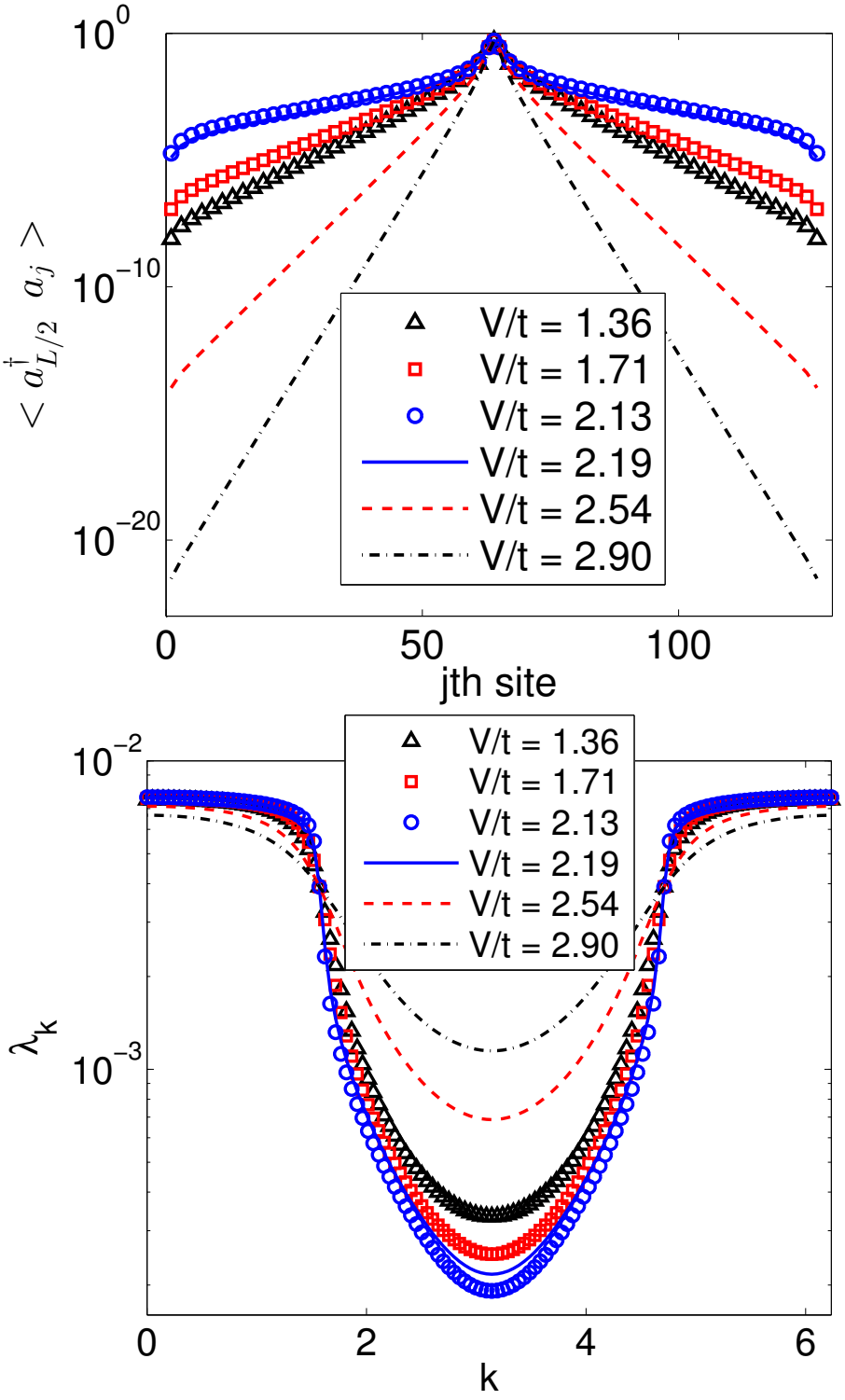

Figure 4.4: **(top)** Single particle quadratures "$\left\langle a^\dagger_{L/2} a_j \right\rangle$" along the lattice sites, and **(bottom)** eigenvalue distribution "λ_k" for the single particle reduced state in a fixed spin sector, as given in Eq.(2.61). We consider a fixed $U/t = 4$. The vertical axis is in log-scale, in order to make clearer the visualisation. As we approach the BOW-CDW quantum phase transition point, at $V/t \approx 2.13$, we see that the quadratures tend to delocalise along the lattice, whereas the eigenvalue distribution becomes more localised.

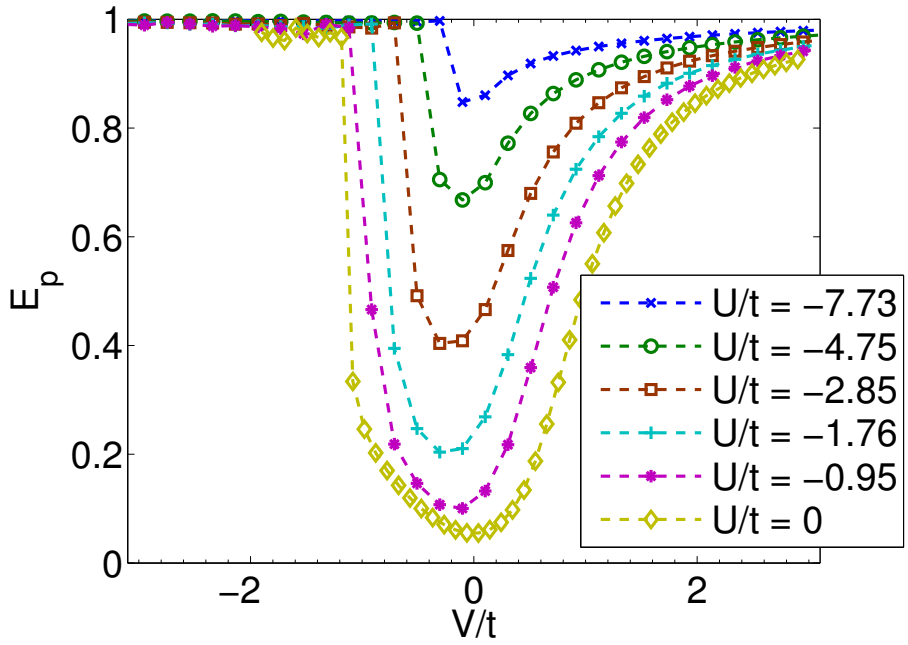

Figure 4.5: Entanglement behavior across the PS-SS-CDW phases. The entanglement, for any fixed atractive on-site interaction (U/t), is characterized by a discontinuity (PS-SS transition), followed by a local minimun (SS-CDW transition).

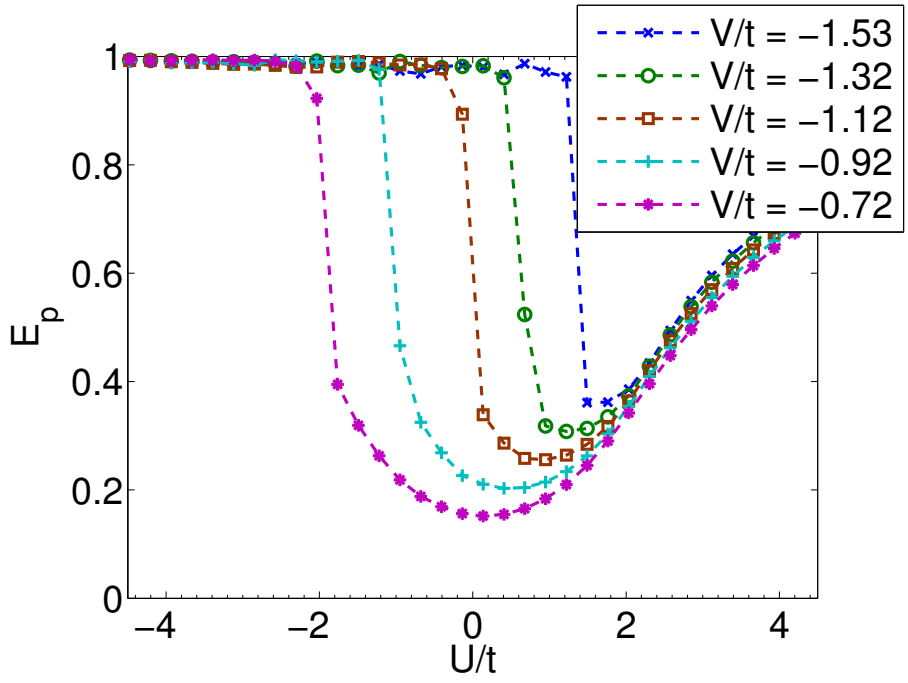

Figure 4.6: Entanglement behavior across the PS-TS-SDW phases. The entanglement, for any fixed atractive inter-site interaction (V/t), is characterized by a discontinuity (PS-TS transition), followed by a local minimun (TS-SDW transition). For large V/t, the two transitions shrink at the same point, and there is no TS phase anymore.

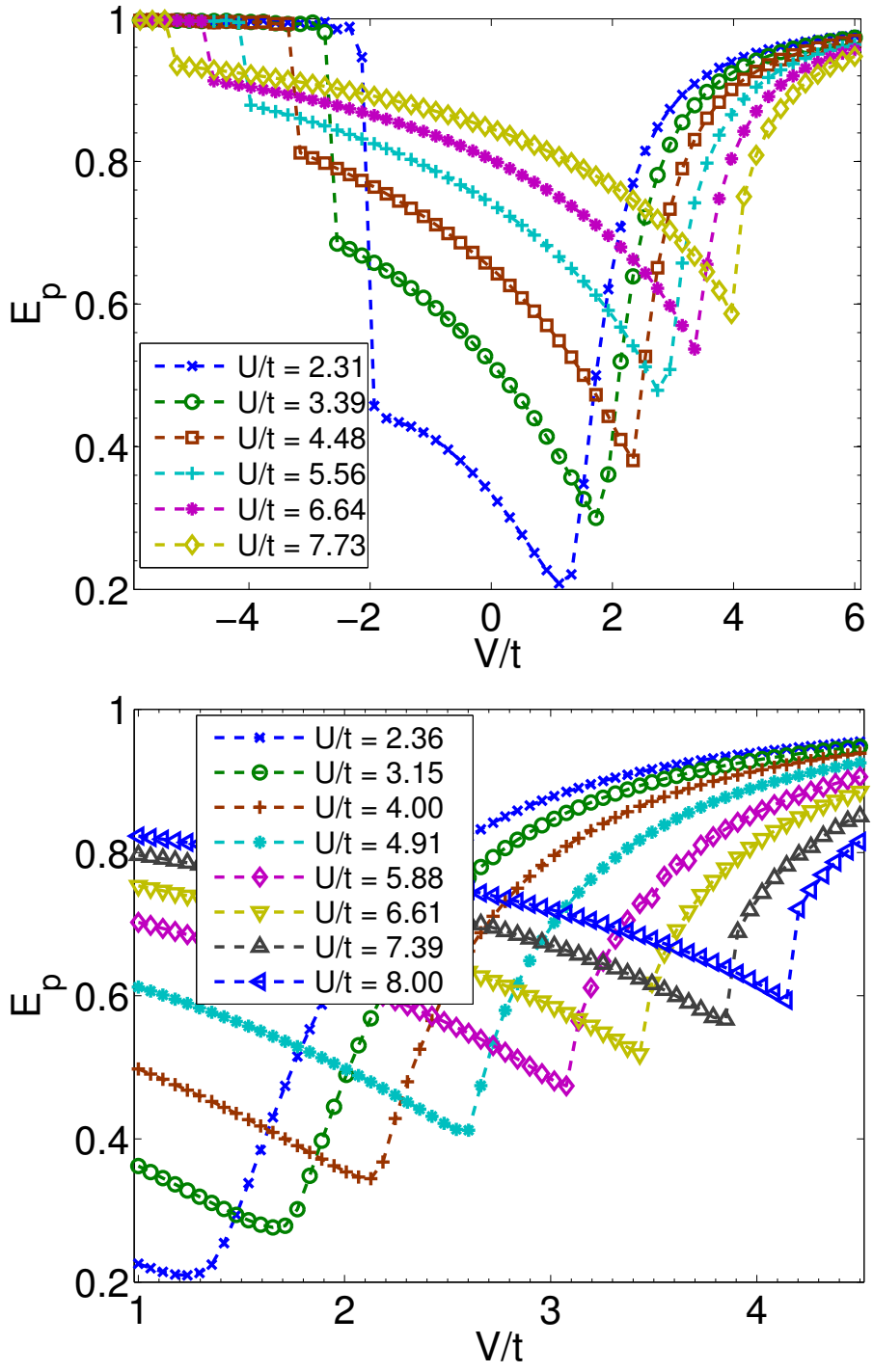

Figure 4.7: Entanglement behavior across the PS-SDW-BOW-CDW phases. The **bottom** panel is a magnification of the **top** panel in the region $1 \leq V/t \leq 4.5$. The entanglement, for any fixed repulsive on-site interaction (U/t), is characterized by a discontinuity (PS-SDW transition), followed by: (i) a discontinuity for large V/t (SDW-CDW transition), or (ii) local minimun points for small V/t (BOW-CDW transition).

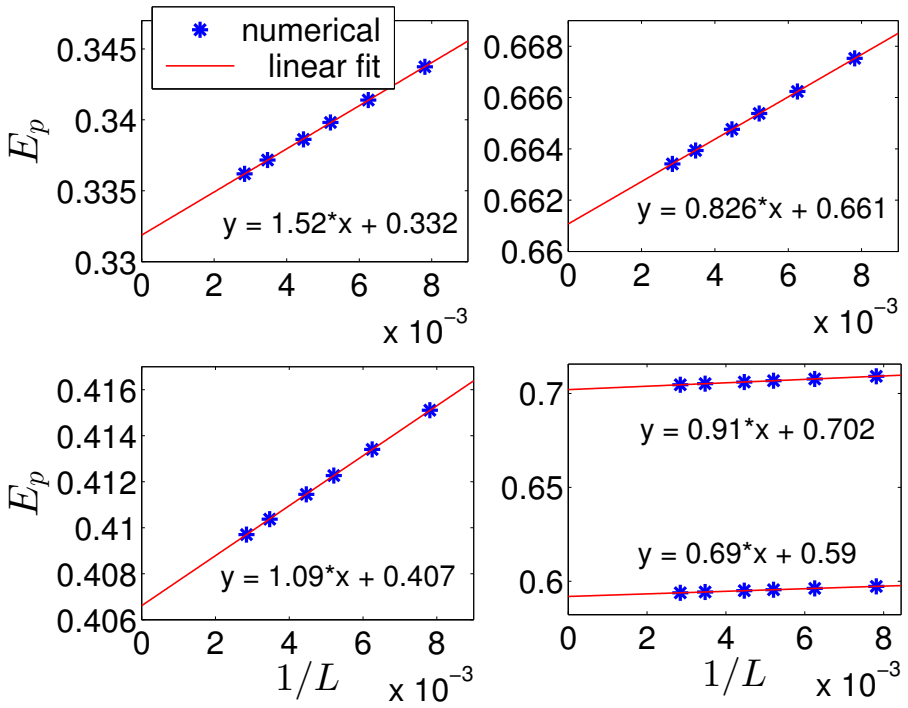

Figure 4.8: Scaling of the entanglement at the SDW-BOW-CDW phase transitions. For a fixed parameter $U/t = 4$, we have: **(upper-left)** minimum entanglement critical point $(V/t)_c = 2.11$; **(upper-right)** $V/t = (V/t)_c + 0.5$; **(bottom-left)** $V/t = (V/t)_c - 0.5$. For a fixed $U/t = 8$ **(bottom-right)**, there is a discontinuity in the entanglement, highlighted by the scaling at $V/t = 4.147$ (bottom curve), and $V/t = 4.153$ (upper curve).

$U/t(\pm 0.01)$	$V/t(\pm 0.01)$	$E_p(L \to \infty)(\pm 0.001)$	$a(\pm 0.001)$
4	1.61	0.407	1.09
4^*	2.11^*	0.332	1.52
4	2.61	0.661	0.826
8	4.147	0.59	0.69
8	4.153	0.702	0.91
5.723^*	3^*	0.457	0.911
-1.76	-0.6	0.273	2.41
-1.76^*	-0.233^*	0.174	3.08
-1.76	0	0.211	2.51
0.4	-1	0.211	2.11
0.67^*	-1^*	0.204	2.59
2	-1	0.33	2.48
-7.73	-2.55	0.995	$-$
-7.73	-2.33	0.884	0.69
-2.03	-0.72	0.978	$-$
-1.875	-0.72	0.403	7.59
3.75	-2.95	0.985	$-$
4.05	-2.95	0.772	0.439

Table 4.1: Scaling constants for the entanglement, $E_p = aL^{-1} + E_p(L \to \infty)$, at different points of the phase diagram, as highlighted in Fig.4.3. The symbol "$*$" denotes the critical points, and "$-$" means that the entanglement is constant, apart from numerical inaccuracy, for the analyzed lattices.

Part II

Topological states of matter in a number conserving setting

CHAPTER 5

Topological states of matter

In a general perspective, matter has many distinct phases, such as ordinary gas, liquid and solid phases, as well as more interesting conductors, insulators, superfluids, and others phases. Despite formed by the same elementary particle constituents, each phase has striking different properties. The properties of a phase emerge from the pattern in which the particles are organized and correlated in the material. These different patterns are usually called the *order* of the phase.

As a very simple example, one could consider an ordinary liquid, such as liquid water. In such a phase the particles (atoms) are randomly distributed in the material, in such a way that it remains invariant under an arbitrary translation of its particles. We say that it has a "continuous translation symmetry". If we increase the external pressure, or decrease the temperature of the material, we know that it becomes a solid after a critical point, with clear distinct macroscopical properties. The material suffers a phase transition at this point. In a solid phase, also called as a crystal phase, the particles are now organized in a regular pattern, remaining unchanged only by some specific translations of its particles. Thus, we say that the crystal has "discrete translation symmetry". We see that such a liquid-solid phase transition *breaks* the symmetries of the state, or equivalently, breaks its internal order. Such a transition is called as *spontaneous symmetry breaking* transition, and constitutes the essence of Landau's theory [84] in order to systematically understand and characterize the different phases of matter. Landau's theory is a very successful theory, and for a long time it was believed that it could describe all possible orders on materials and its phase transitions. We know today, however, that this is not true, and the main reason comes from the fact that such a theory does not takes into account quantum effects, so one should not be surprised if there are states at zero-temperature which can not be characterized by the theory.

We recall that the concept of order for distinct quantum phases was implicitly discussed in Chapter.4, at the presentation of the phase diagram

for the extended Hubbard model. All the phases were there characterized by a distinct local order "O_j" acting at the neighborhood of site j, studying its correlations along the lattice "$\langle O_j O_{j+r}\rangle - \langle O_j\rangle\langle O_{j+r}\rangle$".

We are now able to introduce the main focus of this work: the study of states which present a different kind of order than the ones presented above, a "*topological order*" [87, 88]. Such states can not be described simply by Landau symmetry breaking theory, nor by any local order parameter. A topological order is a kind of order, for systems at zero temperature, which is intrinsically quantum, and involves *non-local order parameters*; in other words, it can be seen, in a general perspective, as a global pattern of collective correlations between the particles in the system, which leads to patterns of *long-range entanglements*. Topological states are very interesting not only due to its paradigm breaks in the understanding and characterization of distinct phases of matter, as well as, due to its amazing physical properties, such states could have wide technological applications, such as in topological quantum computation. We will discuss the aforementioned points in more details now.

Historically, in the late 1980's, it has become apparent in the study of the Quantum Hall Effect (QHE) that some states might not be described by Landau's theory nor any local order parameter. QHE is observed by the confinement of electrons in a $2D$ space, under the influence of a external magnetic field, and cooled to a very low temperature ($\sim 1K^o$). In such a picture, physicists found that the resistivity R_H (Hall coefficient) of the induced current flow presents itself as several plateaus as we vary the external magnetic field. Furthermore, such a resistivity is quantized in a very specific way: as a rational number $R_h = p/q$. An intriguing feature is that the distinct ground states of such system, corresponding to the distinct plateaus in the resistivity, have all the same symmetries according to Landau's theory (chiral symmetry). It was then realized that, in order to completely characterize these states one must take into account other properties of the ground state, as its topological order! Wen [87, 88], in a very beautiful presentation, shows that the different plateaus in the resistivity are related to different "global dancing pattern", where all electrons round around each other in a very specific way. The number of rounds the electrons perform around each other generate the different plateaus in the resistivity. A formal definition of such order could be given by looking at its Berry phase, the fractional statistics of its quasiparticles, and other properties of the phase... we will not go, however, deeper into such subjects for this phase.

In general, topological states share some interesting properties:
- degenerate ground state subspace;
- robustness against local perturbations;
- edge excitations;
- non-local correlations;
- ....

In this thesis we focus into the analysis of topological states of matter in fermionic systems. A minimal setting showcasing all the key aspects of topological states in such systems consist of the paradigmatic Kitaev model.

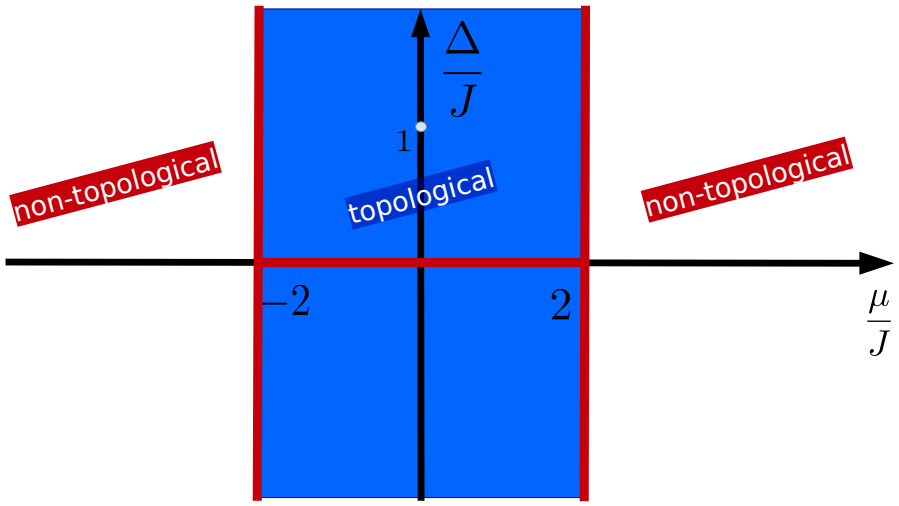

Figure 5.1: Phase diagram of the Kitaev Hamiltonian for a one-dimensional chain of spinless fermions (Eq.(5.1)). The topological phase is within the blue region, $|\mu| < 2J$ and $\Delta \neq 0$, where the red lines correspond to the phase transitions to a non-topological phase. The gray dot at $\mu = 0$, and $\Delta = J > 0$, corresponds to the "sweet point" of the model.

The ground states of such model presents all aforementioned topological properties, which we will discuss in detail now.

5.1 Kitaev Hamiltonian

The Kitaev Hamiltonian for a one-dimensional chain of spinless fermions [89] is given by,

$$\hat{H}_K = \sum_j \left[-J\hat{a}_j^\dagger \hat{a}_{j+1} - \Delta \hat{a}_j \hat{a}_{j+1} + H.c. - \mu\left(\hat{n}_j - 1/2\right)\right].$$

Here, $J > 0$ denotes the hopping amplitude, μ and Δ the chemical potential and the superconducting gap, respectively; $\hat{a}_j^{(\dagger)}$ are fermionic annihilation (creation) operators on site j, and $\hat{n}_j \equiv \hat{a}_j^\dagger \hat{a}_j$. This model has i) two density-driven phase transitions from finite densities to the empty and full states at $|\mu| = 2J$ (for $\Delta \neq 0$), and ii) a transition driven by the competition of kinetic and interaction energy (responsible for pairing) at $\Delta/J = 0$ (for $|\mu| < 2J$) (see Fig.5.1). For $|\mu| < 2J$ and $\Delta \neq 0$, the ground state is unique for periodic boundary conditions, but twofold degenerate for open geometry, hosting localized edge zero-energy Majorana modes. This topological phase is symmetry protected by total fermionic parity $\hat{P} = (-1)^{\hat{N}}$, where $\hat{N} \equiv \sum_j \hat{n}_j$.

Let us focus on the so-called "sweet point", namely $\mu = 0$, and $\Delta = J > 0$ and real, which enjoys the property

$$\hat{H}_K = (J/2)\sum_j \hat{d}_j^\dagger \hat{d}_j = iJ\sum_j \gamma_{2j}\gamma_{2j+1}, \tag{5.1}$$

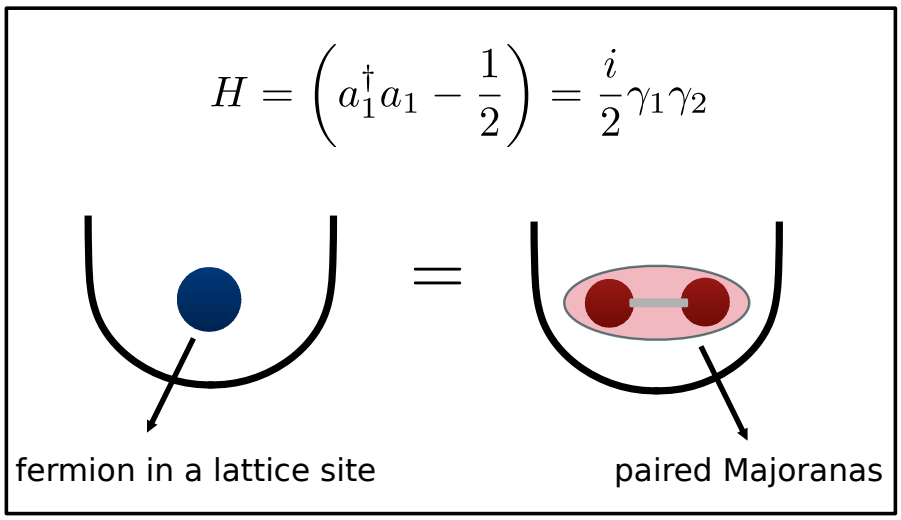

Figure 5.2: Majorana fermions can be roughly seen as "half fermions", representing the real or imaginary part of a fermion. Schematically we represent a fermion in a lattice site (blue circle) as two paired Majorana fermions (red circles connected by a light gray wire).

with $\hat{d}_j = \hat{C}_j^\dagger + \hat{A}_j$, $\hat{C}_j^\dagger = \hat{a}_j^\dagger + \hat{a}_{j+1}^\dagger$, $\hat{A}_j = \hat{a}_j - \hat{a}_{j+1}$ ($\hat{d}_L$ is defined identifying $L+1 \equiv 1$) and $\{\gamma_j\}_{j=1}^{2L}$ are Majorana operators satisfying the Clifford algebra,

$$\gamma_{2j-1} = i(a_j - a_j^\dagger), \tag{5.2}$$

$$\gamma_{2j} = a_j + a_j^\dagger, \tag{5.3}$$

with $\gamma_j^\dagger = \gamma_j$, and $\{\gamma_j, \gamma_l\} = 2\delta_{j,l}$. Such Majorana operators can be seen as "half fermions" representing the real and imaginary part of a fermion (notice the inverse relation $a_j = (\gamma_{2j} - i\gamma_{2j-1})/2$), as schematically presented in Fig.5.2.

The ground state ($|g\rangle$) of such Hamiltonian for periodic boundary conditions, satisfying $\hat{d}_j|g\rangle = 0, \forall j$, is described by a fermionic p-wave superfluid. We see that, if the system has open boundary conditions, the absence of the term "$\hat{d}_L^\dagger \hat{d}_L$" in the Hamiltonian, where $\hat{d}_L = (\gamma_{2L} - i\gamma_1)/2$, induces a degeneracy in the ground state, related to a zero energy mode; more precisely, adding the non-local fermion $\hat{d}_L^\dagger$ does not change the energy, and in this way the ground state subspace will be spanned by the following eigenstates: $|g\rangle$ and $\hat{d}_L^\dagger|g\rangle$. This degeneracy corresponds to a highly delocalized fermion, or alternatively, to completely localized Majorana edge modes γ_1 and γ_{2L}. See a schematically picture in Fig.5.3.

We will use both momentum as well as real space representation in order to describe the ground state. We denote $|G_K\rangle / |\psi\rangle_{e(o)}$ for its momentum/real space representation. In momentum space, the ground state is formally

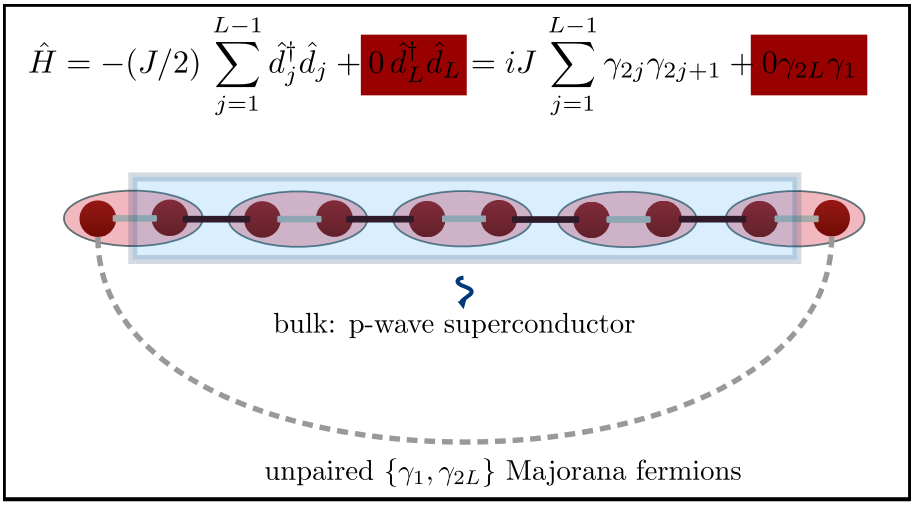

Figure 5.3: Schematic representation for the Kitaev Hamiltonian at the "sweet point" $\mu = 0$, and $\Delta = J > 0$, with periodic conditions. The missing term "$\hat{d}_L^\dagger \hat{d}_L$" leads to a topological degeneracy related to localized edge Majorana fermions γ_1 and γ_{2L}, or alternatively, to a non-local fermion $\hat{d}_L^\dagger$.

described by a p-wave superconductor,

$$\begin{cases} L\,odd: & |G_K\rangle \propto (x_o + x_1 \hat{d}_L^\dagger)|BCS, \alpha = 1\rangle, \\ L\,even: & |G_K\rangle \propto (x_o + x_1 \hat{d}_L^\dagger) a_{k=0}^\dagger |BCS, \alpha = 1\rangle, \end{cases} \tag{5.4}$$

where L is the number of the sites in the chain, $|x_0|^2 + |x_1|^2 = 1$, and $|BCS, \alpha\rangle$ is the BCS state with a fixed phase α. Setting $x_0 = 1, x_1 = 0$ we recover the periodic boundary conditions ground state. The BCS state is defined by,

$$|BCS, \alpha\rangle = \mathcal{N}_\alpha \left[\prod_{k>0} (1 + \alpha \varphi_k a_{-k}^\dagger a_k^\dagger)\right] |vac\rangle \tag{5.5}$$

where $\mathcal{N}_\alpha = \prod_{k>0}(1 + |\alpha\varphi_k|^2)^{-1/2}$ is a global normalization constant, α is an arbitrary complex number, $\varphi_k = -i\,[tan(k/2)]^{-1}$, and $a_k^\dagger = \sum_j e^{-ikj} a_j^\dagger$ are the momentum fermionic operators, where $k = (-\pi, -\pi + 2\pi/L, ..., \pi - 2\pi/L)$. The detailed demonstration is given in Appendix A.

In the real space representation, the ground states can be written [90] as the equal weighted superposition of all even (e) or odd (o) particle number states:

$$|\psi\rangle_{e(o)} = \mathcal{N}_{e(o),L}^{-1/2} \sum_n (-1)^n \sum_{\{\vec{j}_{2n(2n+1)}\}} \left|\vec{j}_{2n(2n+1)}\right\rangle . \tag{5.6}$$

Here $|\vec{j}_m\rangle = \hat{a}_{j_1}^\dagger \hat{a}_{j_2}^\dagger ... \hat{a}_{j_m}^\dagger |\text{vac}\rangle$ with $j_i < j_{i+1}$ ($j_i = 1, \ldots, L$) and $\mathcal{N}_{e,L} = \sum_n \binom{L}{2n}$; $\mathcal{N}_{o,L} = \sum_n \binom{L}{2n+1}$ (see Appendix B).

We are now equipped to present our studies and results concerning topological Majorana edge modes in a number conserving setting.

CHAPTER 6

Localized Majorana-like modes in a number conserving setting: An exactly solvable model

In this chapter we present, in a number conserving framework, a model of interacting fermions in a two-wire geometry supporting non-local zero-energy Majorana-like edge excitations. The model has an exactly solvable line, on varying the density of fermions, described by a topologically non-trivial ground state wave-function. Away from the exactly solvable line we study the system by means of the numerical density matrix renormalization group. We characterize its topological properties through the explicit calculation of a degenerate entanglement spectrum and of the braiding operators which are exponentially localized at the edges. Furthermore, we establish the presence of a gap in its single particle spectrum while the Hamiltonian is gapless, and compute the correlations between the edge modes as well as the superfluid correlations. The topological phase covers a sizeable portion of the phase diagram, the solvable line being one of its boundaries.

6.1 Introduction

Large part of the enormous attention devoted in the last years to topological superconductors owes to the exotic quasiparticles such as Majorana modes, which localize at their boundaries (edges, vortices, ...) [91, 92] and play a key role in several robust quantum information protocols [93]. Kitaev's p-wave superconducting quantum wire [89] provides a minimal setting showcasing all the key aspects of topological states of matter in fermionic systems. The existence of a so-called "sweet point" supporting an exact and easy-to-

handle analytical solution puts this model at the heart of our understanding of systems supporting Majorana modes. Various implementations in solid state [94, 95] and ultracold atoms [96] via proximity to superconducting or superfluid reservoirs have been proposed, and experimental signatures of edge modes were reported [97].

Kitaev's model is an effective mean-field model and its Hamiltonian does not commute with the particle number operator. Considerable activity has been devoted to understanding how this scenario evolves in a number-conserving setting [98, 99, 100, 101, 102]. This effort is motivated both by the fundamental interest in observing a topological parity-symmetry breaking while a U(1) symmetry is intact, and by an experimental perspective, as in several setups (e.g. ultracold atoms) number conservation is naturally present. It was realised that a simple way to promote particle number conservation to a symmetry of the model, while keeping the edge state physics intact, was to consider at least two coupled wires rather than a single one [98, 99, 100]. However, since attractive interactions are pivotal to generate superconducting order in the canonical ensemble, one usually faces a complex interacting many-body problem. Therefore, approximations such as bosonization [98, 99, 100], or numerical approaches [101] were invoked. An exactly solvable model of a topological superconductor in a number conserving setting, which would directly complement Kitaev's scenario, is missing, although recent work pointed out an exacly solvable, number conserving model analogous to a non-local variant of the Kitaev chain [102].

In this chapter we present an exactly solvable model of a topological superconductor which supports exotic Majorana-like quasiparticles at its ends and retains the fermionic number as a well-defined quantum number. The construction of the Hamiltonian with local two-body interactions and of its ground state draws inspiration from recent work on dissipative state preparation for ultracold atomic fermions [103, 104, 105], here applied to spinless fermions in a two-wire geometry. The solution entails explicit ground state wave-functions, which feature all the main qualitative properties highlighted so far for this class of models, with the advantage of being easy-to-handle.

In particular, we establish the following key features: i) The existence of one/two degenerate ground states depending on the periodic/open boundaries with a two-fold degenerate entanglement spectrum; ii) the presence of exponentially localized, symmetry-protected edge states and braiding matrices associated to this degeneracy; iii) exponential decay of the fermionic single particle correlations, even if the Hamiltonian is gapless with collective, quadratically dispersing bosonic modes; iv) p-wave superconducting correlations which saturate at large distance.

By tuning the ratio of interaction vs. kinetic energy of our model, we can explore its properties outside the exactly-solvable line. The full phase diagram (Fig. 6.1) is obtained by means of density matrix renormalization group (DMRG) calculations. The exactly solvable is found to stand between a stable topological phase and a phase-separated state. This finding is rationalized by a relation to the ferromagnetic XXZ chain.

6.2 The model

We begin by recapitulating some properties of the Kitaev chain, as presented in Chapter 5.1, whose Hamiltonian reads [89]

$$\hat{H}_K = \sum_j \big[-J\hat{a}_j^\dagger \hat{a}_{j+1} - \Delta \hat{a}_j \hat{a}_{j+1} + H.c. - \mu\big(\hat{n}_j - 1/2\big)\big].$$

Here, $J > 0$ denotes the hopping amplitude, μ and Δ the chemical potential and the superconducting gap, respectively; $\hat{a}_j^{(\dagger)}$ are fermionic annihilation (creation) operators on site j, and $\hat{n}_j \equiv \hat{a}_j^\dagger \hat{a}_j$. This model has i) two density-driven phase transitions from finite densities to the empty and full states at $|\mu| = 2J$ (for $\Delta \neq 0$), and ii) a transition driven by the competition of kinetic and interaction energy (responsible for pairing) at $\Delta/J = 0$ (for $|\mu| < 2J$). For $|\mu| < 2J$ and $\Delta \neq 0$, the ground state is unique for periodic boundary conditions, but twofold degenerate for open geometry, hosting localized zero-energy Majorana modes. This topological phase is symmetry protected by total fermionic parity $\hat{P} = (-1)^{\hat{N}}$, where $\hat{N} \equiv \sum_j \hat{n}_j$.

Let us focus on the so-called "sweet point", namely $\mu = 0$, and $\Delta = J > 0$ and real, which enjoys the property $\hat{H}_K = (J/2)\sum_j \hat{d}_j^\dagger \hat{d}_j$ with $\hat{d}_j = \hat{C}_j^\dagger + \hat{A}_j$, $\hat{C}_j^\dagger = \hat{a}_j^\dagger + \hat{a}_{j+1}^\dagger$ and $\hat{A}_j = \hat{a}_j - \hat{a}_{j+1}$ ($\hat{d}_L$ is defined identifying $L+1 \equiv 1$). For open geometry, the two ground states with L sites satisfy $\hat{d}_j|\psi\rangle = 0$, for $1 \leq j \leq L-1$, and can be written [90] as the equal weighted superposition of all even (e) or odd (o) particle number states:

$$|\psi\rangle_{e(o)} = \mathcal{N}_{e(o),L}^{-1/2} \sum_n (-1)^n \sum_{\{\vec{j}_{2n(2n+1)}\}} \left|\vec{j}_{2n(2n+1)}\right\rangle . \tag{6.1}$$

Here $|\vec{j}_m\rangle = \hat{a}_{j_1}^\dagger \hat{a}_{j_2}^\dagger ... \hat{a}_{j_m}^\dagger |\text{vac}\rangle$ with $j_i < j_{i+1}$ ($j_i = 1, \ldots, L$) and $\mathcal{N}_{e,L} = \sum_n \binom{L}{2n}$; $\mathcal{N}_{o,L} = \sum_n \binom{L}{2n+1}$.

We now turn to a number conserving version of this model on a single wire [104]. Consider the Hamiltonian $\hat{H}'_K \equiv \sum_j \hat{L}_j^\dagger \hat{L}_j$, with $\hat{L}_j = \hat{C}_j^\dagger \hat{A}_j$, whose exact ground state wave-functions can be obtained as follows. Since $\hat{A}_j|\psi\rangle_{e(o)} = -\hat{C}_j^\dagger|\psi\rangle_{e(o)}$, $|\psi\rangle_{e(o)}$ are also ground states of $\hat{H}'_K$: $\hat{L}_i|\psi\rangle_{e(o)} = 0$ because $(\hat{C}_j^\dagger)^2 = 0$. As $\hat{L}_i$ conserves the particle number, $[\hat{L}_i, \hat{N}] = 0$, we can classify ground states for each fixed particle number sector N by number projection, $|\Psi, N\rangle = \hat{P}_N|\psi\rangle_{e(o)}$. This is implemented by choosing the state with $2n = N$ (or $2n+1 = N$) in the sum over n in Eq. (6.1), and adjusting the normalization to $\mathcal{N}_{L,N} = \binom{L}{N}$. The positive semi-definiteness of $\hat{H}'_K$ implies that these states, having zero energy eigenvalue, are ground states. However, once N is fixed, the ground state $|\Psi, N\rangle$ is unique, as follows from the Jordan-Wigner mapping to the Heisenberg model [84]. The topological twofold degeneracy is lost.

Guided by the previous analysis, we construct an exactly solvable topological two-wire model with canonical fermionic operators $\hat{a}_j^{(\dagger)}$, $\hat{b}_j^{(\dagger)}$. In addition to those involving each wire $\hat{L}_{a(b),j} = \hat{C}_{a(b),j}^\dagger \hat{A}_{a(b),j}$, we introduce new

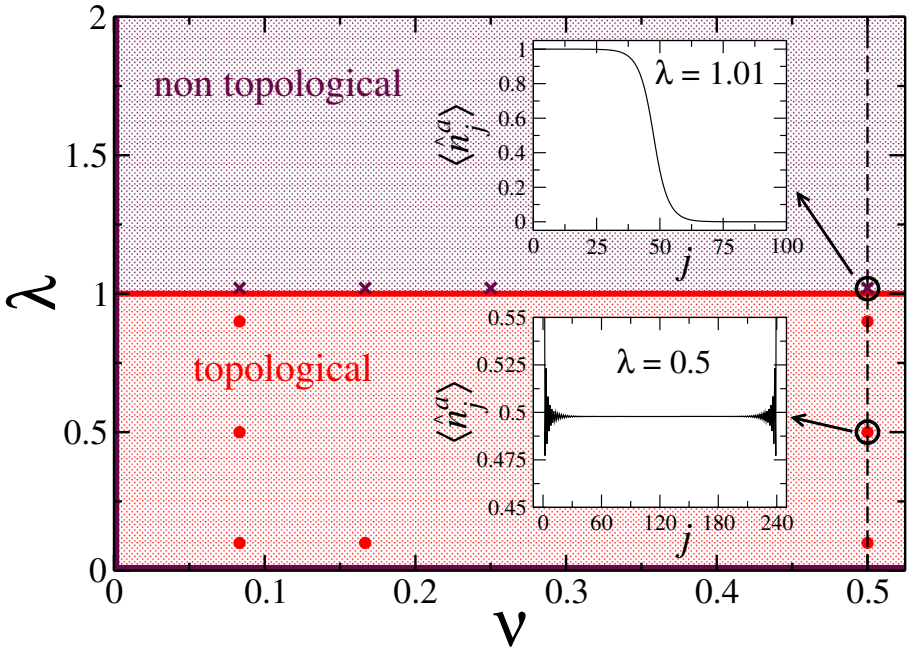

Figure 6.1: Phase diagram for the number and local parity conserving two-wire model (6.3) as a function of λ and filling $\nu = N/2L$ obtained through DRMG simulations. The exactly solvable topological line is at $\lambda = 1$ (another, trivially solvable non-topological line is at $\lambda = 0$). For $\lambda > 1$, the system undergoes phase separation (see the density profile $\langle \hat{n}_j^a \rangle$ in the inset). For $0 < \lambda < 1$ and $\nu \neq 0, 1$, the system is in a homogeneous topological phase (see inset). The phase diagram is symmetric with respect to half filling $\nu = 1/2$ due to particle-hole symmetry of $\hat{H}_\lambda$.

operators $\hat{L}_{I,j} = \hat{C}^\dagger_{a,j}\hat{A}_{b,j} + \hat{C}^\dagger_{b,j}\hat{A}_{a,j}$. The Hamiltonian

$$\hat{H} = \sum_{\alpha=a,b,I} \sum_{j=1}^{L-1} \hat{L}^\dagger_{\alpha,j}\hat{L}_{\alpha,j} \tag{6.2}$$

coincides with the $\lambda = 1$ point of the following more general model:

$$\begin{aligned}\hat{H}_\lambda =& 4\sum_{\substack{j=1\\ \alpha=a,b}}^{L-1}\left[(\hat{\alpha}^\dagger_j\hat{\alpha}_{j+1}+\text{H.c.}) - (\hat{n}^\alpha_j + \hat{n}^\alpha_{j+1}) + \lambda\hat{n}^\alpha_j\hat{n}^\alpha_{j+1}\right] \\ & - 2\lambda\sum_{j=1}^{L-1}\Big[(\hat{n}^a_j + \hat{n}^a_{j+1})(\hat{n}^b_j + \hat{n}^b_{j+1}) - (\hat{a}^\dagger_j\hat{a}_{j+1}\hat{b}^\dagger_j\hat{b}_{j+1} \\ & + \hat{a}^\dagger_j\hat{a}_{j+1}b^\dagger_{j+1}\hat{b}_j - 2\hat{b}^\dagger_j\hat{b}^\dagger_{j+1}\hat{a}_{j+1}\hat{a}_j + H.c.)\Big].\end{aligned} \tag{6.3}$$

$\hat{H}_\lambda$ conserves the total particle number $\hat{N} = \hat{N}_a + \hat{N}_b$ and the local wire parities $\hat{P}_{a,b} = (-1)^{\hat{N}_{a,b}}$, which act as protecting symmetries for the topological

phase. The coupling λ tunes the relative strength of the kinetic and interaction terms similarly to Δ/J in $\hat{H}_K$. Although only $\lambda = 1$ is exactly solvable, we will later consider $\lambda \neq 1$ to explore the robustness of the analytical results. The phase diagram is anticipated in Fig. 6.1.

6.3 Exact results for $\lambda = 1$

For a fixed particle number N and open boundaries, the ground state of $\hat{H}$ is twofold degenerate, due to the freedom in choosing the local parity. For even N, the ground states read

$$|\psi_L(N)\rangle_{ee} = \mathcal{N}_{ee,L,N}^{-1/2} \sum_{n=0}^{N/2} \sum_{\substack{\{\vec{j}_{2n}\},\\ \{\vec{q}_{N-2n}\}}} |\vec{j}_{2n}\rangle_a \otimes |\vec{q}_{N-2n}\rangle_b, \tag{6.4}$$

$$|\psi_L(N)\rangle_{oo} = \mathcal{N}_{oo,L,N}^{-1/2} \sum_{n=0}^{N/2-1} \sum_{\substack{\{\vec{j}_{2n+1}\},\\ \{\vec{q}_{N-2n-1}\}}} |\vec{j}_{2n+1}\rangle_a \otimes |\vec{q}_{N-2n-1}\rangle_b$$

where $\mathcal{N}_{ee,L,N} = \sum_{n=0}^{N/2} \binom{L}{2n}\binom{L}{N-2n}$; $\mathcal{N}_{oo,L,N} = \sum_{n=0}^{N/2-1} \binom{L}{2n+1}\binom{L}{N-2n-1}$. The states $|\vec{j}\rangle_a$ and $|\vec{q}\rangle_b$ are simple generalizations of the states $|\vec{j}\rangle$ defined in Eq.(6.1) to the wire a and b respectively. These describe the cases of even (*ee*) or odd (*oo*) particle numbers in each of the wires. For odd N, the ground states $|\psi_L(N)\rangle_{eo(oe)}$ with an even (odd) number of particles in either wire take the identical sum structure as above with the normalization $\mathcal{N}_{ee,L,N}$ in both cases. The wave-functions (6.4) are the unique ground states of the model (Appendix 6.7). An interesting interpretation of $|\psi_L(N)\rangle_{\sigma\sigma'}$ is in terms of number projection of the ground state of two decoupled even-parity Kitaev chains $|\mathrm{G}\rangle = |\psi\rangle_e^a \otimes |\psi\rangle_e^b$:

$$\begin{aligned} |\psi_L(N)\rangle_{ee} &\propto \hat{P}_N|\mathrm{G}\rangle; \qquad |\psi_L(N)\rangle_{oo} \propto \hat{P}_N \hat{d}_L^{a\dagger}\hat{d}_L^{b\dagger}|\mathrm{G}\rangle; \\ |\psi_L(N)\rangle_{oe} &\propto \hat{P}_N \hat{d}_L^{a\dagger}|\mathrm{G}\rangle; \quad |\psi_L(N)\rangle_{eo} \propto \hat{P}_N \hat{d}_L^{b\dagger}|\mathrm{G}\rangle; \end{aligned} \tag{6.5}$$

where $\hat{d}_L^{a\dagger}$ and $\hat{d}_L^{b\dagger}$ are the zero-energy modes of the decoupled Kitaev wires at half filling. This interpretation provides intuition that the two-fold ground-state degeneracy is absent for periodic boundary conditions: since on a circle $\hat{H}_K$ has a unique ground state, the ground state of $\hat{H}$ with N particles is also unique (Appendix 6.7).

Important evidence of a topologically nontrivial bulk state is obtained from the double degeneracy of the entanglement spectrum, which we now compute for one of the wave-functions (6.4). To this end, we consider the reduced state of l sites on each wire $\rho_l = \mathrm{Tr}_{(L-l)}\left[|\psi_L(N)\rangle_{ee}\langle\psi_L(N)|_{ee}\right]$. Taking the symmetries into account, it can be written in diagonal form as (Appendix 6.7)

$$\rho_l = \sum_{N_l=0}^{min(2l,N)} \sum_{\sigma,\sigma'} \chi^{(L,N)}_{(\sigma\sigma',l,N_l)} |\psi_l(N_l)\rangle_{\sigma\sigma'}\langle\psi_l(N_l)|_{\sigma\sigma'} \tag{6.6}$$

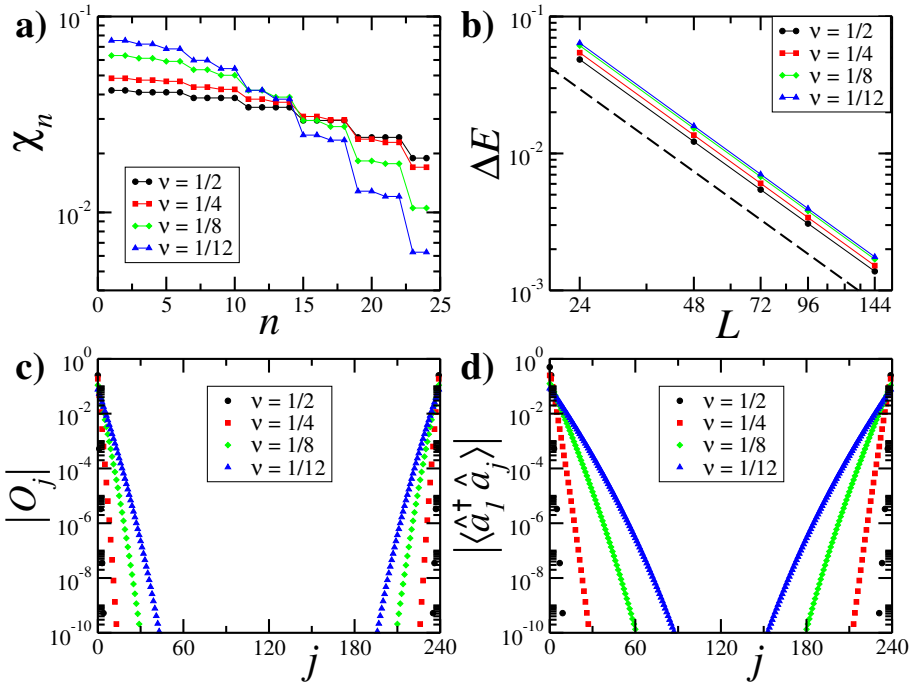

Figure 6.2: Analysis of model $\hat{H}$. (a) Entanglement spectrum for a reduced state ρ_l with $l = 60$ for $L = 240$. (b) DMRG results for the scaling of the gap computed at fixed parity, which is compatible with L^{-2} (dashed line); here the number of kept states is $m = 400$. (c) Localization of the edge mode computed via $|\langle\psi_L(N)|_{oo}\hat{a}_j^\dagger\hat{b}_j|\psi_L(N)\rangle_{ee}|$. (d) Single-fermion edge correlations $|\langle\hat{a}_1^\dagger\hat{a}_j\rangle|$ computed for a system of size $L = 240$. The wave-function is shift invariant, such that $|\langle\hat{a}_i^\dagger\hat{a}_{i+j}\rangle| \equiv |\langle\hat{a}_1^\dagger\hat{a}_j\rangle|$ $(i + j \leq L)$.

with the following nonzero eigenvalues: for N_l even

$$\chi^{(L,N)}_{(ee(oo),l,N_l)} = \mathcal{N}_{ee(oo),l,N_l}\mathcal{N}_{ee(oo),L-l,N-N_l}/\mathcal{N}_{ee,L,N}$$

whereas for N_l odd

$$\chi^{(L,N)}_{(eo,l,N_l)} = \chi^{(L,N)}_{(oe,l,N_l)} = \chi^{(L,N)}_{(ee,l,N_l)}.$$

In the odd-particle number sector the entanglement spectrum is manifestly twofold degenerate. In the even one, such degeneracy appears in the thermodynamic limit: $\chi^{(L,N)}_{(ee,l,N_l)}/\chi^{(L,N)}_{(oo,l,N_l)} \to 1$ (see Appendix 6.7 and Fig. 6.2a).

An interesting insight is provided by $O_j \equiv \langle\psi_L(N)|_{oo}\hat{a}_j^\dagger\hat{b}_j|\psi_L(N)\rangle_{ee}$, where $\hat{a}_j^\dagger\hat{b}_j$ is the only single-site operator which commutes with $\hat{N}$ and changes the local parities $\hat{P}_{a,b}$, so that the two ground states can be locally distinguished. The calculation of such matrix elements leads to a lengthy combinatorial expression (Appendix 6.7) and is shown in Fig. 6.2c. We interpret the exponential decay of O_j into the bulk as a clear signature of localized edge

modes with support in this region only. At half filling the edge states are maximally localized, but away from half filling the number projection increases the localization length. In the thermodynamic limit, this length diverges for $\nu \equiv N/2L \to 0, 1$, indicating a topological phase transition. We emphasize that this exponential behavior is different from [98, 99], reporting algebraic localization of the edge states, but similar to [101, 107]. Non-local correlations of edge states are another clear indication of topological order and can be proven via $\langle \hat{a}_1^\dagger \hat{a}_j \rangle$, which is sizeable both at $j \sim 1$ and $j \sim L$ (see the analytical expression in Appendix (6.7) and Fig. 6.2d).

Furthermore, the Hamiltonian is gapless and hosts long wavelength collective bosonic excitations, while the single fermion excitations experience a finite gap. This is a crucial property of the ground state; the absence of gapless fermion modes in the bulk ensures the robustness of the zero energy edge modes, in analogy to non-interacting topologically non-trivial systems. The gapped nature of single fermion excitations is established via the exponential decay of the fermionic two-point function, e.g. $\langle \hat{a}_i^\dagger \hat{a}_j \rangle$. Again, the resulting formula is a lengthy combinatorial expression (Appendix 6.7), evaluated numerically for very large sizes and plotted in Fig. 6.2d. For $\nu \to 0, 1$, the correlation length diverges, indicating the vanishing of the fermion gap and a thermodynamic, density-driven phase transition in full analogy to the Kitaev chain.

On the other hand, the analysis of the superfluid correlations demonstrates the existence of gapless modes. The p-wave nature of these correlations follows from the correlation of the pairing operator $\hat{a}_{j+1}\hat{a}_j$. A direct calculation (Appendix 6.7) shows a saturation at large distance

$$\left\langle \hat{a}_i^\dagger \hat{a}_{i+1}^\dagger \hat{a}_{j+1} \hat{a}_j \right\rangle \xrightarrow{L\to\infty} \nu^2 (1-\nu)^2 \,. \tag{6.7}$$

Similar expressions hold for cross-correlations between the wires. The finite asymptotic value in Eq. (6.7) hints at the absence of bosonic modes with linear dispersion, which would lead to algebraic decay. A DMRG analysis of the excitation spectrum of $\hat{H}$ for system sizes up to $L = 144$ demonstrates a vanishing of its gap $\sim L^{-2}$ (Fig. 6.2b). This indicates the presence of collective excitations with quadratic dispersion. Further support to this statement is provided from the fact that Eq. (6.3) without the wire coupling term reduces to the XXZ model at the border of its ferromagnetic phase, which hosts quadratically dispersing spin waves, $\omega \sim q^2$. This dispersion, with dynamic exponent $z = 2$, gives rise to an effective phase space dimension $d_{\text{eff}} = z + 1 = 3$ at zero temperature, explaining the constancy of superfluid correlations due to the absence of a divergence in the soft mode correlators. This finding is special for $\lambda = 1$.

6.4 Non-abelian statistics

We now proceed to demonstrate that the edge modes obey a non-abelian statistics completely equivalent to that of Majorana fermions – i.e., Ising anyons. Consider the operator $\hat{B}_{aR,bR}(j) = (\hat{\mathcal{I}} + \hat{Z}_{aR,bR,j})/\sqrt{2}$ with $j <$

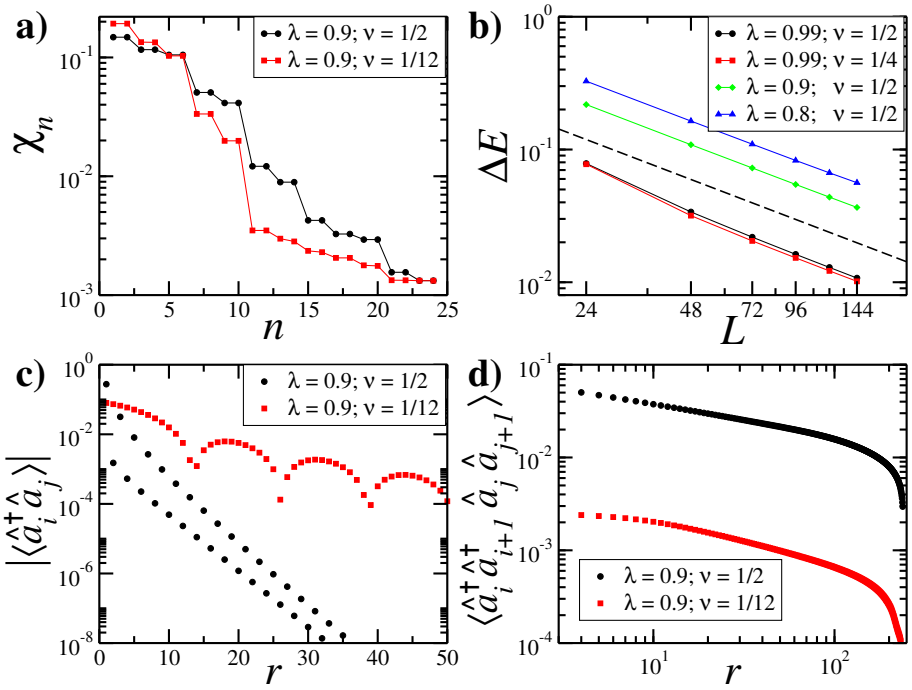

Figure 6.3: DMRG results for model $\hat{H}_\lambda$. (a) Entanglement spectrum for a reduced state ρ_l with $l = 100$ for $L = 240$ ($m = 300$). (b) Algebraic scaling of the gap computed at fixed parity, which is compatible with L^{-1} (dashed line). Here $m = 420$. (c, d) Single-particle $|\langle \hat{a}_i^\dagger \hat{a}_j \rangle|$ and p-wave superfluid $\langle \hat{a}_i^\dagger \hat{a}_{i+1}^\dagger \hat{a}_j \hat{a}_{j+1} \rangle$ correlations at distance $r = |i - j|$ computed in the bulk of system with $L = 240$ ($m = 300$). Analogous data were obtained for other values of ν, λ (red circles in Fig. 6.1).

$L/2$, where $\hat{Z}_{aR,bR,j} = (\sum_{p=1}^{j} [\prod_{q=0}^{p-1} \hat{Y}_{aR,bR,q}] \hat{X}_{aR,bR,p})/\mathcal{F}(j)$, with $\hat{X}_{aR,bR,j} = (a^\dagger_{L+1-j} b_{L+1-j} - b^\dagger_{L+1-j} a_{L+1-j})$, $\hat{Y}_{aR,bR,j} = n^a_{L+1-j} n^b_{L+1-j} + (1 - n^a_{L+1-j})(1 - n^b_{L+1-j})$ for $j > 0$, $\hat{Y}_{aR,bR,0} = \hat{\mathcal{I}}$ and $\mathcal{F}_j = \sqrt{1 - [\nu^{2j} + (1-\nu)^{2j}]}$. $\hat{B}_{aR,bR}(j)$ is thus exponentially localized at the right edge of the ladder and an analogous operator $\hat{B}_{aL,bL}(j)$ can be defined at the left edge through the transformation mapping an operator at site l to site $L + 1 - l$ (and viceversa). Similarly, the operators $\hat{B}_{aR,aL}(j)$ and $\hat{B}_{bL,bR}(j)$ can be defined through the transformations $b_{L+1-l} \to -i a_l$ and $a_{L+1-l} \to -i b_l$, respectively. In general, one can define operators $\hat{B}_{m\Lambda,m'\Lambda'}(j)$ with $m, m' = a, b$ and $\Lambda, \Lambda' = L, R$. These operators have the following key properties: They (i) are exponentially localized at the edges, (ii) act unitarily in the ground state subspace, (iii) are particle number conserving, and (iv) most importantly, provide a representation of Majorana braiding operators. From this we conclude that the localized edge modes behave as non-abelian Majorana fermions [108], in full analogy to the case of two neighboring Kitaev wires. Properties (i)–(iii) are demonstrated in Appendix 6.7, whereas here we focus on (iv). Strictly speaking, properties

(ii) and (iv) are only true apart from an error which is exponentially small in j and L, which can always be made negligible. In this case we can define the braiding operator $\hat{R}_{m\Lambda,m'\Lambda'} \equiv \hat{B}_{m\Lambda,m'\Lambda'}(j)$. We initialize the system in the state $|\psi_L(N)\rangle_{ee}$ and then perform two braiding operations on the edges in different sequences. If we consider for example $\hat{R}_{aR,aL}$ and $\hat{R}_{aR,bR}$ we obtain $[\hat{R}_{aR,aL}, \hat{R}_{aR,bR}]|\psi_L(N)\rangle_{ee} = i|\psi_L(N)\rangle_{oo}$ which demonstrates the non-abelian character of these operations. Moreover, this is the pattern that the conventional braiding operators produce on two neighboring Kitaev wires $\hat{R}'_{m\Lambda,m'\Lambda'} = e^{\frac{\pi}{4}\gamma_{m\Lambda}\gamma_{m'\Lambda'}} = (\mathcal{I} + \gamma_{m\Lambda}\gamma_{m'\Lambda'})/\sqrt{2}$, where $\gamma_{m\Lambda}$ are Majorana operators fulfilling the Clifford algebra appearing at the left and right ($\Lambda = L, R$) edges of two Kitaev wires $m = a, b$. This pattern coincides for the application of $[\hat{R}_{m\Lambda,m'\Lambda'}, \hat{R}_{n\Upsilon,n'\Upsilon'}]$ on all $|\psi_L(N)\rangle_{\sigma\sigma'}$ states (see e.g. [109]). In other words, the operators $\hat{R}_{m\Lambda,m'\Lambda'}$ form a number-conserving representation of Majorana braiding operators on the ground state subspace.

6.5 Numerical results

To further explore the status of these results, we now move to the full model $\hat{H}_\lambda$ away from the solvable line $\lambda = 1$. The study is performed with DMRG on systems with sizes up to $L = 240$ and open boundary conditions.

We first establish the absence of a topological phase for $\lambda > 1$. The density profile, shown in the inset of Fig. 6.1 for $\nu = 0.5$ and $\lambda = 1.01$, displays a clear phase-separation tendency. Analogous data are obtained for other values of ν (see dark crosses in Fig. 6.1). These results can be intuitively understood considering that $\hat{H}_{\lambda>1}$ without interwire coupling can be mapped to a gapped ferromagnetic XXZ model with domain walls dual to fermionic phase separation.

For $\lambda < 1$, simulations support the existence of a homogeneous phase (Fig. 6.1). Note that $\lambda = 0$ is a free-fermion point trivially non-topological. For $\lambda \neq 0$ we observe: i) two quasi-degenerate ground states with different relative parity and same particle numbers, ii) degenerate entanglement spectrum, iii) a gap closing as L^{-1} for fixed parity, iv) exponentially decaying single-fermion correlations, v) power-law decaying superfluid correlators. Plots in Fig. 6.3 display our numerical results. Simulations at lower filling $\nu \to 0$ and small λ are more demanding, owing to the increasing correlation length of the system. The numerics is consistent with the phase diagram in Fig. 6.1 exhibiting a topological phase delimited by three trivial lines at $\lambda = 0$, $\nu = 0$ and $\nu = 1$ and an inhomogeneous non-topological phase for $\lambda > 1$. The exactly solvable topological line at $\lambda = 1$ serves as a boundary; the fixed-ν phase diagram is reminiscent of the ferromagnetic transition in the XXZ model.

6.6 Conclusion

We presented an exactly solvable two-wire fermionic model which conserves the number of particles and features Majorana-like exotic quasiparticles at the edges. Our results can be a valuable guideline to understand topological edge states in number conserving systems. For example, the replacement

$\hat{a}_i \to \hat{c}_{i,\uparrow}, \hat{b}_i \to \hat{c}_{i,\downarrow}$ results in a one-dimensional spinful Hubbard Hamiltonian without continuous spin rotation, but time reversal symmetry. The resulting model with an exactly solvable line belongs to the class of time reversal invariant topological superconductors [112], analyzed in a number conserving setting recently [107], with edge modes protected by the latter symmetry. Moreover, exactly solvable number conserving models can be constructed in arbitrary dimension.

6.7 Appendix

In this Appendix we provide additional information about some details of the analytical results for the exactly solvable two-wire topological system which have been omitted from the main text.

6.7.1 Two-wire ground state

In this section we show that the wave-functions $|\psi_L(N)\rangle_{ee(oo)}$ in Eq. (6.4) of the main text are the only ground states of the two-wire Hamiltonian $\hat{H}_{\lambda=1}$. Our proof actively constructs all of the zero-energy eigenstates of the Hamiltonian, which are the lowest-energy states because $\hat{H}_{\lambda=1} \geq 0$. Such states are obtained projecting the grand-canonical ground state of two decoupled Kitaev chains onto a given particle-number sector.

Let us first consider only the operators $\{\hat{L}_{\alpha,j}, \hat{L}_{\alpha,j}\}$ and the corresponding parent Hamiltonian $\hat{H}_{ab} = \sum_{\alpha=a,b}\sum_j \hat{L}^\dagger_{\alpha,j}\hat{L}_{\alpha,j}$ which corresponds to two decoupled single-wires. We know that the ground states of each single wire are given by $\hat{P}^\alpha_N|\psi\rangle^\alpha_\sigma$. Hamiltonian $\hat{H}_{ab}$ thus has a ground space spanned by

$$\left\{\hat{P}^a_n\hat{P}^b_{N-n}|\psi\rangle^a_\sigma \otimes |\psi\rangle^b_{\sigma'}\right\}^N_{n=0,\,(\sigma,\sigma')=e(o)} \tag{6.8}$$

and (σ,σ') take the values (e,e) and (o,o) when N is even and (e,o) and (o,e) when N is odd.

An important relation holds because $\hat{d}^a_j|\psi\rangle^a_\sigma \otimes |\psi\rangle^b_{\sigma'} = 0$. Upon the insertion of the identity operator $\sum^L_{n,n'=0}\hat{P}^a_n\hat{P}^b_{n'}$ we get

$$\sum_{n,n'}^{L}(\hat{C}^\dagger_{a,j}\hat{P}^a_{n-1} + \hat{A}_{a,j}\hat{P}^a_{n+1})\hat{P}^b_{n'}|\psi\rangle^a_\sigma \otimes |\psi\rangle^b_{\sigma'} = 0. \tag{6.9}$$

Each of the elements in the above sum must vanish independently because of orthogonality, and the important relation

$$\hat{C}^\dagger_{a,j}\hat{P}^a_{n-1}\hat{P}^b_{n'}|\psi\rangle^a_\sigma \otimes |\psi\rangle^b_{\sigma'} = -\hat{A}_{a,j}\hat{P}^a_{n+1}\hat{P}^b_{n'}|\psi\rangle^a_\sigma \otimes |\psi\rangle^b_{\sigma'}, \quad \forall n,n' \tag{6.10}$$

is derived (the same holds for the b wire).

Let us now compute the N-fermions state such that $\hat{H}|\phi_N\rangle = 0$. In general, $|\phi_N\rangle$ must be in the kernel of $\hat{H}_{ab}$:

$$|\phi_N\rangle = \sum_{n=0}^{N}\sum_{\sigma,\sigma'} x_{n,\sigma,\sigma'}\hat{P}^a_n\hat{P}^b_{N-n}|\psi\rangle^a_\sigma \otimes |\psi\rangle^b_{\sigma'}; \quad \sum_{n,\sigma,\sigma'}|x_{n,\sigma,\sigma'}|^2 = 1. \tag{6.11}$$

Imposing now that $\hat{H}_I|\phi_N\rangle = \sum_j \hat{L}^\dagger_{I,j}\hat{L}_{I,j}|\phi_N\rangle = 0$, we obtain that:

$$\begin{aligned}
\hat{L}_{I,j}|\phi_N\rangle &= (\hat{C}^\dagger_{a,j}\hat{A}_{b,j} + \hat{C}^\dagger_{b,j}\hat{A}_{a,j})\sum_{n=0}^{N}\sum_{\sigma,\sigma'} x_{n,\sigma,\sigma'}\hat{P}^a_n\hat{P}^b_{N-n}|\psi\rangle^a_\sigma \otimes |\psi\rangle^b_{\sigma'}, \\
&= \hat{C}^\dagger_{a,j}\hat{A}_{b,j}|\phi_N\rangle - \hat{C}^\dagger_{a,j}\hat{A}_{b,j}\sum_{n}\sum_{\sigma,\sigma'} x_{n,\sigma,\sigma'}\hat{P}^a_{n-2}\hat{P}^b_{N-n+2}|\psi\rangle^a_\sigma \otimes |\psi\rangle^b_{\sigma'}, \\
&= \hat{C}^\dagger_{a,j}\hat{A}_{b,j}\sum_{n}\sum_{\sigma,\sigma'}(x_{n,\sigma,\sigma'} - x_{n+2,\sigma,\sigma'})\hat{P}^a_n\hat{P}^b_{N-n}|\psi\rangle^a_\sigma \otimes |\psi\rangle^b_{\sigma'}, \\
&= 0 \iff x_{n,\sigma,\sigma'} = x_{n+2,\sigma,\sigma'}, \qquad (6.12)
\end{aligned}$$

since $\hat{C}^\dagger_{a,j}\hat{A}_{b,j}\,\hat{P}^a_n\hat{P}^b_{N-n}|\psi\rangle^a_\sigma \otimes |\psi\rangle^b_{\sigma'} \neq 0$. Such a relation uniquely defines a ground state for a fixed local parity (even-even, odd-odd, even-odd, odd-even), and thus, for each fixed particle number N, there is a double degeneracy related to distinct wire parities. Indeed, a general ground state for $2N$ particles is given by

$$|\phi_{2N}\rangle \propto \sum_n \Big[w_0\hat{P}^a_{2n}\hat{P}^b_{2(N-n)}|\psi\rangle^a_e \otimes |\psi\rangle^b_e + w_1\hat{P}^a_{2n+1}\hat{P}^b_{2N-(2n+1)}|\psi\rangle^a_o \otimes |\psi\rangle^b_o\Big], \qquad (6.13)$$

and is parametrized by the complex coefficients w_0 and w_1.

Alternatively, we can consider the ground states of two decoupled even parity Kitaev chains at half filling $\mu = 0$ and $\Delta = J$ on a circle with odd number of sites (no edges), $|G\rangle = |\psi\rangle^a_e \otimes |\psi\rangle^b_e$, and on an open system of the same length,

$$\{|G\rangle, \hat{d}^{a^\dagger}_L|G\rangle, \hat{d}^{b^\dagger}_L|G\rangle, \hat{d}^{a^\dagger}_L\hat{d}^{b^\dagger}_L|G\rangle\},$$

which are related to the edge Majorana fermions $\hat{d}^\alpha_L = \hat{\gamma}^\alpha_{2L} + i\hat{\gamma}^\alpha_1$, where $\{\hat{\gamma}^\alpha_i, \hat{\gamma}^\beta_j\} = 2\delta_{ij}\delta_{\alpha\beta}$, $\hat{\gamma}^\alpha_{2j-1} = i(\hat{\alpha}_j - \hat{\alpha}^\dagger_j)$, and $\hat{\gamma}^\alpha_{2j} = \hat{\alpha}_j + \hat{\alpha}^\dagger_j$, for $\alpha = a, b$. In this writing, we are exploting the highly non-generic properties of Kitaev's wire "sweet point", namely that the ground state of a closed wire (L odd) coincides with the ground state with even parity of an open wire $|\psi\rangle^a$ (L odd).

Thus, the ground states for the two wires number conserving Hamiltonian, as analysed in this section, are described by

$$\begin{aligned}
|\phi_N\rangle &\subset \text{span}\Big\{\hat{P}_N|G\rangle, \hat{P}_N\hat{d}^{a^\dagger}_L\hat{d}^{b^\dagger}_L|G\rangle\Big\} \quad \text{for } N \text{ even}, \\
|\phi_N\rangle &\subset \text{span}\Big\{\hat{P}_N\hat{d}^{a^\dagger}_L|G\rangle, \hat{P}_N\hat{d}^{b^\dagger}_L|G\rangle\Big\} \quad \text{for } N \text{ odd}.
\end{aligned}$$

6.7.2 Entanglement spectrum

In this section we provide the detailed derivation for the entanglement spectrum, presented in the main text. We consider the reduced state of l sites on each wire $\rho_l = \text{Tr}_{(L-l)}\big[|\psi_L(N)\rangle_{ee}\langle\psi_L(N)|_{ee}\big]$ (in the following expression identity operators on the first l sites are omitted):

$$\rho_l = \sum_{\{\vec{j}_m\},\{\vec{q}'_m\}} \langle\vec{j}_m|_a \otimes \langle\vec{q}_{m'}|_b|\psi_L(N)\rangle_{ee}\langle\psi_L(N)|_{ee}\,|\vec{j}_m\rangle_a \otimes |\vec{q}_{m'}\rangle_b.$$

Notice now that for N_l even:

$$\langle \vec{j}_{2m(2m+1)}|_a \otimes \langle \vec{q}_{N-N_l-2m(2m+1)}|_b \, |\psi_L(N)\rangle_{ee} = \sqrt{\frac{\mathcal{N}_{ee(oo),l,N_l}}{\mathcal{N}_{ee,L,N}}} \, |\psi_l(N_l)\rangle_{ee(oo)}, \tag{6.14}$$

which, as we see, does not depend on the specific $\vec{j}$ or $\vec{q}$. A similar relation exists for N_l odd,

$$\langle \vec{j}_{2m(2m+1)}|_a \otimes \langle \vec{q}_{N-N_l-2m(2m+1)}|_b \, |\psi_L(N)\rangle_{ee} = \sqrt{\frac{\mathcal{N}_{ee,l,N_l}}{\mathcal{N}_{ee,L,N}}} \, |\psi_l(N_l)\rangle_{eo(oe)}, \tag{6.15}$$

Summing up such terms, we obtain the reduced state in diagonal form and its eigenvalues, as given in the main text.

The demonstration for the double degeneracy in the entanglement spectrum in the limit of large L and $L-l$ (i.e., large lattices and bipartitions not close to its edges), is related to the fact that, in this limit, $\mathcal{N}_{ee,l,N_l} \sim \mathcal{N}_{oo,l,N_l}$. Even if we do not have an explicit analytical proof of the previous relation, numerical tests in several regimes corroborate this intuitive result.

From the eigenvalues computed in this section, we can also compute the entanglement entropy of the block matrices, and see how it scales with the size of the block. We see in Fig. 6.4 a behavior typical of a gapless Hamiltonian, which does not scale as an area law.

6.7.3 Edge modes

As discussed in the main text, in order to directly characterize the localization length of the edge modes we may compute the local parity breaking perturbation $\langle g_2|\hat{a}_i^\dagger \hat{b}_i|g_1\rangle$, where $\left|g_{1(2)}\right\rangle$ correspond to the two ground states for fixed N in Eq. (6.5). The task of computing these observables reduces merely to counting the suitable configurations, by looking at the ground states as given in Eq. (6.4). Let us consider, for simplicity, the case of an even number of particles N, and $\left|g_{1(2)}\right\rangle$ the even-even (odd-odd) local parity ground state.

If we act with the $\hat{V}_j = \hat{a}_j^\dagger \hat{b}_j$ operator on the *even-even* ground state, the only states $\left|\vec{j}_{2n}\right\rangle_a \otimes |\vec{q}_{N-2n}\rangle_a$ (see Eq.(6.4) in the main text) which are not annnihilated bt $\hat{V}_j$ are those which have a particle at site b_j, and a hole at site a_j. Due to the anticommutation relations, each of these configurations obtain a phase $(-1)^{(n_R^a+n_L^b)}$, where $n_R^a = \sum_{r=j+1}^{L} n_r^a$ is the number of particles located at the right of the jth site in the a-wire, and $n_L^b = \sum_{r=1}^{j-1} n_r^b$ the number of particles located at the left of the jth site in the b-wire. These phases describe the parity of the configuration on the segments $[j+1, L]$ for the a-wire and $[1, j-1]$ for the b-wire. Since the ground state is an equal superposition of all configurations distributing N particles between the two wires and fixing the parity of the number of particles for each wire, n_R^a varies from a minimum value equal to $\max(0, N-j)$ to a maximum value $\min(N, L-j)$. Analogous

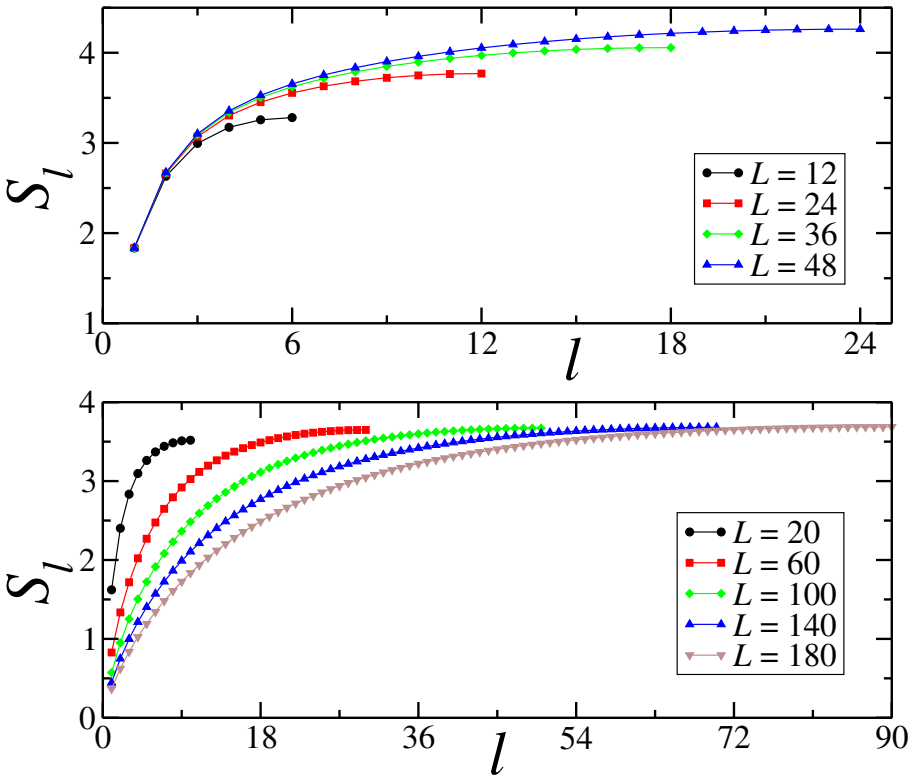

Figure 6.4: Entanglement entropy S_l for a block with l sites, (*upper panel*) considering a fixed filling $n = \frac{N}{2L} = \frac{1}{3}$, (*lower panel*) or a fixed particle number sector $N = 10$.

relations exist for n_R^b. The matrix element O_j defined in the text is thus related to a simple counting argument of particle configurations which takes into account the phase $(-1)^{(n_R^a + n_L^b)}$. Realizing then the expectation value of these configurations with the *odd-odd* ground state, it will be simply related to the number of such configurations weighted by its corresponding phases.

Let us discuss this in more detail. The total number of configurations for the *even-even* state, is given by

$$\sum_n \underbrace{\binom{L}{2n}}_{b-wire} \underbrace{\binom{L}{N-2n}}_{a-wire}, \tag{6.16}$$

whereas those which have a particle at site b_j and a hole at site a_j correspond to

$$\sum_n \underbrace{\binom{L-1}{2n-1}}_{b-wire} \underbrace{\binom{L-1}{N-2n}}_{a-wire} = \sum_n \underbrace{\left(\sum_{n_L^b} \binom{j-1}{n_L^b} \binom{L-j}{2n-1-n_L^b} \right)}_{b-wire} \underbrace{\left(\sum_{n_R^a} \binom{L-j}{n_R^a} \binom{j-1}{N-2n-n_R^a} \right)}_{a-wire}.$$

Taking into account the phase $(-1)^{(n_R^a+n_L^b)}$, we have that

$$\langle\psi_L(N)|_{oo}\hat{a}_j^\dagger\hat{b}_j|\psi_L(N)\rangle_{ee} = \frac{1}{\sqrt{\mathcal{N}_{ee,L,N}\mathcal{N}_{oo,L,N}}}\sum_{n,n_L^b,n_R^a}(-1)^{(n_L^b+n_R^a)}\underbrace{\binom{j-1}{n_L^b}\binom{L-j}{2n-1-n_L^b}}_{b-wire}\underbrace{\binom{L-j}{n_R^a}\binom{j-1}{N-2n-n_R^a}}_{a-wire}$$

Following the same steps as above, it is not hard to see that for a general single-particle operator we have

$$\langle\psi_L(N)|_{oo}\hat{a}_j^\dagger\hat{b}_r|\psi_L(N)\rangle_{ee} = \frac{1}{\sqrt{\mathcal{N}_{ee,L,N}\mathcal{N}_{oo,L,N}}}\sum_{n,n_L^b,n_R^a}(-1)^{(n_L^b+n_R^a)}\underbrace{\binom{r-1}{n_L^b}\binom{L-r}{2n-1-n_L^b}}_{b-wire}\underbrace{\binom{L-j}{n_R^a}\binom{j-1}{N-2n-n_R^a}}_{a-wire}.$$

for $(L+r)-j>1$.

In particular, the edge-edge correlations can be reduced to a simple expression in the thermodynamic limit,

$$\begin{aligned}\langle\psi_L(N)|_{oo}\hat{a}_1^\dagger\hat{b}_L|\psi_L(N)\rangle_{ee} &= \frac{1}{\sqrt{\mathcal{N}_{ee,L,N}\mathcal{N}_{oo,L,N}}}\sum_n(-1)^{(N-1)}\underbrace{\binom{L-1}{2n-1}}_{b-wire}\underbrace{\binom{L-1}{N-2n}}_{a-wire},\\ \langle\psi_L(N)|_{oo}\hat{a}_L^\dagger\hat{b}_1|\psi_L(N)\rangle_{ee} &= \frac{1}{\sqrt{\mathcal{N}_{ee,L,N}\mathcal{N}_{oo,L,N}}}\sum_n\underbrace{\binom{L-1}{2n-1}}_{b-wire}\underbrace{\binom{L-1}{N-2n}}_{a-wire}.\end{aligned} \tag{6.17}$$

Using the Chu-Vandermonde identity, $\sum_{k=0}^r\binom{m}{k}\binom{n}{r-k}=\binom{m+n}{r}$, for non-negative integer m,n,r, we obtain in the limit of large lattices,

$$\sum_n\underbrace{\binom{L-1}{2n-1}}_{b-wire}\underbrace{\binom{L-1}{N-2n-1}}_{a-wire} \approx \frac{1}{2}\binom{2L-2}{N-1}, \tag{6.18}$$

and $\mathcal{N}_{ee(oo),L,N}\approx\frac{1}{2}\binom{2L}{N}$. Thus, the edge-edge correlations are

$$\langle\psi_L(N)|_{oo}\hat{a}_1^\dagger\hat{b}_L|\psi_L(N)\rangle_{ee}\approx\frac{\nu(1-\nu)}{(1-\frac{1}{2L})}\overset{L\to\infty}{\longrightarrow}\nu(1-\nu). \tag{6.19}$$

and similarly for $\langle g_2|\hat{a}_L^\dagger\hat{b}_1|g_1\rangle$. Note that, if N is *odd*, we would have a minus sign in the above correlation, $\langle g_2|\hat{a}_1^\dagger\hat{b}_L|g_1\rangle\overset{L\to\infty}{\longrightarrow}-\nu(1-\nu)$, due to the overall phase $(-1)^{(N-1)}$ in Eq. (6.17).

6.7.4 Single-particle and superfluid correlations

In a general way, any ground state observable can be computed as in the previous section through a simple counting of the suitable configurations. In this section we evaluate the single particle correlations $\langle\hat{a}_j^\dagger\hat{a}_{j+r}\rangle$, as well as the

superfluid correlations $\langle \hat{a}_i^\dagger \hat{a}_{i+1}^\dagger \hat{a}_{j+1} \hat{a}_j \rangle$. We skip unnecessary details and focus mainly on the presentation of the final results. We only consider ground states with even-even or odd-odd local parities because the even-odd and odd-even cases are mathematically equivalent to the even-even one.

Single particle correlations:

$$\langle \psi_L(N)|_{ee(oo)} \hat{a}_j^\dagger \hat{a}_{j+r} |\psi_L(N)\rangle_{ee(oo)} = \\ \frac{1}{\mathcal{N}_{ee(oo),L,N}} \sum_{n,n^a_{(j,r)}} (-1)^{n^a_{(j,r)}} \underbrace{\binom{L}{2n(2n+1)}}_{b-wire} \underbrace{\binom{r-1}{n^a_{(j,r)}} \binom{L-r-1}{N-2n(2n+1)-1-n^a_{(j,r)}}}_{a-wire}, \tag{6.20}$$

if $r > 1$, and

$$\langle \psi_L(N)|_{ee(oo)} \hat{a}_j^\dagger \hat{a}_{j+r} |\psi_L(N)\rangle_{ee(oo)} = \\ \frac{1}{\mathcal{N}_{ee(oo),L,N}} \sum_{n} \underbrace{\binom{L}{2n(2n+1)}}_{b-wire} \underbrace{\binom{L-r-1}{N-2n(2n+1)-1}}_{a-wire}, \tag{6.21}$$

if $r \leq 1$, where $n^a_{(j,r)} = \sum_{i=1}^{r-1} n^a_{j+i}$ is the number of particles between the sites j and $j+r$, which varies from a minimum of zero (where all the particles are in the b-wire), to a maximum value equal to $\min(N-1, r-1)$ (where all the remaining $N-1$ particles lie between these sites, or it is completely filled).

Superfluid correlations:

The superfluid order can be characterized by the following p-wave superconducting correlators "$\hat{a}_i^\dagger \hat{a}_{i+1}^\dagger \hat{a}_{j+1} \hat{a}_j$". We compute it analytically, and show that it saturates along the lattice, $\hat{a}_i^\dagger \hat{a}_{i+1}^\dagger \hat{a}_{j+1} \hat{a}_j \overset{L\to\infty}{\longrightarrow} \nu^2(1-\nu)^2$. The evaluation is similar as the previous ones, following through a simple counting of the suitable configurations.

$$\langle \psi_L(N)|_{ee(oo)} \hat{a}_i^\dagger \hat{a}_{i+1}^\dagger \hat{a}_{j+1} \hat{a}_j |\psi_L(N)\rangle_{ee(oo)} = \frac{1}{\mathcal{N}_{ee(oo)}(L,N)} \sum_{n} \underbrace{\binom{L}{2n}}_{b-wire} \underbrace{\binom{L-4}{N-2n-2}}_{a-wire}, \tag{6.22}$$

for $i+1 < j$. Using the Chu-Vandermonde identity, we obtain in the limit of large lattices,

$$\sum_{n} \underbrace{\binom{L}{2n}}_{b-wire} \underbrace{\binom{L-4}{N-2n-2}}_{a-wire} \approx \frac{1}{2}\binom{2L-4}{N-2}, \tag{6.23}$$

and $\mathcal{N}_{ee(oo)}(L,N) \approx \frac{1}{2}\binom{2L}{N}$. Thus, the superfluid correlations is

$$\langle\psi_L(N)|_{ee(oo)}\hat{a}_i^\dagger\hat{a}_{i+1}^\dagger\hat{a}_{j+1}\hat{a}_j|\psi_L(N)\rangle_{ee(oo)} \approx \frac{2^4\nu^2(1-\nu)^2L^4+\mathcal{O}(L^3)}{2^4L^4+\mathcal{O}(L^3)} \xrightarrow{L\to\infty} \nu^2(1-\nu)^2. \tag{6.24}$$

6.7.5 Braiding

In this section we demonstrate the properties of the braiding operator $\hat{B}_{aR,bR}(j) = (\hat{\mathcal{I}}+\hat{Z}_{aR,bR,j})/\sqrt{2}$ presented in the main text. To that end, it is useful to first study the action of $\hat{Z}_{aR,bR,j}$, starting from the simpler case $j=1$:

$$\hat{Z}_{aR,bR,1} = \frac{\hat{X}_{aR,bR,1}}{\mathcal{F}_1}; \qquad \hat{X}_{aR,bR,1} = a_L^\dagger b_L - b_L^\dagger a_L; \qquad \mathcal{F}_1 = \sqrt{1-[\nu^2+(1-\nu)^2]}; \tag{6.25}$$

with $\nu = \frac{N}{2L}$. The action of $a_L^\dagger b_L$ on $|\psi_L(N)\rangle_{ee}$ produces an unnormalized state proportional to the equal-weighted superposition of all fermionic configurations with (i) N fermions, (ii) odd wire parities, (iii) a hole in the L-th site of the wire a, and (iv) a particle in the L-th site of the wire b. Due to the anticommuting properties of fermionic operators, this state gets a global phase $(-1)^{(N-1)+(N_a)} = (-1)^{N_b-1}$ (recall that $(-1)^{N_a}$ and $(-1)^{N_b}$ are well-defined although N_a and N_b are not fixed). With similar reasoning one can also characterize $b_L^\dagger a_L|\psi_L(N)\rangle_{ee}$ (here the hole (fermion) is in the L-th site of the wire a (b) and the global phase is $(-1)^{(N_a-1)+(N-1)} = (-1)^{N_b}$). The state $\hat{Z}_{aR,bR,1}|\psi_L(N)\rangle_{ee}$ is the normalized state described by the equal weighted superposition of all fermionic configurations with (i) N fermions and (ii) odd wire parities and without (iii) the simultaneous presence of two holes or two particles at the L-th site of both wires a and b. The normalization constant F_1 corresponds to the "fidelity" of the state with the ground state with such local parities, $\mathcal{F}_1 = \sqrt{\langle\psi_L(N)|_{oo}\hat{Z}_{aR,bR,1}|\psi_L(N)\rangle_{ee}} = \sqrt{1-[\nu^2+(1-\nu)^2]}$.

The operator $\hat{Z}_{aR,bR,j}$ acts on the last j sites of the wires. Let us consider for example $j=2$:

$$\begin{aligned}\hat{Z}_{aR,bR,2} =& \frac{\hat{X}_{aR,bR,1}+\hat{Y}_{aR,bR,1}\hat{X}_{aR,bR,2}}{\mathcal{F}_2};\\ \hat{Y}_{aR,bR,1}\hat{X}_{aR,bR,2} =& \Big(n_L^a n_L^b + (1-n_L^a)(1-n_L^b)\Big)\Big(a_{L-1}^\dagger b_{L-1} - b_{L-1}^\dagger a_{L-1}\Big);\\ \mathcal{F}_2 =& \sqrt{1-[\nu^4+(1-\nu)^4]}.\end{aligned} \tag{6.26}$$

Note that the term $\hat{Y}_{aR,bR,1}\hat{X}_{aR,bR,2}|\psi_L(N)\rangle_{ee}$ acts only on the fermionic configurations which were missing in $\hat{X}_{aR,bR,1}|\psi_L(N)\rangle_{ee}$. However, it is clear that $\hat{Z}_{aR,bR,2}|\psi_L(N)\rangle_{ee}$ does not contain any configuration with four holes or four particles in the L-th and $(L-1)$-th sites of both wires. Whereas this still makes $\hat{Z}_{aR,bR,2}|\psi_L(N)\rangle_{ee}$ different from $|\psi_L(N)\rangle_{oo}$, it is a considerable improvement with respect to the previous case. In general, the state $\hat{Z}_{aR,bR,j}|\psi_L(N)\rangle_{ee}$ is the equal weighted superposition of all fermionic configurations with (i) N fermions and (ii) odd wire parities, and without (iii) the simultaneous

presence of $2j$ holes or $2j$ particles in the last j sites of both wires. $\mathcal{F}_j$ corresponds to the fidelity of the state to the ground state with such local parity pattern, $\mathcal{F}_j = \sqrt{\langle\psi_L(N)|_{oo}\hat{Z}_{aR,bR,j}|\psi_L(N)\rangle_{ee}} = \sqrt{1-\left[\nu^{2j}+(1-\nu)^{2j}\right]}$. For a large enough $j < L/2$, the difference between $\hat{Z}_{aR,bR,j}|\psi_L(N)\rangle_{ee}$ and $|\psi_L(N)\rangle_{oo}$ becomes exponentially small, so that the above operator *in the zero-energy subspace* reads

$$\hat{Z}_{aR,bR,j} \sim \sum_{N\,even}(|\psi_L(N)\rangle_{ee}\langle\psi_L(N)|_{oo} - |\psi_L(N)\rangle_{oo}\langle\psi_L(N)|_{ee}) + \\ + \sum_{N\,odd}(|\psi_L(N)\rangle_{oe}\langle\psi_L(N)|_{eo} - |\psi_L(N)\rangle_{eo}\langle\psi_L(N)|_{oe}). \tag{6.27}$$

For j and L are such that the error is negligible, we define the *number conserving* operator $\hat{R}_{aR,bR} = \hat{B}_{aR,bR}(j)$.

We observe that $\hat{R}_{aR,bR}$ acts on the zero-energy states in the same way done in the conventional *number non-conserving* scenario of two neighboring Kitaev wires by the braiding operator $\hat{R}'_{aR,bR} = e^{\frac{\pi}{4}\gamma_{aR}\gamma_{bR}} = (\mathcal{I}+\gamma_{aR}\gamma_{bR})/\sqrt{2}$, where $\gamma_{m\Lambda}$ are the zero-energy Majorana operators exponentially localized at the $\Lambda = R, L$ edge of the wire $m = a, b$. In order to verify this explicitly, we first recall that the number non-conserving edges Majoranas are related to a non-local fermion as $\hat{f}_m = \hat{\gamma}_{mL} - i\gamma_{mR}$ which is the Bogoliubov zero-energy mode. The two degenerate ground states of the wire $m = a, b$, $|\psi\rangle_{m\sigma}$ (σ is the parity of the number of fermions, even, e or odd, o, and labels the two ground states), correspond to the presence or absence of the non-local fermion $\hat{f}_m$: $\hat{f}_m|\psi\rangle_{me} = 0$, and $\hat{f}^\dagger_m|\psi\rangle_{me} = |\psi\rangle_{mo}$. Using the inverse relations $\hat{\gamma}_{mL} \propto \left(\hat{f}_m + \hat{f}^\dagger_m\right)$ and $\hat{\gamma}_{mR} \propto i\left(\hat{f}_m - \hat{f}^\dagger_m\right)$, it is now easy to see that:

$$\begin{aligned}\hat{\gamma}_{aR}\hat{\gamma}_{bR}|\psi\rangle_{a\sigma}|\psi\rangle_{b\tau} &= p_\sigma(\hat{\gamma}_{aR}|\psi\rangle_{a\sigma})(\hat{\gamma}_{bR}|\psi\rangle_{b\tau}) = p_\sigma(-ip_\sigma)(-ip_\tau)|\psi\rangle_{a\bar{\sigma}}|\psi\rangle_{b\bar{\tau}} \\ &= -p_\tau|\psi\rangle_{a\bar{\sigma}}|\psi\rangle_{b\bar{\tau}}\end{aligned} \tag{6.28}$$

where $p_\sigma = 1$ for $\sigma = e$ and $p_\sigma = -1$ for $\sigma = o$; $\bar{\sigma}, \bar{\tau}$ are the flipped σ, τ. As claimed, $\hat{\gamma}_{aR}\hat{\gamma}_{bR}$ acts on the ground space in a way which is completely analogous to that of $\hat{Z}^R_{ab}$ in Eq. (6.27) for the number-conserving model. The equivalence of $\hat{R}_{aR,bR}$ and $\hat{R}'_{aR,bR}$ follows directly.

The unitarity of the braiding operator $\hat{R}_{aR,bR}$ restricted to the ground subspace can be proved explicitly. Let us first notice that:

$$\begin{aligned}&\langle\psi_L(N)|_{\sigma\tau}\hat{R}^\dagger_{aR,bR}\hat{R}_{aR,bR}|\psi_L(N)\rangle_{\sigma'\tau'} \\ &= \frac{1}{2}\langle\psi_L(N)|_{\sigma\tau}\left(\mathcal{I}+\hat{Z}_{aR,bR,j}+\hat{Z}^\dagger_{aR,bR,j}+\hat{Z}^\dagger_{aR,bR,j}\hat{Z}_{aR,bR,j}\right)|\psi_L(N)\rangle_{\sigma'\tau'} \\ &= \frac{1}{2}\langle\psi_L(N)|_{\sigma\tau}\left(\mathcal{I}+\hat{Z}^\dagger_{aR,bR,j}\hat{Z}_{aR,bR,j}\right)|\psi_L(N)\rangle_{\sigma'\tau'} \\ &= \delta_{\sigma,\sigma'}\delta_{\tau,\tau'}\end{aligned} \tag{6.29}$$

where in the second line we used the fact that $\hat{Z}_{aR,bR,j}$ is anti-Hermitian. Thus, in the ground state subspace we have,

$$\hat{P}_g\,\hat{R}^\dagger_{aR,bR}\,\hat{R}_{aR,bR}\,\hat{P}^\dagger_g = \hat{P}_g \tag{6.30}$$

With similar procedures we can define other braiding operators with completely analogous properties. For example, let us consider the transformation $i \leftrightarrow (L+1-i)$ which maps an operator at site i to site $(L+1-i)$, thus mapping the right edge to the left one and viceversa. When we apply it to $\hat{Z}_{aR,bR,j}$, we can define $\hat{Z}_{aL,bL,j}$, which is exponentially localized at the left edge of the wire. For j and L large enough, its explicit expression is:

$$\begin{aligned}\hat{Z}_{aL,bL,j} \sim & \sum_{N\,even} (-|\psi_L(N)\rangle_{ee}\langle\psi_L(N)|_{oo} + |\psi_L(N)\rangle_{oo}\langle\psi_L(N)|_{ee}) \\ & + \sum_{N\,odd} (|\psi_L(N)\rangle_{oe}\langle\psi_L(N)|_{eo} - |\psi_L(N)\rangle_{eo}\langle\psi_L(N)|_{oe}).\end{aligned} \tag{6.31}$$

The braiding operator $\hat{R}_{aL,bL}$ can be defined, and an explicit calculation shows that it is unitary and that it resembles the operator $\hat{R}'_{aL,bL}$ for the number non-conserving case.

As a second example, let us consider the transformation $b_{L+1-j} \to -ia_j$ for $j < L/2$ which maps the right edge of the wire b to the left edge of the wire a, leaving the other two edges unchanged. When we apply it to $\hat{Z}_{aR,bR,j}$, we can define the operator $\hat{Z}_{aR,aL,j}$, whose explicit expression for j and L large enough is:

$$\begin{aligned}\hat{Z}_{aR,aL,j} \sim & \sum_{N\,even} i\,(|\psi_L(N)\rangle_{ee}\langle\psi_L(N)|_{ee} - |\psi_L(N)\rangle_{oo}\langle\psi_L(N)|_{oo}) \\ & + \sum_{N\,odd} i\,(|\psi_L(N)\rangle_{eo}\langle\psi_L(N)|_{eo} - |\psi_L(N)\rangle_{oe}\langle\psi_L(N)|_{oe}).\end{aligned} \tag{6.32}$$

Again, everything follows as before. In general, with this method one can define sixteen braiding operators $\hat{R}_{m\Lambda,m'\Lambda}$, with $m, m' = a, b$ labeling the wires and $\Lambda, \Lambda' = L, R$ labeling the left and right edge.

Let us conclude with an explicit verification of the non-abelian character of these operators; to this aim, we initialize the system in the state $|\psi_L(N)\rangle_{ee}$. We then perform two braiding operations on the edges in different sequences:

$$\begin{aligned}&(\hat{R}_{aR,aL}\hat{R}_{aR,bR} - \hat{R}_{aR,bR}\hat{R}_{aR,aL})|\psi_L(N)\rangle_{ee} \\ &= \frac{1}{2}\Big(\hat{Z}_{aR,aL,j}\hat{Z}_{aR,bR,j} - \hat{Z}_{aR,bR,j}\hat{Z}_{aR,aL,j}\Big)|\psi_L(N)\rangle_{ee} \\ &= i|\psi_L(N)\rangle_{oo}.\end{aligned} \tag{6.33}$$

The result shows explicitly the non-commutativity of the braiding operations.

CHAPTER 7

Dissipative preparation of topological superconductors in a number-conserving setting

In this chapter we discuss the dissipative preparation of p-wave superconductors in number-conserving one-dimensional fermionic systems. We focus on two setups: the first one entails a single wire coupled to a bath, whereas in the second one the environment is connected to a two-leg ladder. Both settings lead to stationary states which feature the bulk properties of a p-wave superconductor, identified in this number-conserving setting through the long-distance behavior of the proper p-wave correlations. The two schemes differ in the fact that the steady state of the single wire is not characterized by topological order, whereas the two-leg ladder hosts Majorana zero modes, which are decoupled from damping and exponentially localized at the edges. Our analytical results are complemented by an extensive numerical study of the steady-state properties, of the asymptotic decay rate and of the robustness of the protocols.

7.1 Introduction

Topological quantum computation has recently emerged as one of the most intriguing paradigms for the storage and manipulation of quantum information [85, 86]. The defining features of topological order, namely the existence of degenerate ground states which (i) share the same thermodynamic properties and (ii) can only be distinguished by a global measurement, portend for a true many-body protection of quantum information. Additionally, the

non-Abelian anyons which typically appear in these models are crucial for the active manipulation of the information, to be accomplished through their adiabatic braiding [123, 124].

Among the several systems featuring topological order, free p-wave superconducting systems with symmetry protected topological properties have lately attracted a significant amount of attention [125, 126, 127]. On the one hand, they are exactly-solvable fermionic models which help building a clear physical intuition of some aspects of topological order [89, 108]. On the other one, they are physically relevant, and several articles have recently reported experimental evidences to be linked to p-wave-like superconductors featuring zero-energy Majorana modes [97, 128, 129, 130, 131].

Whereas up to now these experimental results have been obtained in solid-state setups, it is natural to ask whether such physics might as well be observed in cold atomic gases [132], which owing to their well-controlled microscopic physics should allow for a more thorough understanding of these peculiar phases of matter. Important theoretical efforts have thus proposed a variety of schemes which exploit in different ways several properties of such setups [133, 134, 96, 104, 135, 101, 136].

Among these ideas, that of a dissipative preparation of interesting many-body quantum states [113, 114] is particularly appealing: rather than suffering from some unavoidable open-system dynamics, such as three-body losses or spontaneous emission, one tries to take advantage of it (see Refs. [137, 104, 105, 138, 139] for the case of states with topological order, such as p-wave superconductors). The key point is the engineering of an environment that in the long-time limit drives the system into the desired quantum state. This approach has the remarkable advantage of being a workaround to the ultra-low temperatures necessary for the observation of important quantum phenomena which constitute a particularly severe obstacle in fermionic systems. The trust is thus that the mentioned "non-equilibrium cooling" may open the path towards the experimental investigation of currently unattainable states, e.g. characterized by p-wave superconductivity.

In this chapter we discuss the dissipative engineering of a p-wave superconductor with a fixed number of particles, an important constraint in cold-atom experiments. We consider two different setups: (i) A single quantum wire, introduced in Ref. [104]; this system displays the typical features of a p-wave superconductor but it is not topological in its number conserving variant. (ii) A two-leg ladder [98, 99, 100, 101, 102, 115, 140], supporting a dissipative dynamics which entails a two-dimensional steady state space characterized by p-wave superconducting order with boundary Majorana modes for every fixed particle number.

We identify the p-wave superconducting nature of the steady states by studying the proper correlators, which saturate to a finite value in the long distance limit. Their topological properties are best discussed using a mathematical connection between dark states of the Markovian dynamics and ground states of a suitable parent Hamiltonian. In both setups we demonstrate that the dissipative gap closes at least polynomially in the system size and thus that the typical decay time to the steady state diverges in the ther-

modynamic limit. This contrasts with the case where number conservation is not enforced. In this case typically the decay time is finite in the thermodynamic limit [104, 105], and reflects the presence of dynamical slow modes related to the particle-number conservation [141, 142], which also exist in non-equilibrium systems (see also Ref. [143, 144, 145]).

Our exact analytical findings are complemented by a numerical study based on a matrix-product-operator representation of the density matrix [117, 118], one of the techniques for open quantum systems which are recently attracting an increasing attention [146, 119, 147, 148, 149, 150, 151, 152, 153]. These methods are employed to test the robustness of these setups to perturbations, which is thoroughly discussed.

The chapter is organized as follows: in Sec. 7.2 we review the key facts behind the idea of dissipative state preparation using the dark states of a many body problem, and exemplify them recalling the problem studied in Ref. [104]. A simple criterion for signalling the divergence of the decay-time with the system size is also introduced. In Sec. 7.3 we present the exact analytical study of the single-wire protocol, and in Sec. 7.4 a numerical analysis complements the previous discussion with the characterization of the robustness to perturbations of these setups. In Sec. 7.5 we discuss the protocol based on the ladder geometry. Finally, in Sec. 7.6 we present our conclusions.

7.2 Dissipative state preparation of Majorana fermions: known facts

7.2.1 Dark states and parent Hamiltonian of Markovian dynamics

The dissipative dynamics considered in this chapter is Markovian and, in the absence of a coherent part, can be cast in the following Lindblad form:

$$\frac{\partial}{\partial t}\hat{\rho} = \mathcal{L}[\hat{\rho}] = \sum_{j=1}^{m}\left[\hat{L}_j\hat{\rho}\hat{L}_j^\dagger - \frac{1}{2}\{\hat{L}_j^\dagger\hat{L}_j,\hat{\rho}\}\right], \tag{7.1}$$

where $\mathcal{L}$ is the so-called Lindbladian super-operator and the $\hat{L}_j$ are the (local) Lindblad operators. We now discuss a fact which will be extensively used in the following. Let us assume that a pure state $|\Psi\rangle$ exists, with the property:

$$\hat{L}_j|\Psi\rangle = 0; \quad \forall\, j = 1,\dots,m. \tag{7.2}$$

A simple inspection of Eq. (7.1) shows that $|\Psi\rangle$ is a steady state of the dynamics, and it is usually referred to as *dark state*. Although the existence of a state satisfying Eq. (7.2) is usually not guaranteed, in this chapter we will mainly consider master equations which enjoy this property.

A remarkable feature of dark states is that they can be searched through the minimization of a *parent Hamiltonian*. Let us first observe that Eq. (7.2) implies that $\langle\Psi|\hat{L}_j^\dagger\hat{L}_j|\Psi\rangle = 0$ and since every operator $\hat{L}_j^\dagger\hat{L}_j$ is positive semi-definite, $|\Psi\rangle$ minimizes it. Consequently, $|\Psi\rangle$ is a ground state of the parent Hamiltonian:

$$\hat{\mathcal{H}}_p = \sum_{j=1}^{m}\hat{L}_j^\dagger\hat{L}_j. \tag{7.3}$$

Conversely, every zero-energy ground state $|\Phi\rangle$ of Hamiltonian (7.3) is a steady state of the dynamics (7.1). Indeed, $\hat{\mathcal{H}}_p|\Phi\rangle = 0$ implies that $\langle\Phi|\hat{L}_j^\dagger \hat{L}_j|\Phi\rangle = 0$ for all $j = 1, \ldots, m$. The last relation means that the norm of the states $\hat{L}_j|\Phi\rangle$ is zero, and thus that the states themselves are zero: $\hat{L}_j|\Phi\rangle = 0$. As we have already shown, this is sufficient to imply that $|\Phi\rangle$ is a steady-state of the dynamics.

In order to quantify the typical time-scale of the convergence to the steady state, it is customary to consider the right eigenvalues of the super-operator $\mathcal{L}$, which are defined through the secular equation $\mathcal{L}[\hat{\theta}_\lambda] = \lambda\hat{\theta}_\lambda$. The asymptotic decay rate for a finite system is defined as

$$\lambda_{ADR} = \inf_{\substack{\lambda \text{ is eigenvalue of } \mathcal{L} \\ \Re(\lambda)\neq 0}} \{-\Re(\lambda)\}. \tag{7.4}$$

The minus sign in the previous equation follows from the fact that the real part of the eigenvalues of a Lindbladian super-operator satisfy the following inequality: $\Re(\lambda) \leq 0$.

Remarkably, for every eigenvalue ξ of $\hat{\mathcal{H}}_p$ there is an eigenvalue $\lambda = -\xi/2$ of $\mathcal{L}$ which is at least two-fold degenerate. Indeed, given the state $|\psi_\xi\rangle$ such that $\hat{\mathcal{H}}_p|\psi_\xi\rangle = \xi|\psi_\xi\rangle$, the operators made up of the dark state $|\Psi\rangle$ and of $|\psi_\xi\rangle$

$$\hat{\theta}^{(1)}_{-\xi/2} = |\Psi\rangle\langle\psi_\xi|, \quad \hat{\theta}^{(2)}_{-\xi/2} = |\psi_\xi\rangle\langle\Psi| \tag{7.5}$$

satisfy the appropriate secular equation. This has an important consequence: if $\hat{\mathcal{H}}_p$ is gapless, then $\lambda_{ADR} \xrightarrow{L\to\infty} 0$ in the thermodynamic limit, where L is the size of the system. Indeed:

$$0 < \lambda_{ADR} \leq \frac{\xi}{2}, \tag{7.6}$$

for every eigenvalue ξ of $\hat{\mathcal{H}}_p$; if ξ closes as $L^{-\alpha}$ ($\alpha > 0$), then the dissipative gap closes at least polynomially in the system size. Note that this argument also implies that if $\mathcal{L}$ is gapped, then the parent Hamiltonian is gapped as well.

It is important to stress that the spectral properties of the parent Hamiltonian $\hat{\mathcal{H}}_p$ do not contain all the information concerning the long-time dissipative dynamics. As an example, let us assume that the Markovian dynamics in Eq. (7.1) (i) supports at least one dark state and (ii) has an associated parent Hamiltonian which is gapped. If the Lindblad operators are Hermitian, then the fully-mixed state is a steady state of the master equation too. The presence of such stationary state is not signaled by the parent Hamiltonian, which is gapped and only detects the pure steady states of the dynamics.

Whereas the some of the above relations have been often pointed out in the literature [113, 114], to the best of our knowledge the remarks on the relation between the spectral properties of $\mathcal{L}$ and $\hat{\mathcal{H}}_p$ are original.

7.2.2 The Kitaev chain and the dissipative preparation of its ground states

Let us now briefly review the results in Ref. [104] and use them to exemplify how property (7.2) can be used as a guideline for dissipative state preparation in the number non-conserving case. This will be valuable for our detailed studies of its number conserving variant below.

The simplest model displaying zero-energy unpaired Majorana modes is the one-dimensional Kitaev model at the so-called "sweet point" [89]:

$$\hat{\mathcal{H}}_K = -J\sum_j \Big[\hat{a}_j^\dagger \hat{a}_{j+1} + \hat{a}_j \hat{a}_{j+1} + \text{H.c.}\Big], \quad J>0, \tag{7.7}$$

where the fermionic operators $\hat{a}_j^{(\dagger)}$ satisfy canonical anticommutation relations and describe the annihilation (creation) of a spinless fermion at site j. The model can be solved with the Bogoliubov-de-Gennes transformation, and, when considered on a chain of length L with open boundaries, it takes the form:

$$\hat{\mathcal{H}}_K = E_0 + \frac{J}{2}\sum_{j=1}^{L-1} \hat{\ell}_j^\dagger \hat{\ell}_j\,, \tag{7.8}$$

with

$$\hat{\ell}_j = \hat{C}_j^\dagger + \hat{A}_j, \tag{7.9}$$

$$\hat{C}_j^\dagger = \hat{a}_j^\dagger + \hat{a}_{j+1}^\dagger, \quad \hat{A}_j = \hat{a}_j - \hat{a}_{j+1}. \tag{7.10}$$

The ground state has energy E_0 and is two-fold degenerate: there are two linearly independent states $|\psi_e\rangle$ and $|\psi_o\rangle$ which satisfy:

$$\hat{\ell}_j|\psi_\sigma\rangle = 0; \quad \forall\, j=1,\dots,L-1; \qquad \sigma = e,o. \tag{7.11}$$

The quantum number distinguishing the two states is the parity of the number of fermions, $\hat{P} = (-1)^{\sum \hat{a}_j^\dagger \hat{a}_j}$, which is a symmetry of the model (the subscripts e and o stand for *even* and *odd*). Both states $|\psi_\sigma\rangle$ are p-wave superconductors, as it can be explicitly proven by computing the expectation value of the corresponding order parameter:

$$\langle\psi_\sigma|\hat{a}_j\hat{a}_{j+1}|\psi_\sigma\rangle \xrightarrow{L\to\infty} \frac{1}{4}. \tag{7.12}$$

It is thus relevant to develop a master equation which features $|\psi_e\rangle$ and $|\psi_o\rangle$ as steady states of the dynamics [104, 105]. Property (7.11) provides the catch: upon identification of the $\hat{\ell}_j$ operators with the Lindblad operators of a Markovian dynamics, Eq. (7.2) ensures that the states $|\psi_\sigma\rangle$ are steady states of the dynamics and that in the long-time limit the system evolves into a subspace described in terms of p-wave superconducting states. This becomes particularly clear once it is noticed that the parent Hamiltonian of this Markov process coincides with $\hat{\mathcal{H}}_K$ in Eq. (7.8) apart from an additive constant.

Let us conclude mentioning that the obtained dynamics satisfies an important physical requirement, namely *locality*. The Lindblad operators $\hat{\ell}_j$ only

act on two neighboring fermionic modes; this fact makes the dynamics both physical and experimentally feasible. On the other hand, they do not conserve the number of particles, thus making their engineering quite challenging with cold-atom experiments. The goal of this chapter is to provide dissipative schemes with Lindblad operators which commute with the number operator and feature the typical properties of a p-wave superconductor.

7.3 Single wire: Analytical results

The simplest way to generalize the previous results to systems where the number of particles is conserved is to consider the master equation induced by the Lindblad operators [104, 105]:

$$\hat{L}'_j = \hat{C}_j^\dagger \hat{A}_j, \quad \forall\, j = 1, \dots, L-1, \tag{7.13}$$

for a chain with hard-wall boundaries and spinless fermions:

$$\frac{\partial}{\partial t}\hat{\rho} = \mathcal{L}'[\hat{\rho}] = \gamma \sum_{j=1}^{L-1} \left[\hat{L}'_j \hat{\rho} \hat{L}'^\dagger_j - \frac{1}{2}\{\hat{L}'^\dagger_j \hat{L}'_j, \hat{\rho}\} \right]; \quad \gamma > 0; \tag{7.14}$$

where γ is the damping rate. This Markovian dynamics has already been considered in Refs. [104, 105]. Using the results presented in Ref. [115], where the parent Hamiltonian related to the dynamics in Eq. (7.14) is considered, it is possible to conclude that for a chain with periodic boundary conditions (i) there is a unique dark state for every particle number density $\nu = N/L$, and (ii) this state is a p-wave superconductor. A remarkable point is that the $\hat{L}'_j$ are local and do not change the number of particles: their experimental engineering is discussed in Ref. [104], see also [154].

Here we clarify that for the master equation for a single wire with hard-wall boundaries, the steady state is not topological and does not feature Majorana edge physics, although they still display the bulk properties of a p-wave superconductor (instead, the two-wire version studied below *has* topological properties associated to dissipative Majorana zero modes). The asymptotic decay rate of the master equation is also characterized. An extensive numerical study of the stability of this protocol is postponed to Sec. 7.4.

7.3.1 Steady states

In order to characterize the stationary states of the dynamics, let us first observe that Eq. (7.11) implies [115]

$$\hat{C}_j^\dagger |\psi_\sigma\rangle = -\hat{A}_j |\psi_\sigma\rangle, \tag{7.15}$$

so that:

$$\hat{L}'_j |\psi_\sigma\rangle = \hat{C}_j^\dagger \hat{A}_j |\psi_\sigma\rangle = -\hat{C}_j^\dagger \hat{C}_j^\dagger |\psi_\sigma\rangle = 0. \tag{7.16}$$

Thus, $|\psi_\sigma\rangle$ are steady states of the dynamics. Let us define the states

$$|\psi_N\rangle = \hat{\Pi}_N |\psi_\sigma\rangle, \tag{7.17}$$

where $\hat{\Pi}_N$ is the projector onto the subspace of the global Hilbert (Fock) space with N fermions ($\hat{\Pi}_N|\psi_\sigma\rangle = 0$ when the parity of N differs from σ and thus we avoid the redundant notation $|\psi_{\sigma,N}\rangle$). Since $[\hat{L}'_j, \hat{N}] = 0$, where $\hat{N} = \sum_j \hat{a}_j^\dagger \hat{a}_j$ is the particle-number operator, it holds that $\hat{L}'_j|\psi_N\rangle = 0$ for all $j = 1, \ldots, L-1$ and thus the $|\psi_N\rangle$ are dark states. Let us show that there is only one dark state $|\psi_N\rangle$ once the value of N is fixed. To this end, we consider the parent Hamiltonian (7.3) associated to the Lindblad operators (7.13):

$$\hat{\mathcal{H}}'_p = 2J \sum_{j=1}^{L-1} \Big[\hat{n}_j + \hat{n}_{j+1} - 2\hat{n}_j\hat{n}_{j+1} - \hat{a}_{j+1}^\dagger \hat{a}_j - \hat{a}_j^\dagger \hat{a}_{j+1} \Big], \tag{7.18}$$

where $\hat{n}_j \equiv \hat{a}_j^\dagger \hat{a}_j$ and $J > 0$ is a typical energy scale setting the units of measurement. Upon application of the Jordan-Wigner transformation, the model $\hat{\mathcal{H}}'_p$ is unitarily equivalent to the following spin-1/2 chain model:

$$\hat{\mathcal{H}}'_{p,spin} = J \sum_{j=1}^{L-1} \Big[1 + \hat{\sigma}_j^x \hat{\sigma}_{j+1}^x + \hat{\sigma}_j^y \hat{\sigma}_{j+1}^y - \hat{\sigma}_j^z \hat{\sigma}_{j+1}^z \Big], \tag{7.19}$$

where $\hat{\sigma}_j^\alpha$ are Pauli matrices. Apart from a constant proportional to $L-1$, $\hat{\mathcal{H}}'_{p,spin}$ is the ferromagnetic Heisenberg model. The particle-number conservation corresponds to the conservation of the total magnetization along the $\hat{z}$ direction. It is a well-known fact that this model has a highly degenerate ground state but that there is only one ground state for each magnetization sector, both for finite and infinite lattices. Thus, this state corresponds to the state $|\psi_N\rangle$ identified above; therefore, the possibility that the ground state of $\hat{\mathcal{H}}'_p$ is two-fold degenerate (as would be required for the existence of Majorana modes) for fixed number of fermions and hard-wall boundary conditions is ruled out.

Summarizing, the dynamics induced by the Lindblad operators in (7.13) conserves the number of particles and drives the system into a quantum state with the properties of a p-wave superconductor (in the thermodynamic limit $|\psi_e\rangle$ and $\hat{\Pi}_N|\psi_e\rangle$ have the same bulk properties, as it is explicitly checked in Ref. [104, 105], but see also the discussion below). Since the steady states of the system for open boundary conditions are unique, they do not display any topological edge property.

7.3.2 P-wave superconductivity

Let us explicitly check that the states $|\psi_N\rangle$ have the properties of a p-wave superconductor. Since each state has a definite number of fermions, the order parameter defined in Eq. (7.12) is zero by symmetry arguments. In a number-conserving setting, we thus rely on the p-wave pairing correlations:

$$G_{j,l}^{(p)} = \langle \psi_N | \hat{O}_j^{(p)\dagger} \hat{O}_l^{(p)} | \psi_N \rangle = \langle \psi_N | \hat{a}_j^\dagger \hat{a}_{j+1}^\dagger \hat{a}_{l+1} \hat{a}_l | \psi_N \rangle. \tag{7.20}$$

If in the long-distance limit, $|l-j| \to \infty$, the expectation value saturates to a finite value or shows a power-law behavior, the system displays p-wave superconducting (quasi-)long-range order. If the decay is faster, e.g. exponential, the system is disordered.

In this specific case, the explicit calculation shows a saturation at large distance (see also Ref. [115]):

$$G^{(p)}_{j,l} \xrightarrow{|j-l|\to\infty} \nu^2(1-\nu)^2 \tag{7.21}$$

in the thermodynamic limit. The saturation to a finite value captures the p-wave superconducting nature of the states. Note that the breaking of a continuous symmetry in a one-dimensional system signaled by Eq. (7.21) is a non-generic feature: a perturbation of Hamiltonian $\hat{\mathcal{H}}'_p$ would turn that relation into a power-law decay to zero as a function of $|j-l|$ (see Ref. [115] for an explicit example).

7.3.3 Dissipative gap

An interesting feature of $\hat{\mathcal{H}}'_{p,spin}$ is that it is gapless; the gap closes as L^{-2} due to the fact that the low-energy excitations have energy-momentum relation $\omega_q \sim q^2$, as follows from well-known properties of the ferromagnetic Heisenberg model. The Jordan-Wigner transformation conserves the spectral properties and thus $\hat{\mathcal{H}}'_p$ is also gapless. Thus, according to the discussion in Sec. 7.2.1, the asymptotic decay rate λ'_{ADR} associated to the Lindbladian $\mathcal{L}'$ closes in the thermodynamic limit. This is true both for periodic and hard-wall boundary conditions.

This fact has two important consequences. The first is that the dissipative preparation of a fixed-number p-wave superconductor through this method requires at least a typical time τ' that scales like L^2. In Sec. 7.4 we numerically confirm this polynomial scaling. Although this requires an effort which is polynomial in the system size, and which is thus efficient, it is a slower dynamical scenario than that of the non-number-conserving dynamics considered in Refs. [104, 105] and summarized in Sec. 7.2.2, where τ does not scale with L (the super-operator $\mathcal{L}$ in that case is gapped), and thus the approach to stationarity is exponential in time. The difference can be traced to the presence of dynamical slow modes related to exact particle number conservation, a property which is abandoned in the mean field approximation of Refs. [104, 105].

The second consequence is that a gapless Lindbladian $\mathcal{L}$ does not ensure an *a priori* stability of the dissipative quantum state preparation. Roughly speaking, even a small perturbation $\epsilon\mathcal{M}'$ ($\epsilon \ll 1$) to the Lindbladian $\mathcal{L}'$ such that the dynamics is ruled by $\mathcal{L}' + \epsilon\mathcal{M}'$ has the potential to qualitatively change the physics of the steady-state (see Refs. [156, 157, 158] for some examples where the presence of a gap is exploited for a perturbative analysis of the steady states). This concerns, in particular, the long-distance behavior of correlation functions. To further understand this last point, in Sec. 7.4 we have analyzed the effect of several perturbations through numerical simulations. In the case in which the steady state has topological properties, they may still be robust. We further elaborate on this point in Sec. 7.5, where we study the ladder setup.

Notwithstanding the gapless nature of the Lindbladian $\mathcal{L}'$, we can show that waiting for longer times is beneficial to the quantum state preparation.

If we define $p_0(t) = \mathrm{tr}\big[\hat{P}_0\hat{\rho}(t)\big]$, where $\hat{P}_0$ is the projector onto the ground space of the parent Hamiltonian $\hat{\mathcal{H}}'_p$, then the following monotonicity property holds:

$$\frac{\mathrm{d}}{\mathrm{d}t}p_0(t) \geq 0. \tag{7.22}$$

Indeed, $\frac{\mathrm{d}}{\mathrm{d}t}p_0(t) = \mathrm{tr}\big[\hat{P}_0\mathcal{L}'[\hat{\rho}(t)]\big] = \mathrm{tr}\big[\mathcal{L}'^{*}[\hat{P}_0]\hat{\rho}(t)\big]$, where $\mathcal{L}'^{*}$ is the adjoint Lindbladian. It is easy to see that $\mathcal{L}'^{*}[\hat{P}_0] = \gamma\sum_j \hat{L}'^{\dagger}_j\hat{P}_0\hat{L}'_j$, which is a non-negative operator because for any state $|\phi\rangle$ it holds that:

$$\begin{aligned}\langle\phi|\mathcal{L}'^{*}[\hat{P}_0]|\phi\rangle =&\gamma\sum_j\langle\phi|\hat{L}'^{\dagger}_j\hat{P}_0\hat{L}'_j|\phi\rangle = \\ =&\gamma\sum_{j,\alpha}|\langle\psi_\alpha|\hat{L}'_j|\phi\rangle|^2 > 0\end{aligned} \tag{7.23}$$

where $\{|\psi_\alpha\rangle\}$ are a basis of the ground space of the parent Hamiltonian $\hat{\mathcal{H}}'_p$. If we consider the spectral decomposition of $\hat{\rho}(t) = \sum_\beta p_\beta|\phi_\beta\rangle\langle\phi_\beta|$, with $p_\beta > 0$, we obtain Eq. (7.22).

7.4 Single wire: Numerical results

Although the previous analysis, based on the study of the dark states of the dynamics, has already identified many distinguishing properties of the system, there are several features which lie outside its prediction range. Let us list for instance the exact size scaling of the asymptotic decay rate or the resilience of the scheme to perturbations. In order to complement the analysis of the dissipative dynamics with these data, we now rely on a numerical approach.

The numerical analysis that we are going to present is restricted to systems with hard-wall boundary conditions. In order to characterize the time evolution described by the master equation (7.14), we use two different numerical methods. The first is a Runge-Kutta (RK) integration for systems of small size (up to $L = 10$) [116]. This method entails an error due to inaccuracies in the numerical integration, but the density matrix is represented without any approximation.

On the contrary, the second method, based on a Matrix-Product-Density-Operator (MPDO) representation of the density matrix, allows the study of longer systems through an efficient approximation of $\hat{\rho}$ [117, 118, 119]. The time evolution is performed through the Time-Evolving Block Decimation (TEBD) algorithm, which is essentially based on the Trotter decomposition of the Liouville super-operator $e^{t\mathcal{L}'}$. Although this method has been shown to be able to reliably describe problems with up to ~ 100 sites [150], in this case we are not able to consider lengths beyond $L = 22$ because of the highly-entangled structure of the states encountered during the dynamics. It is an interesting perspective to investigate whether algorithms based on an MPDO representation of the density matrix, which compute the steady state through maximization of the Lindbladian super-operator $\mathcal{L}'$, might prove more fruitful in this context [149, 152].

Finally, we have also performed Exact-Diagonalization (ED) studies of system sizes up to $L = 5$ in order to access properties of $\mathcal{L}'$, such as its spectrum, which cannot be observed with the time-evolution.

7.4.1 Asymptotic decay rate

Let us first assess that the asymptotic decay rate of the system closes polynomially with the system size (from the previous analysis we know that it closes *at least* polynomially. As we discuss in Appendix 7.7.1, in the asymptotic limit, it is possible to represent the expectation value of any observable $\hat{A}$ as:

$$\langle \hat{A} \rangle(t) - \langle \hat{A} \rangle_{ss} \sim \kappa e^{-\lambda_{ADR} t} + \dots \tag{7.24}$$

where $\langle \hat{A} \rangle(t) = tr\left[\hat{A}\,\hat{\rho}(t)\right]$, $\langle \hat{A} \rangle_{ss} = \lim_{t\to\infty} \langle \hat{A} \rangle(t)$ and κ is a non-universal constant. The notation $-\lambda_{ADR}$ is due to the fact that λ_{ADR} is positive, being defined through the additive inverse of the real part of the eigenvalues, see Eq. (7.4). It is possible to envision situations where $\kappa = 0$ and thus the long-time decay is dominated by eigenvalues of $\mathcal{L}'$ with smaller real part.

The study of the long-time dependence of any observable can be used to extract the value of λ_{ADR}; among all the possible choices, we employ the pairing correlator $G^{(p)}_{j,l}(t) = \langle \hat{O}^{(p)\dagger}_j \hat{O}^{(p)}_l \rangle(t)$ [see Eq. (7.20)] because of its special physical significance. In Fig. 7.1(top), we consider $L = 10$ and plot the time evolution of $G^{(p)}_{j,l}(t)$ for $j = 1$ and $l = L - 1$ (no relevant boundary effects have been observed as far as the estimation of λ_{ADR} is concerned). The calculation is performed through RK integration of the master equation. The initial state of the evolution is given by the ground state of the non-interacting Hamiltonian, $\hat{\mathcal{H}}_0 = -J \sum_j \hat{a}^\dagger_j \hat{a}_{j+1} + H.c.$ ($N = L/2$ for L even, and $N = (L+1)/2$ for L odd).

In order to benchmark the reliability of the RK integration for getting the steady state, we compare the expectation value of several observables (in particular of pairing correlators) with the exactly-known results (Sec. 7.3 provides the exact wavefunction of the steady state, from which several observables can be computed). In all cases the absolute differences are below 10^{-6}. Similar results are obtained for smaller system sizes, where it is even possible to compute the trace-distance of the RK steady-state from the $\lambda = 0$ eigenstate of the Liouvillian computed with ED.

In the long-time limit, the observable (7.20) displays a clear stationary behavior, $\left[G^{(p)}_{j,l}\right]_{ss} = \lim_{\tau\to\infty} G^{(p)}_{j,l}(\tau)$, consistently with Eq. (7.24). Once such stationary value is subtracted, it is possible to fit λ_{ADR} from the exponential decay of

$$G^{(p)}_{j,l}(t) - \left[G^{(p)}_{j,l}\right]_{ss} \tag{7.25}$$

The subtraction is possible to high precision because the value of $\left[G^{(p)}_{j,l}\right]_{ss}$ is known from the previous analytical considerations. Moreover, as we have already pointed out, the evolution continues up to times such that $G^{(p)}_{j,l}(t)$ differs in absolute terms from the analytical value for $\lesssim 10^{-6}$, which makes the whole procedure reliable.

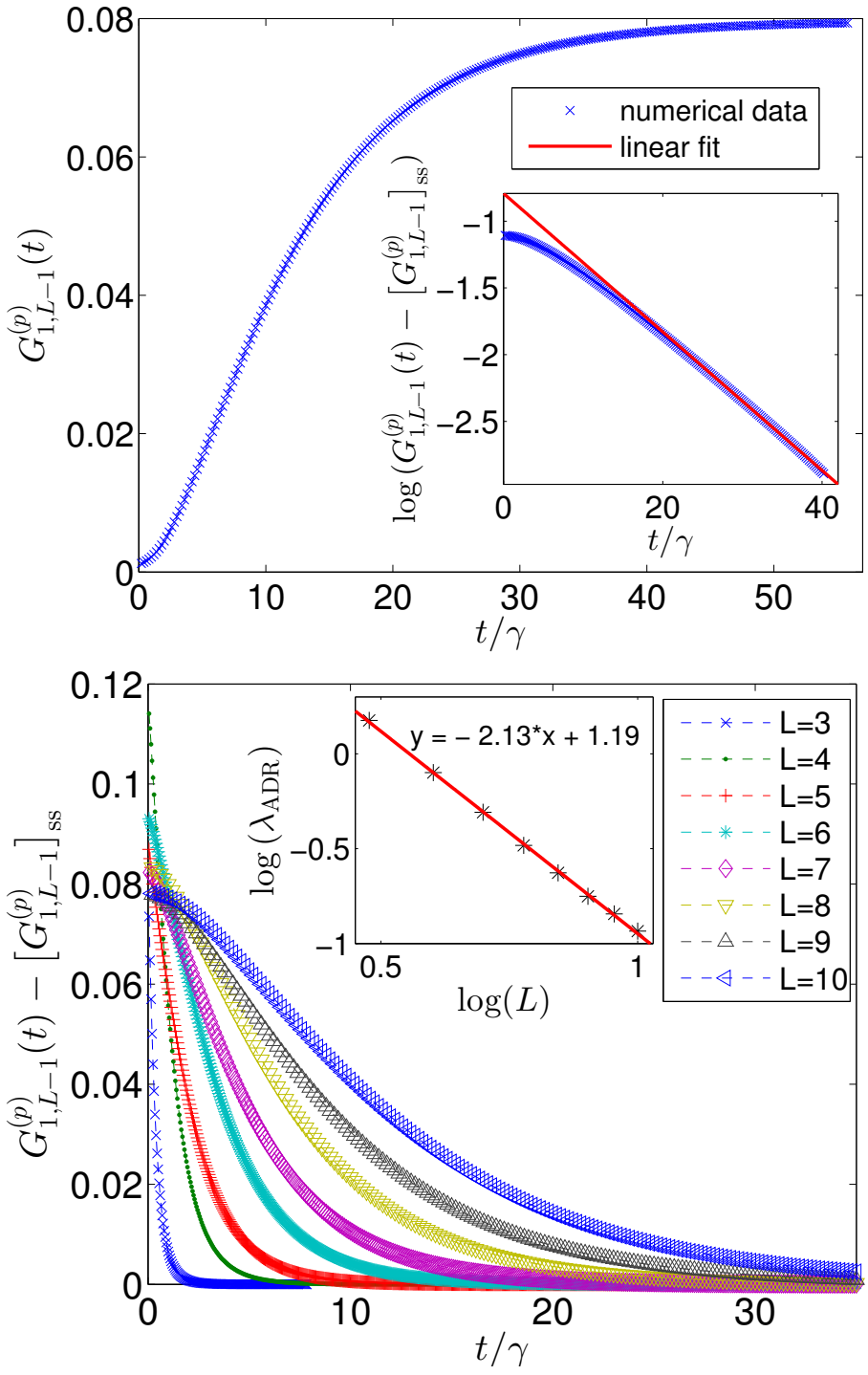

Figure 7.1: (Top) Runge-Kutta time evolution of the pairing correlator $G^{(p)}_{1,L-1}(t)$ for the largest available system size, $L = 10$. The inset shows that upon subtraction of the steady value, an exponential decay is observed, from which λ_{ADR} is extracted. (Bottom) Time evolution of $G^{(p)}_{1,L-1}(t) - \left[G^{(p)}_{1,L-1}\right]_{ss}$ for several system sizes. The inset shows the scaling of λ_{ADR} with L, which is fitted by an algebraic function.

In Fig. 7.1(bottom) we display the quantity in (7.25) for various lattice sizes L. It is clear that the convergence of the observable requires an amount of time which increases with L. A systematic fit of λ_{ADR} for several chain lengths allows for an estimate of its dependence on L [see Fig. 7.1(bottom)]: the finite-size dissipative gap scales as

$$\lambda_{ADR} \propto L^{-2.13\pm0.05} \,. \tag{7.26}$$

The exact diagonalization (ED) of the Liouvillian up to $L = 5$ allows a number of further considerations. First, the Liouvillian eigenvalues with largest real part ($\Re(\lambda) \lesssim 0$) are independent of the number of particles (the check has been performed for every value of $N = 1, ..., 5$). Second, comparing the ED with the previous analysis, we observe that the λ_{ADR} in Eq. (7.26) coincides with the second eigenvalue of the Liouvillian, rather than with the first [here the generalized eigenvalues are ordered according to the additive inverse of their real part $-\Re(\lambda)$]. Numerical inspection of small systems (up to $L = 5$) shows that the first excited eigenvalue of $\mathcal{L}'$ is two-fold degenerate and takes the value $-\xi/2$, where ξ is the energy of the first excited state of $\hat{\mathcal{H}}'_p$ (see the discussion in Sec. 7.2.1). Our numerics suggests that it does not play any role in this particular dissipative evolution, hinting at the fact that the chosen $\hat{\rho}(0)$ does not overlap with the eigensubspace relative to $-\xi/2$. In this case, the value of κ in Eq. (7.24) is zero.

7.4.2 Perturbations

In order to test the robustness of the dissipative scheme for the preparation of a p-wave superconductor, we now consider several perturbations of the Lindbladian $\mathcal{L}'$ of both dissipative and Hamiltonian form. The robustness of the dissipative state preparation of the p-wave superconductor is probed through the behavior of the correlations $G^{(p)}_{j,l}(t)$, which define such phase.

Perturbations of the Lindblad operators

Let us define the following perturbed Lindblad operator:

$$\hat{L}'_{j,\epsilon} = \hat{C}^\dagger_j \hat{A}_{j,\epsilon}; \quad \hat{A}_{j,\epsilon} = \hat{a}_j - (1-\epsilon)\hat{a}_{j+1}; \quad \epsilon \in \mathbb{R}, \tag{7.27}$$

which allows for slight asymmetries in the action of the dissipation between sites j and $j+1$. The continuity equation associated to the dynamics, $\partial_t \hat{n}_i = -(\hat{j}_i - \hat{j}_{i-1})$, is characterized by the following current operator: $\hat{j}_i = \hat{n}_i - (1-\epsilon)^2\hat{n}_j + (\epsilon^2 - 2\epsilon)\hat{n}_i\hat{n}_{i+1}$. When $\epsilon \neq 0$, $\hat{j}_i$ is not anymore odd under space reflection around the link between sites i and $i+1$, so that in the stationary state a non-zero current can flow even if the density profile is homogeneous (and even under the previous space-inversion transformation), which is quite intuitive given the explicit breaking of inversion symmetry in this problem.

We employ the MPDO method to analyze the steady-state properties of a system with size $L = 22$ initialized in the ground state of the free Hamiltonian $\hat{\mathcal{H}}_0$ for $N = 11$ and subject to such dissipation. The results in the inset of Fig. 7.2 show that the steady state is not homogeneous and that a

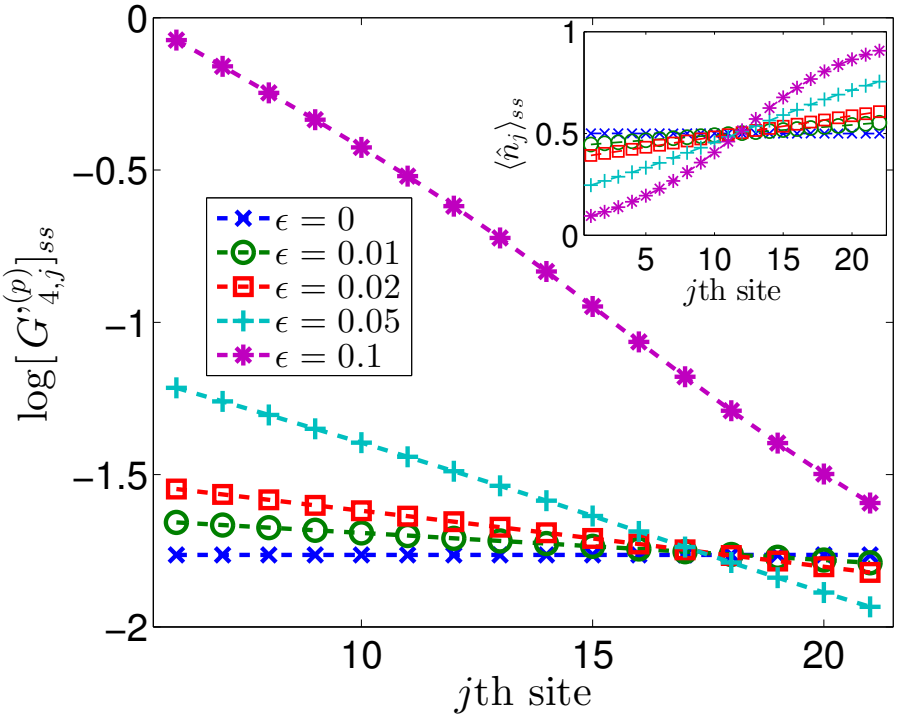

Figure 7.2: Steady-state values of $\left[G'^{(p)}_{4,j}\right]_{ss}$ [see Eq. (7.28)] for a lattice with $L = 22$ sites at half-filling, $\nu = 1/2$, computed with MPDO for different values of ϵ in $\hat{L}'_{j,\epsilon}$ [see Eq. (7.27)]. The inset displays the steady-state values of the local number of fermions $\langle \hat{n}_j \rangle_{ss}$ for the same systems.

relatively high degree of inhomogeneity $\frac{\langle \hat{n}_L \rangle - \langle \hat{n}_1 \rangle}{\langle \hat{n}_{L/2} \rangle} \approx 1$ is found also for small perturbations $\epsilon = 0.05$. This is not to be confused with the phase-separation instability which characterizes the ferromagnetic parent Hamiltonian $\hat{\mathcal{H}}'_{p,\text{spin}}$. Indeed, if PBC are considered, the system becomes homogeneous and a current starts flowing in it (not shown here).

P-wave superconducting correlations are affected by such inhomogeneity. Whereas for $\epsilon = 0$ the correlations $\left[G^{(p)}_{j,l}\right]_{ss}$ do not show a significant dependence on $|j-l|$, this is not true even for small perturbations $\epsilon \leq 0.05$. In order to remove the effect of the inhomogeneous density, in Fig. 7.2 we show the value of properly rescaled p-wave correlations:

$$\left[G'^{(p)}_{j,l}\right]_{ss} \equiv \langle \hat{O}'^{(p)\dagger}_j \hat{O}'^{(p)}_l \rangle_{ss} = \frac{(N/L)^4 \langle \hat{O}^{(p)\dagger}_j \hat{O}^{(p)}_l \rangle_{ss}}{\langle \hat{n}_j \rangle_{ss} \langle \hat{n}_{j+1} \rangle_{ss} \langle \hat{n}_l \rangle_{ss} \langle \hat{n}_{l+1} \rangle_{ss}} \tag{7.28}$$

where $\hat{O}'^{(p)}_j = (N/L)^2 \hat{O}^{(p)}_j / (\langle \hat{n}_j \rangle_{ss} \langle \hat{n}_{j+1} \rangle_{ss})$. An exponential decay behavior appears as a function of $|j-l|$, which becomes more pronounced when ϵ is increased. Even if the simulation is performed on a finite short system, for significant perturbations, $\epsilon = 0.1$, the value of $\left[G'^{(p)}_{j,l}\right]_{ss}$ decays of almost

two decades, so that the exponential behavior is identified with reasonable certainty.

In Appendix 7.7.2 we discuss some interesting analogies of these results with the properties of the ground state of the parent Hamiltonian $\hat{\mathcal{H}}'_{p,\epsilon} = J\sum_j \hat{L}'^{\dagger}_{j,\epsilon}\hat{L}'_{j,\epsilon}$. It should be stressed that, since $\hat{\mathcal{H}}'_{p,\epsilon}$ does not have a zero-energy ground state, there is no exact correspondence between its ground state and the steady states of $\mathcal{L}'_\epsilon$.

Concluding, we mention that a similar analysis can be done introducing an analogous perturbation in the operator $\hat{C}^{\dagger}_j$; our study did not observe any qualitative difference (not shown).

Perturbations due to unitary dynamics

An alternative way of perturbing the dynamics of $\mathcal{L}'$ in Eq. (7.14) is to introduce a Hamiltonian into the system, chosen for simplicity to be the already-introduced free Hamiltonian $\hat{\mathcal{H}}_0$:

$$\frac{\partial}{\partial t}\hat{\rho} = -i[\epsilon\hat{\mathcal{H}}_0, \hat{\rho}] + \mathcal{L}[\hat{\rho}]. \tag{7.29}$$

Using the MPDO method to characterize the steady state of the dynamics, we analyze the spatial decay of the pairing correlations for $L = 22$ and at half-filling ($N = 11$); the initial state is set in the same way as in the previous section. In Fig. 7.3 (top) we display the results: even for very small perturbations the pairing correlator $\left[G^{(p)}_{4,j}\right]_{ss}$ decays rapidly in space. The long-distance saturation observed in the absence of perturbations is lost and qualitatively different from this result. In Fig. 7.3 (bottom) we highlight that the decay is exponential.

Summarizing, in all the cases that we have considered, the p-wave pairing correlations of the stationary state $\left[G^{(p)}_{j,l}\right]_{ss}$ are observed to decay as a function of $|j-l|$. Due to the interplay between the targeted dissipative dynamics and the perturbations, which do not support a p-wave ordered dark state, the steady state is mixed, similar to a finite temperature state. From this intuition, the result is easily rationalized: Any (quasi) long range order is destroyed in one-dimensional systems at finite temperature. We note that the true long range order found in the unperturbed case (correlators saturating at large distance; opposed to the more generic quasi-long range order defined with algebraic decay) is non-generic in one-dimensional systems and a special feature of our model, see [115] for a thorough discussion. However, the destruction of any such order via effective finite temperature effects must be expected on general grounds. The absence of quasi-long-range p-wave superconducting order, which in one-dimension only occurs at zero-temperature for pure state, is likely to be in connection with this fact.

Perturbation strength

Finally, we perform a quantitative investigation of the dependence of the pairing correlations on the perturbation strength, ϵ.

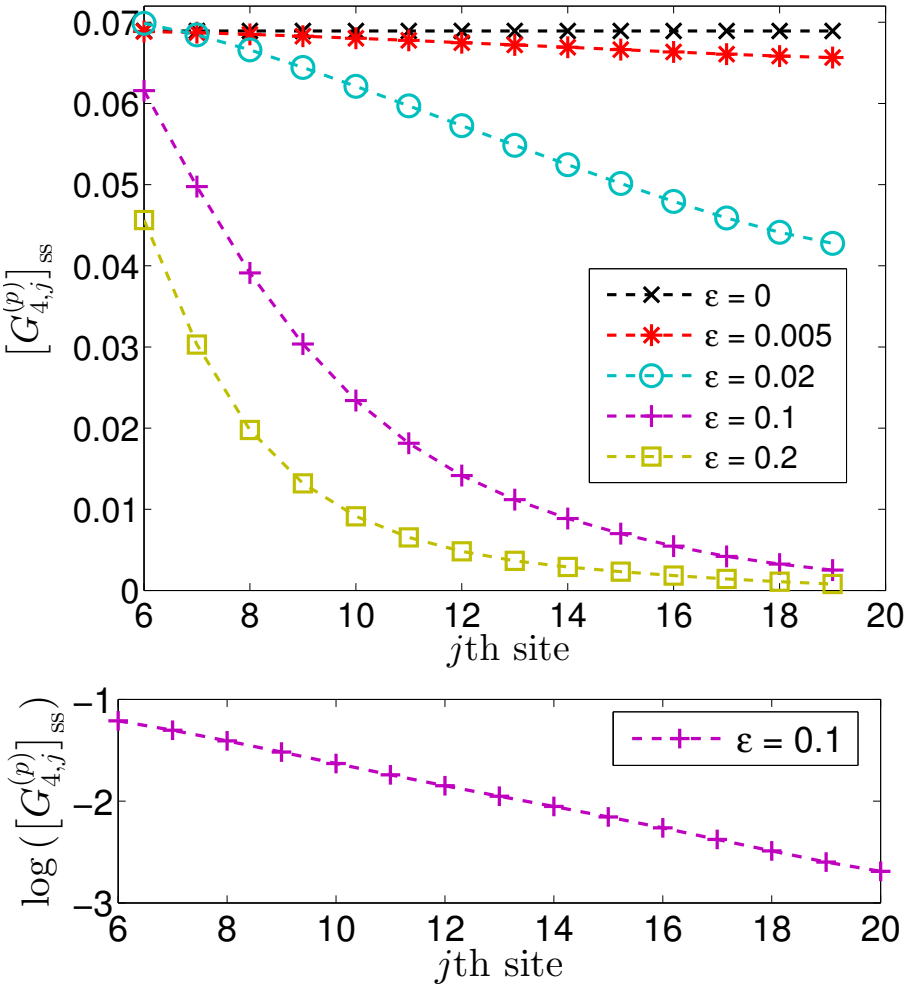

Figure 7.3: (Top) Pairing correlations $[G^{(p)}_{4,j}]_{ss}$ for the steady state of the dynamics in the presence of a Hamiltonian perturbation (7.29). The calculation of the steady state is performed with MPDO technique for $L = 22$ and $N = 11$. (Bottom) The decay of $[G^{(p)}_{4,j}]_{ss}$ is exponential in j (here, $\epsilon = 0.1$).

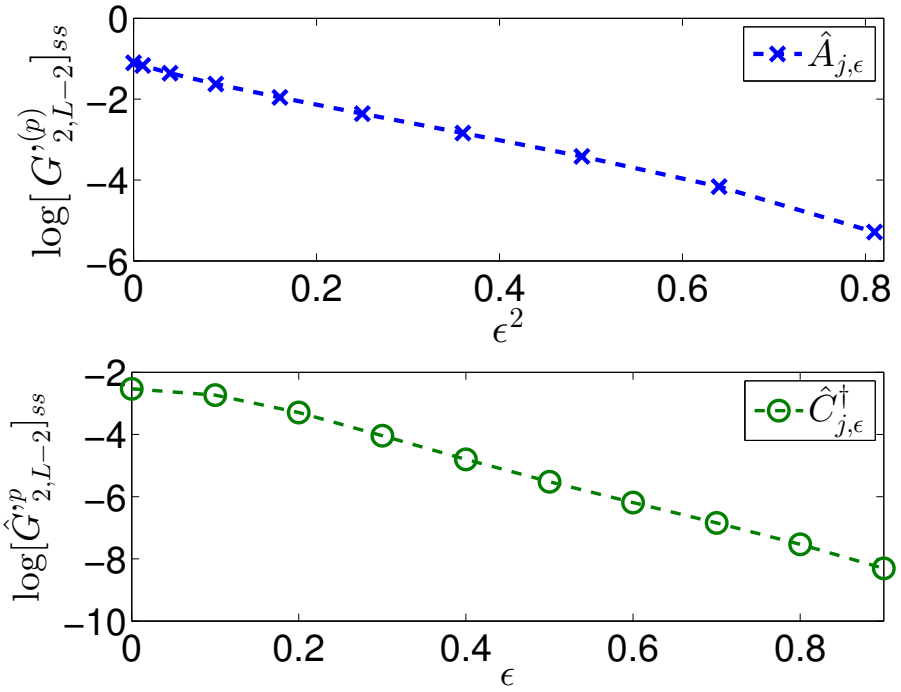

Figure 7.4: $\left[G'^{(p)}_{2,L-2}\right]_{ss}$ in the presence of a perturbed Lindblad operator as a function of the perturbation strength ϵ. The perturbation is considered both for the $\hat{A}_j$ (top) and $\hat{C}^{\dagger}_j$ (bottom) operators (see text for the definitions). The calculation is done with RK integration of the equation of motion for $L = 8$ and $N = 4$.

Lindblad perturbation – In Fig. 7.4 we plot the p-wave superconducting correlation $\left[G^{(p)}_{2,L-2}\right]_{ss}$ of a system of length $L = 8$ as a function of the intensity of the perturbation ϵ in $\hat{L}'_{j,\epsilon}$ (for completeness, the complementary case $\hat{L}'^{(2)}_{j,\epsilon} = \hat{C}^{\dagger}_{j,\epsilon}\hat{A}_j$, with $\hat{C}^{\dagger}_{j,\epsilon} = \hat{a}^{\dagger}_j + (1-\epsilon)\hat{a}^{\dagger}_{j+1}$, is also included). Our data confirm that correlations undergo a clear suppression in the presence of $\epsilon \neq 0$, which in one case is exponential in ϵ and in the other in ϵ^2. The calculation is performed through RK integration of the dynamics.

Hamiltonian perturbation – We begin with the two cases: $\hat{\mathcal{H}}_0$ and $\hat{\mathcal{H}}_{nn} = -J\sum_j \hat{n}_j\hat{n}_{j+1}$. Fig. 7.5 shows, in both cases, an exponential decay to zero of $\left[G'^{(p)}_{2,L-2}\right]_{ss}$ when ϵ is increased. On the contrary, a Hamiltonian which introduces p-wave correlations in the system, such as

$$\hat{\mathcal{H}}_{pair} = -J\sum_{j,l}(\hat{a}^{\dagger}_j\hat{a}^{\dagger}_{j+1}\hat{a}_{l+1}\hat{a}_l + H.c.), \tag{7.30}$$

changes the value and the sign of $\left[G'^{(p)}_{2,L-2}\right]_{ss}$, leaving it different from zero.

Concluding, we have shown that in all the considered cases, perturbations of both dissipative and Hamiltonian form are detrimental to the creation of a p-wave superconductor. This is rationalized by the mixedness of the stationary

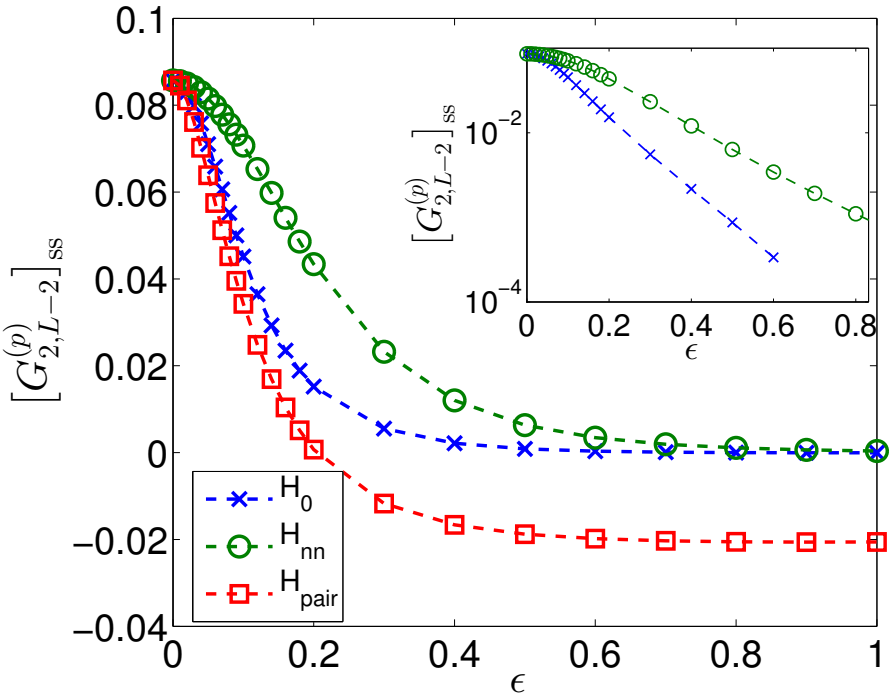

Figure 7.5: $\left[G^{(p)}_{2,L-2}\right]_{ss}$ in the presence of a perturbing Hamiltonian as a function of the perturbation strength ϵ. We consider $\hat{\mathcal{H}}_0$, $\hat{\mathcal{H}}_{nn}$ and $\hat{\mathcal{H}}_{pair}$ (see text for the definitions). The inset highlights the exponential decay with ϵ.

state in that case, and parallels a finite temperature situation. In any generic, algebraically ordered system at T=0, one has gapless modes.

7.5 Two wires

An intuitive explanation of why the dissipative setup discussed in Sec. 7.3 does not show topological dark states with fixed number of particles is the fact that this constraint fixes the parity of the state, and thus no topological degeneracy can occur. It has already been realized in several works that a setup with two parallel wires can overcome this issue [98, 99, 100, 101, 102, 115, 140]. In this case it is possible to envision a number-conserving p-wave superconducting Hamiltonian which conserves the parity of the number of fermions in each wire: such symmetry can play the role of the parity of the number of fermions for $\hat{\mathcal{H}}_K$ in Eq. (7.8). Several equilibrium models have already been discussed in this context; here we consider the novel possibility of engineering a topological number-conserving p-wave superconductor with Markovian dynamics.

7.5.1 Steady states

Let us study a system composed of two wires with spinless fermions described by the canonical fermionic operators $\hat{a}_j^{(\dagger)}$ and $\hat{b}_j^{(\dagger)}$. For this model we consider three kinds of Lindblad operators:

$$\hat{L}''_{a,j} = \hat{C}^\dagger_{a,j}\hat{A}_{a,j}; \tag{7.31a}$$

$$\hat{L}''_{b,j} = \hat{C}^\dagger_{b,j}\hat{A}_{b,j}; \tag{7.31b}$$

$$\hat{L}''_{I,j} = \hat{C}^\dagger_{a,j}\hat{A}_{b,j} + \hat{C}^\dagger_{b,j}\hat{A}_{a,j}. \tag{7.31c}$$

We now characterize the dark states of the Markovian dynamics induced by these operators for a two-leg ladder of length L with hard-wall boundary conditions:

$$\frac{\partial}{\partial t}\hat{\rho} = \mathcal{L}''[\hat{\rho}] = \gamma \sum_{j=1}^{L-1} \sum_{\Lambda=a,b,I} \left[\hat{L}''_{\Lambda,j}\hat{\rho}\hat{L}''^\dagger_{\Lambda,j} - \frac{1}{2}\{\hat{L}''^\dagger_{\Lambda,j}\hat{L}''_{\Lambda,j}, \hat{\rho}\}\right]. \tag{7.32}$$

In particular, we will show that, for every fermionic density different from the completely empty and filled cases, there are always two steady states.

It is easy to identify the linear space $\mathcal{S}_N$ of states which are annihilated by the $\hat{L}''_{a,j}$ and $\hat{L}''_{b,j}$ and have a total number of particles N:

$$\mathcal{S}_N = \mathrm{span}\{|\psi_{a,0}\rangle|\psi_{b,N}\rangle, |\psi_{a,1}\rangle|\psi_{b,N-1}\rangle, \ldots, |\psi_{a,N}\rangle|\psi_{b,0}\rangle\}. \tag{7.33}$$

where the states $|\psi_{\alpha,N}\rangle$ are those defined in Eq. (7.17) for the wire $\alpha = a, b$. Let us consider a generic state in $\mathcal{S}_N$:

$$|\psi\rangle = \sum_{m=0}^{N} \alpha_m |\psi_{a,m}\rangle|\psi_{b,N-m}\rangle, \quad \sum_{m=0}^{N} |\alpha_m|^2 = 1. \tag{7.34}$$

From the condition $\hat{C}^\dagger_j|\psi_\sigma\rangle = -\hat{A}_j|\psi_\sigma\rangle$ we obtain:

$$\hat{C}^\dagger_j|\psi_{N-1}\rangle = -\hat{A}_j|\psi_{N+1}\rangle, \quad N \in (0, 2L) \tag{7.35a}$$

$$0 = -\hat{A}_j|\psi_1\rangle, \tag{7.35b}$$

$$\hat{C}^\dagger_j|\psi_{2L-1}\rangle = 0, \tag{7.35c}$$

and when we impose the condition $\hat{L}''_{I,j}|\psi\rangle = 0$:

$$\begin{aligned}\hat{L}''_{I,j}|\psi\rangle &= \sum_{m=0}^{N-1} \alpha_m \hat{C}^\dagger_{a,j}\hat{A}_{b,j}|\psi_{a,m}\rangle|\psi_{b,N-m}\rangle + \sum_{m=1}^{N} \alpha_m \hat{C}^\dagger_{b,j}\hat{A}_{a,j}|\psi_{a,m}\rangle|\psi_{b,N-m}\rangle = \\ &= \sum_{m=0}^{N-1} \alpha_m \hat{C}^\dagger_{a,j}\hat{A}_{b,j}|\psi_{a,m}\rangle|\psi_{b,N-m}\rangle - \sum_{m=2}^{N+1} \alpha_m \hat{C}^\dagger_{a,j}\hat{A}_{b,j}|\psi_{a,m-2}\rangle|\psi_{b,N-m+2}\rangle = 0.\end{aligned} \tag{7.36}$$

The result is $\alpha_m = \alpha_{m+2}$, so that two linearly independent states can be constructed which are annihilated by all the Lindblad operators in (7.31):

$$|\psi_{N,ee}\rangle = \frac{1}{\mathcal{N}_{N,ee}^{1/2}} \sum_m |\psi_{a,2m}\rangle |\psi_{b,N-2m}\rangle, \tag{7.37a}$$

$$|\psi_{N,oo}\rangle = \frac{1}{\mathcal{N}_{N,oo}^{1/2}} \sum_m |\psi_{a,2m-1}\rangle |\psi_{b,N-2m+1}\rangle. \tag{7.37b}$$

The subscripts ee and oo refer to the fermionic parities in the first and second wire assuming that N is even; $\mathcal{N}_{N,ee}$ and $\mathcal{N}_{N,oo}$ are normalization constants [115]. For N odd one can similarly construct the states $|\psi_{N,eo}\rangle$ and $|\psi_{N,oe}\rangle$. By construction, the states that we have just identified are the only dark states of the dynamics.

It is an interesting fact that at least two parent Hamiltonians are known for the states in (7.37), as discussed in Refs. [115, 140]. We refer the reader interested in the full characterization of the topological properties of these steady-states to those articles.

Finally, let us mention that the form of the Lindblad operators in (7.31) is not uniquely defined. For example one could replace $\hat{L}''_{I,j}$ in Eq. (7.31c) with the following:

$$\hat{L}''_{I,j} = \left(\hat{C}^\dagger_{a,j} + \hat{C}^\dagger_{b,j}\right)\left(\hat{A}_{a,j} + \hat{A}_{b,j}\right), \tag{7.38}$$

without affecting the results [115]. The latter operator is most realistic for an experimental implementation, as we point out below.

7.5.2 P-wave superconductivity

Let us now check that the obtained states are p-wave superconductors. Similarly to the single-wire protocol discussed in Eq. (7.21), the explicit calculation [115] shows that p-wave correlations saturate to a final value at large distances in the thermodynamic limit [for the two-leg ladder we consider $\nu = N/(2L)$]

$$\langle \psi_{N,ee}|\hat{O}_j^{(p)\dagger}\hat{O}_l^{(p)}|\psi_{N,ee}\rangle \xrightarrow{|j-l|\to\infty} \nu^2(1-\nu)^2. \tag{7.39}$$

This relation clearly highlights the p-wave superconducting nature of the states.

7.5.3 Dissipative gap

In order to demonstrate that the asymptotic decay rate λ_{ADR} associated to $\mathcal{L}''$ tends to 0 in the thermodynamic limit, we consider the parent Hamiltonian of

the model:

$$\begin{aligned}\hat{\mathcal{H}}''_p = &-4J\sum_{\substack{j=1\\ \alpha=a,b}}^{L-1}\Big[(\hat{\alpha}_j^\dagger\hat{\alpha}_{j+1}+\text{H.c.})-(\hat{n}_j^\alpha+\hat{n}_{j+1}^\alpha)+\hat{n}_j^\alpha\hat{n}_{j+1}^\alpha\Big]\\ &-2J\sum_{j=1}^{L-1}\Big[(\hat{n}_j^a+\hat{n}_{j+1}^a)(\hat{n}_j^b+\hat{n}_{j+1}^b)-(\hat{a}_j^\dagger\hat{a}_{j+1}\hat{b}_j^\dagger\hat{b}_{j+1}\\ &+\hat{a}_j^\dagger\hat{a}_{j+1}\hat{b}_{j+1}^\dagger\hat{b}_j-2\hat{b}_j^\dagger\hat{b}_{j+1}^\dagger\hat{a}_{j+1}\hat{a}_j+H.c.)\Big],\end{aligned} \tag{7.40}$$

where $J>0$ is a typical energy scale setting the units of measurement. This Hamiltonian has been extensively analyzed in Ref. [115]. Numerical simulations performed with the density-matrix renormalization-group algorithm assess that $\hat{\mathcal{H}}''_p$ is gapless and that the gap is closing as $1/L^2$. According to the discussion in Sec. 7.2.1, the asymptotic decay rate λ_{ADR} associated to the Lindbladian $\mathcal{L}''$ closes in the thermodynamic limit with a scaling which is equal to $\sim L^{-2}$ or faster. This is true both for periodic and hard-wall boundary conditions.

7.5.4 Experimental implementation

The Lindblad operators in Eqs. (7.31a), (7.31b) and (7.38) lend themselves to a natural experimental implementation. The engineering of terms like $\hat{L}''_{a,j}$ and $\hat{L}''_{b,j}$ has been extensively discussed in Ref. [104] starting from ideas originally presented in Ref. [113]. As we will see, the Lindblad operator $\hat{L}''_{I,j}$ in Eq. (7.38) is just a simple generalization.

The idea is as follows: a superlattice is imposed which introduces in the system additional higher-energy auxiliary sites located in the middle of each square of the lower sites target lattice. Driving lasers are then applied to the system, whose phases are chosen such that the excitation to the auxiliary sites happens only for states $|\varphi\rangle$ such that $(\hat{A}_{a,j}+\hat{A}_{b,j})|\varphi\rangle\neq 0$. If the whole system is immersed into, e.g., a Bose-Einstein condensate reservoir, atoms located in the auxiliary sites can decay to the original wire by emission of a Bogoliubov phonon of the condensate. This process is isotropic and, for a wavelength of the emitted phonons comparable to the lattice spacing, gives rise to the four-site creation part with relative plus sign: $\hat{C}^\dagger_{a,j}+\hat{C}^\dagger_{b,j}$.

7.5.5 Perturbations

An important property of topological Hamiltonians is the robustness of their edge physics to local perturbations. Similar features have been highlighted in the case of topological superconductors where the setup is not number conserving [104, 105]. The goal of this section is to probe the resilience of the twofold-degenerate steady states of $\mathcal{L}''$. A conclusive analysis is beyond our current numerical possibilities; here we present some preliminary results obtained via exact diagonalization methods.

We consider the natural choice of Lindblad operators Eqs. (7.31a,7.31b,7.38), subject to perturbations:

$$\hat{L}''_{a,j,\epsilon} = \hat{C}^{\dagger}_{a,j}\hat{A}_{a,j,\epsilon}; \quad \hat{A}_{a,j,\epsilon} = \hat{a}_j - (1-\epsilon)\hat{a}_{j+1}; \tag{7.41a}$$

$$\hat{L}''_{b,j,\epsilon} = \hat{C}^{\dagger}_{b,j}\hat{A}_{b,j,\epsilon}; \quad \hat{A}_{b,j,\epsilon} = \hat{b}_j - (1-\epsilon)\hat{b}_{j+1}; \tag{7.41b}$$

$$\hat{L}''_{I,j} = \left(\hat{C}^{\dagger}_{a,j} + \hat{C}^{\dagger}_{b,j}\right)\left(\hat{A}_{a,j,\epsilon} + \hat{A}_{b,j,\epsilon}\right); \quad \epsilon \in \mathbb{R} \tag{7.41c}$$

Those define a perturbed Lindbladian $\mathcal{L}''_{\epsilon}$. They are a simple generalization of those defined in Eq. (7.27) for the single-wire setup.

Let us begin our analysis by showing that for small sizes $L \sim 6$ the degeneracy of the steady space for $\epsilon = 0$ is broken. Let us first remark that for $\epsilon = 0$ the steady space is four-fold degenerate; a possible parameterization is:

$$\mathcal{B} = \{|\psi_{N,ee}\rangle\langle\psi_{N,ee}|, \quad |\psi_{N,ee}\rangle\langle\psi_{N,oo}|, \tag{7.42}$$

$$|\psi_{N,oo}\rangle\langle\psi_{N,ee}|, \quad |\psi_{N,oo}\rangle\langle\psi_{N,oo}|\}. \tag{7.43}$$

A direct inspection of the eigenvalues of $\mathcal{L}_{\epsilon}$ shows that this degeneracy is broken once $\epsilon \neq 0$. Results, shown in Fig. 7.6 for a fixed lattice size $L = 6$ and $N = 6$, display a quadratic splitting of the steady steady degeneracy with the perturbation strength.

Let us now check the behavior with the system size of the first eigenvalues of the system for longer system sizes. In order to obtain a reasonable number of data, the extreme choice of setting $N = 2$ in all simulations has been taken, which allows us to analyze system sizes up to $L = 20$. Results shown in Fig. 7.7 (top) show that the Liouvillian eigenvalues related to the steady-state degeneracy display an algebraic scaling $\lambda_{ADR} \sim L^{-1}$ in the accessible regime of system sizes for small perturbations ($\epsilon = 10^{-2}$), while they are gapped for larger perturbations ($\epsilon = 10^{-1}$). Note that, for the system sizes which could be accessed, larger eigenvalues clear display an algebraic decay, as shown in Fig. 7.7 (bottom), also for $\epsilon = 0.1$. The scaling of the eigenvalues related to the steady state degeneracy is not exponential and thus in principle should not be connected to the topological properties of the system. However, these preliminary considerations suffer from two significant biases: (i) the small considered sizes, (ii) the fact that they are not performed at exactly fixed density, and (iii) the very low filling. A more thorough analysis is left for future work.

7.6 Conclusions

In this chapter we have discussed the dissipative quantum state preparation of a p-wave superconductor in one-dimensional fermionic systems with fixed number of particles. In particular, we have presented two protocols which have been fully characterized in the presence of hard-wall boundaries. Whereas the former does not display topological property, the latter features a two-dimensional steady space to be understood in terms of boundary Majorana modes for any number of fermions. Through the analysis of a related parent

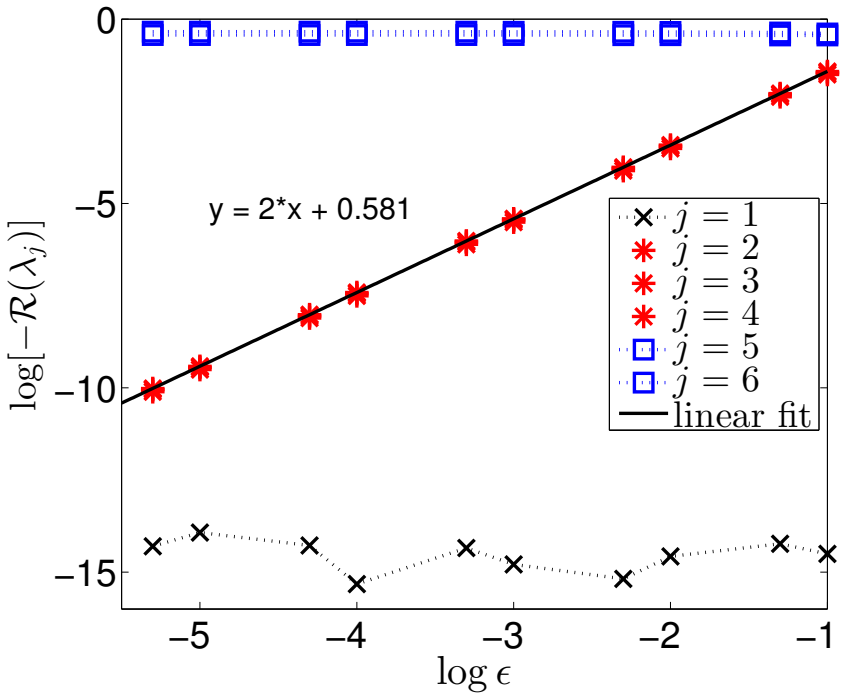

Figure 7.6: Real part of the first six eigenvalues of the Lindbladian operator $\mathcal{L}''_\epsilon$ for $L = 6$ and $N = 6$ as a function of ϵ. Eigenvalues λ_j are sorted according to increasing $-\Re(\lambda_j)$. The plot highlights the presence of a $\lambda = 0$ eigenvalue (within numerical accuracy 10^{-15}), of three eigenvalues which scale as ϵ^2 and of other eigenvalues of magnitude ~ 1.

Hamiltonian, we are able to make precise statements about the gapless nature of the Lindbladian super-operators associated to both dynamics.

The peculiar form of the master equations considered in this chapter allows for the exact characterization of several properties of the system, and in particular of the steady state, even if the dynamics is not solvable with the methods of fermionic linear optics [120, 121] exploited in Refs. [104, 105]. This result is very interesting *per se*, as such examples are usually rare but can drive physical intuition into regimes inaccessible without approximations. It is a remarkable challenge to investigate which of the properties presented so far are general and survive to modifications of the environment, and which ones are peculiar of this setup.

Using several numerical methods for the study of dissipative many-body systems, we have presented a detailed analysis of the robustness to perturbations of these setups. Through the calculation of the proper p-wave correlations we have discussed how external perturbations can modify the nature of the steady state. In the ladder setup, where the steady states are topological, we have presented preliminary results on the stability of the

degenerate steady-space of the system.

The analysis presented here has greatly benefited from exact mathematical relations between the properties of the Lindbladian and of a related parent Hamiltonian. Since the study of closed systems is much more developed than that of open systems both from the analytical and from the numerical points of view, a more detailed understanding of the relations between Lindbladians and associated parent Hamiltonian operators stands as a priority research program.

7.7 Appendix

7.7.1 Spectral properties of the Lindbladian super-operator

In order to discuss the long-time properties of the dissipative dynamics, it is convenient to start from the spectral decomposition of the Lindbladian. Since $\mathcal{L}$ is in general a non-Hermitian operator, its eigenvalues are related to its Jordan canonical form [159]. Let us briefly review these results. The Hilbert space of linear operators on the fermionic Fock space, $\mathbb{H}$, can be decomposed into the direct sum of linear spaces $\mathbb{M}_j$ (usually not orthogonal) such that if we denote with $\mathcal{P}_j$ the projectors onto such subspaces (usually not orthogonal) and with $\mathcal{N}_j$ a nilpotent super-operator acting on $\mathbb{M}_j$, the following is true:

$$\mathcal{L} = \sum_j [\lambda_j \mathcal{P}_j + \mathcal{N}_j]. \tag{7.44}$$

The $\{\lambda_j\}$ are the generalized complex eigenvalues of the super-operator $\mathcal{L}$ and, for the case of a Lindbladian, have non-positive real part; the $\mathcal{N}_j$ can also be equal to zero. By this explicit construction it is possible to observe that the $\{\mathcal{P}_j\}$ and $\{\mathcal{N}_j\}$ are all mutually commuting ($\mathcal{P}_j\mathcal{P}_k = \delta_{j,k}\mathcal{P}_j$, $\mathcal{P}_j\mathcal{N}_k = \mathcal{N}_k\mathcal{P}_j = \delta_{j,k}\mathcal{N}_j$ and $\mathcal{N}_j\mathcal{N}_k = \delta_{j,k}\mathcal{N}_j^2$).

Using these properties, the time evolution can be written as:

$$\hat{\rho}(t) = e^{t\mathcal{L}'}[\hat{\rho}(0)] = \sum_j e^{\lambda_j t} e^{t\mathcal{N}_j} \mathcal{P}_j[\hat{\rho}(0)], \tag{7.45}$$

which highlights that at a given time t only the terms of the sum such that $|\Re(\lambda_j)\, t| \ll 1$ play a role. In the long-time limit, it is possible to represent the expectation value of any observable $\hat{A}$ as:

$$\langle \hat{A} \rangle(t) \approx \mathrm{tr}[\hat{A}\, \mathcal{P}_0[\hat{\rho}(0)]] + e^{-\lambda_{ADR} t}\, \mathrm{tr}[\hat{A}\, e^{t\mathcal{N}_{ADR}} \mathcal{P}_{ADR}[\hat{\rho}(0)]]. \tag{7.46}$$

Eq. (7.46) is the mathematical formula motivating Eq. (7.24) in the text, defining also the meaning of κ.

Let us mention that in the example discussed in the text $\mathcal{N}_{ADR} = 0$: this is observed by explicit inspection via exact diagonalization of small systems ($L = 5$). Since the presence of a non-zero nilpotent super-operator is a fine-tuned property, it is reasonable to assume that the situation remains similar for longer systems.

7.7.2 Analogies with the parent Hamiltonian

In this Appendix we discuss some interesting analogies between the steady state $\hat{\rho}_{ss}$ of the dissipative dynamics for the perturbed Lindblad operator $\hat{L}'_{j,\epsilon}$ in Eq. (7.27) with the ground state $|g\rangle$ of its parent Hamiltonian $\hat{\mathcal{H}}'_{p,\epsilon} = J\sum_j \hat{L}'^{\dagger}_{j,\epsilon}\hat{L}'_{j,\epsilon}$. It should be stressed that, since $\hat{\mathcal{H}}'_{p,\epsilon}$ does not have a zero-energy ground state, there is no exact correspondence between both states.

We first study a small lattice with $L = 8$ sites at half-filling, performing a Runge-Kutta integration of the master equation. The initial state of the evolution is the ground state of $\hat{\mathcal{H}}_0$. In Fig. 7.8 it is shown that both the purity of the steady state $\mathcal{P}(\rho_{ss}) = tr\left[\hat{\rho}^2_{ss}\right]$ and its fidelity with the ground state of the parent Hamiltonian decrease with the perturbation strength. Notice, however, that for small perturbations the fidelity $\mathcal{F}(\hat{\rho}_{ss}, |g\rangle) = \langle g|\hat{\rho}_{ss}|g\rangle$ remains close to one, thus revealing the similarity of the states in such regime.

Such feature is also observed for larger lattices. Using the MPDO method for $\hat{\rho}_{ss}$ and an algorithm based on matrix product states for $|g\rangle$, we analyze a lattice with $L = 22$ sites at half-filling. We compare the pairing correlations and density profiles for both states, which differ only for $\mathcal{O}(10^{-2})$, when the perturbation strength is $\epsilon \lesssim 0.05$ (not shown). Let us explicitly show the results for the Hamiltonian case. In Fig. 7.9 we show that, for a lattice with $L = 40$ sites at half-filling, even a small perturbation ($\epsilon \sim 10^{-3}$) produces a non-negligible inhomogeneity. Moreover, the pairing correlations decay, indicating that such perturbation breaks the p-wave ordered nature of the purely dissipative dark state.

This similarity encourages the possibility of accessing some steady-state properties for large lattices through the study of the ground states of the corresponding parent Hamiltonians, even if no mathematical connection is present and the mixedness of the state is expected to act like a finite temperature, washing out several ground-state properties.

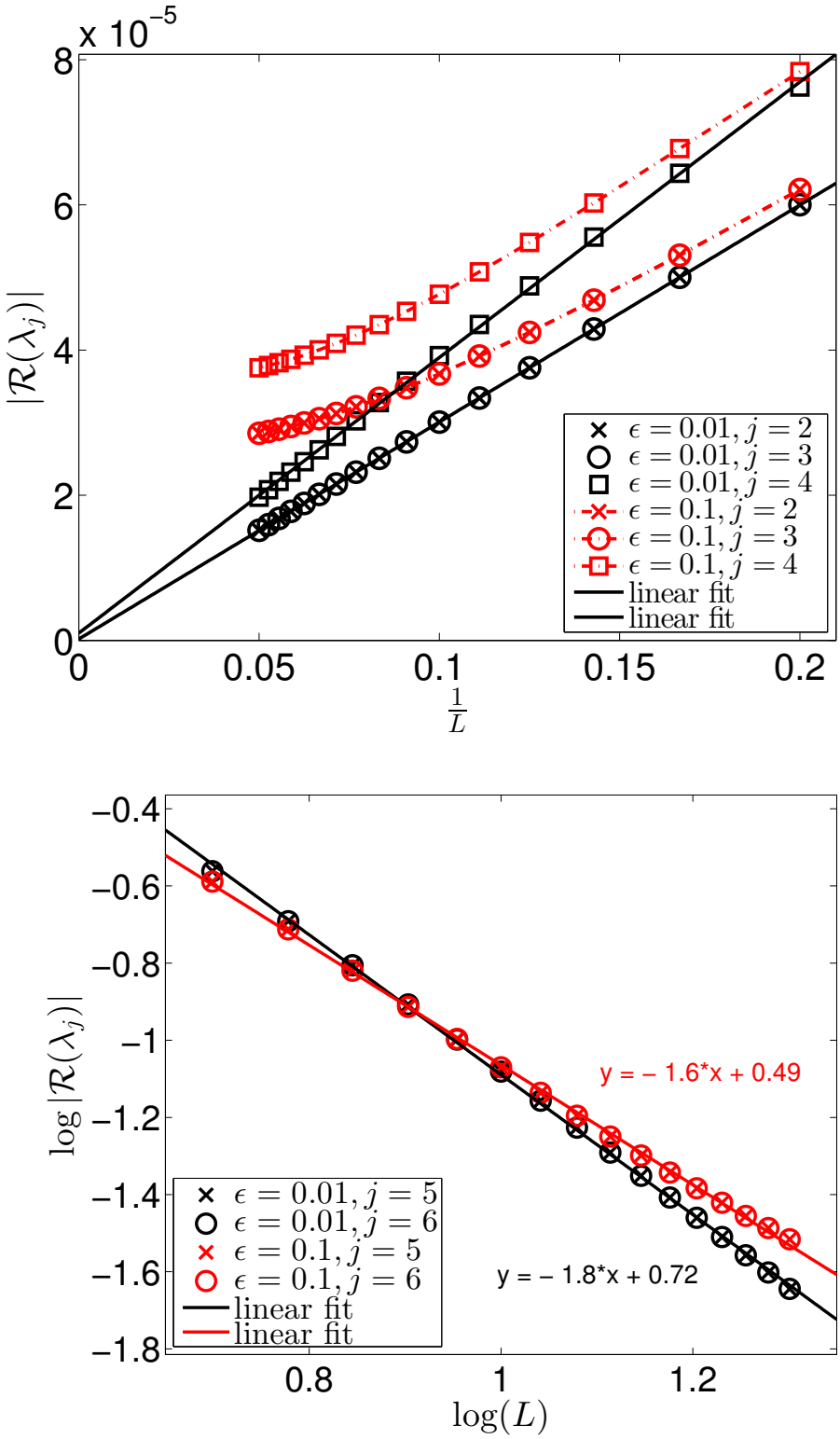

Figure 7.7: Real part of the eigenvalues $j = 2$, 3 and 4 (top) and $j = 5$ and 6 (bottom) of the Lindbladian operator $\mathcal{L}''_\epsilon$ for $N = 2$ as a function of L (here, $L \leq 20$). The two values $\epsilon = 0.1$ and $\epsilon = 0.01$ are considered. In the top panel, the values of the eigenvalues relative to $\epsilon = 0.1$ have been rescaled by 0.01 in order to facilitate the readability of the plot.

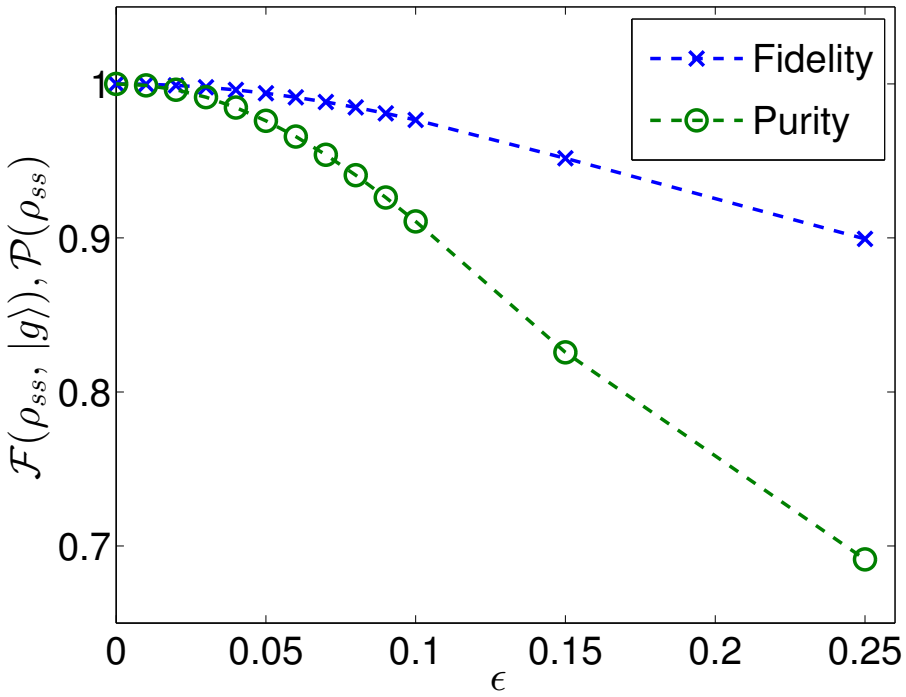

Figure 7.8: Fidelity $\mathcal{F}(\rho_{ss}, |g\rangle)$ and purity $\mathcal{P}(\rho_{ss})$ for different values of ϵ in $\hat{L}'_{j,\epsilon}$ [see Eq. (7.27)].

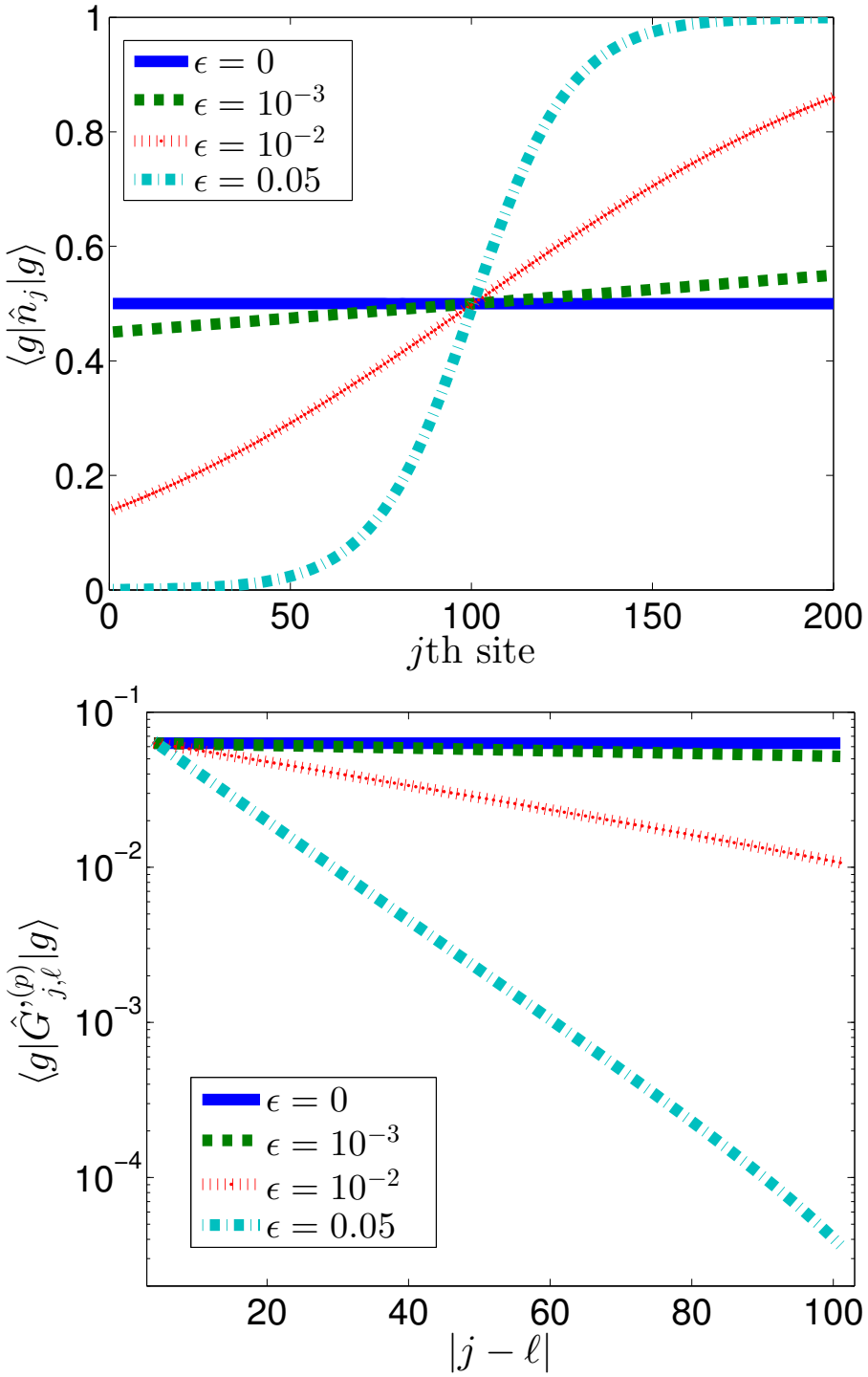

Figure 7.9: (top) Density profile $\langle g|\hat{n}_j|g\rangle$ and (bottom) renormalized pairing correlations $\langle g|\hat{O}'^{(p)\dagger}_j \hat{O}'^{(p)}_\ell|g\rangle$, with $j = (L/2) - 2$ and $\ell > j$. The computation is performed for a lattice with $L = 200$ sites at half-filling and different values of ϵ in $\hat{L}'_{j,\epsilon}$ [see Eq. (7.27)].

Part III

Non-Markovian dynamics and the divisibility criterion

CHAPTER 8

Witnessing non-Markovian dynamics with the divisibility criterion: a qubit interacting with an Ising model environment

By means of the divisibility criterion, *i.e.*, the non-positivity of the dynamical matrix for some intermediate time, we characterize the dynamics of a qubit interacting with an arbitrary quadratic fermionic environment. We obtain an analytical expression for the Kraus decomposition of the quantum map, and check its non-positivity with a simple function. With an efficient sufficient criterion to map the non-Markovian regions of the dynamics, we analyze the particular case of an environment described by the Ising Hamiltonian with a transverse field.

8.1 Introduction

The need to fight decoherence, to guarantee the proper working of the quantum enhanced technologies of information and computation [1], has renovated the motivation for the in-depth study of system-environment interaction dynamics. In particular, the Markovian or non-Markovian nature of the dynamics is of great interest [161]. Several witnesses and measures have been proposed in order to characterize the non-Markovianity of quantum processes [162]. For instance, the information flow between system and environment, quantified by the distinguishability of any two quantum states [163, 164], or by the Fisher information [165], or mutual information [166]; the Loschmidt echo [167, 168]; the entanglement between system and environment [169].

In this work, we will focus on the divisibility criterion [169, 170, 171], which consists in checking the non-positivity of intermediate time quatum maps. The system we will consider is formed by qubits governed by general fermionic quadratic Hamiltonians. Performing an exact diagonalization of the system-environment Hamiltonian [84], we will obtain, analytically, the Kraus representation of the quantum map [46]. Then we will propose a non-Markovianity measure, and will investigate in detail a model governed by the Ising Hamiltonian.

The chapter is organized as follows. We briefly revise the formalism of dynamical maps and the divisibility criterion in Sec.8.2. Our first result appears in Sec.8.3, where we present the exact Kraus decomposition for general quadratic fermionic Hamiltonians, and introduce a witness of non-Markovianity. In Sec.8.4, we introduce the model we shall investigate numerically, and relate it to the formalism of Sec.III. Our results for the dynamics of a qubit interacting with an environment governed by the Ising model are presented in Sec.8.5, and then we conclude.

8.2 Quantum Dynamical Maps and the Divisibility Criterion

The evolution of an open quantum system ($\rho' = \Phi(\rho)$) can be written in the well known operator sum representation as:

$$\rho' = \sum_{\mu} K_{\mu} \rho K_{\mu}^{\dagger}, \qquad \sum_{\mu} K_{\mu}^{\dagger} K_{\mu} = \mathbb{I}, \tag{8.1}$$

where the K_{μ} are the Kraus operators related to the quantum map Φ, and $\mathbb{I}$ is the identity in the Hilbert space of the system. Using the *vec* operation, defined by:

$$vec(|x\rangle\langle y|) = |x\rangle \otimes |y\rangle, \tag{8.2}$$

and the following relation,

$$ABC = (A \otimes C^{T}) vec(B), \tag{8.3}$$

where A,B,C are matrices, the evolution (Eq.(8.1)) can be rewritten as:

$$\left|\rho'\right\rangle = \Phi|\rho\rangle, \;\; \Phi = \sum_{\mu} K_{\mu} \otimes K_{\mu}^{*}, \tag{8.4}$$

where $|\rho\rangle \equiv vec(\rho)$.

Consider the evolution of the system from an initial time t_0 to a final time t_f,

$$\left|\rho(t_f)\right\rangle = \Phi(t_f, t_0)|\rho(t_0)\rangle. \tag{8.5}$$

Suppose this evolution is broken in two steps with an intermediate time, $t_f > t_m > t_0$, namely:

$$\left|\rho(t_f)\right\rangle = \Phi(t_f, t_m)\Phi(t_m, t_0)|\rho(t_0)\rangle. \tag{8.6}$$

Whereas $\Phi(t_f, t_0)$ is a completely positive (CP) map for arbitrary t_f, the map corresponding to the intermediate step, $\Phi(t_f, t_m)$, may be non-CP for some t_m. As realizable maps are always CP, $\Phi(t_f, t_m)$ being non-CP for the particular time t_m witnesses the fact that such a division is not possible. A trivial case in which any intermediate division is possible corresponds to unitary evolutions. Markovian evolutions also admit arbitrary intermediate steps. The intermediate map may fail to be CP only in the case of non-Markovian evolutions. This *divisibility criterion* [169] is therefore a sufficient condition to detect non-Markovianity.

In order the check the complete positivity of a map, we use the well known duality between CP maps and positive operators, expressed by the Choi's theorem [46]. First we define the unique dynamical matrix associated to the map:

$$D_{\mu\nu}^{mn} = \Phi_{n\nu}^{m\mu} = \langle m\mu|\Phi|n\nu\rangle, \tag{8.7}$$

where latin and greek indices correspond to system and environment Hilbert spaces, respectively. The Choi's theorem states that the map (Φ) is CP if and only if its dynamical matrix (D) is a positive semidefinite operator. Finally, to check the complete positivity of the intermediate map, we form the matrix of its super-operator by means of the product:

$$\Phi(t_f, t_m) = \Phi(t_f, t_0)\Phi^{-1}(t_m, t_0). \tag{8.8}$$

8.3 Dynamical Matrix for a General Fermionic Quadratic Hamiltonian

In the previous section, we reviewed the formalism of quantum maps and the divisibility criterion. We now apply such formalism to environments described by general fermionic quadratic Hamiltonians, interacting with a qubit. We will show how to obtain the exact expression for the Kraus decomposition of the dynamical matrix.

Let us then consider a general fermionic quadratic Hamiltonian, namely,

$$H_g = \sum_{m,n=1}^{L} (x_{m,n} a_m^\dagger a_n + y_{m,n} a_m^\dagger a_n^\dagger + h.c.). \tag{8.9}$$

where L is the lattice size, and $x_{m,n}, y_{m,n}$ are arbitrary complex numbers, $a_j^\dagger (a_j)$ is the creation (annihilation) operator, satisfying the usual anti-commutation relations:

$$\{a_i, a_j^\dagger\} = \delta_{ij}, \ \{a_i, a_j\} = 0. \tag{8.10}$$

For the interaction of the qubit with this environment, we consider the following Hamiltonian:

$$H_{int} = -\delta|e\rangle\langle e| \otimes V_e, \tag{8.11}$$

where $|g\rangle$ and $|e\rangle$ are the qubit ground and excited states, respectively, and V_e is a fermionic quadratic Hamiltonian. We consider that the qubit and

environment are initially uncorrelated, and they are in an arbitrary pure initial state,

$$|\psi(0)\rangle = |\chi(0)\rangle \otimes |\varphi(0)\rangle = (c_g|g\rangle + c_e|e\rangle) \otimes |\varphi(0)\rangle, \tag{8.12}$$

where $|\chi(0)\rangle = c_g|g\rangle + c_e|e\rangle$, with $|c_g|^2 + |c_e|^2 = 1$, is the initial qubit state. The evolution under the total Hamiltonian,

$$H = H_g + H_{int}, \tag{8.13}$$

is given by:

$$|\psi(t)\rangle = e^{-iHt/\hbar}|\chi(0)\rangle \otimes |\varphi(0)\rangle, \tag{8.14}$$

$$|\psi(t)\rangle = c_g|g\rangle \otimes \underbrace{e^{-iH_g t/\hbar}|\varphi(0)\rangle}_{|\varphi_g(t)\rangle} + c_e|e\rangle \otimes \underbrace{e^{-iH_e t/\hbar}|\varphi(0)\rangle}_{|\varphi_e(t)\rangle}, \tag{8.15}$$

where

$$H_e = H_g + V_e. \tag{8.16}$$

Such Hamiltonians, H_e and H_g, can be easily diagonalized by a Bogoliubov transformation [84], namely:

$$B_k \equiv \cos(\theta_b^k)a_k - i\sin(\theta_b^k)a_{-k}^\dagger, \tag{8.17}$$

$$A_k \equiv \cos(\theta_a^k)a_k - i\sin(\theta_a^k)a_{-k}^\dagger. \tag{8.18}$$

These new fermionic operators are related according to

$$B_{\pm k} = \cos(\alpha_k)A_{\pm k} - i\sin(\alpha_k)A_{\mp k}^\dagger, \tag{8.19}$$

where $\alpha_k = (\theta_g^k - \theta_e^k)/2$. The Hamiltonians in diagonal form read:

$$H_g = \sum_k \epsilon_g^k (B_k^\dagger B_k + C_g), \;\; H_e = \sum_k \epsilon_e^k (A_k^\dagger A_k + C_e), \tag{8.20}$$

where C_g and C_e are both real constants, and $\epsilon_{g(e)}^k$ are the single-particle eigenvalues. The ground states of H_g (G_g) and H_e (G_e) are related by:

$$|G_g\rangle = \prod_{k>0}\Big[\cos(\alpha_k) - i\sin(\alpha_k)A_k^\dagger A_{-k}^\dagger\Big]|G_e\rangle. \tag{8.21}$$

Now we derive the Kraus decomposition of the map super-operator (Φ). The Kraus operators of the evolution are:

$$K_i = (\mathbb{I}_S \otimes \langle i|)\, e^{-iHt/\hbar}\, (\mathbb{I}_S \otimes |\varphi(0)\rangle), \tag{8.22}$$

with $\mathbb{I}_S = |g\rangle\langle g| + |e\rangle\langle e|$. Assuming, without loss of generality (the map does not depend on the initial states of the qubit-environment), that the environment is initially in its ground state , $|\varphi(0)\rangle = |G_g\rangle$, and using Eq.(8.15), we obtain:

$$K_i = \mathbb{I}_S \otimes \langle i|\big[|g\rangle\langle g| \otimes |\varphi_g(t)\rangle + |e\rangle\langle e| \otimes |\varphi_e(t)\rangle\big]. \tag{8.23}$$

The environment states $|\varphi_g(t)\rangle$ and $|\varphi_e(t)\rangle$ are given by:

$$|\varphi_g(t)\rangle = e^{-iH_g t/\hbar}|G_g\rangle = e^{-iE_g t/\hbar}|G_g\rangle = \tag{8.24}$$
$$e^{-iE_g t/\hbar}\prod_{k>0}\Big[\cos(\alpha_k) - i\sin(\alpha_k)A_k^\dagger A_{-k}^\dagger\Big]|G_e\rangle,$$

where E_g is the ground state energy of H_g. Likewise, using Eq.(8.21), we obtain:

$$|\varphi_e(t)\rangle = e^{-iH_e t/\hbar}\times \tag{8.25}$$
$$\prod_{k>0}\Big[\cos(\alpha_k) - i\sin(\alpha_k)A_k^\dagger A_{-k}^\dagger\Big]|G_e\rangle =$$
$$\prod_{k>0}\Big[\cos(\alpha_k) - e^{-i(\epsilon_e^k+\epsilon_e^{-k})t/\hbar}i\sin(\alpha_k)A_k^\dagger A_{-k}^\dagger\Big]\times$$
$$e^{-iE_e t/\hbar}|G_e\rangle.$$

In order to obtain the Kraus operators, it is enough to calculate the overlaps $\langle i|\varphi_g(t)\rangle$ and $\langle i|\varphi_e(t)\rangle$, for a given environment basis $\{|i\rangle\}$, as shown in Eq.(8.23). A convenient basis is formed by the eigenstates of H_e, namely:

$$\{|i\rangle\} = \{|G_e\rangle, A_{\vec{k}_N}^\dagger|G_e\rangle\}, \tag{8.26}$$

where $\vec{k}_N = (k_1, k_2, ..., k_N)$ is the vector representing the momentum of the $N(= 1, \ldots, L)$ excitations, and $A_{\vec{k}}^\dagger = A_{k_1}^\dagger A_{k_2}^\dagger ... A_{k_N}^\dagger$. It is easy to see that the only non null elements for "$\langle i|\varphi_g(t)\rangle$", using Eq.(8.24), are given by,

$$\langle G_e|\varphi_g(t)\rangle = e^{-iE_g t/\hbar}(\prod_{k>0}\cos(\alpha_k)), \tag{8.27}$$

and

$$a_{\vec{k}_N}(t) \equiv \langle G_e|A_{-\vec{k}_N}A_{\vec{k}_N}^\dagger|\varphi_g(t)\rangle = \tag{8.28}$$
$$e^{-iE_g t/\hbar}\prod_{k\in\vec{k}_N}(-i\sin(\alpha_k))(\prod_{k>0,k\notin\vec{k}_N}\cos(\alpha_k)),$$

where N varies from 1 to $L/2$. Analogously, the non null terms for "$\langle i|\varphi_e(t)\rangle$", using Eq.(8.25), are given by,

$$b_{\vec{k}_N}(t) \equiv \langle G_e|A_{-\vec{k}_N}A_{\vec{k}_N}^\dagger|\varphi_e(t)\rangle = \tag{8.29}$$
$$e^{-iE_e t/\hbar}\prod_{k\in\vec{k}_N}\Big[-i\sin(\alpha_k)\exp(-i(\epsilon_e^k+\epsilon_e^{-k})t/\hbar)\Big]\times$$
$$(\prod_{k>0,k\notin\vec{k}_N}\cos(\alpha_k)).$$

It is easy to check the following relation:

$$b_{\vec{k}_N}(t) = a_{\vec{k}_N}(t)f_{\vec{k}_N}(t), \tag{8.30}$$

where

$$f_{\vec{k}_N}(t) \equiv e^{-i(E_e-E_g)t/\hbar}\exp(-i\sum_{k\in\vec{k}_N}^{N}(\epsilon_e^k+\epsilon_e^{-k})t/\hbar). \tag{8.31}$$

Finally, we reach the first result of this work, obtaining a simple expression for the Kraus operators of the quantum map,

$$K_{\vec{k}_N} = a_{\vec{k}_N}(t)(|g\rangle\langle g| + f_{\vec{k}_N}(t)|e\rangle\langle e|). \tag{8.32}$$

Note that $\left|a_{\vec{k}_N}(t)\right|^2$ is not a time dependent variable, and

$$\sum_{\{\vec{k}_N\}} \left|a_{\vec{k}_N}(t)\right|^2 = Tr(|\varphi_g(t)\rangle\langle\varphi_g(t)|) = 1. \tag{8.33}$$

By using this fact, we can then write the quantum map in terms of the Kraus operators as follows,

$$\begin{aligned}\Phi(t,0) \quad = \quad & \sum_{\{\vec{k}_N\}} K_{\vec{k}_N} \otimes K^*_{\vec{k}_N} = \\ & \sum_{\{\vec{k}_N\}} [|g\rangle\langle g| \otimes |g\rangle\langle g| + |e\rangle\langle e| \otimes |e\rangle\langle e| + \\ & |g\rangle\langle g| \otimes |e\rangle\langle e| \ \left|a_{\vec{k}_N}(t)\right|^2 f_{\vec{k}_N}(t)^* + \\ & + |e\rangle\langle e| \otimes |g\rangle\langle g| \ \left|a_{\vec{k}_N}(t)\right|^2 f_{\vec{k}_N}(t)\Big].\end{aligned} \tag{8.34}$$

If we define the following variable,

$$x(t) \equiv \sum_{\{\vec{k}_N\}} \left|a_{\vec{k}_N}(t)\right|^2 f_{\vec{k}_N}(t), \tag{8.35}$$

the quantum map can be rewritten as,

$$\begin{aligned}\Phi(t,0) = \ & [|g\rangle\langle g| \otimes |g\rangle\langle g| + |e\rangle\langle e| \otimes |e\rangle\langle e| + \\ & |g\rangle\langle g| \otimes |e\rangle\langle e| x(t)^* + |e\rangle\langle e| \otimes |g\rangle\langle g| x(t)].\end{aligned} \tag{8.36}$$

As expected, the quantum map consists in a decoherence channel, and thus we can identify the variable "$x(t)$" with the known Loschmidt echo $\mathcal{L}(t)$ [167, 168],

$$\mathcal{L}(t) = |x(t)|^2 = |\langle\phi_g(t)|\phi_e(t)\rangle|^2. \tag{8.37}$$

The above relation follows just by noticing that the qubit reduced state, $\rho_S(t) = Tr_E(|\psi(t)\rangle\langle\psi(t)|)$, taking the partial trace of Eq.(8.12), is given by $\rho_S(t) = |c_g|^2|g\rangle\langle g| + |c_e|^2|e\rangle\langle e| + c_g^* c_e \mu(t)|e\rangle\langle g| + H.c.$, where $\mu(t) = \langle\phi_g(t)|\phi_e(t)\rangle$ is the decoherence factor. The quantum map corresponding to such an evolution is the decoherence channel, as described before.

Using now Eq.(8.8), we have the following expression for the intermediate map:

$$\begin{aligned}\Phi(t_f,t_m) = \ & [|g\rangle\langle g| \otimes |g\rangle\langle g| + |e\rangle\langle e| \otimes |e\rangle\langle e| + \\ & |g\rangle\langle g| \otimes |e\rangle\langle e| y(t_f,t_m)^* + \\ & |e\rangle\langle e| \otimes |g\rangle\langle g| y(t_f,t_m)\Big],\end{aligned} \tag{8.38}$$

where

$$y(t_f, t_m) \equiv \frac{x(t_f)}{x(t_m)}. \tag{8.39}$$

The dynamical matrix of this quantum map is

$$D_{\Phi(t_f,t_m)} = \begin{pmatrix} 1 & 0 & 0 & y(t_f,t_m)^* \\ 0 & 0 & 0 & 0 \\ 0 & 0 & 0 & 0 \\ y(t_f,t_m) & 0 & 0 & 1 \end{pmatrix}. \tag{8.40}$$

Using the Schur's complement, we arrive at the following simple sufficient condition for the positive-semidefiniteness of the dynamical matrix:

$$1 - |y(t_f, t_m)|^2 \geq 0. \tag{8.41}$$

Therefore we have obtained a simple function capable to witness the non-Markovianity of the dynamics, *i.e.*, Φ is non-Markovian if $|y(t_f, t_m)|^2 > 1$.

8.4 Ising Hamiltonian

In this section we will analyze an specific environment and interaction Hamiltonians, in order to exemplify our method. We focus on an environment described by the Ising Hamiltonian in a transverse field (H_{ising}), with periodic boundary conditions ($L + 1 = 1$). The interaction with the environment (H_{int}) is by means of the transverse magnetic field in the Z direction (see Fig.8.1), more precisely,

$$H_{Ising} = -J \sum_{j=1}^{L} (\sigma_j^x \sigma_{j+1}^x + \lambda \sigma_j^z), \tag{8.42}$$

$$H_{int} = -\delta |e\rangle\langle e| \otimes \sum_{j=1}^{L} \sigma_j^z. \tag{8.43}$$

In order to employ the previous section's results, we first do the identification:

$$H_e = H_{ising} - \delta \sum_{j=1}^{L} \sigma_j^z, \tag{8.44}$$

$$H_g = H_{ising}. \tag{8.45}$$

We now diagonalize the Ising Hamiltonian [172]. First we use the usual Jordan-Wigner transformation,

$$\sigma_j^+ = \exp\left(i\pi \sum_{l<j} a_l^\dagger a_l\right) = \prod_{l<j} (1 - 2a_l^\dagger a_l) a_j, \tag{8.46}$$

$$a_j = \left(\prod_{l<j} \sigma_l^z\right) \sigma_j^+. \tag{8.47}$$

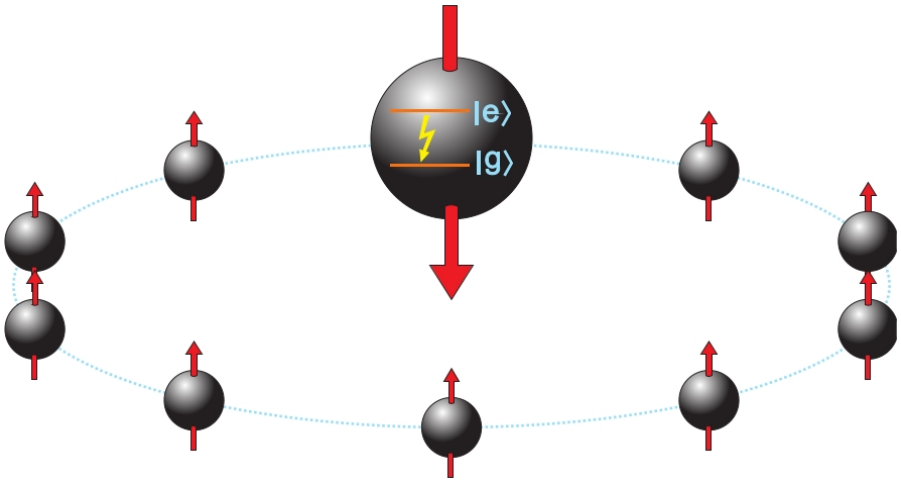

Figure 8.1: Schematic view of spins forming a ring array, described by the environment Ising Hamiltonian (Eq.(8.42)). The central spin is the qubit interacting with the environment according to Eq.(8.43).

The Ising Hamiltonian can then be rewritten in terms of quadratic fermionic operators:

$$H_{ising} = -J\Bigg[\sum_{j=1}^{L-1}(a_j^\dagger a_{j+1} + a_j^\dagger a_{j+1}^\dagger + h.c.) + e^{(i\pi)\hat{N}}(a_L^\dagger a_1 + a_L^\dagger a_1^\dagger + h.c.) + 2\lambda\hat{N} - \lambda L\Bigg], \tag{8.48}$$

where $\hat{N} = \sum_j a_j^\dagger a_j$. The Hamiltonian conserves the parity, $\left[H, e^{(i\pi)\hat{N}}\right] = 0$. Thus we can analyze its *odd*/*even* subspaces separately. The gap between the ground state energy of these two subspaces obviously closes in the thermodynamic limit. For simplicity, we shall proceed the analysis in the *odd* sector, which leads to a simple quadratic Hamiltonian with periodic boundary conditions. Using the momentum eigenstates,

$$a_k = \frac{1}{\sqrt{L}}\sum_j e^{(-ikj)}a_j, \tag{8.49}$$

with $k = \frac{2\pi}{L}q$, $q = 0, ..., L-1$, and the Bogoliubov transformation (Eq.(8.18)), with phases

$$\theta_e^k(\delta) = \frac{1}{2}\arctan\left[\frac{-\sin(k)}{\cos(k) - (\lambda+\delta)}\right], \tag{8.50}$$

the Hamiltonian assumes the desired diagonal form:

$$H_e = \sum_k \epsilon_e^k\,(A_k^\dagger A_k - 1/2), \tag{8.51}$$

with eigenvalues given by:

$$\epsilon_e^k(\delta) = \sqrt{1 + (\lambda+\delta)^2 - 2(\lambda+\delta)\cos(k)}. \tag{8.52}$$

8.5 Witnessing the non-Markovianity in the Ising Model

Now we are equipped to characterize the dynamics of a qubit interacting with an environment governed by the Ising model (Fig.8.1). We consider lattices up to $L = 5 \times 10^5$ sites, and investigate the non-Markovianity in the vicinity of the critical point of the quantum Ising model, which is well known to be equal to $\lambda^* \equiv \lambda + \delta = 1$.

Let us define a measure (η) of non-Markovianity as the minimum of the eigenvalues for the intermediate quantum dynamical matrix $D_{\Phi(t_t,t_m)}$ over all final times t_f and over all time partitions t_m, precisely:

$$\eta = \min_{\{t_f\}} \min_{\{t_m<t_f\}} eig\{D_{\Phi(t_t,t_m)}\}, \tag{8.53}$$

where *eig* is the set of eigenvalues of the intermediate dynamical matrix $D_{\Phi(t_f,t_m)}$. In order to exemplify such a non-Markovianity measure, we plot, in Fig.8.2, the smallest eingenvalue of the intermediate map as a function of the final (t_f) and intermediate (t_m) times, at the critical point of the Ising model, for a lattice with $L = 10$ sites. As the values of t_m and t_f are swept, the non-Markovian regions of the dynamics are revealed.

In Fig.8.3, the non-Markovianity, quantified by η (Eq.(8.53)), is plotted against the transverse field (λ), in the vicinity of the Ising model critical point, for a fixed interaction coupling constant $\delta = 0.01$. We see that the larger the lattice, the larger the non-Markovianity. The most interesting feature shown in this figure is the maximum of non-Markovianity occurring precisely at the Ising model critical point. The behavior of this measure for larger lattice sizes, and in the thermodynamic limit, for the particular model studied in this section could also be inferred by the Loschimdt echo [167, 168], from Eqs.(8.37) and (8.41). Note, however, that this equivalence between η and the Loschimdt echo is not necessarily true in general.

In Fig. 8.4 ,we see the behavior of the Loschmidt echo, for different lattice sizes, at the critical point ($\lambda^* = 1$). We highlight some of its features: (i) the Loschmidt echo has an abrupt decay followed by a revival, with a time period "τ", which is proportional to the lattice size, $\tau \propto L$; (ii) the difference between the minimun value of the decay (which we shall denote by $\mathcal{L}_{dec}$) and the maximal of the revival ($\mathcal{L}_{rev}$) becomes higher as we increase the lattice size. In this way, the non-Markovianity measure is simply given by $\eta = \mathcal{L}_{rev}/\mathcal{L}_{dec}$. Performing a finite-size scaling analysis, we see, in Fig. 8.5, that such a measure grows exponentially with lattice size, $\eta(\lambda^*) \propto exp(\alpha_* L)$, with $\alpha_* \sim 2.36 \times 10^{-3}$. Notice however that, despite such exponentially increasing behavior, at the thermodynamic limit the period τ diverges, and there is no revival of the function, consequently, the non-Markovianity pointed by this measure must be null: $\eta(\lambda^*) = 0$ for $L \to \infty$.

The behavior of the Loschmidt echo out of the critical point is plotted in Fig. 8.6. We highlight some of its features: (i) due to finite size effects, we see that after a certain time (Γ), which increases with the lattice size ($\Gamma \propto L$), the function has a chaotic behavior; (ii) the "shape" of the function before the chaotic behavior is invariant with the lattice size, only its amplitude is changed. Performing then a finite-size scaling analysis, we see, in Fig. 8.7, that

the non-Markovianity measure grows exponentially with lattice size, $\eta(\lambda^* - 0.1) \propto exp(\beta_l L)$, with $\beta_l \sim 1.43 \times 10^{-5}$, and $\eta(\lambda^* + 0.1) \propto exp(\beta_r L)$, with $\beta_r \sim 1.29 \times 10^{-5}$. Notice that although the measure also has an exponential scaling, as in the critical point, its exponential factors are much smaller, namely, $\beta_{l(r)}/\alpha_* \sim 10^{-2}$.

In summary, we see that the non-Markovianity measure, for finite size systems, reaches its maximal at the critical point, whereas in the thermodynamic limit it is zero exactly at the critical point, and it diverges out of the critical point.

8.6 Conclusion

We derived an analytical expression for the Kraus representation of the map corresponding to the evolution of a qubit interacting with an environment, for a general quadratic fermionic Hamiltonian, and introduced a simple function which is sufficient to check the non-Markovianity of the dynamics. We analyzed our proposed non-Markovianity function for the quantum map of a qubit interacting with an environment governed by the Ising model. For lattices up to 10^5 sites we studied the non-Markovianity of the dynamics, in the vicinity of the Ising model critical point. We quantified the non-Markovianity by the most negative eigenvalue (η) of the dynamical matrix, and obtained that, for finite size systems, it reaches its maximum at the critical point, whereas in the thermodynamic limit it is zero exactly at the critical point, diverging outside the critical point. In the particular case of the *Ising environment*, we obtained that the Loschmidt echo and our measure η are equivalent.

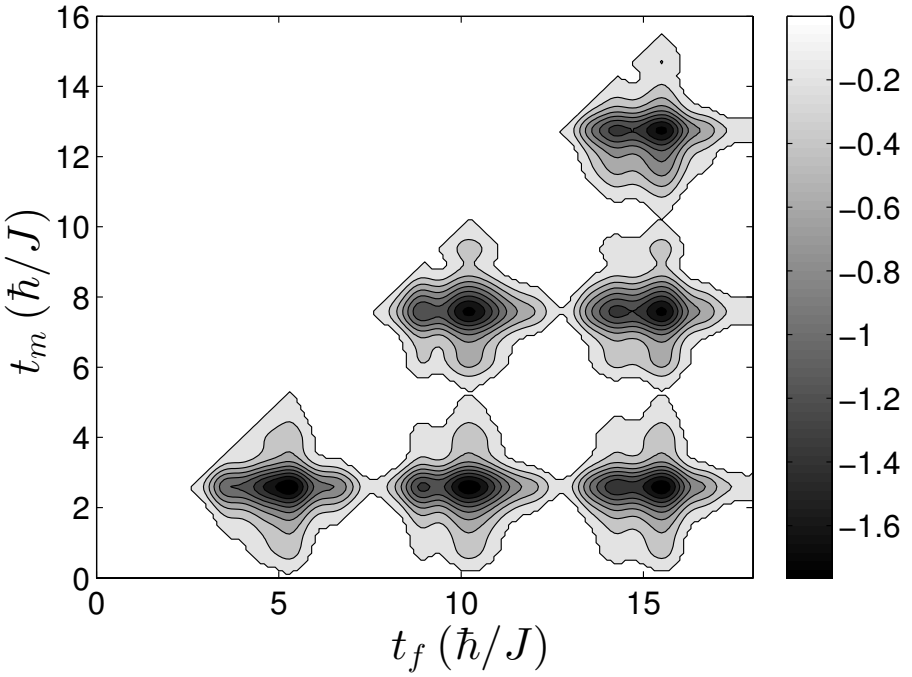

Figure 8.2: Manifestation of the non-Markovianity by means of the most negative eigenvalue of the intermediate quantum map $D_{\Phi(t_f,t_m)}$ (greyscale), in function of t_f and t_m, for a lattice with parameters $L = 10$, $\lambda = 0.5$ and $\delta = 0.5$.

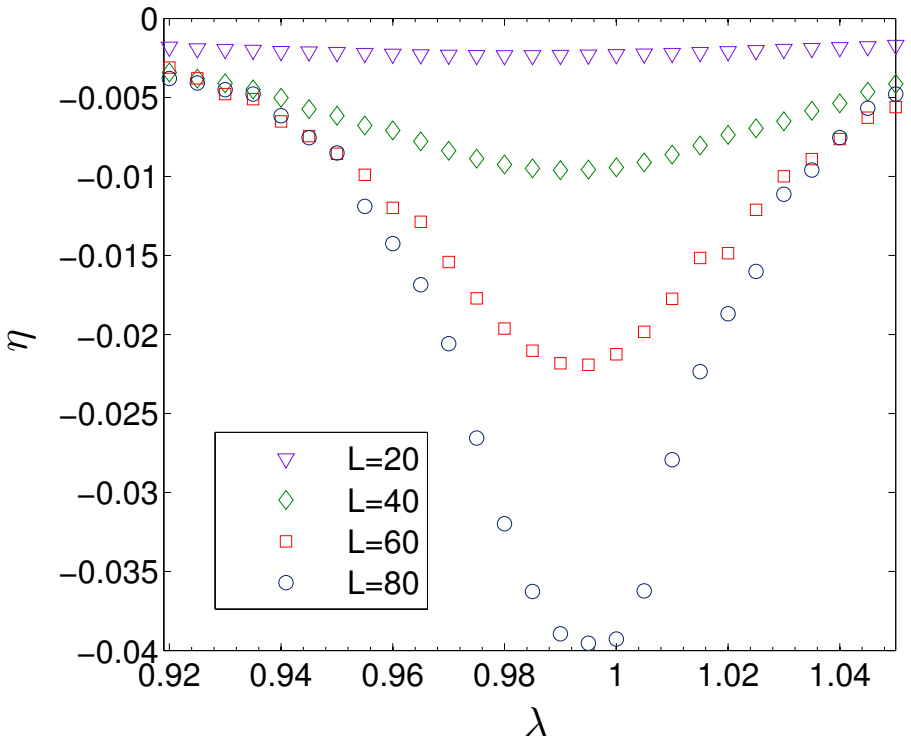

Figure 8.3: The non-Markovianity measure η (Eq. (8.53)) in function of the transverse field λ, for $\delta = 0.01$, and for different lattice sizes (L), in the vicinity of the Ising model critical point.

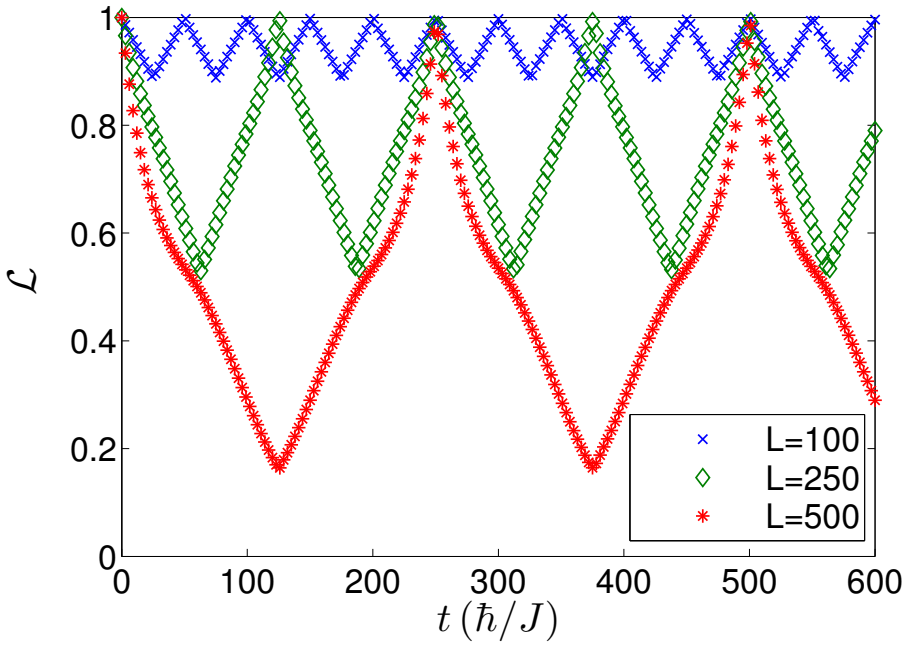

Figure 8.4: The Loschmidt echo $\mathcal{L}$ (Eq. (37)) as a function of the time, at the critical point $\lambda^* = \lambda + \delta = 1$, with $\delta = 10^{-2}$, for different lattice sizes.

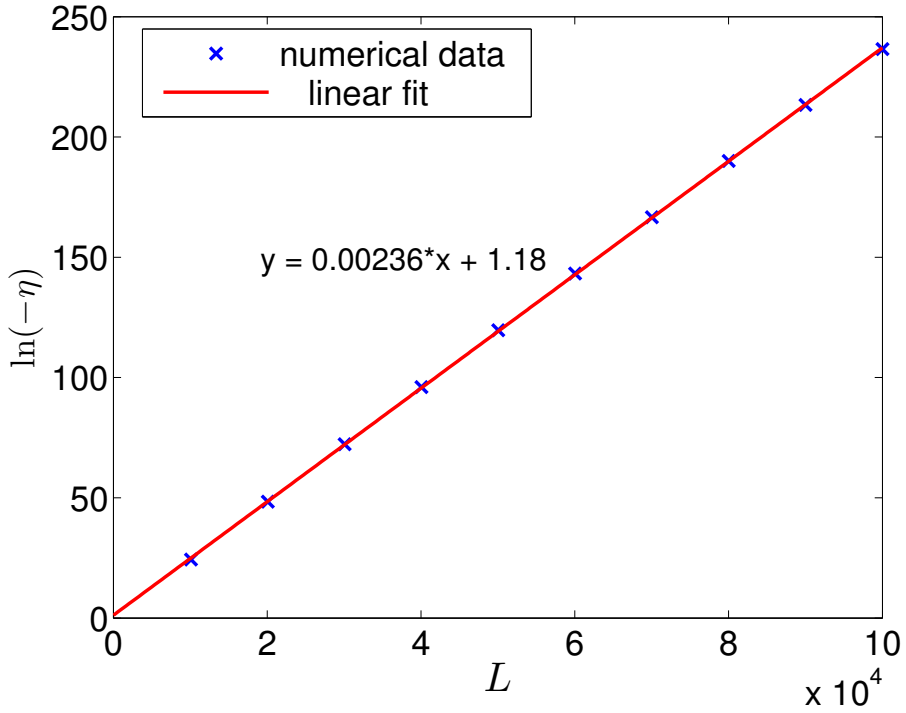

Figure 8.5: Finite size scaling analysis: $ln(-\eta)$ as a function of L, for $L = 100$ to $L = 10^5$ sites, at the critical point $\lambda^* = 1$, with $\delta = 10^{-2}$. The linear fit reveals an exponential divergence of the non-Markovianity with the lattice size.

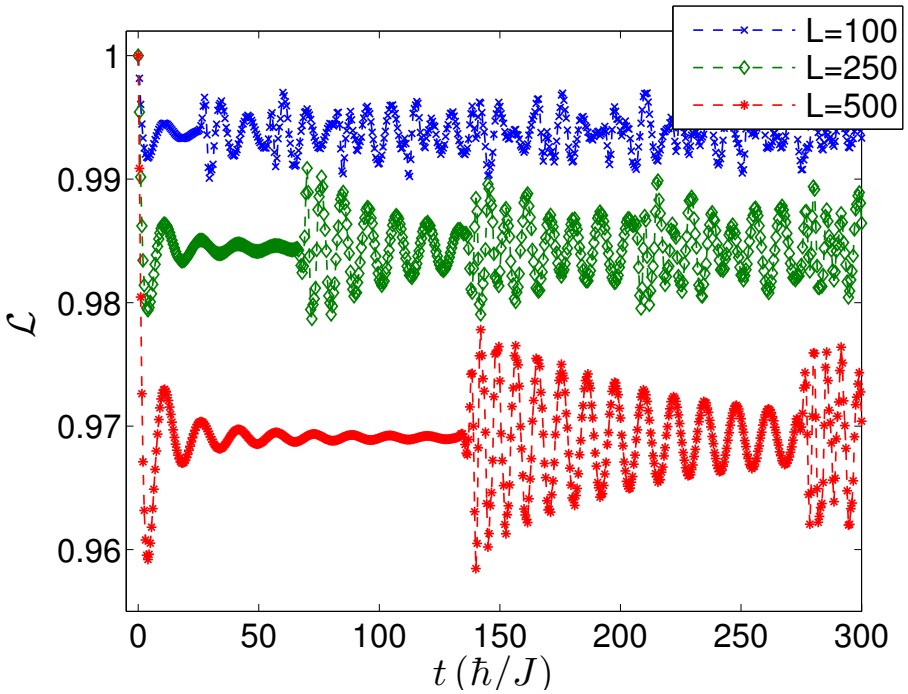

Figure 8.6: The Loschmidt echo $\mathcal{L}$ (Eq. (37)) as a function of the time, out of the critical point; more precisely, for $\lambda = \lambda^* - 0.1$, and $\delta = 10^{-2}$. The behavior for $\lambda = \lambda^* + 0.1$ is completely similar to this one.

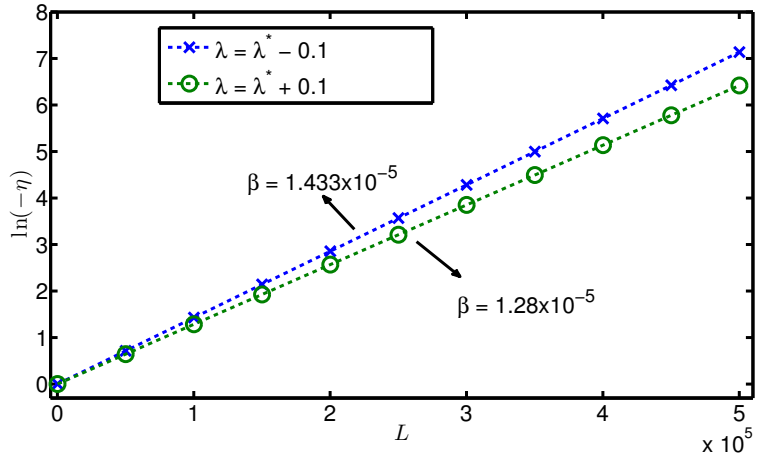

Figure 8.7: Finite size scaling analysis: $ln(-\eta)$ as a function of L, for $L = 100$ to $L = 5 \times 10^5$ sites, out of the critical point, more precisely, for $\lambda = \lambda^* \pm 0.1$, and $\delta = 10^{-2}$. The linear fit reveals an exponential divergence of the non-Markovianity with the lattice size, $(-\eta) \propto e^{\beta L}$.

APPENDIX A

Mean-field dark state

Dark states for linear Lindblad operators: Given a one-dimensional lattice governed uniquely by a dissipative evolution given by the linear Lindblad operators $\hat{\ell}_j = \alpha C_j^\dagger + A_j$ (Eq.(7.9)), here neglecting the Hamiltonian contribution ($\hat{H} = 0$), we have that its pure dark states are uniquely given by,

$$\begin{cases} L\,odd: & |d\rangle \propto (x_0 + x_1 \hat{\ell}_L^\dagger)\,|BCS, \alpha\rangle, \\ L\,even: & |d\rangle \propto (x_0 + x_1 \hat{\ell}_L^\dagger)\,a_{k=0}^\dagger |BCS, \alpha\rangle, \end{cases} \tag{A.1}$$

with $|BCS, \alpha\rangle$ as given in Eq.(5.5), and $x_0 = 1, x_1 = 0$ for periodic boundary conditions ($L + 1 = 1$), while a topological degeneracy is generated for open boundary conditions, $|x_0|^2 + |x_1|^2 = 1$. We see that the Kitaev ground state at the "sweet point", namely $\mu = 0$, and $\Delta = J > 0$, is the particular case for $\alpha = 1$.

Proof: The proof below is similar to the one given in [105]. Since the lindblad operators are translational invariant it's convenient to work in momentum space,

$$C_k^\dagger = \sum_j e^{-ikj} C_j^\dagger = \sum_l e^{-ikl} a_l^\dagger \underbrace{\left(\sum_j e^{-ik(j-l)} v_{j,l}\right)}_{v_k\,(independent\,of\,"l")}, \tag{A.2}$$

and since $v_{j,l} = v_{j-l,0}$, we have that,

$$C_k^\dagger = v_k a_k^\dagger, \qquad A_k = \sum_j e^{ikj} A_j = u_k a_k, \tag{A.3}$$

for $k = -\pi + \frac{2\pi}{L}(j-1)$, $j = 1, ..., L$, where,

$$v_k = \sum_{j=-L}^{L} e^{-ikj} v_{j,0}, \qquad u_k = \sum_{j=-L}^{L} e^{ikj} u_{j,0}. \tag{A.4}$$

This way the Lindblad operators are local in momentum space,

$$\hat{\ell}_k = \sum_j e^{ikj}\hat{\ell}_j = \alpha C^\dagger_{-k} + A_k, = \alpha v_{-k} a^\dagger_{-k} + u_k a_k, \tag{A.5}$$

It's easy to see that, if we assume $v_{-k} = \pm\, v_k, u_{-k} = \mp u_k$, such that $\phi_k = v_k/u_k$ is antissimetric, the above momentum operators satisfy the following properties,

$$\left\{\hat{\ell}^\dagger_k, \hat{\ell}^\dagger_{k'}\right\} = \left\{\hat{\ell}_k, \hat{\ell}_{k'}\right\} = 0, \tag{A.6}$$

$$\left\{\hat{\ell}_k, \hat{\ell}^\dagger_{k'}\right\} = \left(|u_k|^2 + |\alpha v_k|^2\right)\delta_{k,k'}, \tag{A.7}$$

i.e., they satisfy the anti-commutation relations, forming a complete Dirac algebra. These operators can thus be seen as "creation" and "annhilitation" operators, and the dark state shall be the "vacuum state", being unique, and satisfying $\hat{\ell}_k|d\rangle = 0, \forall k$. The dark state is given simply by,

$$|d\rangle = \prod_{\{k\}} \hat{\ell}_k |vac\rangle, \tag{A.8}$$

where is trivial to see that $\hat{\ell}_{k'}|d\rangle = \prod_{\{k\}-k'} \hat{\ell}_k \left(\hat{\ell}_{k'}\hat{\ell}_{k'}\right)|vac\rangle = 0, \forall k'$. In the particular linear Lindblad operators proposed in [104], we have $v_k = 2e^{ik/2}\cos(k/2), u_k = -2ie^{ik/2}\sin(k/2)$, such that $\hat{\ell}_{k=-\pi} \propto a_{k=\pi}$, and $\hat{\ell}_{k=0} \propto a^\dagger_{k=0}$; since $a_{k=\pi}|BCS, \alpha\rangle = 0$, we can write the dark states as,

$$|d\rangle = \hat{\ell}_{k=0} \prod_{\{k\neq\pi\}} \hat{\ell}_{-k}\hat{\ell}_k |vac\rangle \propto a^\dagger_{k=0}|BCS, \alpha\rangle. \tag{A.9}$$

In case $L = odd$, where there isn't zero momentum, the dark state are simply the fixed phase BCS state.

If we are dealing with open boundary conditions, then $\nexists\, \hat{\ell}_L$ acting in the dissipation, and it generates a degeneracy in the dark states given by the subspace $\{|d\rangle, \hat{\ell}^\dagger_L|d\rangle\}$.

APPENDIX B

Real-space representation of the Kitaev ground state

For the Kitaev model at the "sweet point", namely $\mu = 0$, and $\Delta = J > 0$ and real, one can check that its degenerate ground states can be written as a equal weighted superposition of all real space configurations with fixed fermion parity (even or odd). E.g., the even sector would be given by,

$$|g_K\rangle \propto \sum_{n=even} (-1)^{n/2} \left[\sum_{\{\vec{j}\}} \left| \psi_{\vec{j}}(n) \right\rangle \right], \tag{B.1}$$

where $\left| \psi_{\vec{j}}(n) \right\rangle \equiv \left| \vec{j}_n \right\rangle$ (as in Eq.(6.1)), and the sum runs over all the possible configurations with even number of particles. Let us first look the action of the $C_i^\dagger$ and A_i operators in their respective local subspace:

$$\{|vac\rangle, a_i^\dagger|vac\rangle, a_{i+1}^\dagger|vac\rangle, a_i^\dagger a_{i+1}^\dagger|vac\rangle\}, \tag{B.2}$$

where we see that,

$$\begin{array}{ll} C_i^\dagger|vac\rangle = C_i^\dagger|vac\rangle, & A_i|vac\rangle = 0 \\ C_i^\dagger a_i^\dagger|vac\rangle = a_{i+1}^\dagger a_i^\dagger|vac\rangle, & A_i a_i^\dagger|vac\rangle = |vac\rangle \\ C_i^\dagger a_{i+1}^\dagger|vac\rangle = a_i^\dagger a_{i+1}^\dagger|vac\rangle, & A_i a_{i+1}^\dagger|vac\rangle = -|vac\rangle \\ C_i^\dagger a_i^\dagger a_{i+1}^\dagger|vac\rangle = 0, & A_i a_i^\dagger a_{i+1}^\dagger|vac\rangle = C_i^\dagger|vac\rangle \end{array} \tag{B.3}$$

In this way one can note the following relations,

$$C_i^\dagger \sum_{\{\vec{j}\}} \left| \psi_{\vec{j}}(n) \right\rangle = C_i^\dagger \sum_{\{\vec{J}\}} \left| \psi_{\vec{J}}(n) \right\rangle, \tag{B.4}$$

$$A_i \sum_{\{\vec{j}\}} \left| \psi_{\vec{j}}(n) \right\rangle = C_i^\dagger \sum_{\{\vec{J}\}} \left| \psi_{\vec{J}}(n-2) \right\rangle, \tag{B.5}$$

where $\vec{J} = (j_1, j_2, .., j_n)$, $j_m \neq i$, $j_{m'} \neq i+1$ are the configurations with no particles at both sites "i" and "$i+1$". We have then that,

$$\begin{aligned}
\hat{d}_i|g_K\rangle &= \sum_{n=even} (-1)^{n/2} \left[C_i^\dagger \sum_{\{\vec{j}\}} \left|\psi_{\vec{j}}(n)\right\rangle + A_i \sum_{\{\vec{j}\}} \left|\psi_{\vec{j}}(n)\right\rangle \right], \\
&= \sum_{n=even} (-1)^{n/2} C_i^\dagger \left[\sum_{\{\vec{J}\}} \left|\psi_{\vec{J}}(n)\right\rangle + \sum_{\{\vec{J}\}} \left|\psi_{\vec{J}}(n-2)\right\rangle \right], \\
&= \sum_{n=even} (-1)^{n/2} C_i^\dagger \left[\sum_{\{\vec{J}\}} \left|\psi_{\vec{J}}(n)\right\rangle - \sum_{\{\vec{J}\}} \left|\psi_{\vec{J}}(n)\right\rangle \right], \\
&= 0, \qquad \text{(B.6)}
\end{aligned}$$

where in the second line we used the relations from Eqs.(B.4), (B.5); and then in the third line we just made change of index for the second term of the sum.

Conclusion and Perspectives

In the first part of this thesis we studied quantum correlations and entanglement in systems of indistinguishable particles. Entanglement of distinguishable particles is related to the notion of separability, *i.e.* the possibility of describing the system by a simple tensor product of individual states. In systems of indistinguishable particles, the symmetrization or antisymmetrization of the many-particle state eliminates the notion of separability, and the concept of entanglement becomes subtler. If one is interested in the different modes (or configurations) the system of indistinguishable particles can assume, it is possible to use the same tools employed in systems of distinguishable particles to calculate the *entanglement of modes*. On the other hand, if one is interested in the genuine entanglement between the particles, as discussed in the present work, one needs new tools. In this case, we have seen that entanglement of particles in fermionic systems is simple, in the sense that the necessary tools are obtained by simply antisymmetrizing the distinguishable case, and one is led to the conclusion that unentangled fermionic systems are represented by convex combinations of Slater determinants. The bosonic case, however, does not follow straightforwardly by symmetrization of the distinguishable case. The possibility of multiple occupation implies that a many-particle state of Slater rank one in one basis can be of higher rank in another basis. This ambiguity reflects on the possibility of multiple values of the von Neumann entropy for the one-particle reduced state of a pure many-particle state. Aware of the subtleties of the bosonic case, we have proven that a *shifted* von Neumann entropy and a *shifted* Negativity can be used to quantify entanglement of particles. We presented fermionic and bosonic entanglement witnesses, and showed an algorithm able to efficiently determine OEW's for such systems. We have shown, however, that the bosonic entanglement witness are not completely optimal, due to the possibility of multiple occupation. Nonetheless, numerical calculations have shown that the bosonic witness improves with the increase of the single-particle Hilbert space dimension. Finally, we have illustrated how the tools presented in this section could be useful in analysing the properties of entanglement in many-body systems, obtaining in particular analytic expressions for the entanglement of particles according to the von Neumann entropy of the single-particle reduced state in homogeneous D-dimensional Hamiltonians.

We also discussed how to define a more general notion of correlation, called quantumness of correlations, in fermionic and bosonic indistinguishable particles, and presented equivalent ways to quantify it, addressing the

notion of an activation protocol, the minimum disturbance in a single-particle von Neumann measurement, and a geometrical view for its quantification. An important result of our approach concerns to the equivalence of these correlations to the entanglement in distinguishable subsystems via the activation protocol, thus settling its usefulness for quantum information processing. It is interesting to note that the approach used in this work is essentially based on the definition of the algebra of single-particle observables, dealing here with the algebra of indistinguishable fermionic, or bosonic, single-particle observables, but we could apply the same idea for identical particles of general statistics, e.g. braid-group statistics, simply by defining the correct single-particle algebra of observables.

Finally, we studied the entanglement of indistinguishable particles in the extended Hubbard model at half-filling, with focus on its behavior when crossing the quantum phase transitions. Our results showed that the entanglement either has discontinuities, or presents local minima, at the critical points. We identified the discontinuities as first order transitions, and the minima as second order transitions. In this way, we concluded that the entanglement of particles can "detect" all transitions of the known diagram, except for the subtle transitions between the superconductor phases TS-SS, and the transition SDW-BOW. It is also interesting to compare our results with other entanglement measures, such as the entanglement of modes, which was widely studied in several models, as well as in the extended Hubbard model [82, 83, 81]. Gu *et al.* [82] firstly showed that the entanglement of modes, i.e., the entanglement of a single site with the rest of the lattice, could detect three main symmetry broken phases, more specifically, the CDW, SDW and PS. Other phases were not identified due to the fact that they are associated to off-diagonal long-range order. Further investigation were performed analysing the block-block entanglement [83, 81], i.e., the entanglement of a block with l sites with the rest of the lattice ($L - l$ sites), showing that this more general measure could then detect the transition to the superconducting phase, as well as the bond-order phase. The measure, however, could not detect the SS-TS transition, besides presenting some undesirable finite-size effects in the PS phase. On the other hand, the entanglement of particles studied in this work showed no undesirable finite-size effects in the PS phase, but could not detect the superconductor SS-TS transition either. Regarding the BOW phase, from the above discussion we see that it would be worth to analyze more general measures for the entanglement of particles, which goes beyond single particle information. Some steps in this direction were made in [12], where a notion of entanglement of "subgroups" of indistinguishable particles was defined.

In the second part of this thesis we addressed the generation of topological states of matter, similar to the Kitaev model ground states, in a number conserving setting. Working in a Hamiltonian setting, we then presented an exactly solvable two-wire fermionic model which conserves the number of particles and features Majorana-like exotic quasiparticles at the edges. Our results can be a valuable guideline to understand topological edge states in number conserving systems. For example, the replacement $\hat{a}_i \to \hat{c}_{i,\uparrow}, \hat{b}_i \to \hat{c}_{i,\downarrow}$

in our Hamiltonian (Eq.(6.3)) results in a one-dimensional spinful Hubbard Hamiltonian without continuous spin rotation, but time reversal symmetry. The resulting model with an exactly solvable line belongs to the class of time reversal invariant topological superconductors [112], analyzed in a number conserving setting recently [107], with edge modes protected by the latter symmetry. Moreover, exactly solvable number conserving models can be constructed in arbitrary dimension.

We also analysed the problem in a dissipative setting, i.e., the dissipative quantum state preparation of a fixed-number p-wave superconductor in one-dimensional fermionic system. In particular, we have presented two protocols which have been fully characterized in the situation of open boundary conditions. Whereas the former does not display any topological property, the latter features a two-dimensional steady space to be understood in terms of boundary Majorana modes for any number of fermions. Through the analysis of a related parent Hamiltonian, we are able to make precise statements about the gapless nature of the Lindbladian super-operators associated to both dynamics.

The peculiar form of the master equations considered in this thesis allows for the exact characterization of several properties of the system, most importantly the steady state, even if the dynamics is not solvable with the methods of fermionic linear optics [120, 121] exploited in Refs. [104, 105]. This result is very interesting *per se*, as such examples are usually rare but can drive physical intuition into regimes unaccessible without proper approximations. It is a remarkable challenge to investigate which of the properties presented so far are general and survive to modifications of the environment, and which ones are peculiar of this setup.

The analysis presented in this thesis has greatly benefited from exact mathematical relations between the properties of the Lindbladian and of a related parent Hamiltonian. Since the study of closed systems is much more developed than that of open systems both from the analytical and from the numerical points of view, the complete characterization of all the possible relations between Lindbladians and associated Hermitian operators stands as a priority research program.

In the third part of this thesis we analysed the non-Markovian nature of the dynamics by means of the divisibility criterion. We derived an analytical expression for the Kraus representation of the map corresponding to the evolution of a qubit interacting with an environment, for a general quadratic fermionic Hamiltionian, and introduced a simple function which is sufficient to check the non-Markovianity of the dynamics. We analyzed our proposed non-Markovianity function for the quantum map of a qubit interacting with an environment governed by the Ising model. For lattices up to 10^5 sites we studied the non-Markovianity of the dynamics, in the vicinity of the Ising model critical point. We quantified the non-Markovianity by the most negative eigenvalue (η) of the dynamical matrix, and obtained that, for finite size systems, it reaches its maximum at the critical point, whereas in the thermodynamic limit it is zero exactly at the critical point, diverging outside

the critical point. In the particular case of the *Ising environment*, we obtained that the Loschmidt echo and our measure η are equivalent.

Bibliography

[1] M. A. Nielsen and I. L. Chuang, Quantum Computation and Quantum Information (Cambridge University, New York, 2000).

[2] R. Horodecki, P. Horodecki, M. Horodecki, K. Horodecki, Rev. Mod. Phys. **81**, 865 (2009).

[3] L. Amico, R. Fazio, A. Osterloh and V. Vedral, Rev. Mod. Phys. **80**, 517 (2008).

[4] S. Kais, in *Reduced-Density-Matrix Mechanics: With Application to Many-Electron Atoms and Molecules,* Advances in Chemical Physics Vol. 134, edited by David A. Mazziotti (Wiley, New York, 2007).

[5] L. Amico, R. Fazio, A. Osterloh and V. Vedral, Rev. Mod. Phys., **80**, 517 (2008).

[6] A. Einstein, B. Podolsky and N. Rosen, Phys. Rev. **47**, 77 (1935).

[7] E. Schrodinger, Proc. Camb. Phil. Soc. **31**, 555 (1935).

[8] E. Schrodinger, Proc. Camb. Phil. Soc. **32**, 446 (1936).

[9] J. S. Bell, "On the Einstein-Poldolsky-Rosen paradox", Physics (1964).

[10] A. Aspect, Nature, **398**, 189 (1999).

[11] A. P. Balachandran, T. R. Govindarajan, A. R. de Queiroz and A. F. Reyes-Lega, Phys. Rev. Lett. **110**, 080503 (2013); A. P. Balachandran, T. R. Govindarajan, A. R. de Queiroz and A. F. Reyes-Lega, Phys. Rev. A **88**, 022301 (2013).

[12] G.C. Ghirardi, L. Marinatto and T. Weber, J. Stat. Phys. **108**, 49 (2002); G.C Ghirardi and L. Marinatto, Phys. Rev. A **70**, 012109 (2004).

[13] G.C Ghirardi and L. Marinatto, Phys. Rev. A **70**, 012109 (2004).

[14] F. Iemini, T. Debarba, and R. O. Vianna, Phys. Rev. A, **89**, 032324 (2014).

[15] J. Schliemann, D. Loss, and A. H. MacDonald, Phys. Rev B **63**, 085311 (2001); J. Schliemann, J. I. Cirac, M. Kus, M. Lewenstein and D. Loss, Phys. Rev. A **64**, 022303 (2001).

[16] K. Eckert, J. Schliemann, D. Bruss and M. Lewenstein, Ann. Phys. **299**, 88 (2002).

[17] Y. S. Li, B. Zeng, X. S. Liu and G. L. Long, Phys. Rev. A **64**, 054302 (2001).

[18] Rolando Somma, Gerardo Ortiz, Howard Barnum, Emanuel Knill and Lorenza Viola, Physic. Rev. A **70**, 042311 (2004).

[19] P. Zanardi, Phys. Rev. A **65**, 042101 (2002).

[20] H. M. Wiseman and J. A. Vaccaro, Phys. Rev. Lett. **91**, 097902 (2003).

[21] F. Benatti, R. Floreanini and U. Marzolino, Ann. Phys. **325**, 924 (2010).

[22] M.C. Banuls, J. I. Cirac and M. M. Wolf, Phys. Rev. A **76**, 022311 (2007).

[23] J. Grabowski, M. Kus and G. Marmo, J. Phys. A: Math. Theor. **44**, 175302 (2011). J. Grabowski, M. Kus and G. Marmo, J. Phys. A: Math. Theor. **45**, 105301 (2012).

[24] T. Sasaki, T. Ichikawa and I. Tsutsui, Phys. Rev. A **83**, 012113 (2011).

[25] H. Barnum, E. Knill, G. Ortiz, R. Somma, and L. Viola, Phys. Rev. Lett. **92**, 107902 (2004).

[26] Gerardo Ortiz, Rolando Somma, Howard Barnum, Emanuel Knill and Lorenza Viola, arXiv:quant-ph/0403043v2

[27] F. Iemini, T. O. Maciel, T. Debarba, and R. O. Vianna, Quantum Inf. Process., **12**, 733 (2013).

[28] F. Iemini, and R. O. Vianna, Phys. Rev. A **87**, 022327 (2013).

[29] R. Paskauskas and L. You, Phys. Rev. A **64**, 042310 (2001).

[30] A. R. Plastino, D. Manzano and J. S. Dehesa, Europhys. Lett **86**, 20005 (2009).

[31] C. Zander and A. R. Plastino, Phys. Rev. A **81**, 062128 (2010).

[32] A. Reusch, J. Sperling and W. Vogel, Phys. Rev. A **91** 042324, (2015).

[33] A. Peres, Phys. Rev. Lett. **77**, 1413 (1996).

[34] M. Piani, S. Gharibian, G. Adesso, J. Calsamiglia, P. Horodecki and A. Winter, Phys. Rev. Lett. **106**, 220403 (2011).

[35] John F. Clauser, Michael A. Horne, Abner Shimony, and Richard A. Holt, Phys. Rev. Lett. **23**, 880 (1969).

[36] R. G. Parr and W. Yang, Density Matrices: The N-representability of reduced density matrices. In: Density-Functional Theory of Atoms and Molecules, The International Series of Monographs on Chemistry - 16, Oxford Science Publications. 1989.

[37] K. Eckert, J. Schliemann, D. Bruss and M. Lewenstein, Ann. Phys. **299**, 88-127 (2002).

[38] William K. Wootters, Phys. Rev. Lett. **80**, 2245 (1998).

[39] M. Lewentein, *Quantum Information Theory Wintersemester 2000/2001*, url: www.quantware.ups-tlse.fr/IHP2006/lectures/lewenstein2.pdf

[40] F.G.S.L. Brandão, Phys. Rev. A **72**, 022310 (2005).

[41] Guifré Vidal and Rolf Tarrach, Phys, Rev. A, **59**, 1 (1999).

[42] Michael Steiner, Phys. Rev. A, **67**, 054305 (2003).

[43] Stephen Boyd and Lieven Vandenberghe, Convex Optimization, Cambridge University Press (2004).

[44] F.G.S.L. Brandão and R.O. Vianna, Phys. Rev. Lett. **93**, 220503 (2004).

[45] Fernando G. S. L. Brandão and Reinaldo O. Vianna, Phys. Rev. A **70**, 062309 (2004).

[46] Ingemar Bengtsson and Karol Zyczkowski, Quantum Entanglement. In: Geometry of Quantum States, An Introduction to Quantum Entanglement - Cambridge University Press 2006.

[47] A. Streltsov, H. Kampermann and D. Bruss, Phys. Rev. Lett. **106**, 160401 (2011).

[48] H. Ollivier and W. H. Zurek, Phys. Rev. Lett. **88**, 017901 (2001).

[49] L. Henderson and V. Vedral, J. Phys. A **34**, 6899 (2001).

[50] J. Oppenheim, M. Horodecki, P. Horodecki and R. Horodecki, Phys. Rev. Lett. **89**, 180402 (2002).

[51] M. Horodecki, P. Horodecki, R. Horodecki, J. Oppenheim, A. Sen, U. Sen and B. Synak-Radtke, Phys. Rev. A **71**, 062307 (2005).

[52] S. Luo, Phys. Rev. A **77**, 022301 (2008).

[53] Kavan Modi, Tomasz Paterek, Wonmin Son, Vladko Vedral and Mark Williamson, Phys. Rev. Lett. **104**, 080501 (2010).

[54] W.H. Zurek, Rev. Mod. Phys. **75**, 715–775 (2003)

[55] S. Gharibian, M. Piani, G. Adesso, J. Calsamiglia and P. Horodecki, Int. J. Quantum Inform. **09**, 1701 (2011).

[56] M. Piani and G. Adesso, Phys. Rev. A **85**, 040301(R) (2012).

[57] T. Nakano, M. Piani and G. Adesso, Phys. Rev. A **88**, 012117 (2013).

[58] Paolo Zanardi, Phys. Rev. Lett. **87**, 077901 (2001). Paolo Zanardi, Daniel A. Lidar and Seth Lloyd, Phys. Rev. Lett. **92**, 060402 (2004).

[59] N. L. Harshman and K. S. Ranade, Phys. Rev. A **84**, 012303 (2011).

[60] L. Derkacz, M. Gwózdz, and L. Jakóbczyk, J. Phys. A 45, 025302 (2012).

[61] C.H. Bennett, D.P. DiVincenzo, J.A. Smolin and W.K. Wootters, Phys. Rev. A **54**, 3824 (1996).

[62] V. Vedral and M.B. Plenio, Phys. Rev. A **57**, 1619 (1998).

[63] V. Vedral, M.B. Plenio, M.A. Rippin and P.L. Knight, Phys. Rev. Lett. **78**, 2275 (1997).

[64] E.M. Rains, IEEE Trans. Inf. Theory **47**, 2921 (2001).

[65] Tohya Hiroshima and Masahito Hayashi, Phys. Rev. A **70**, 030302 (2004).

[66] Ana P. Majtey, C. Zander, and Angel R. Plastino, Eur. Phys. J. D (2013) 67:79, DOI: 10.1140/epjd/e2013-30594-7.

[67] Fernando Iemini, Thiago O. Maciel and Reinaldo O. Vianna, Phys. Rev. B **92**, 075423 (2015).

[68] J. Hubbard, Proc. R. Soc. Lond. A **276**, 238-257 (1963).

[69] J. Sólymon, Adv. Phys., **28**, 201-303 (1979).

[70] U. Schollwöck, Ann. Phys., **326**, 96-192 (2011).

[71] B. Bauer, L.D. Carr, H.G Evertz, A. Feiguin, J. Freire, S. Fuchs, L. Gamper, J. Gukelberger, E. Gull, S. Guertler, A. Hehn, R. Igarashi, S.V. Isakov, D. Koop, P.N. Ma, P. Mates, H. Matsuo, O. Parcollet, G. Pawłowski, J.D. Picon, L. Pollet, E. Santos, V.W. Scarola, U. Schollwöck, C. Silva, B. Surer, S. Todo, S. Trebst, M. Troyer, M.L. Wall, P. Werner, and S. Wessel, J. Stat. Mech, **2011**, P05001 (2011).

[72] H. Q. Lin, D. K. Campbell and R. T. Clay, Chinese Journal of Physics **38**, 1 (2000).

[73] M. Nakamura, Phys. Rev. B **61**, 16377 (2000).

[74] P. Sengupta, A. W. Sandvik and D. K. Campbell, Phys. Rev. B **65**, 155113 (2002).

[75] Y. Z. Zhang, Phys. Rev. Lett. **92**, 246404 (2004).

[76] M. D., J. Carrasquilla, L. Taddia, E. Ercolessi and M. Rigol, arXiv:1412.5624v1

[77] E. Jeckelmann, Phys. Rev. Lett. **89**, 236401 (2002).

[78] Satoshi Ejima and S. Nishimoto, Phys. Rev. Lett. **99**, 216403 (2007).

[79] A. W. Sandvik, L. Balents and D. K. Campbell, Phys. Rev. Lett. **92**, 236401 (2004).

[80] T. Giamarchi, *Quantum Physics in One Dimension* (Oxford University Press, New York, 2004).

[81] C. Mund, Ö. Legeza and R. M. Noack, Phys. Rev. B **79**, 245130 (2009).

[82] Shi-Jian Gu, Shu-Sa Deng, You-Quan Li and Hai-Qing Lin, Phys. Rev. Lett. **93**, 086402 (2004).

[83] Shu-Sa Deng, Shi-Jian Gu and Hai-Qing Lin, Phys. Rev. B **74**, 045103 (2006).

[84] S. Sachdev, *Quantum Phase Transitions* (Cambridge University Press, 1999).

[85] C. Nayak, S. H. Simon, A. Stern, M. Freedman and S. Das Sarma, Rev. Mod. Phys. **80**, 1083 (2008).

[86] J. K. Pachos, *Introduction to Topological Quantum Computation* (Cambridge University Press, Cambridge, 2012)

[87] Xiao-Gang Wen, ISRN Condensed Matter Physics, Volume 2013, Article ID 198710, http://dx.doi.org/10.1155/2013/198710

[88] Xiao-Gang Wen, *An Introduction of Topological Orders*, http://dao.mit.edu/ wen

[89] A. Y. Kitaev, Physics Uspekhi **44**, 131 (2001).

[90] A. M. Turner, F. Pollmann, and E. Berg, Phys. Rev. B **83**, 075102 (2011).

[91] M. Z. Hasan and C. L. Kane, Rev. Mod. Phys. **82**, 3045 (2010).

[92] X.-L. Qi and S.-C. Zhang, Rev. Mod. Phys. **83**, 1057 (2011).

[93] C. Nayak, S. H. Simon, A. Stern, M. Freedman, and S. Das Sarma, Rev. Mod. Phys. **80**, 1083 (2008).

[94] R. M. Lutchyn, J. D. Sau, and S. Das Sarma, Phys. Rev. Lett. **105**, 077001 (2010).

[95] Y. Oreg, G. Refael, and F. von Oppen, Phys. Rev. Lett. **105**, 177002 (2010).

[96] L Jiang, T. Kitagawa, J. Alicea, A. R. Akhmerov, D. Pekker, G. Refael, J. I. Cirac, E. Demler, M. D. Lukin, and P. Zoller, Phys. Rev. Lett. **106**, 220402 (2011).

[97] V. Mourik, K. Zuo, S. M. Frolov, S. R. Plissard, E. P. A. M. Bakkers, and L. P. Kouwenhoven, Science **336**, 1003 (2012).

[98] L. Fidkowski, R. M. Lutchyn, C. Nayak, and M. P. A. Fisher, Phys. Rev. B **84**, 195436 (2011).

[99] J. D. Sau, B. I. Halperin, K. Flensberg, and S. Das Sarma, Phys. Rev. B, **84**, 144509 (2011).

[100] M. Cheng and H.-H. Tu, Phys. Rev. B., **84**, 094503 (2011).

[101] C. V. Kraus, M. Dalmonte, M. A. Baranov, A. M. Läuchli, and P. Zoller, Phys. Rev. Lett., **111**, 173004 (2013).

[102] G. Ortiz, J. Dukelsky, E. Cobanera, C. Esebbag, and C. Beenakker, Phys. Rev. Lett. **113**, 267002 (2014).

[103] S. Diehl, W. Yi, A. J. Daley, and P. Zoller, Phys. Rev. Lett. **105**, 227001 (2010).

[104] S. Diehl, E. Rico, M. A. Baranov, and P. Zoller, Nature Phys. **7**, 971 (2011).

[105] C.-E. Bardyn, M. A. Baranov, C. V. Kraus, E. Rico, A. Imamoglu, P. Zoller, and S. Diehl, New J. Phys. **15**, 085001 (2013).

[106] J. Ruhman, E. Berg, E. Altman, Phys. Rev. Lett. 1**114**, 100401 (2015).

[107] A. Keselman and E. Berg, arXiv:1502.02037 (2015).

[108] A. Yu Kitaev, Annals of Physics **321** 2 (2006).

[109] C. Laflamme, M. A. Baranov, P. Zoller and C. V. Kraus Phys. Rev. A **89**, 022319 (2014).

[110] S. Bravyi, Phys. Rev. B **73**, 042313 (2006).

[111] M. Freedman, C. Nayak, and K. Walker, Phys. Rev. B **73**, 245307 (2006).

[112] X.-L. Qi, T. L. Hughes, S. Raghu, and S.-C. Zhang, Phys. Rev. Lett. **102**, 187001 (2009).

[113] S. Diehl, A. Micheli, A. Kantian, B. Kraus, H.P. Buchler and P. Zoller P, Nature Phys. **4**, 878–83 (2008).

[114] Frank Verstraete, Michael M. Wolf and J. Ignacio Cirac, Nature Phys. **5**, 633 (2009).

[115] F. Iemini, L. Mazza, D. Rossini, R. Fazio, and S. Diehl, Phys. Rev. Lett. **115**, 156402 (2015).

[116] Willian H. Press, Saul A. Teukolsky, William T. Vetterling and Brian P. Flannery, Chapter 16.1: Numerical Recipes in C, The Art of Scientific Computing, Second Edition.

[117] F. Verstraete, J.I. Garcia-Ripoll and J.I. Cirac, Phys. Rev Lett., **93**, 207204 (2004).

[118] M. Zwolak and G. Vidal, Phys. Rev. Lett., **93**, 207205 (2004).

[119] T. Prosen and M. Znidaric, J. Stat. Mech., P02035 (2009).

[120] T. Prosen, New J. Phys. **10**, 043026 (2008).

[121] S. Bravyi and R. Koenig, Quant. Inf. Comp. **12**, 925 (2012).

[122] Fernando Iemini, Davide Rossini, Sebastian Diehl, Rosario Fazio and Leonardo Mazza, Phys. Rev. B **93**, 115113 (2016).

[123] A. Kitaev, Ann. Phys. **303**, 2 (2003); and arXiv:quant-ph/9707021 (1997).

[124] E. Dennis, A. Kitaev, A. Landahl, and J. Preskill, J. Math. Phys. **43**, 4452 (2002).

[125] J. Alicea, Rep. Prog. Phys. **75**, 076501 (2012).

[126] C. W. J. Beenakker, Annu. Rev. Con. Mat. Phys. **4**, 113 (2013).

[127] S. Das Sarma, M. Freedman, and C. Nayak, arXiv:1501.02813v2 (2015).

[128] A. Das, Y. Ronen, Y. Most, Y. Oreg, M. Heiblum, and H. Shtrikman, Nat. Phys. **8**, 887 (2012).

[129] H. O. H. Churchill, V. Fatemi, K. Grove-Rasmussen, M. T. Deng, P. Caroff, H. Q. Xu, and C. M. Marcus, Phys. Rev. B **87**, 241401 (2013).

[130] A. D. K. Finck, D. J. Van Harlingen, P. K. Mohseni, K. Jung, and X. Li, Phys. Rev. Lett. **110**, 126406 (2013).

[131] S. Nadj-Perge, I. K. Drozdov, J. Li, H. Chen, S. Jeon, J. Seo, A. H. MacDonald, B. A. Bernevig, and A. Yazdani, Science **346**, 602 (2014).

[132] L. Radzihovsky and V. Gurarie, Ann. Phys. **322**, 2 (2007).

[133] M. Sato, Y. Takahashi, and S. Fujimoto, Phys. Rev. Lett. **103**, 020401 (2009).

[134] J. D. Sau, R. Sensarma, S. Powell, I. B. Spielman, and S. Das Sarma, Phys. Rev. B **83** 140510(R) (2011).

[135] S. Nascimbène, J. Phys. B: At. Mol. Opt. Phys. **46**, 134005 (2013).

[136] A. Bühler, N. Lang, C. V. Kraus, G. Möller, S. D. Huber, and H. P. Büchler, Nat. Commun. **5**, 4504 (2014).

[137] M. Roncaglia, M. Rizzi, and J. I. Cirac, Phys. Rev. Lett. **104**, 096803 (2010).

[138] J. C. Budich, P. Zoller, and S. Diehl, Phys. Rev. A **91**, 042117 (2015).

[139] Hendrik Weimer, Markus Müller, Igor Lesanovsky, Peter Zoller and Hans Peter Büchler, Nature Physics **6**, 382 - 388 (2010).

[140] N. Lang and H. P. Büchler, Phys. Rev. B **92**, 041118 (2015).

[141] Z. Cai and T. Barthel, Phys. Rev. Lett. **111**, 150403 (2013).

[142] P. Hohenberg and B. Halperin, Rev. Mod. Phys. **49**, 435–479 (1977).

[143] M. J. Kastoryano, D. Reeb, and M. M. Wolf, J. Phys. A: Math. Theor. **45** 075307 (2012).

[144] M. Buchhold and S. Diehl, Phys. Rev. A **92**, 013603 (2015).

[145] S. Caspar, F. Hebenstreit, D. Mesterházy and U.-J. Wiese, arXiv:1511.08733 (2105).

[146] R. Orus and G. Vidal, Phys. Rev. B **78**, 155117 (2008).

[147] M. J. Hartmann, J. Prior, S. R. Clark and M. B. Plenio, Phys. Rev. Lett. **102**, 057202 (2009).

[148] A. J. Daley, Adv. Phys. **63**, 77 (2014).

[149] J. Cui, J. I. Cirac, and M. C. Banuls, Phys. Rev. Lett. **114**, 220601 (2015).

[150] A. Biella, L. Mazza, I. Carusotto, D. Rossini, and R. Fazio, Phys. Rev. A **91**, 053815 (2015).

[151] S. Finazzi, A. Le Boité, F. Storme, A. Baksic, and C. Ciuti, Phys. Rev. Lett. **115**, 080604 (2015).

[152] E. Mascarenhas, H. Flayac, and V. Savona, Phys. Rev. A **92**, 022116 (2015).

[153] A. H. Werner, D. Jaschke, P. Silvi, M. Kliesch, T. Calarco, J. Eisert, and S. Montangero, arXiv:1412:5746 (2014).

[154] M. Müller, S. Diehl, G. Pupillo, P. Zoller, Advances in Atomic, Molecular, and Optical Physics **61**, 1-80 (2012)

[155] J. Alicea, Y. Oreg, G. Refael, F. von Oppen, and M. P. A. Fisher, Nat. Phys. **7**, 412 (2011).

[156] N. Syassen, D. M. Bauer, M. Lettner, T. Volz, D. Dietze, J. J. Garcia-Ripoll, J. I. Cirac, G. Rempe and S. Dürr, Science **320**, 1329 (2008).

[157] A. C. Y. Li, F. Petruccione, and J. Koch, Sci. Rep. **4**, 4887 (2014).

[158] M. Ippoliti, L. Mazza, M. Rizzi, and V. Giovannetti, Phys. Rev. A **91**, 042322 (2015).

[159] T. Kato, *Perturbation Theory for Linear Operators* Springer-Verlag, Berlin heidelberg New York (1980).

[160] Fernando Iemini, Andre T. Cesário and Reinaldo O. Vianna, arXiv:1507.02267

[161] B. Bylicka, D. Chruściński, S. Maniscalco, Sci. Rep., **4**, 5720 (2014).

[162] P. Haikka, J.D. Cresser, S. Maniscalco, Phys. Rev. A, **83**, 012112 (2011).

[163] E. M. Laine, J. Piilo, and H. P. Breuer, Phys. Rev. A, **81**, 062115 (2010).

[164] D. Chruściński, A. Kossakowski, Eur. Phys. J. D, **68**, 7 (2014).

[165] X.M. Lu, X. Wang, C.P. Sun, Phys. Rev. A, **82**, 042103 (2010).

[166] S. Luo, S. Fu, H. Song, Phys. Rev. A, **86**, 044101 (2012).

[167] H. T. Quan, Z. Song, X. F. Liu, P. Zanardi, and C.P. Sun, Phys. Rev. Lett., **96**, 140604 (2006).

[168] P. Haikka, J. Goold, S. McEndoo, F. Plastina, and S. Maniscalco, Phys. Rev. A **85**, 060101(R) (2012); P. Haikka and S. Maniscalco, Open Syst. Inf. Dyn. 21, 1440005 (2014).

[169] A. Rivas, S.F. Huelga, M.B. Plenio, Phys. Rev. Lett., **105**, 050403 (2010).

[170] C.A. Rodríguez-Rosario, E.C.G. Sudarshan , Int. J. Quantum Inform., **09**, 1617 (2011).

[171] A. Devi, A. Rajagopal, S. Shenoy and R. Rendell, J. Q. Inf. Sci., **2**, 47-54 (2012).

[172] F. Franchini, Notes on Bethe Ansatz Techniques, SISSA, the International School for Advanced Studies in Trieste, Italy (2011), http://people.sissa.it/∼ffranchi/BAnotes.pdf.